INTERNATIONAL HYDROLOGICAL PROGRAMME

Progress in surface and subsurface water studies at plot and small basin scale

10th Conference of the Euromediterranean Network of Experimental and Representative Basins (ERB)
Turin, Italy, 13 – 17 October 2004

Convened by : ERB, UNESCO/IHP (NE FRIEND Project 5) and National Research Council of Italy (CNR) – Research Institute for Geo-Hydrological Protection

PROCEEDINGS

Edited by F. Maraga and M. Arattano

IHP-VI | Technical Documents in Hydrology | No. 77
UNESCO, Paris, 2005

Published in 2005 by the International Hydrological Programme (IHP) of the United Nations Educational, Scientific and Cultural Organization (UNESCO)
1 rue Miollis, 75732 Paris Cedex 15, France

IHP-VI Technical Document in Hydrology N°77
UNESCO Working Series SC-2005/WS/56

The designations employed and the presentation of material throughout the publication do not imply the expression of any opinion whatsoever on the part of UNESCO concerning the legal status of any country, territory, city or of its authorities, or concerning the delimitation of its frontiers or boundaries.

Publications in the series of *IHP Technical Documents in Hydrology* are available from:

IHP Secretariat | UNESCO | Division of Water Sciences
1 rue Miollis, 75732 Paris Cedex 15, France
Tel: +33 (0)1 45 68 40 01 | Fax: +33 (0)1 45 68 58 11
E-mail: ihp@unesco.org
http://www.unesco.org/water/ihp

Printed in UNESCO's workshops
Paris, France

PROGRESS
IN SURFACE AND SUBSURFACE WATER STUDIES
AT PLOT AND SMALL BASIN SCALE

International Conference held in Turin, Italy
October 13th – 17th 2004

Convened by:

Euromediterranean Network of Experimental and Representative Basins (ERB)
IHP - UNESCO - Northern European FRIEND Project 5
National Research Council of Italy (CNR) - Research Institute for Geo-Hydrological Protection

Organized by:

Italian Committee for Hydrology – NC IHP UNESCO
CNR - Research Institute for Geo-Hydrological Protection

Scientific Advisory Committee:

Mike Bonell, UNESCO, Paris, France
Virgilio Anselmo, Turin, Italy
Wojciech Chelmicki, Crakow, Poland
Siegfried Demuth, Freiburg, Germany
Francesc Gallart, Barcelona, Spain
George Ivanov Gergov, Sofia, Bulgaria
Ladislav Holko, Liptovsky Mikulas, Slovakia
Hubert Holzman, Vienna, Austria
Pompiliu Mita, Bucharest, Romania
Laurent Pfister, Luxembourg, Luxembourg
Manfred Spreafico, Bern, Switzerland
Miroslav Tesar, Prague, Czech Republic
Lucio Ubertini, Perugia, Italy
Piet Warmerdam, Wageningen, The Netherlands

Local Organizing Committee:

Enrico Giacomasso, Giorgio Lollino, Franca Maraga, Caterina Tantaro, Domenico Tropeano (CNR-Research Institute for Geo-Hydrological Protection) Virgilio Anselmo (University of Turin) and Giovanni Maria Zuppi (University of Venice). Secretary: Chiara Pellissero.

Scientific Reviewers:

Massimo Arattano, Elpidio Caroni, Wojciech Chelmicki, Roel Dijksma, Francesc Gallart, Ladislav Holko, Hubert Holzmann, Pompiliu Mita, Laurent Pfister, Daniel Viville, Piet Warmerdam.

Linguistic review:

Alexander Cameron-Curry and Joseph Gerard Dorrity

Previous ERB conferences and proceedings:

Oct 1986 Aix en Provence (France)

Oct 1988 Perugia (Italy)
Erosion and sediment transport
Bull. of Ass. It. di Idronomia, Quaderni Idronomia Montana No. 9 [Special Issue], Padua, 1999, 204 pp.

Sep 1990 Wageningen (The Netherlands)
Hydrological research basins and the environment
TNO Comm. On Hydrol. Res., Proc. and Informat. No. 44, The Hague, 347 pp.

Sep 1992 Oxford (United Kingdom)
Methods of hydrological basin comparison
Institute of Hydrology Rep. No. 120, Wallingford, 198 pp.

Sep 1994 Barcelona (Spain)
Assessment of hydrological temporal variability and changes
Acta Geol. Hisp. [Special Issue], vol. 28, No. 2-3, Barcelona, 1995, 138 pp.

Sep 1996 Strasbourg (France)
Ecohydrological processes in small basins
Technical Documents in Hydrology 14, IHP UNESCO, Paris, 1997, 199 pp.

Sep 1998 Liblice (Czech Republic)
Catchment hydrological and biochemical processes in a changing environment Technical Documents in Hydrology 37, IHP UNESCO, Paris, 2000, 296 pp.

Sep 2000 Ghent (Belgium)
Monitoring and modelling catchment water quantity and quality
Technical Documents in Hydrology 66, IHP UNESCO, Paris, 2003, 112 pp.

Sep 2002 Demanovska Dolina (Slovakia)
Interdisciplinary approaches in small catchment hydrology: monitoring and research
Technical Documents in Hydrology 67, IHP UNESCO, Paris, 2003, 256 pp.

ERB Member Countries and National Correspondents (in 2004):

Austria	Hubert Holzmann	Poland	Wojciech Chelmicki
Belgium	François de Troch	Rumania	Pompiliu Mita
Bulgaria	George Gergov	Russia	Sergey Zhuravin
Czech Republic	Miroslav Tesar	Slovakia	Pavol Miklanek
Finland	Pertti Seuna	Slovenia	Brilly Mitja
France	Daniel Viville	Spain	Francesc Gallart
Germany	Stefan Uhlenbrook	Switzerland	Manfred Spreafico
Italy	Franca Maraga	The Netherlands	Piet Warmerdam*
Luxembourg	Laurent Pfister	United Kingdom	Ian Littlewood

**Co-ordinator since 2002*

NE FRIEND Project 5 participating countries (in 2004):

Czech Republic, Finland, Germany, The Netherlands, Poland, Russia, Slovakia, Sweden.
Co-ordinator Ladislav Holko (Slovakia)

Preface

The Proceedings contain contributions selected for oral presentation at the 10th International Conference of the Euromediterranean Network of Experimental and Research Basins (ERB) of Unesco. The conference was organized jointly with the IHP UNESCO Northern European FRIEND Project 5 "Catchment hydrological and biogeochemical processes in a changing environment" and the Research Institute for Geo-Hydrological Protection (IRPI) in Turin, Italy.

The ***Euromediterranean Network of Experimental and Research Basins (ERB)*** was recommended by the European Council and launched in 1986. The main objectives of the network are:

- to establish and maintain relationships between member countries and research teams by means of information exchange, mobility and regular conferences
- to initiate and enable co-operation between members and other organisations
- to maintain a database of small research and experimental basins

The *ERB* network currently has 18 member countries. Member countries are represented by their national correspondents in the ERB Steering Committee, which assembles once per year. National correspondents are appointed by National Committees for IHP of Unesco. The ERB General Assembly meets once every two years during the ERB international conference. Regular *ERB* conferences represent the main forum for meeting and exchanging knowledge among the ERB participants.

The ERB reports on its activities in the *ERB* Newsletter, which is published approximately once a year. It provides information about the Steering Committee meetings, national and international activities, catchments, research findings and progress with the ERB database. Editor of the Newsletter is Laurent Pfister (laurent.pfister@lippmann.lu)

The ERB database ICARE (Inventory of the Catchments for Research in Europe) contains metadata from about 142 basins and several sets of validation data measured during short time intervals. The database is maintained by CEMAGREF in Lyon, France.

The ***Northern European FRIEND Project 5 "Catchment hydrological and biogeochemical processes in a changing environment"*** is focused on a better understanding and synthesis of the processes and mechanisms responsible for streamflow generation, variation in flow components and cycling of the main nutrients under different physiographic and climatic conditions. FRIEND is a bottom-up programme with free participation. About 10-15 participants representing universities and research institutes typically contribute to Project 5.

Similar interests of ERB and NE FRIEND Project 5 communities have lead to close co-operation in the exchange of knowledge and organisation of the latest ERB conferences.

Additional information about the ERB can be obtained from the National Correspondents and from the International Co-ordinator of ERB Piet Warmerdam (Piet.Warmerdam@wur.nl) and about NE FRIEND Project 5 from the International Co-ordinator Ladislav Holko (holko@uh.savba.sk) or on:

http://erb.lyon.cemagref.fr/en/index.html
http://www.ih.savba.sk/ihp/friend5/index.html

Note from the editors

The ERB International Conference 2004 was jointly organized with the 10th General Assembly of Experimental and Representative Basins network members and the UNESCO IHP Northern European FRIEND Project 5 meeting.
The conference was attended by nearly 100 participants representing 17 countries: Austria, Bulgaria, Czech Republic, France, Georgia, Germany, Italy, Lithuania, Luxembourg, Poland, Portugal, Rumania, Slovakia, Slovenia, Spain, Switzerland, The Netherlands.
Funding from Unesco enabled the Organizing Committee to support the participation of twelve scientists from requesting countries.

Five scientific sessions were organized as oral and poster presentations focusing on the following topics:

1) Surface and subsurface water flow;
2) Precipitation – runoff processes;
3) Water quality and quantity relationships;
4) Water and sediment relationships in channel and slope erosion, sediment transport, mass movement and debris flow;
5) Approaches and experiences on earth process studies involving development on innovative devices.

Three field trips were settled on the final day of the Conference in order to show some experiences carried out in Alpine and Apennine regions related to soil erosion studies on vineyard hill, water body monitoring on cave hydrogeologic system, sediment transport measurements in small mountain basin.

This volume contains the contributions of 30 selected oral presentations and the list of 38 exhibited posters, proposed by authors coming from 16 different countries (Bulgaria, Czech Republic, France, Georgia, Germany, Italy, Lithuania, Luxembourg, Poland, Portugal, Rumania, Slovakia, Slovenia, Spain, Switzerland, The Netherlands).
The contributions present results obtained in experimental sites located in different regional landscapes and geographical positions.

The editors are very grateful to the reviewers (listed on pag. *i*) for their kind devotion to the heavy review work of the papers, regarding a large range of topics and to the ERB Co-ordinator for his continuous organizational support and his scientific help for a good success of the ERB 2004 Conference Proceedings.

Franca MARAGA and Massimo ARATTANO
Caterina Tantaro (assistant)
Research Institute for Geo-hydrological Protection, National Research Council of Italy

ERB and Northern European FRIEND Project 5
International Conference
PROGRESS IN SURFACE AND SUBSURFACE WATER STUDIES AT PLOT AND SMALL BASIN SCALE
Turin, Italy
13th – 17th October 2004

TABLE OF CONTENTS

Session 3: Water quality and quantity relationships

Session 4: Water and sediment relationships in channel and slope erosion, sediment transport, mass movement and debris flow

EMPIRICAL AND CONCEPTUAL APPROACHES FOR SOIL MOISTURE ESTIMATION IN VIEW OF EVENT-BASED RAINFALL-RUNOFF MODELING

L. Brocca, F. Melone and T. Moramarco

National Research Council (CNR), Institute for Geo-Hydrological Protection (IRPI), Via Madonna Alta 126, 06128 Perugia, Italy
e-mail Luca Brocca: brocca@irpi.cnr.it

ABSTRACT

The estimation of soil water content before a given storm event, which is generally an arbitrary parameter in rainfall-runoff modeling, is addressed. Empirical approaches and a simple conceptual model of water balance in the upper soil layer are investigated. The empirical approaches concern different formulations widely employed in hydrological practice and based on indexes for taking account of the degree of catchment wetness. Neglecting the evapotranspiration process, they consider only the precipitation data. The conceptual model is based on that proposed by Georgakakos and Baumer (1996) and uses routinely measured meteorological variables: rainfall and air temperature. The performance of each method was tested through local measurements of soil moisture carried out continuously on an experimental plot in central Italy. In the verification stage, the conceptual model was found to be significantly more efficient and its reliability independent of the period of the year. In addition, preliminary results on the relation of the local measurements with the hydrological response of the catchment including the plot are presented.

Key words: soil moisture, Antecedent Precipitation Index, land surface models, rainfall-runoff, experimental basins.

INTRODUCTION

The characterization of soil moisture space-time variability is a fundamental issue in modeling the hydrological response of a basin and land-atmosphere interactions. In fact, root-zone soil moisture is addressed as a key-variable controlling surface water (evapotranspiration, infiltration and surface runoff) and energy exchange between the land surface and the first layer of the atmosphere. In particular, soil moisture is very important for real-time flood forecast modeling (Kitanidis and Bras, 1980) and for the prediction of precipitation at local scale (Entekhabi et al., 1996).
The event-based streamflow simulation models require knowledge of the basin's soil moisture conditions before a given storm event. Indeed, many studies show that for Mediterranean catchments, in which extreme events occur when the soil is close to saturation, soil moisture is the main factor affecting the flood formation process (Aronica and Candela, 2004). This issue is frequently addressed through an index based on the cumulated rainfall within a short period preceding the event, the Antecedent Precipitation Index (API). A very popular index is that adopted by the American Soil Conservation Service method (SCS-CN) for representation of losses in rainfall-runoff models and which uses the precipitation depth of the previous five days (Chow et al., 1988). Because of its empirical basis the application to basins with different characteristics could be inappropriate (Ponce and Hawkins, 1996; Corradini et al., 2000). Other relations involving different weights for precipitations in accordance with the time in which they occur, have been developed (Pan et al., 2003). These weights depend on a parameter which considers the drop in soil moisture during the rainless periods and which is linked to both evapotranspiration and infiltration processes. Due to this dependence its estimation remains quite doubtful.
The need to predict the evolution of soil moisture led to the advent of land surface models (LSMs) able to simulate the mass and energy transfer between the land and the first layer of the atmosphere (Georgakakos and Baumer, 1996). These models are physically based and, in general, the surface moisture and energy balance equation provides details of soil moisture and soil thermal conditions over time (Famiglietti and Wood, 1994). Their limitation is linked to the availability of the meteorological data and to the considerable number of parameters that have to be estimated.

The main objective of the present study is to investigate both the reliability of a simple conceptual model of the soil water balance based on the approach proposed by Georgakakos and Baumer (1996) and the problems of its use in the hydrological practice with respect to the empirical methods based on the antecedent precipitation. An experimental data set collected in an equipped hillslope located in the Colorso basin, Central Italy, has been used for this purpose.

METHODS

In order to evaluate the temporal pattern of soil moisture both empirical approaches and a relatively simple model of water balance in the upper soil layer are used.
The empirical approaches are based only on the antecedent precipitation, with a general formulation written as (Gray, 1970):

$$API_t = \sum_{i=1}^{N} b_i P_{t-i} \tag{1}$$

in which t is time; N is the number of the antecedent days; b_i and P_{t-i} are the weight and the daily precipitation depth, respectively. The API index is based on daily rainfall records, but in order to take account of rainfall variability, the formulation is here extended for time series with temporal resolution of 0.5 hours. In particular, assuming that b_i are functions of time, the following cases are considered:

$$b_i = 1 \Rightarrow API_t^N = \sum_{i=0}^{48N-1} P_{t-i} \tag{2}$$

$$b_i = e^{-Ki} \Rightarrow API_t^{N,K} = \sum_{i=1}^{N} \left(\sum_{j=48(i-1)}^{48i-1} P_{t-j} e^{-Ki} \right) \tag{3}$$

$$b_i = K^i \Rightarrow API_t = K \cdot API_{t-1} + P_t \tag{4}$$

where K is a decay parameter to be estimated by calibration. Eq.(2) involves only one parameter, the number of days. For the other relations, two parameters have to be estimated: K and N in Eq.(3), again K and the initial value of API, API_0, in Eq.(4). It is to be noted that N represents the memory of the system while K is linked to the drop in soil moisture in the periods without rainfall, which is mainly due to the evapotranspiration process. In order to take account of this process, a formulation of Eq.(4) with K varying monthly is also investigated with an increase in the parameters to thirteen.
The conceptual model used in this study is based on the following water content balance equation for the upper soil layer of thickness z (Georgakakos and Baumer, 1996):

$$\frac{dW}{dt} = p(t) - s(t) - e(t) - b(t) \tag{5}$$

where p(t) is precipitation, s(t) is surface runoff, e(t) is evapotranspiration and b(t) is the sum of interflow and deep percolation (see Fig. 1). The amount of water in the investigated soil layer, W(t), is given by:

$$W(t) = (\theta - \theta_r) \cdot z \tag{6}$$

with θ volumetric water content and θ_r residual volumetric water content. At natural saturation ($\theta=\theta_s$), this amount is equal to the capacity of the soil to hold water, W_{max}.

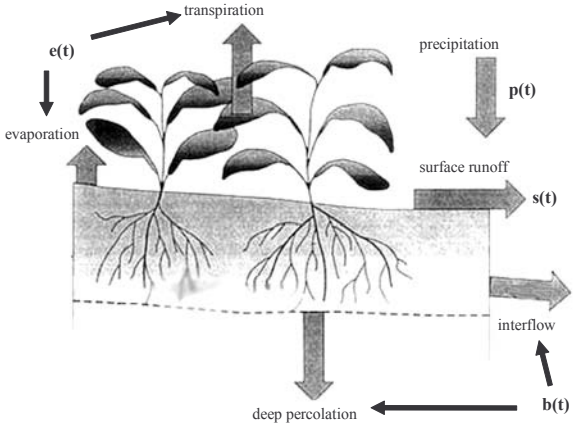

Fig 1: Components of the conceptual model.

Specifically, the equations describing the components of the model are:

$$s(t) = p(t) \cdot \left(\frac{W(t)}{W_{max}} \right)^m \tag{7}$$

$$e(t) = ETp(t) \cdot \frac{W(t)}{W_{max}} \tag{8}$$

$$b(t) = K_s \cdot \left(\frac{W(t)}{W_{max}} \right)^n \tag{9}$$

where m is a parameter for non linearity in the infiltration process, K_s is the saturated hydraulic conductivity, n is a parameter linked to the structure of the soil and ETp(t) is the potential evapotranspiration. The model represents the evapotranspiration, in a simple way, which is the key variable controlling the soil moisture temporal pattern in the periods without rainfall. It is computed through the empirical relation of Thornthwaite (Xu and Singh, 2001) for the potential evapotranspiration and involves only air temperature. Such a simple approach is considered here because the physical methods (Penman-Monteith, energy balance) requiring meteorological variables that are difficult to measure can be applied only for small basins. The model requires the calibration of five parameters which are physically based and linked to the characteristics of soil and surface runoff.

STUDY AREA AND RESULTS

The reliability of the methods proposed here was tested through an experimental data set collected in the period July 2002 - May 2004 in a plot of the Colorso catchment (central Italy) where eighteen sensors (Sentek Sensor Technologies, 1997) were installed. They provide continuous monitoring of the water content at three different depths: 10, 20 and 40 cm. Measurement cycles for all probes were carried out at 0.5 hourly intervals. No data were collected from July to September 2003 because of failure of an instrument. The plot is also equipped with a raingauge station, while two meteorological stations close to the study area provide air temperature data. Fig. 2 shows the trend of the precipitation and the "observed" soil moisture of the upper soil layer which was assumed as the mean of the measurements at a 10 cm depth. As can be seen, soil water content shows a rapid rise during heavy precipitations and differing decreases during the rainfall hiatus depending on the period of the year. We divided the observation period in two parts, the first (July 2002-June 2003) for the calibration and the second (September 2003-May 2004) for the verification of the investigated methods.

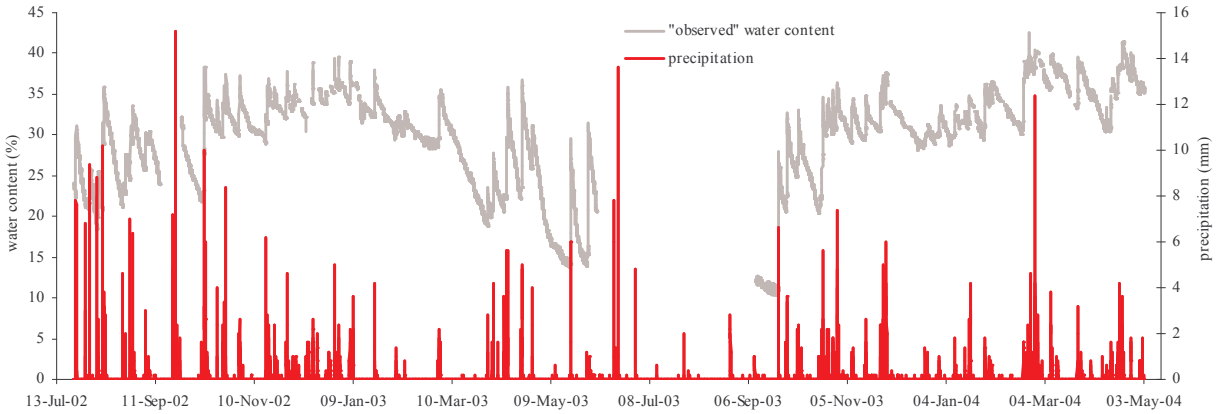

Fig 2: Half-hourly upper soil layer water content trend "observed" in the experimental plot. Precipitation is also shown.

In order to test the influence of the parameter K in the API relations (Eqs.2-4), an analysis was carried out for two different periods of the calibration phase, the first one (March 2003 - June 2003) characterized by an

almost uniform soil moisture drop during the interstorm time. For this period, Fig. 3a illustrates the time evolution of the half-hourly "observed" water content and the wetness conditions given by the API relations. The API values are expressed as dimensionless quantities in order to have an easier visual comparison with the "observed" data. From the figure it can be seen that the API relation (2) did not provide reliable results especially during the falling limbs, while the other two relations showed a comparable accuracy.
As can be seen in Table 1, the best results in terms of coefficient of determination, R^2, were achieved for the API relation (4) with K=0.91, which belongs to the range reported in the literature (0.80-0.98), while the optimal number of antecedent days in relation (2) was ten which is two times the value proposed in the SCS-CN method.

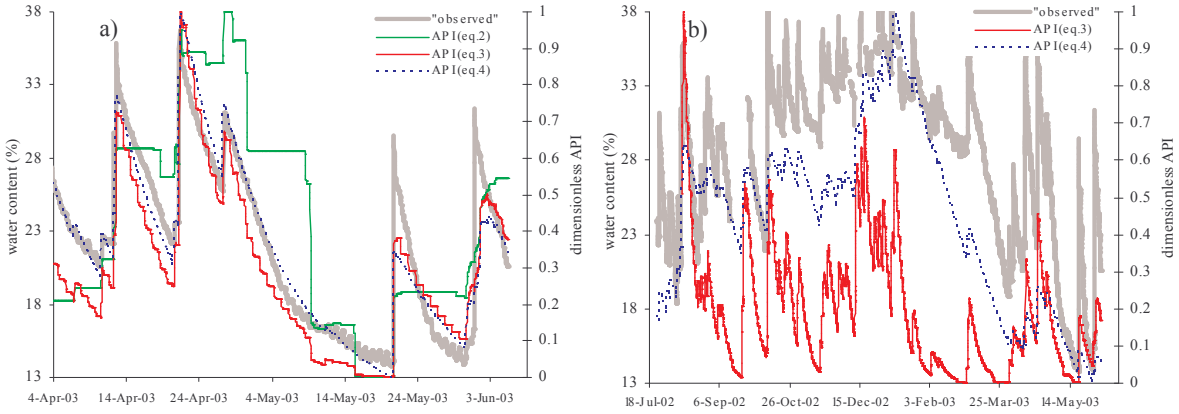

Fig 3: Half-hourly "observed" soil water content and simulated soil wetness conditions by the API relations: a) spring period and b) whole calibration period.

Table 1: Coefficient of determination, R^2, for different parameter sets of the API approaches. For symbols see text

Period		16/03/03-05/06/03			23/07/02-05/06/03		
Parameters		K	N	R^2	K	N	R^2
$API_t^N = \sum_{j=0}^{48N-1} P_{t-j}$	Eq. (2)	0	5	0.59	0	5	0.18
		0	10	**0.69**	0	10	**0.19**
		0	18	0.56	0	18	0.18
$API_t^{N,K} = \sum_{i=1}^{N}\left(\sum_{j=48(i-1)}^{48i-1} P_{t-j}e^{-Ki}\right)$	Eq. (3)	0.18	5	0.63	0.17	5	0.18
		0.13	10	0.82	0.19	10	0.22
		0.14	18	**0.86**	0.15	18	**0.24**
Parameters		K^{48}	API_0	R^2	K^{48}	API_0	R^2
$API_t = K \cdot API_{t-1} + P_t$	Eq. (4)	0.80	20	0.79	0.80	0	0.21
		0.98	20	0.02	0.98	0	0.56
		0.91	20	**0.90**	0.992	245	**0.67**

However, for the whole calibration period, characterized by a more variable soil moisture pattern, all the API relations gave very poor results as shown in Table 1 and Fig. 3b. Also in this case the highest value of R^2 was obtained for relation (4) (R^2=0.67), but for meaningless parameters.
On the basis of the above results, the API relation (4) with K monthly varying was adopted as well as the conceptual model (Eq. 5) to represent the soil moisture pattern from season to season. The estimated values of K were found to be related to the inverse of the evapotranspiration pattern during the year, with high values in winter and low values in summer. For the calibration period the model and the API relation provided reasonable results (Fig. 4a), with R^2=0.82 for both approaches. At the validation stage (Fig. 4b), the conceptual model kept the same degree of reliability (R^2=0.89), while the empirical approach gave poor results (R^2=0.56).

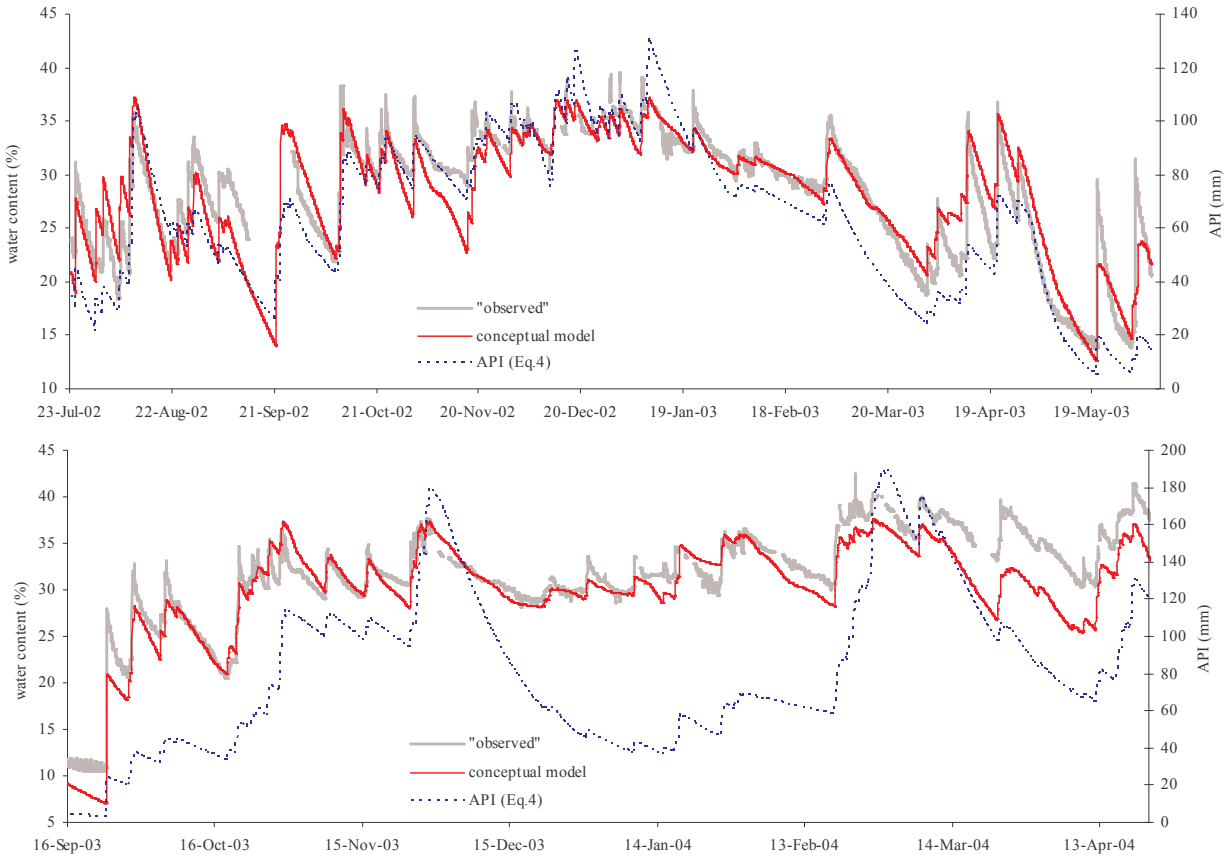

Fig 4: Comparison of soil wetness conditions derived from the conceptual model and the Antecedent Precipitation Index incorporating a monthly varying parameter for the a) calibration, and b) validation stage.

Moreover, it should be noted that the API relation requires a very long calibration period, at least one year, whereas, as its parameters are physically based and vary in a limited range, the conceptual model calibration could be done by using some spot measurements of the near surface soil moisture carried out, for example, by portable Time Domain Reflectometry equipment. The above results mean that the representation of evapotranspiration, even if in a simple way, cannot be disregarded when evaluating the soil moisture state of a basin.

In order to assess the reliability of the last two methods as a component of an event-based rainfall-runoff model, an analysis of their accuracy in estimating the soil wetness conditions before a rainfall event was performed. Specifically, all the rainfall events in the verification period with a cumulated value greater than 5 mm were selected since these events can cause floods in the Colorso stream. Also for this analysis, Figure 5 confirms that the conceptual model is more reliable than the empirical approaches based only on the rainfall data.

Finally, at basin scale, the relationship between the soil wetness conditions before a flood event and the corresponding runoff coefficients, that is the ratio between the volume of direct runoff and the precipitation volume, was investigated. In particular, the antecedent wetness conditions are taken as the "observed" soil moisture for the plot and the API relation (2) with N=5. As the direct runoff volume depends not only on the antecedent soil wetness conditions, SWC, but also on the rainfall pattern, the investigated relation was:

$$C_q = \alpha \cdot P_s + \beta \cdot SWC + \gamma \cdot p_s \qquad (10)$$

where C_q is the runoff coefficient; P_s and p_s are respectively the basin averaged storm rainfall depth and mean intensity, and α, β and γ the coefficients of the linear regression. As can be seen from Figure 6a, the near-surface soil moisture of the plot could be considered representative for assessing the antecedent SWC of the whole catchment. In contrast, when SWC was given by the classical approach of the Soil Conservation Service based on the total 5-day antecedent rainfall, the linear relationship for the runoff coefficient was not found to be very accurate (see Fig. 6b).

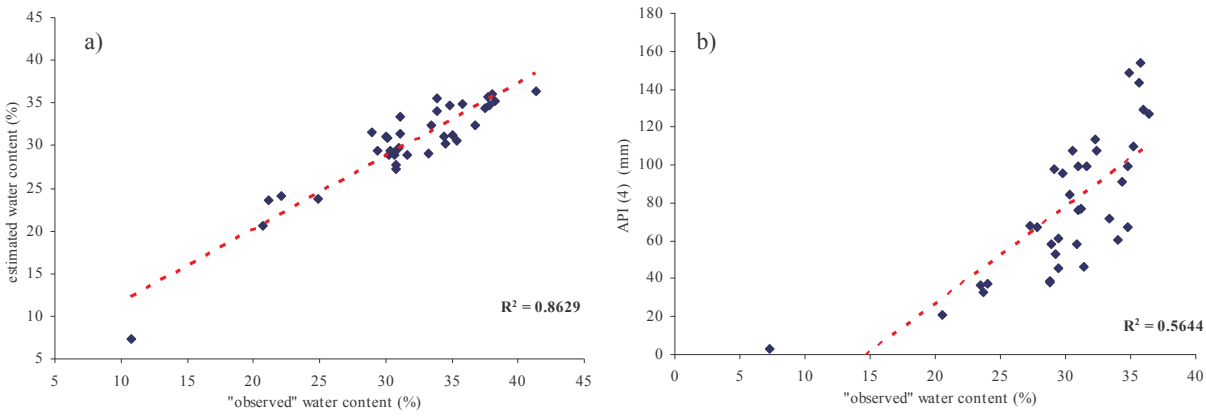

Fig 5: "Observed" versus estimated soil wetness conditions before a rainfall event. Estimation was performed with: a) conceptual model, and b) API relation (4) with the parameter monthly varying.

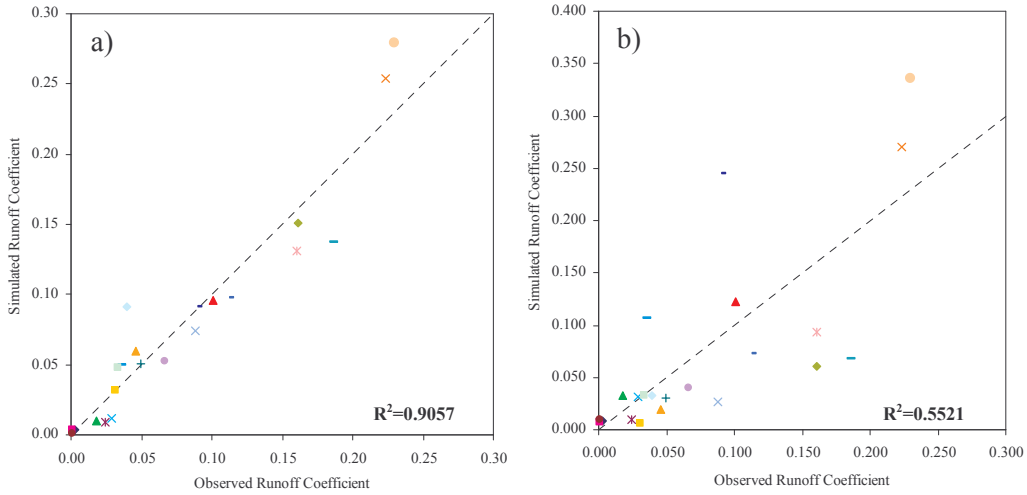

Fig 6: Runoff coefficient for flood events that occurred in the Colorso stream estimated by Eq.10 using for soil wetness conditions a) pre-event soil moisture "observed" in an inlet experimental plot and b) the Antecedent Precipitation Index based on 5-day precipitation depth.

CONCLUSION

For soil moisture state estimation, the empirical relations based only on precipitation can be applied to periods characterized by a uniform drop in soil moisture during the interstorm time interval. To estimate the soil moisture from season to season evapotranspiration should be taken into account using a model which considers the temporal evolution of this variable. The simple conceptual model of water content balance implemented in this study has shown a high degree of reliability in simulating the soil moisture evolution pattern for the whole validation period, when the floods generally occur in the study area. As a good correlation between the soil moisture measurements carried out at the plot and the runoff coefficient of the whole basin was found, the conceptual model of water content balance can be considered as a practical tool for event-based rainfall-runoff modeling.

REFERENCES

Aronica, G., Candela, A. (2004). A regional methodology for deriving Flood Frequency Curves (FFC) in catchments with uncertain knowledge of soil moisture conditions. iEMSs 2004 International Conference, 14-17 June 2004 University of Osnabrück, Germany.

Chow, V.T., Maidment, D.R. and Mays, L.W. (1988). Applied Hydrology. McGraw-Hill, New York.
Corradini,C., Melone, F., Morbidelli, R., Neri, N. and Saltalippi, C. (2000). Semi-distributed rainfall-runoff models and representation of losses. In: M.H. Hamza (Ed.) Modelling and Simulation, IASTED Acta Press, Anaheim (CA), 345-349.
Entekhabi, D., Rodriguez-lturbe, I., Castelli, F. (1996). Mutual interaction of soil moisture state and atmospheric process. Journal of Hydrology, 3-17 (184).
Famiglietti, J.S., Wood, E.F. (1994). Multiscale modeling of spatially variable water and energy balance processes. Water Resources Research, 3061-3078 (11).
Georgakakos, K.P. and Baumer, O.W. (1996). Measurement and utilization of on-site soil moisture data. Journal of Hydrology, 131-152 (184).
Gray, D.M. ed. (1970). Handbook on the principles of hydrology**.** Water Information Center, INC., Port Washington (NY).
Kitanidis, P.K., Bras, R.L. (1980). Real time forecasting with a conceptual hydrologic model, 2. Applications and results. Water Resources Research, 1034-1044 (31).
Ponce, V.M., Hawkins, R.H. (1996). Runoff curve number: Has it reached maturity?. Journal of Hydrologic Engineering, 11-19 (1).
Pan, F., Peters Lidard, C.D., Sale, M.J. (2003). An analytical method for predicting surface soil moisture from rainfall observations. Water Resources Research, 1314-1328 (39).
Sentek Sensor Technologies (1997). Enviroscan: Hardware Manual, version 3.0. Sentek Pty Ltd, Australia.
Xu, C.Y. and Singh, V.P. (2001). Evaluation and generalization of temperature-based methods for calculating evaporation. Hydrological Processes, 305-319 (15).

ASSESSMENT OF BASEFLOW CONTRIBUTION IN A MEDITERRANEAN CATCHMENT USING HYDROMETRIC, GEOCHEMICAL AND MODELLING APPROACHES

J. Latron[1], P. Llorens[2], A.Butturini[2] and F. Gallart[2]

[1]*CSIC, Instituto Pirenaico de Ecología, Avda. Montañana, 1005, 50059 Zaragoza, Spain*
[2]*CSIC, Institut de Ciències de la Terra "Jaume Almera", Solé i Sabarís s/n, 08028 Barcelona, Spain.*
E-mail Jerome Latron: jlatron@ipe.csic.es

ABSTRACT

This work presents the results obtained through three different approaches, used to characterize baseflow contribution in the Can Vila catchment (0.56 km^2) located in the Catalan Pre-Pyrenees. The first approach is purely hydrometric, and makes use of the observed relationship between water table depth and discharge during recession periods. The second approach relies on geochemistry and uses DOC as a conservative tracer. Finally, the third approach derives from an application of TOPMODEL (conditioned on the master recession curve and on the relationships between recession discharge, water table depth and the extension of saturated areas). All of these three approaches establish a 2 components separation of the hydrograph, between "storm runoff" and "baseflow". The study period is a sequence of 4 successive floods in late 2003 (illustrating the typical autumn transition from dry to wet conditions) that allow characterizing changes in runoff generation dynamics. Results show a relatively good coherence between the different approaches, concerning the relative contribution of subsurface flow during floods. However, each of the methods suggests somewhat different within-flood dynamics of the subsurface contribution and illustrates the necessity to complete this analysis with internal information of the catchment in order to draw a more detailed picture of its hydrological functioning.

Key words: hydrograph separation, baseflow contribution, Mediterranean catchment, water table, DOC, Topmodel.

INTRODUCTION

The assessment of runoff generation dynamics is a relevant issue in hydrology both from the quantitative and qualitative points of view. The great variety of processes makes it difficult, however, to evaluate hydrological behaviour, especially where a marked seasonality, as in Mediterranean regions increases the non-linearity of the hydrological response within a catchment. To deal with this heterogeneity of the hydrological response, a combination of different approaches is often recommended (Bonell and Fritsch, 1997; Grésillon et al., 1997) as a way to reduce possible misconceptions in the elaboration of a perceptual model of the hydrological behaviour of the catchment.

This work presents the results obtained on the hydrological dynamics of the small Mediterranean Can Vila catchment during a wetting-up period with three different approaches (based on hydrometric measurements, geochemical analysis and model application). The different approaches were used to perform a two components hydrograph separation for a sequence of four successive floods in late 2003.

Hydrograph separation is a long-established technique in hydrology, often linked with the unit hydrograph theory (see for example Sherman, 1932). The aim of the method is the separation of the storm hydrographs into two components representing "storm runoff" and "baseflow". However, as sometimes (but not so often!) stressed (for example Hewlett and Hibbert, 1967; Beven, 1991), hydrograph separation procedures are largely arbitrary and imply subjective assumptions about the sources of waters and/or about the runoff processes. Despite this, hydrograph separation based on different approaches may provide some complementary information on the hydrological dynamics of one catchment, especially if a previous knowledge of the catchment behaviour is available as in the Can Vila catchment.

STUDY AREA

The Can Vila catchment (ERBES 30) is located in the headwaters of the Llobregat river in the Catalan Pre-Pyrenees, north-eastern Spain (Fig 1). The catchment has an area of 0.56 km^2, with elevations ranging from 1115 to 1458 m a.s.l. The climate is sub-Mediterranean with a mean annual rainfall of 924 mm and a mean annual reference evapotranspiration around 700 mm (Gallart et al., 2002). The catchment is mainly covered by pasture, however, as a result of spontaneous afforestation of agricultural land, forest covers 34% of the catchment. Outside the terraced areas, non-forested areas are covered by scrub.

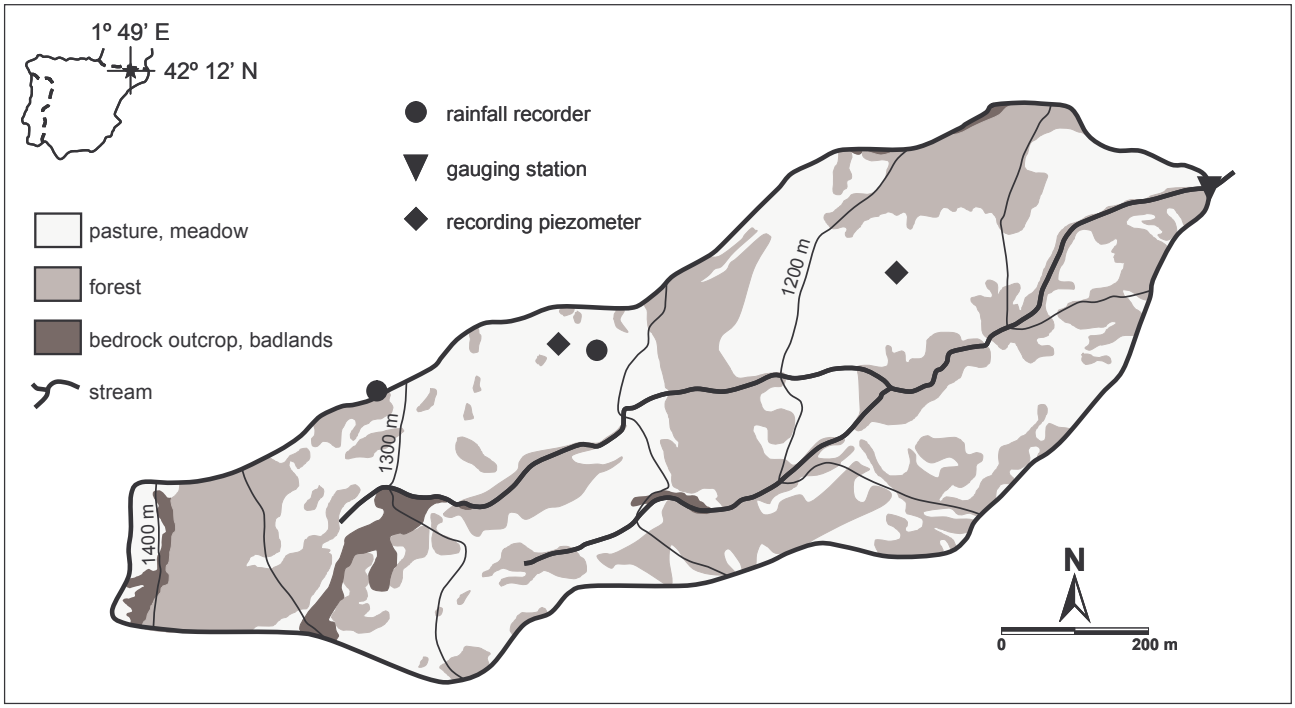

Fig 1: Map of the Can Vila research catchment, showing location of the instruments.

The results obtained to date (Latron and Gallart, 2002; Gallart et al., 2002; Latron, 2003) show that the seasonal dynamics of both rainfall and evapotranspiration have a significant influence on the hydrological response of the catchment. During the year, the dominant runoff generation mechanisms change gradually, as a result of both varying catchment antecedent wetness conditions and changing rainfall events characteristics (intensity and duration).

DATA AND METHODS

The period considered in this study is a typical wetting-up phase (Fig 2) that occurs every year in this Mediterranean environment at the end of the summer dry period. During this period there is a progressive wetting up of the catchment due to successive rainfall events. The shift from dry to wetter conditions is illustrated by the progressive rise of the water table. Within this wetting-up period, four single events have been selected to perform a two components hydrograph separation.

The first method used to obtain a two components separation is purely hydrometric and is based on the relationship between water table depth (measured at one single location) and discharge observed during recession periods. During the days with no rainfall, an exponential regression can be defined between both. For the Can Vila catchment:

$$Q = 0.134\, e^{-0.014\, z} \qquad n=3341,\ r^2=0.91,\ p<0.01$$

Where Q is the runoff (mm.20min^{-1}), and z is the depth to the water table (cm).

Using this relationship, baseflow contribution can be obtained from the depth to the water table, and the difference between the baseflow estimates and the discharge measured at the outlet is interpreted as storm runoff.
One source of uncertainty associated with this approach is due to the fact that the response of the water table can vary at different locations within the catchment. Another source of uncertainty is the validity of the relationship during high flow periods, when the water table is close to the surface. In order to take into account the scatter of this relationship, and to consider the uncertainty associated with this method of baseflow estimation, two relationships representing the 90% confidence limits have been finally considered.

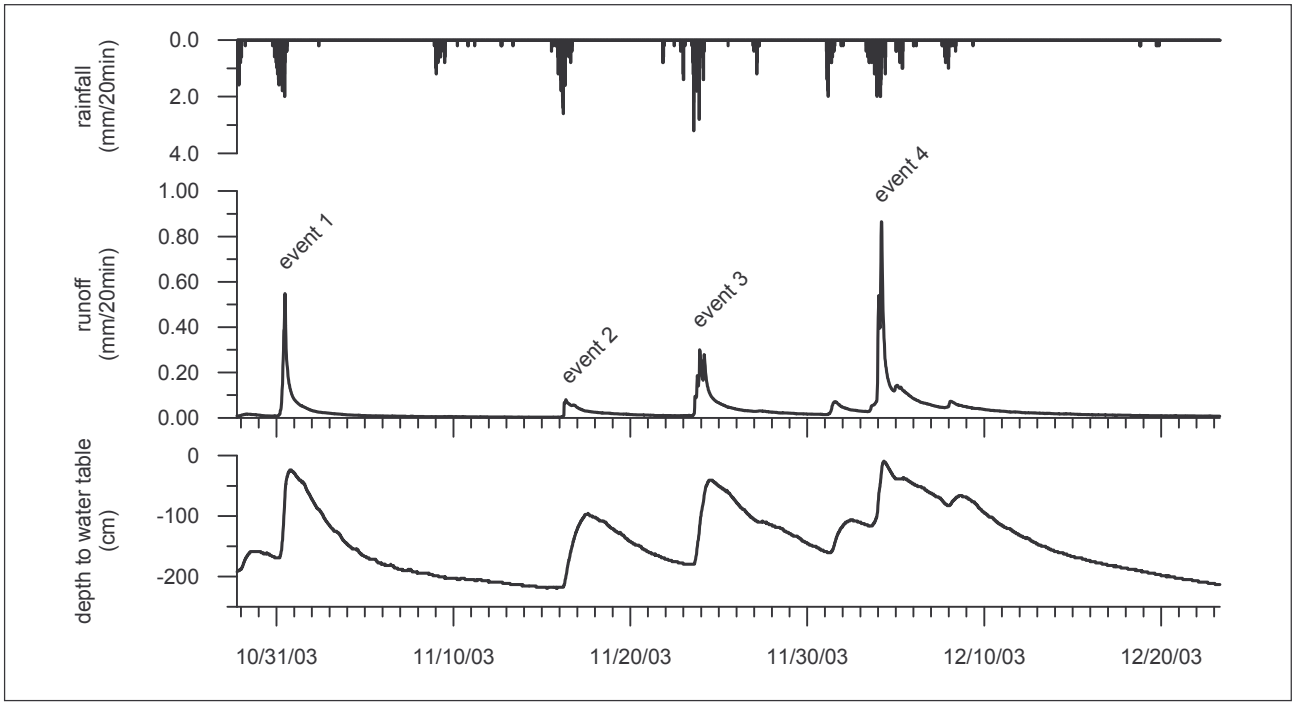

Fig 2: Rainfall, runoff and depth to the water table time series, for the 3 month period considered in this study, showing the 4 events used for a two components hydrograph separation.

The second approach relies on geochemistry and used dissolved organic carbon (DOC) as a conservative tracer. During each of the four events, samples were taken at a variable time step, depending on discharge variations at the outlet (Butturini et al., submitted). After collection, water samples were filtered through fibreglass filters and DOC was analysed using a Skalar 12 SK TOC analyser. A two components chemical hydrograph separation was performed using the classical mixing model of Pinder and Jones (1969). The two end members considered correspond to groundwater with low DOC concentrations (2.4 ± 0.1 mg.l^{-1}) and water from the soils in the terraced area (where saturated areas develop) with high DOC concentrations (5.4 ± 0.3 mg.l^{-1}). For the purpose of hydrograph separation, groundwater was considered as baseflow and soil water as stormflow, although this is largely arbitrary, as the information provided by DOC merely allows separation of groundwater and soil water components.
The main sources of uncertainty with this method come on the one hand from the assumption of the existence of only two components in the total runoff, and on the other hand from the unknown dynamics of the end members during the flood, as only stream water was sampled during the event. In order to consider the uncertainty associated with this method of baseflow estimation, some variation was introduced in the end member concentration to obtain the 90% confidence limits of baseflow contribution.

Finally, the third approach derived from an application of the hydrological model TOPMODEL (Beven and Kirkby, 1979). The model was not calibrated, but used within a Generalized Likelihood Uncertainty Estimation (GLUE) framework (Beven and Freer, 2001). A total of 10000 simulations were performed with reasonable “a priori” parameters ranges.
The main source of uncertainty with this approach is associated with the simulation of the total flow and baseflow, with a model not calibrated for this period, but used in a predictive mode. The determination of the

90% confidence limits was achieved following the method described by Beven and Binley (1992), with simulated baseflow values ranked in order of magnitude, and the likelihood of the parameter sets used as weighting functions to assess the uncertainty associated with model predictions. As described in Gallart et al., (submitted), the likelihood weights in this model application were determined through a composed criteria, based on information on the master recession curve, and on the relationships between recession discharge and the extension of saturated areas.

RESULTS AND DISCUSSION

The results showed some coherence between the different approaches, concerning the relative contribution of baseflow during floods. Contributions estimated from the water table depth were however somewhat lower than with the other two approaches. Contributions derived from the application of TOPMODEL were characterized by a larger uncertainty, due to the difficulty the model has to simulate adequately the total flow during the wetting up transition (without calibration for this period). For the wettest conditions (event 4) the uncertainty on baseflow contribution with the model was however of the same order as with the other approaches (Fig. 3).
In spite of this overall coherence, differences were apparent between the different approaches, both in the amount of baseflow contribution and in the dynamics of this contribution during the flood. Nevertheless, all three approaches reproduced a dynamic contribution of baseflow, with a maximum during the flood peak, even if the peak of baseflow contribution derived from DOC preceded the peaks derived from the other two methods, suggesting a possible contribution from another component like rainwater with low DOC concentration.

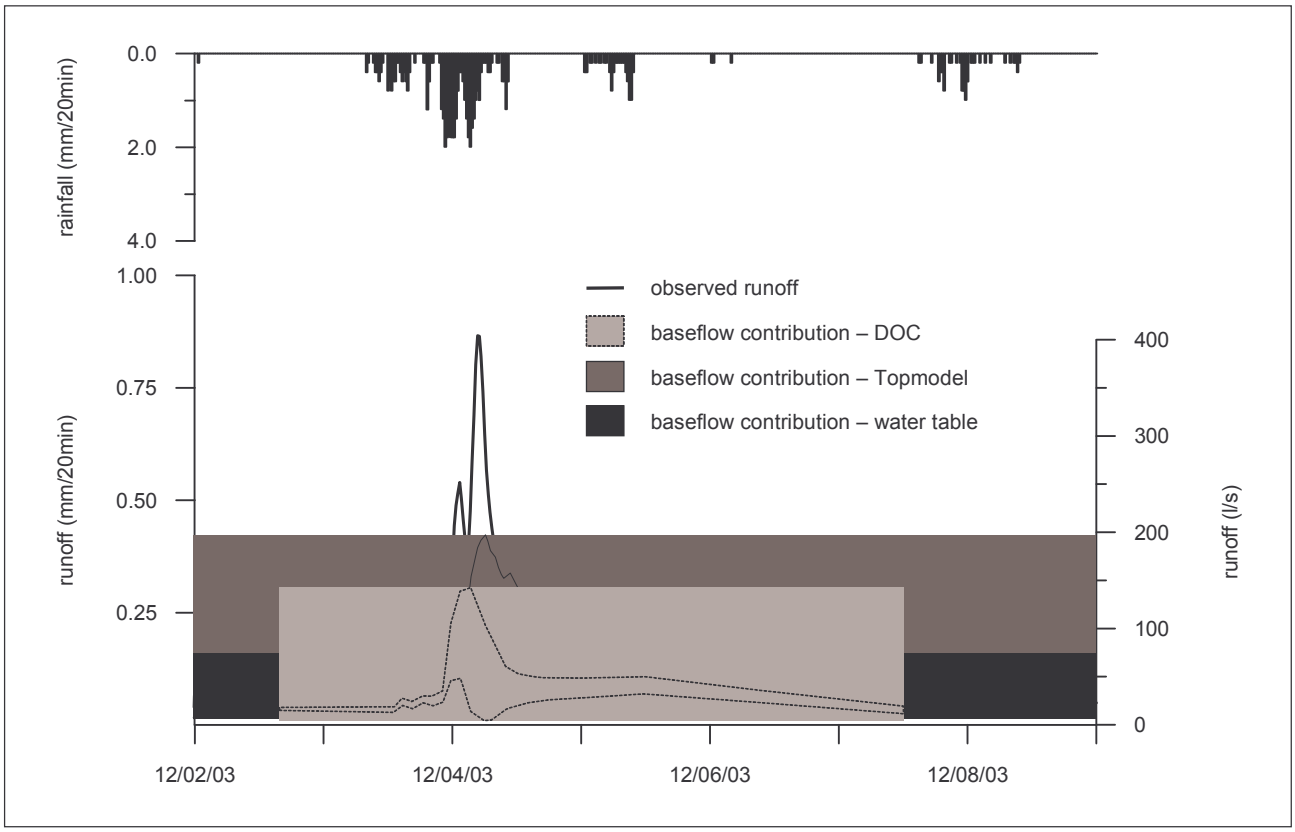

Fig 3: Observed runoff and baseflow contribution 90 % confidence limits, using water table information, DOC and Topmodel for event 4.

The range of baseflow contribution obtained with the different methods for the four events, showed that even if there were some differences between the approaches, the evolution of baseflow contribution along the different floods was similar (Table 1). There was an increase in baseflow component between event 1 and 2, a decrease between event 2 and 3 and a new increase for the last event. So even if the study period

corresponded to a wetting-up transition after a dry summer period (and that therefore antecedent conditions for event 1 were much drier than for event 4) there was no clear increase in baseflow contribution from the first to the last event.

The relationship between the amount of baseflow contribution and the hydrological status of the catchment is not therefore straightforward, but seems closely related with the hydrological behaviour of the catchment and with the dynamics of saturation observed within the terraced area. Using previous knowledge concerning the functioning of the catchment (Latron and Gallart, 2002; Latron, 2003), the following scheme may be suggested:
- During dry conditions (before and during the rainfall events) there were only a few saturated areas in the catchment, and baseflow was the most important contribution to runoff in the "absence" of surface runoff (runoff coefficients were around 20 to 30 %).

Table 1: Rainfall, runoff coefficient and ranges of baseflow contribution (corresponding to 90% confidence limits), using water table information, DOC and Topmodel for the 4 events

	Rainfall (mm)	Runoff coefficient (%)	Baseflow cont. (water table) (%)	Baseflow cont. (DOC) (%)	Baseflow cont. (Topmodel) (%)*
Event 1	45.3	30.0	[42-63]	[58-62]	[78-99]
Event 2	28.8	19.8	[51-75]	[83-85]	[95-98]
Event 3	45.6	39.0	[25-48]	[36-66]	[75-90]
Event 4	64.7	45.9	[40-73]	[45-79]	[81-92]

* percentage of Topmodel simulated flow.

- During the wetting up period, the superficial saturation often observed in the inner part of the terraces increased surface contribution, and decreased relative baseflow contribution, and at the same time the water table showed a very delayed response (runoff coefficients were around 40%).
- Finally during wet conditions, the significant rise of the water table observed in the catchment generated some new saturated areas, but at the same time increased baseflow contribution significantly, resulting in an increase in the relative amount of baseflow contribution.

CONCLUSION

The use of different methods to estimate baseflow contribution and its associated uncertainty during a wetting up sequence in a Mediterranean catchment has provided some coherent results, even if some differences in the amount of baseflow contribution and in the within flood dynamics of baseflow are apparent between the different approaches.
All along the wetting up period the potential increase of baseflow contribution (favoured by an increase in the baseflow itself) seems to be counterbalanced by an increasing contribution of storm runoff related to the progressive development of saturated areas within the catchment.
In spite of the many assumptions behind the two components hydrograph separation, results obtained here provide a complementary way of investigating runoff generation dynamics in a Mediterranean catchment. This information should however not be over interpreted as stressed by Beven (1991), that reminds us that the major problem with the use of hydrograph separation is in the physical interpretation of components.
The results presented here should be considered as preliminary as each of the methods can be easily improved in order to reduce part of the associated uncertainty.
Finally, it would be interesting to perform the same kind of analysis at different times of the year in order to characterize the seasonal dynamics associated with baseflow contribution in the catchment.

ACKNOWLEDGMENTS

This research was carried out with the support the PROHISEM (REN2001-2268-C02-01/HID) and the PIRIHEROS (REN2003-08678/HID) projects funded by the Spanish Government, and the TEMPQSIM (EVK1-CT-2002-00112) project funded by the European Commission. J. Latron and A. Butturini have benefited from a CSIC research contract (I3P programme). Support provided by O. Avila and X. Huguet during fieldwork is acknowledged.

REFERENCES

Beven K. J. (1991). Hydrograph separation. *Proceedings of the 3rd National Hydrology Symposium*, Southampton, U.K., 3.1-3.7.

Beven K., Binley A. (1992). The future of distributed models: Model calibration and uncertainty prediction. In: K. J. Beven and I. D. Moore (Eds), "*Terrain Analysis and Distributed Modelling in Hydrology*", J. Wiley & Sons, 227-246.

Beven K. J., Kirkby M. J. (1979). A physically-based variable contributing area model of basin hydrology. *Hydrological Sciences Bulletin*, 24 (1): 43-69.

Beven K., Freer J. (2001). Equifinality, data assimilation, and uncertainty estimation in mechanistic modelling of complex environmental systems using the GLUE methodology**.** *Journal of Hydrology*, 249 (1-4), 11-29 .

Bonell M., Fritsch J. M. (1997). Combining hydrometric-hydrochemistry methods: a challenge for advancing runoff generation process research. "*Hydrochemistry*", IAHS Publ., nº 244, 165-184.

Butturini A., Gallart F., Latron J., Vasquez E., Sabater F. (submitted). Cross-site comparison of variability of DOC and nitrate c-q hysteresis during fall-winter period in three Mediterranean headwater streams. A synthetic approach. (submitted to *Biogeochemistry*)

Gallart F., Latron J., Llorens P., Beven K. (submitted). Using internal catchment information to reduce the uncertainty of discharge and baseflow predictions. (submitted to *Advances in Water Resources*)

Gallart F., Llorens P., Latron J., Regüés D. (2002). Hydrological processes and their seasonal controls in a small Mediterranean mountain catchment in the Pyrenees. *Hydrology and Earth System Sciences*, 6 (3): 527-537.

Grésillon J. M., Marc V., Schober A., Taha A. (1997). Confrontation des méthodes de la géochimie, de l'hydrodynamique et de l'hydrologie statistique pour l'étude des crues. "*Hydrochemistry*", IAHS Publ., nº 244, 133-140.

Hewlett J. D., Hibbert A. R. (1967). Factors affecting the response of small watersheds to precipitation in humid areas. In: W. E. Sopper and H. W. Lull (Eds), "*Forest Hydrology*", Pergamon, 275-290.

Latron J. (2003). Estudio del funcionamiento hidrológico de una cuenca mediterránea de montaña (Vallcebre, Pirineos Catalanes). Ph.D. Thesis, Universitat de Barcelona, 269p.

Latron J., Gallart F. (2002). Seasonal dynamics of runoff variable contributing areas in a Mediterranean mountain catchment (Vallcebre, Catalan Pyrenees). In: L. Holko, P Miklánek, J. Parajka and Z. Kostka (Eds), "*Interdisciplinary approaches in small catchment hydrology: monitoring and research*", proceedings of the ERB 2002 International Conference, Demänovská dolina, Slovakia, 25-28/09/2002, 173-179.

Pinder G. F., Jones J. F. (1969). Determination of the groundwater component of peak discharge from the chemistry of total runoff. *Water Resources Research*, 5 (2): 438-445.

Sherman L. K. (1932). Streamflow from rainfall by the unit-graph method. *Eng. News Record*, 108: 501-505.

VARIABILITY IN THE PROCESS OF LAKE FEEDING BY GROUNDWATER (CASE STUDY OF SMALL BASIN IN SOUTH POMERANIAN LAKE DISTRICT)

B. Nowicka and M. Lenartowicz

Department of Hydrology, Faculty of Geography and Regional Studies, University of Warsaw, 30 Krakowskie Przedmieście Street, 00-927 Warsaw, Poland
e-mail Barbara Nowicka: benowick@uw.edu.pl
e-mail Maciej Lenartowicz: mlenarto@uw.edu.pl

ABSTRACT

This paper presents the results of research on three selected ribbon lakes in the Bory Tucholskie National Park – PNBT (North Poland). The lakes are all located within a short distance of each other, yet differ significantly in terms of their morphological, hydrochemical and biological features. The main goal was the recognition of hydrogeological conditions and estimates of vertical and horizontal water exchange components. Research was conducted between 2000 and 2003 when water resources restoration after the hydrological drought of the mid 1990s was observed. An indirect approach, namely the water balance method to evaluate underground exchange of water in the lakes, was applied. The analysis of the influence of lake water exchange (vertical and horizontal) on surface and underground storage used the mass curves method. The research results confirm that there are differences in the reaction of selected lakes to variable conditions of atmospheric recharge. Despite their close location, there are differences in course of water exchange processes. Comparison of underground and atmospheric water exchange mass curves shows variable delay in the reaction of underground and atmospheric water exchange.

Key words: ribbon lakes, outwash plain, water balance of lakes, exchange of lake waters, lake water – groundwater relations, mass curve method, protected areas.

INTRODUCTION

Lakes of outwash (sandur) plains are important elements of the last-glaciation landscapes in Europe. The lakes are characterised by morphological, hydrological, hydrogeochemical and biological heterogeneity, each at a different stage of evolution. Preservation of their natural values and protection of water resources require a detailed recognition of conditions prevailing throughout the circulation and interaction of surface water and groundwater.
It appears particularly difficult to assess relations between groundwater and lakes. Investigated closely by many (e.g. Winter, 1978; Anderson and Munter, 1981; Cheng and Anderson, 1993), the issue remains open. In most cases, deep lake bowls cut across several aquifers. On the other hand, bottom sediments isolating lake bowls limit the exchange of water. Time and again, their complex lithological structure impedes a proper evaluation of the water exchange processes. This particularly applies to the marginal zone of the last glaciation.

The objective of this study is the recognition of water exchange conditions in ribbon lakes of sandur areas in the South Pomeranian Lake District. The lakes of the Bory Tucholskie National Park (PNBT) were chosen as a study area as a dataset of hydrometeorological monitoring is available (Fig. 1). Research focussing on the recognition of hydrogeological conditions and estimates of vertical and horizontal exchange components in selected lakes attempts to shed some light on the directions of relations between groundwater and lakes (drainage – accretion) that underlie the evaluation of impact of the underground and surface water exchange on changes in lake and groundwater storage.
This paper presents the results of research on three lakes located within a small distance of each other (Fig. 1), yet differing significantly in terms of their morphological, hydrochemical and biological features. The substantial differences between the lakes give grounds for the belief that they are the result of different groundwater exchange conditions. The research was conducted over the 2000 to 2003 period of water resource restoration after the hydrological drought of the mid 1990s.

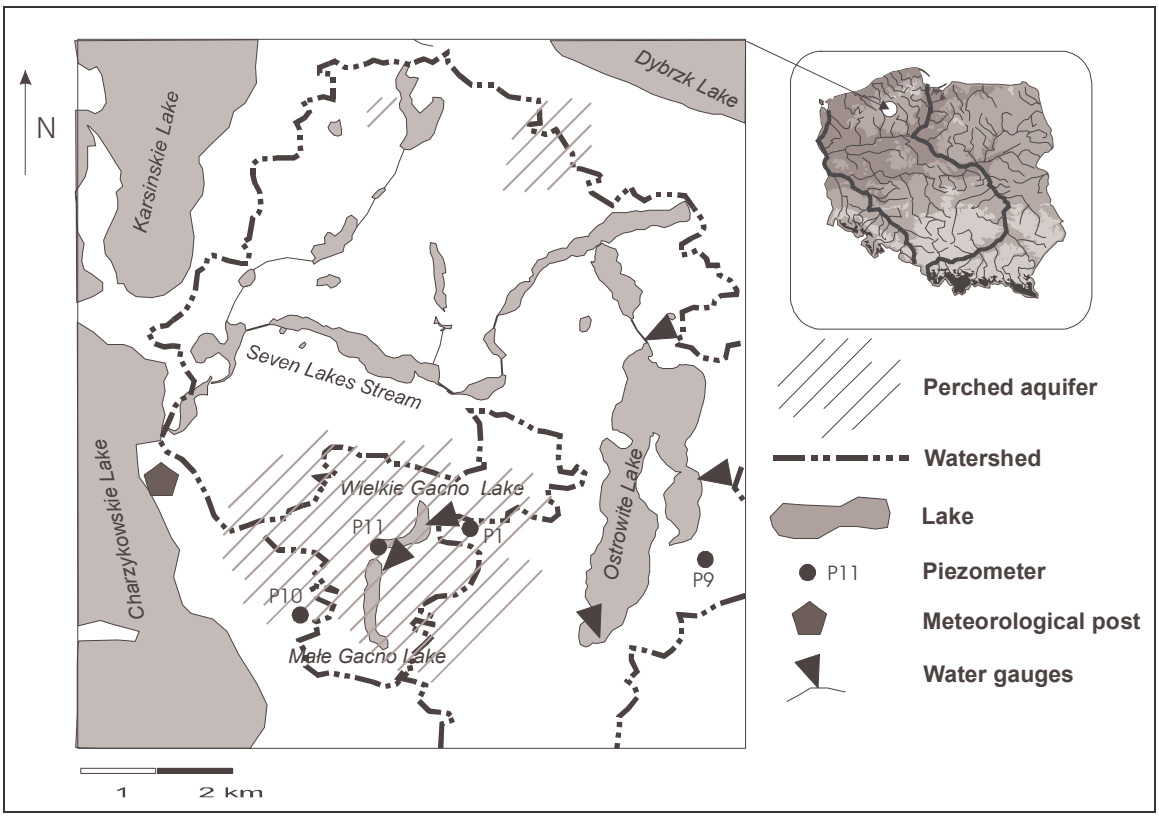

Fig. 1.: Location of investigated lakes.

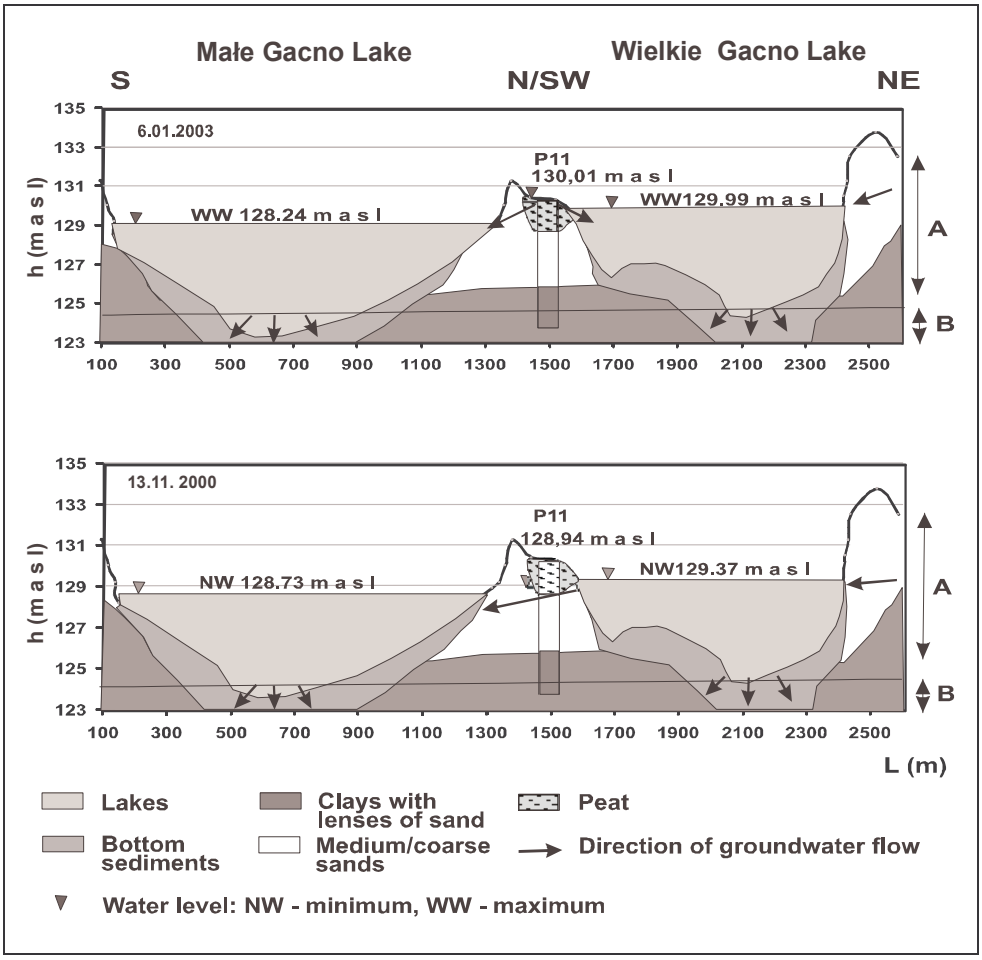

Fig. 2: Groundwater and surface water levels in subglacial channel of lakes: Wielkie Gacno and Małe Gacno (A- perched aquifer zone, B – main continuous aquifer zone).

PROFILE OF THE RIBBON LAKES STUDIED

The lakes are all located within a short distance of each other (Fig. 1). Two of them, Małe Gacno and Wielkie Gacno, are landlocked lakes. They are oligothropic, acid (pH5.0), humus lakes hosting precious species of Atlantic period relict plants (e.g. *Lobelia dortmnanna*). The lakes fill small shallow lake bowls (15.4 ha and 14.2 ha with a maximum depth of 5.6 m and 6.2 m respectively). The bowls are padded with bottom deposits approximately 6.0 m thick. In their geological past the two lakes were connected. Forming a cascade structure, the lakes are separated by a small hill, approximately 350 m in length (Fig. 2). Differences in water stages between them reach 75 cm at times. Małe Gacno and Wielkie Gacno lakes are in hydraulic contact.

The third lake, Ostrowite is located in a parallel subglacial channel approximately 2.5 km east of the two lakes described above. The water in this mesothropic lake is of a neutral reaction (pH7.0) and dominated by four ions: SO_4^{-2}, HCO_3^{-}, Mg^{+2}, and Ca^{+2} (Wicik, 2002). Numerous species of *Hara* algae occur in the lake. Its water level is nearly 4.0 m lower than the Wielkie and Małe Gacno lakes. The lake is nearly 20 times larger and its maximum depth exceeds 43.0 m. The lake bowl is padded with a thick layer of bottom sediments. Being an outflow lake, it is the first part of the drainage network of the Seven Lakes Stream.

METHODS OF ANALYSIS

The hydrogeological profile of the lakes has been derived from over 50 borings (up to 5.0 m deep), archive data and piezometric measurements. Sadly though, even a large number of boring tests and intense geological sounding cannot answer many questions related to the hydrogeological structure of the studied area. Therefore, an indirect procedure was used, namely the water balance method to evaluate the underground exchange of water in the lakes (Mikulski, 1970; Bajkiewicz-Grabowska, 2002). Three components of water exchange in the lakes were analysed, namely the vertical (atmospheric), horizontal (surface) and underground component. These components are the results of the input and output elements of the water balance (Bajkiewicz-Grabowska, 2002). The underground exchange ($Z_{pdz\ \Delta t}$) was calculated with a one month time interval (Δt = 1 month), applying the water balance equation:

a) Landlocked lakes (Wielkie Gacno and Małe Gacno)

$$(P_{\Delta t} - E_{\Delta t}) + (R_t - R_{t+1}) + Z_{pdz\ \Delta t} = 0 \quad (1)$$

b) Lakes with outflow (Ostrowite Lake)

$$(P_{\Delta t} - E_{\Delta t}) + (R_t - R_{t+1}) - H_{\Delta t} + Z_{pdz\ \Delta t} = 0 \quad (2)$$

where:

$$Z_{pdz\ \Delta t} = D_{\Delta t} - A_{\Delta t} \quad (3)$$

where $P_{\Delta t}$ represents the monthly precipitation total on the lake (mm); $E_{\Delta t}$ represents the monthly evaporation total from the lake (mm); $H_{\Delta t}$ represents outflow from the lake over Δt (mm); R_t represents retention at the beginning of Δt (mm) and R_{t+1} retention at the end of Δt (mm); $D_{\Delta t}$ and $A_{\Delta t}$ represent drainage and accretion of the aquifer respectively (mm).
The above data have been estimated based on the results of hydrometeorological monitoring by PNBT[1] service (Fig. 1). Evaporation from free water surface was calculated using empirical Penman formula (Penman, 1948) and evaporation in the ice cover period was estimated following the Konstantinov method (Konstantinov et al., 1971)[2].

The result of underground exchange is positive when the lake is fed by aquifer over the balance period, and negative when the lake water is flowing into the aquifer.

[1] As of 2000, Department of Hydrology (University of Warsaw) has supervised the monitoring network.
[2] Those methods were accepted based on tests run in the nearest lake subjected to evaporometric monitoring.

The analysis of the influence of lake water exchange on surface and underground storage in hydrologic years 2000-2003 uses the mass curves method (Fig. 3), with the retention at 1st November 1999 as the initial condition. It has been further assumed that the **mass curve of atmospheric exchange** (vertical component) explains potential changes of water stages in a landlocked lake, isolated from an aquifer. When set against the curves showing real fluctuations of water stages in the lakes, this curve shows an impact of atmospheric factors on lake storage and conditions of groundwater exchange. The **mass curve of underground exchange** in turn enables an estimate of the lake's role in the accretion or drainage of aquifers. In the lakes with an unstable function, it depicts the predominant direction of the long-term water exchange. Mutual relations of the curves were assessed by comparing them to those describing changes in groundwater storage. Changes in groundwater storage were calculated using the Bindemann method (Zamanov, 1970) based on piezometric measurements (piezometers P1 and P9: unconfined main continuous aquifer and piezometers P10 and P11: the perched aquifer).

HYDROGEOLOGICAL CONDITIONS

The lithological structure of the studied area is extremely complex. During glaciation and deglaciation the series of sediments deposited in the region were deformed, dislocated and eroded. Hence the problem of correctly recognising the individual aquifers arises. One can reasonably infer that two aquifers are active in the process of water exchange with the lakes under examination, namely the continuous aquifer and non-continuous, perched aquifer.

The main continuous aquifer in the medium and coarse sands with gravel and cobbles is about 20 m thick and founded on a series of clays. Ordinates of the groundwater table range between 120.5 m a.s.l. near Charzykowskie lake and 126.0 m a.s.l. east of Ostrowite lake. The aquifer is drained by Charzykowskie lake, a part of the Brda river system. The groundwater divide between the two lakes is not particularly distinct. The slope of the groundwater table varies from 0.1 % to 0.2 % and only locally reaches 1 %, that is below the edges of the subglacial channels. The water table of the main aquifer is mostly unconfined, except for the basin of lakes Wielkie Gacno and Małe Gacno, featuring a non-continuous but extensive packet of clays with the interbedding of fine sands. In places it is found at 0.5 m below terrain level. It is hard to specify the degree of isolation of the lakes caused by the clay sediments, or find clear evidence of hydraulic contact between the lakes and the main aquifer. On the other hand, the ordinates of the lakes bottoms are lower than its local piezometric surface. Lens of impermeable clays has an important role in keeping the local perched aquifer. Elevation of its water table ranges between 128.9 (near Małe Gacno) and 134.0 m a.s.l. (west of Wielkie Gacno). This aquifer stays in hydraulic contact with the two landlocked lakes of. Wielkie Gacno and Małe Gacno.

Analysis of changes in the water stages of both lakes and the groundwater stages observed on the inter-lake piezometer (P11) show that directions of groundwater flow vary over time. Lower lake Małe Gacno is only periodically recharged by Wielkie Gacno (Fig. 2). At the highest water stages (over 129.5 m a.s.l.), stoppage of groundwater flow between lakes was observed several times. The phenomenon may be the consequence of the lower hydraulic conductivity of peat in the upper soil layers (Fig. 2).

EXCHANGE OF WATER IN THE LAKES

Research was conducted after damage to the lakes' ecosystems as a consequence of the hydrological drought of the 1990s. Analysis was related to the wet periods between 2000 and 2003. The shapes of mass curves of vertical water exchange P-E (Fig. 3) confirm that this period was favourable for lake water resource restoration. The curves mentioned above show that four shorter wet periods between 2000 and 2003 can be distinguished. They differ in terms of time of duration and rate of potential water resource increase. The longest one lasted from June 2000 to April 2002. The increase in lake water levels as a result of atmospheric exchange (P-E) could then potentially reach 605 mm.

The reaction of individual lakes to the atmospheric exchange of water differed. There was a quick reaction in the landlocked lakes of Małe Gacno and Wielkie Gacno (Fig. 3A), and changes recorded in the water levels of both lakes followed the curve of cumulated atmospheric exchange of water (P-E). There were two distinct

stages of mutual relationships between the two lakes over the period of water resource increase. The first was observed as Małe Gacno was recharged by Wielkie Gacno. The second stage was related to stoppage of groundwater flow towards the lower lake (Małe Gacno). Also, in Wielkie Gacno, the amplitude of water levels (720 mm) was greater than in the lower Małe Gacno (540 mm). Regression relationships between cumulated values of atmospheric water exchange (P-E), representing potential changes in water storage and real changes in water storage of both lakes at different stages have been depicted in Fig. 4. Those relationships appear to be closely interlinked (R^2> 0.97 at confidence level 0.05). Water storage of larger, outflow lake - Ostrowite is considerably more stable; the amplitude of water levels was 270 mm. (Fig. 3B).

Between 2000 and 2003, the periods of groundwater drainage and accretion in the lakes followed one another (Fig. 3). However, in the case of the landlocked lakes, groundwater accretion prevailed over groundwater drainage (over 100 mm over the 4 years). It mostly relates to the main aquifer. It is hard to draw an authoritative conclusion, as to what is the role of a perched aquifer in water exchange. Infiltration waters stored on the lens of impermeable clays are most likely drained by both landlocked lakes. This phenomenon is indicated by the shape of mass curves showing underground exchange resulting from the landlocked lakes and changes in groundwater storage of perched aquifer observed on the piezometers (P10, P11) as well as by the ordinates of the groundwater table documented in August 2000.

Lake Ostrowite is mainly a draining lake. Storage losses are caused by river runoff to the Stream of Seven Lakes and water is replenished by aquifer drainage. Over the four years, underground water exchange (lake feeding by groundwater and aquifer accretion) hit 744mm.

Comparison of underground and atmospheric water exchange mass curves shows a delay in the reaction of underground and atmospheric water exchange.

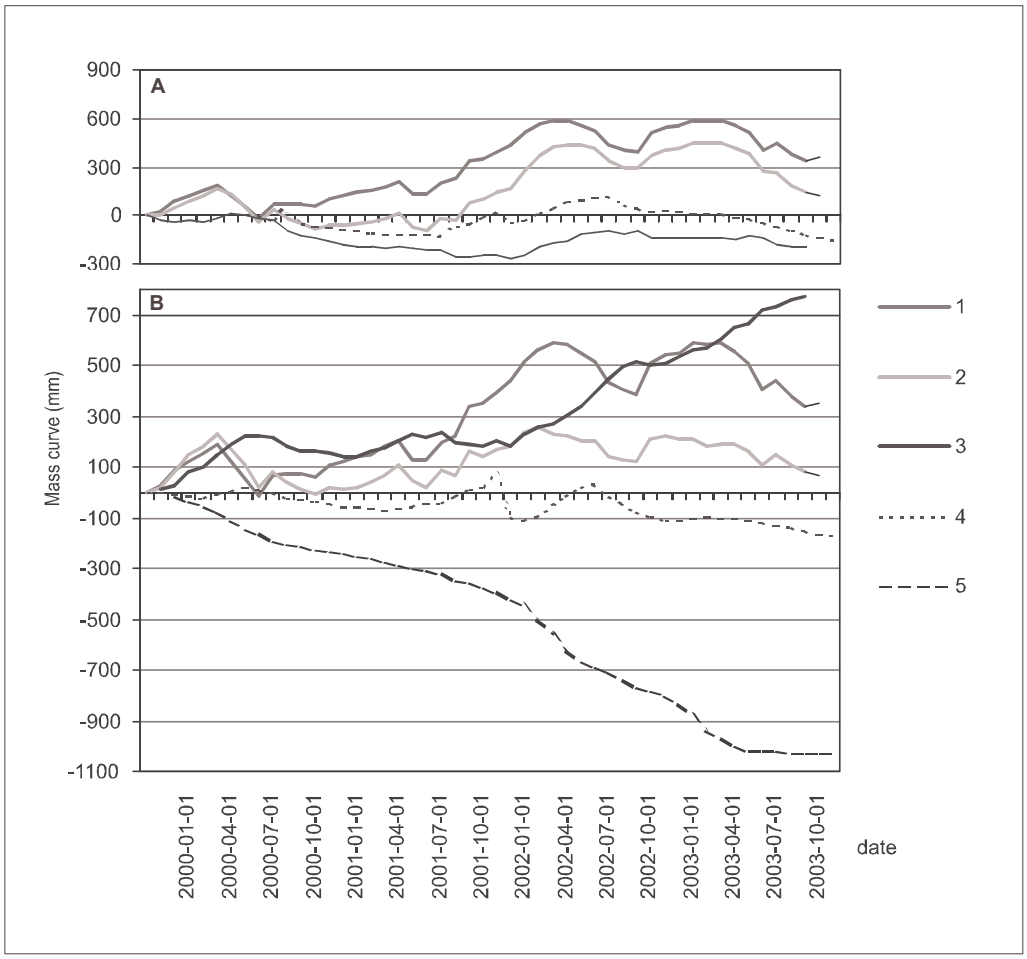

Fig. 3: Comparison of selected water balance elements of the lakes between 2000 and 2003: A – Małe Gacno Lake, piezometer P 10; B – Ostrowite Lake, piezometer P 9. (1 – vertical exchange, 2 – lake water levels fluctuations, 3 – underground exchange, 4 – changes in groundwater storage, 5 – surface outflow from the lakes)

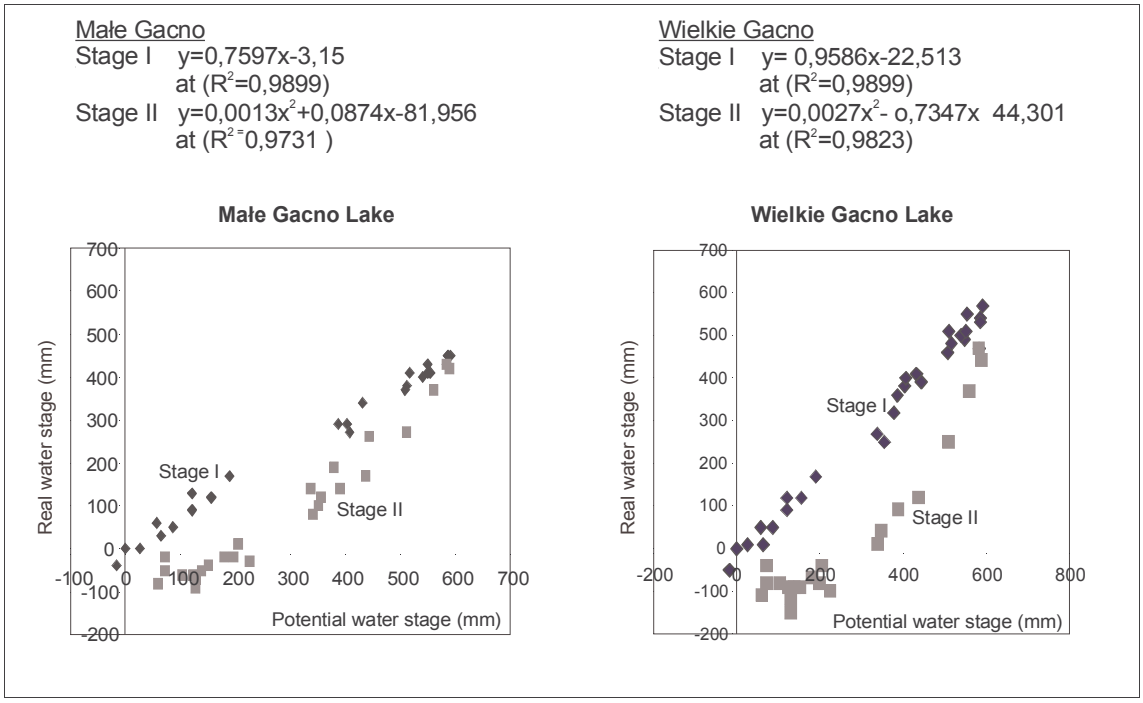

Fig. 4: Regression relationships between potential and real changes in water stages in lakes Wielkie Gacno and Małe Gacno (according to cumulated values).

RECAPITULATION

Research results show that the selected ribbon lakes react differently to variable conditions of atmospheric recharge. Despite their close location and shared origin, there are clear differences in course of water exchange processes. This is not only the case in the lakes which are significantly different in terms of their morphometric features and hydrological pattern (Wielkie Gacno and Ostrowite). One can observe this phenomenon also in the lakes with similar profiles (Wielkie Gacno and Małe Gacno). This is an effect of the cascade structure of the lakes, hence the impact of the higher located lake on the subordinated one. The high variability of geological structure is yet another element disturbing relations between the lakes.

REFERENCES

Anderson, M.P, Munter, J.A. (1981) *Seasonal reversals in ground-water flow around lakes and the relevance to stagnation points and lake budgets.* Water Resour. Res. 17(4), 1139-1150.

Bajkiewicz-Grabowska, E. (2002) *Obieg materii w systemach rzeczno-jeziornych*. Wyd. UW, Warszawa.

Cheng, X., Anderson M.P. (1993) *Numerical simulation of ground-water interaction with lakes allowing for fluctuating lake level*. Ground Water 31(6), 929-933.

Konstantinov, A.R., Astachova, N.I., Levenko, A.A. (1971) *Metody rasczeta isparienija sielskochozjajstwiennych polej*. Gidromietieoizdat, Leningrad.

Mikulski, Z. (1970) *Kształtowanie się bilansu wodnego jezior w Polsce*. Przegląd Geograficzny, vol. 42, no. 3.

Penman, H.L. (1948) *Natural evaporation from open water, bare soil and grass*. Proceedings of the Royal Society, 193, 120 – 145.

Wicik, B. (2002) *Cechy chemiczne wód powierzchniowych*. In: Nowicka, B. (ed.) *Plan Ochrony Parku Narodowego Bory Tucholskie*. NFOŚ, manuscript PNBT/NFOŚ, Warszawa, 251 - 255.

Winter, T.C. (1978), *Numerical simulation of steady state three-dimensional groundwater flow near lakes*. Water Resour. Res. 14(2), 245-254.

Zamanov, Ch.D. (1970) *Rasczot podziemnogo stoka iż oziera Bolszoj Ałagiel mietodom wodnogo bałansa*. Izw. Wsiesoj. Gieogr. Obszcz., vol. 102, no. 1.

HYDROGRAPH FORMATION IN A HILLSLOPE TRANSECT

M. Šanda, T. Vogel and M. Císlerová

Czech Technical University, Thákurova 7, 166 29 Prague 6, Czech Republic
e-mail Martin Šanda: sanmartin@seznam.cz

ABSTRACT

Continuous data monitoring was set up in the Uhlířská experimental watershed, located in the northern part of the Czech Republic in the Jizera Mountain range to identify and evaluate the rainfall transformation mechanism into soil profile runoff where subsurface flow plays a dominant hydrological and climatic role in runoff formation. Soil profile classed as Dystric Cambisol is shallow and highly heterogeneous, formed on weathered granite bedrock. Subsurface outflow in the subsurface trench was monitored in three soil horizons and soil water suction scanned by triplets of tensiometers complete with pressure transducers adjacent the trench. The unsaturated regime within the soil profile prevailed though soil moisture content was close to saturation. Almost simultaneous reaction of suction change in all soil horizons implied rapid vertical flow. Local preferential flow paths conducted water at significantly variable rates.
Several numerical codes based on Richard's equation were tested to simulate outflow from the experimental hillslope area. The assumption that soil is a single-continuum system is often inadequate when seeking a reasonably realistic description of water field scale movement due to existing preferential flow. Dual domain models were developed to simulate mobile water in soils (Vogel et al., 2000), conceptualized to have two pore systems: a matrix and a preferential flow domain. Darcian flow assumption was taken to be valid for each of the two flow domains separately, allowing for local non-equilibrium between then. The tested dual-permeability model provided significantly better agreement of measured and simulated outflow hydrographs from the soil profile on the Uhlířská watershed hillslope than the single domain model (Vogel, 1987).

Key words: subsurface, preferential flow, hydrological monitoring, dual domain models.

OBJECTIVES

The purpose of the hydrological research was to identify the flow mechanism transforming rainfall into runoff in variably saturated soil profiles on the instrumented hillslope (Šanda and Císlerová, 2000), with focus on the subsurface flow process. Two-domain modelling approaches using S_2D_Dual model (Vogel et al., 2000) were used to clarify the outflow mechanism.

INTRODUCTION

Experimental watershed Uhlířská (Fig. 1) is located in the northern part of the Czech Republic at the highest elevation of the Jizera Mountains. The watershed area is 1.87 km^2, 50% of which deforested in the early 1980s. Average altitude is 822 metres above sea level. Average slope is 2.3% and average hillslope length is 450 m. The watershed belongs to a humid region, where annual rainfall exceeds 1300 mm. The soil profile at the hillslope site subject of this study is shallow and highly heterogeneous. It consists of some 80 cm of Dystric Cambisol, formed on the decayed fractured granite bedrock. The about 15 cm deep topsoil is peaty, covered by bush grass vegetation. The profile below the organic layer consists of 10 cm of grey-black clayey loam, 25 cm of brown sandy loam and 30 cm of light brown loam with a high bedrock particle content (Císlerová et al., 1998).

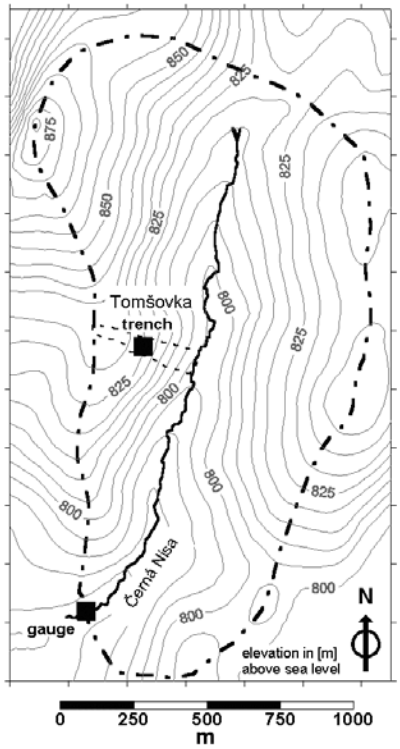

Fig 1: Map of Uhlířská watershed.

Hydrological and climatic process data monitoring focussed on soil profile processes to evaluate the subsurface flow mechanism. One typical hillslope location at Tomšovka was outlined. The location studied is a transect, defined as a vertical plane of the soil profile running perpendicular to surface contour lines.

Several measurements were completed to obtain data on the subsurface flow region inner geometry and its boundaries. The set of 10 shallow boreholes in the main East/West axis of the hillslope was completed for upper soil and rock layer formation stratification. Geophysical spatial measurements with two-pole electromagnetic profiling and vertical electrical survey (Fig. 2) were selected to identify bedrock surface geometry and the flow region geological fracture system. A series of 100 infiltration tests was performed to investigate infiltration rate spatial variability.

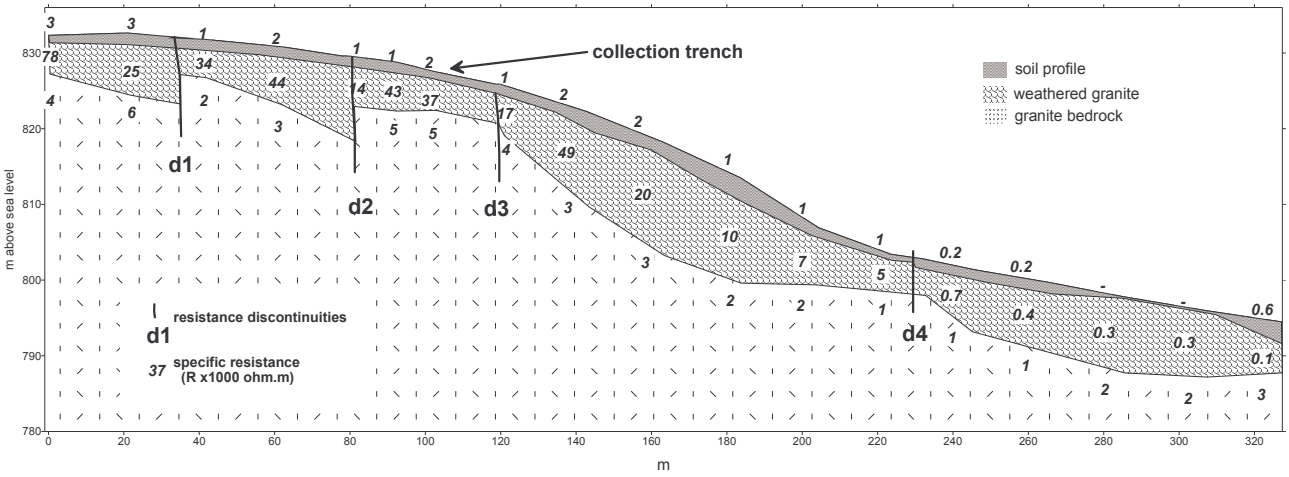

Fig. 2: Geological formation by vertical electrical survey.

The research focusing on subsurface storm flow generation concentrated on some 20 x 20 meters of the experimental plot located above the hillslope steepest part where the shallow soil profile was excavated and the subsurface collection trench built for collecting subsurface through-flow (Fig. 3).

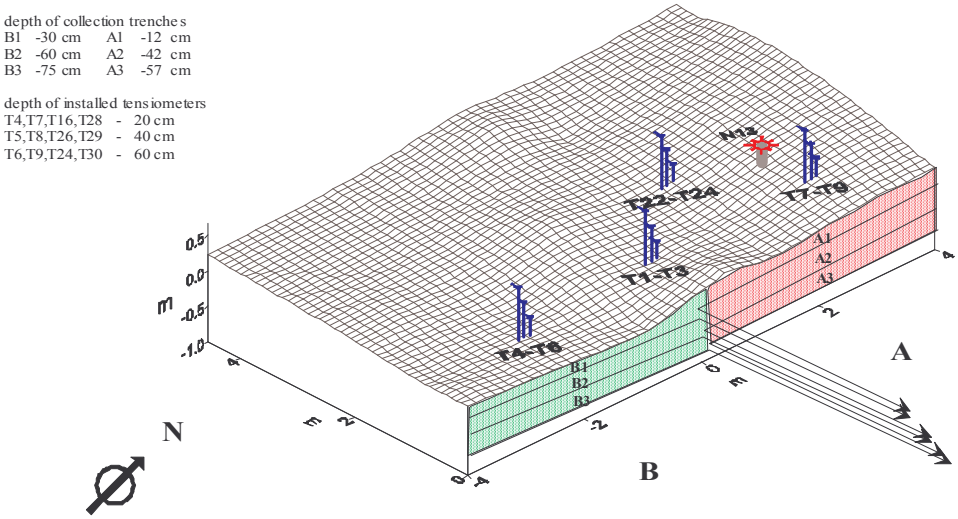

Fig. 3: Subsurface outflow collection trench.

Subsurface outflow in the collection trench was gathered into three two-section (A and B) soil horizons, each fitted with a 4 m long stainless steel collector. Flow was then gravitationally channelled into 6 tipping-bucket flow meters and recorded. Soil water pressure was monitored at several depths with the triplet-nested tensiometers and installed into typical soil layers (some 15, 30 and 60 cm below soil surface) at several locations above the trench. The site was also equipped with a set of soil and air

thermometers, anemometer, net radiometer and rain gauges. Automated data collection devices were used for continuous subsurface runoff and soil water regime monitoring in 10-minute time steps for short inflow/outflow hydrological events as well as year-round soil water regime and climate (Šanda and Císlerová, 2000). Soil water regime monitoring has been running since 1998.

SUBSURFACE WATER REGIME MONITORING RESULTS

Data collected showed relatively fast decreased soil water suction response to rainfall. Almost simultaneous reaction in all soil horizons implied rapid vertical flow. The unsaturated regime within the soil profile prevailed though soil moisture content was close to saturation. No permanent water table was noted on the slope. Only a narrow range of soil moisture variation was observed, so step change between saturated and unsaturated flow regime and vice versa was fast and sudden. Subsurface flow heterogeneity was documented by comparing very different outflow amounts between two sections and three subsurface trench soil horizons. Local preferential flow paths transfer water at significantly variable rates.

Measurement results led to the following conclusions on the nature of storm flow generation in the watershed under review: a significant fraction of the rain falling on the hillslope infiltrated vertically towards the practically impermeable weathered bedrock via preferential pathways and the remaining part infiltrated the soil matrix slowly. A saturated layer built up in the soil profile above the weathered granite layer and a rapid subsurface flow formed there. Significant relationships exist between groundwater table, soil moisture, subsurface runoff and total outflow from the watershed, showing that subsurface water content or soil suction control rainfall transformation into runoff in the shallow soil area.

DISCHARGE NUMERICAL SIMULATION

Several numerical codes were tested to simulate experimental hillslope area outflow. The results of two of them, both based on Richard's equation describing variably saturated porous media flow are compared here. The latest version of SWM II model of two-dimensional flow in a variably saturated porous medium (Vogel, 1987) and the two-dimensional dual-permeability model S_2D_Dual (Vogel et al., 2000) were used. Soil water dynamics simulation was performed in the vertical plane along the Tomšovka hillslope during the selected rainfall measured in June 1998 (Fig. 4).

The assumption that soil is a single-continuum system is often inadequate when seeking a reasonably realistic description of water field scale movement due to existing preferential flow. Two domain models (Gerke and van Genuchten, 1993a, 1993b; Vogel et al., 2000) were developed in the last few decades to simulate soil mobile water designed to feature two pore systems: the matrix and the preferential flow (PF) domain. These models are commonly referred to as dual-permeability models. Darcian flow assumption in these models was taken to be valid for each of the two flow domains separately, allowing for local non-equilibrium between them.

Figure 5 shows modelled results as the best fit to represent measured outflow peaks from subsurface horizon A3 simulated by SWM II model compared with the same problem solved using S_2D_Dual dual domain model. The fit of measured and simulated hydrographs is very close for the model considering preferential flow domain, unlike that for the single domain model.

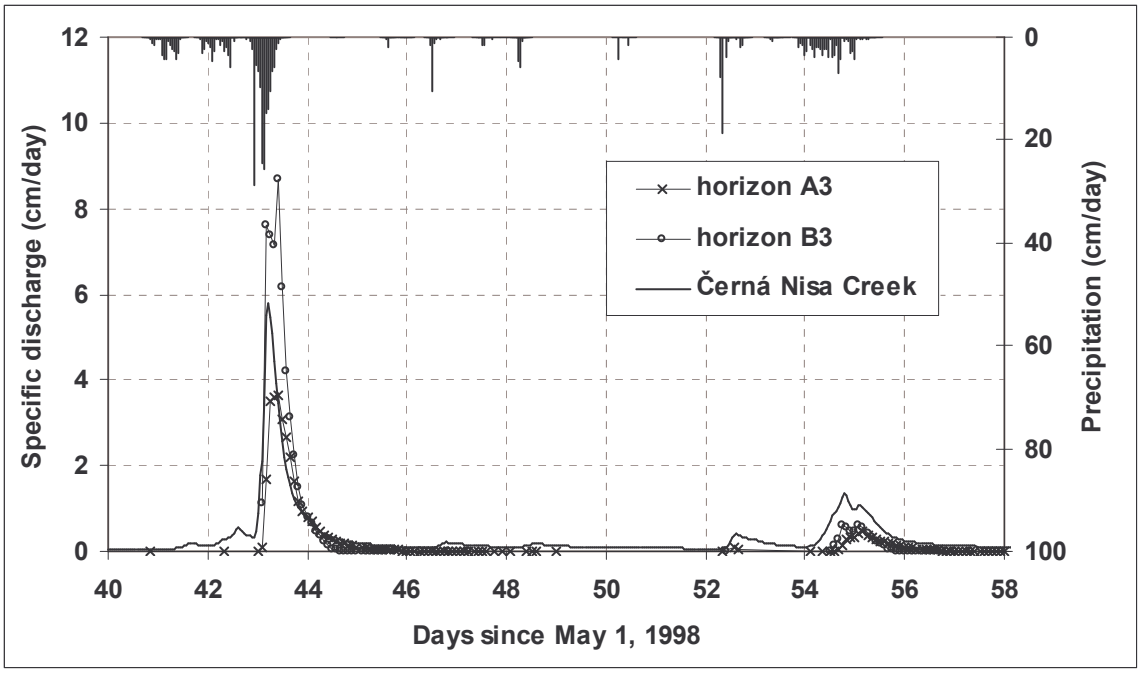

Fig. 4: Daily overall rainfall and specific outflow from soil profile deepest horizons A3 and B3 and specific discharge measured in the Uhlířská watershed closing profile.

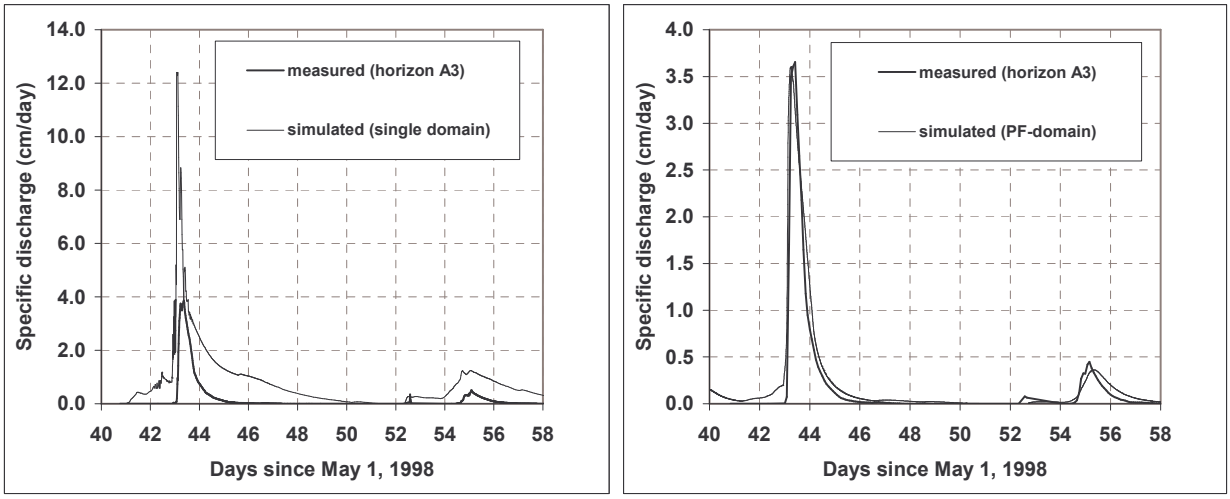

Fig. 5: Soil profile response to rainfall. Measured hillslope discharge rates observed at section A3 and simulated discharge by the 2D SWM-II model (single domain) and by S_2D_Dual (dual permeability approach) in two-dimensional vertical plane.

MODELLED SUBSURFACE FLOW COMPONENTS

Figure 6 shows subsurface flow components simulated by the dual domain model. Rainwater infiltrates to the deeper horizons below the simulated flow region by deep percolation, (free drainage boundary condition). The through-flow component comes from saturated flow above the less permeable layer at 70 cm depth. As expected, preferential flow domain discharge was significantly greater than soil matrix discharge in terms of through-flow. Deep percolation continued throughout the whole period, rainfall intervals included. The soil matrix exclusively generates it.

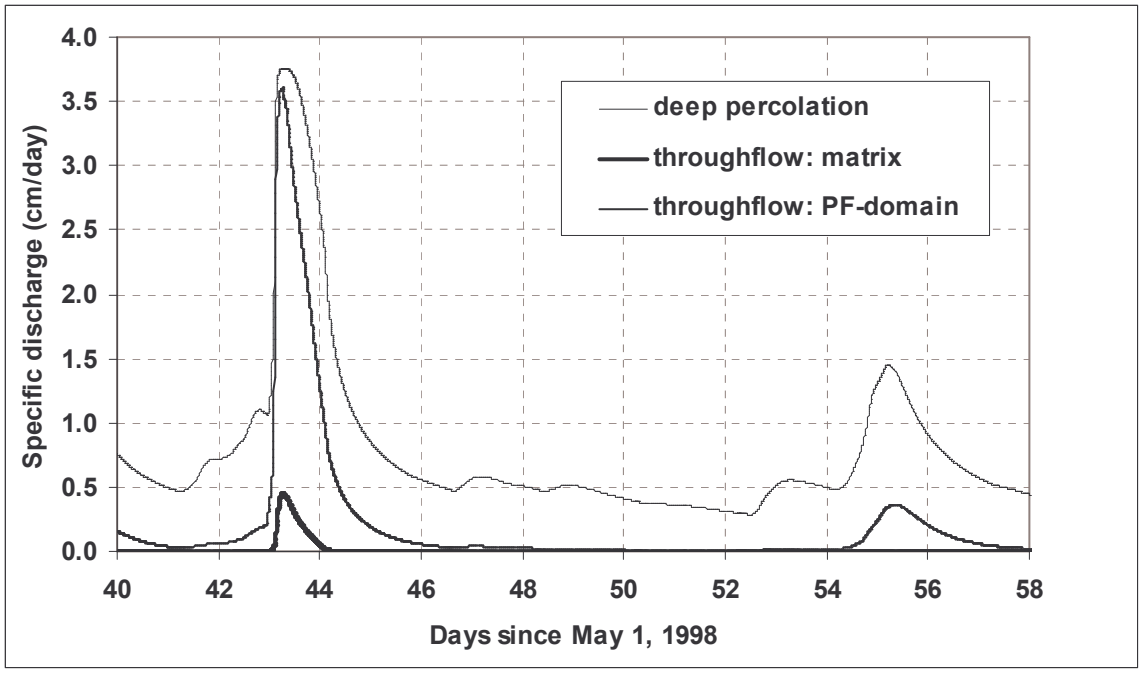

Fig. 6: Simulated components of hillslope subsurface runoff obtained by applying the dual-porosity model.

Hydrograph shape with the observed base flow in the stream is shown in Figure 7 using two different scales. Deep percolation is supposed to be the major water source for the Uhlířská watershed base flow.

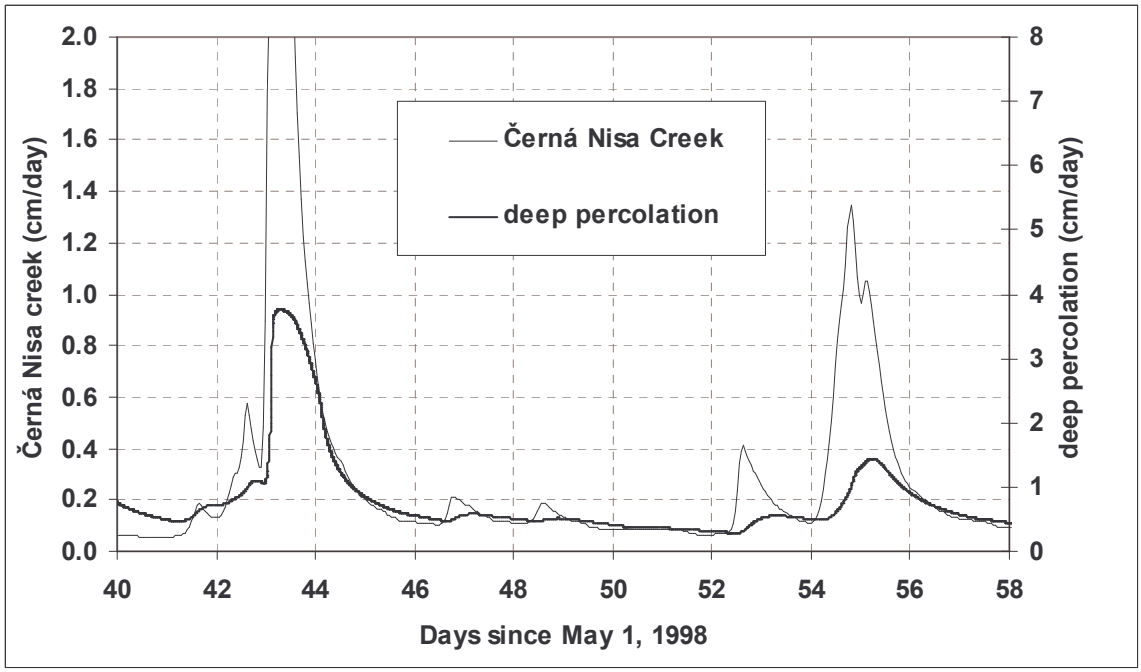

Fig. 7: Simulated deep percolation from the hillslope compared with measured watershed discharge.

CONCLUSIONS

Measurement results show that a significant fraction of rain falling on hill slopes infiltrates vertically towards the practically impermeable weathered bedrock via preferential pathways and the remaining part slowly infiltrates the soil matrix and leaves it gradually over a longer time period. Rapid flow is formed in the saturated layer on the top of weathered granite. The narrow range of water close to saturation controlled rainfall transformation into runoff at the Uhlířská watershed. Overland flow occurred very seldom due to highly conductive preferential pathways and only when the whole soil profile is fully saturated.

Three runoff components were identified when modelling the runoff formation in response to a rainstorm at the Uhlířská watershed hillslope scale: overland flow, shallow subsurface flow or through-flow and deep subsurface flow or deep percolation. Through flow in the soil profile dominates - these components in transforming a rainfall into quick runoff in the response time and hydrograph magnitude. Deep percolation as one of the dual domain model outcomes is supposedly the major base flow water source. Overland flow did not occur. Dual domain approach based modelling clearly shows better results in interpreting quick subsurface runoff than the single domain model where hydraulic properties are inadequately averaged into one domain, considering slow and fast flow domains with a certain degree of communication.

At Tomšovka, a representative Uhlířská watershed slope, magnitudes of partial contributions in through-flow and deep percolation may change overall hillslope response to rainfall under certain conditions. To a large extent, these components depend on hydraulic properties of porous formations the soil profile and weathered crystalline bedrock consist of. Detailed knowledge of the soil water regime is clearly essential for understanding the mechanism governing runoff formation at the hillslope scale in the shallow soil profile, and preferential flow has to be considered in interpreting observations and modelling the environment studied.

ACKNOWLEDGEMENTS

The research has been supported by the research project VaV/650/5/03 DU 11 of the Ministry of Environment of the Czech Republic and project of Czech Academy of Science S2060104.

REFERENCES

M. Císlerová, M. Šanda, T. Vogel, P. Tachecí, A Grünwald, J, Zeithammerová, A. Stodolovská, J. Votrubová, J. Kundratová and T. Picek (1998). The Research of the Transport Processes at the Watershed Affected by the Rainfall-Runoff Relationship Change. In Czech. Project Report VaV/510/3/96, DÚ 01, VÚV, ČVUT, Praha.

H.H. Gerke and M.Th. van Genuchten (1993a). A Dual-Porosity Model for Simulating the Preferential Movement of Water and Solutes in Structured Porous Media. Water Resources. Res., 29(2), 305-319.

H.H. Gerke and M.Th. van Genuchten (1993b). Evaluation of a First-Order Water Transfer Term for Variably Saturated Dual-Porosity Models. Water Resources Res., 29(4), 1225-1238.

M. Šanda and M. Císlerová (2000). Observation of Subsurface Hillslope Flow Processes in the Jizera Mountains Region, Czech Republic, Proc. Catchment Hydrology and Biogeochemistry. Processes in Changing Environment, IHP-V Technical documents in Hydrology, UNESCO Paris, Nr. 37, 219-226.

T. Vogel (1987). WM II - Numerical Model of Two-Dimensional Flow in a Variably Saturated Porous Medium, Research Report Nr. 87, Department of Hydraulics. and Catchment Hydrology, Agricultural University, Wageningen, The Netherlands.

T. Vogel, H. H. Gerke, R. Zhang and M. Th. van Genuchten (2000). Modelling Flow and Transport in a Two-Dimensional Dual-Permeability System with Spatially Variable Hydraulic Properties, J. Hydrology, 238, 78-89.

TEMPORAL PATTERNS OF SUBSURFACE WATER STORAGE INFERRED FROM SOIL MOISTURE TDR MEASUREMENTS

U. Somorowska

Warsaw University, Faculty of Geography and Regional Studies, Department of Hydrology , Krakowskie Przedmiescie 30, 00-927 Warsaw, Poland
e-mail Urszula Somorowska: usomorow@uw.edu.pl

ABSTRACT

The objective of this paper is to describe certain relationships between the components of subsurface water storage and discharge. Soil water storage and dynamic groundwater storage are investigated. Temporal patterns of subsurface water storage are inferred from the soil moisture measurements using a portable TDR meter. Soil water storage is calculated from the volumetric soil moisture content and linked with the groundwater level. Moreover, temporal differences in soil water storage are linked with the corresponding differences in dynamic groundwater storage inferred from the recession curve analysis of discharge data. Master recession curves are derived according to the theoretical framework proposed by Lamb and Beven (1997) using MRC Tool. The methodology is applied to the 362 km^2 lowland basin of the Łasica River located in central Poland on the Mazovian Lowland.

Key words: Time Domain Reflectometry (TDR) technique, soil-moisture-groundwater interface, patterns of hydrologic response.

INTRODUCTION

The soil moisture content considered as the hydrologic variable represents water retention in the top soil layers. Playing a significant role in soil-vegetation-atmosphere interactions, its estimates are necessary in the anticipation of wetness conditions in hydrological investigations. The in-situ data collected from reference sites form an integral part of the research strategy for a better understanding and assessment of water storage and fluxes. While quantifying the soil moisture content at one point is straightforward through direct measurements, characterizing the relationship between subsurface water storage and discharge at a basin scale is still a challenging opportunity.

The purpose of this study is to identify dominant stages of wetness conditions that control the hydrological response at a basin scale. The approach applied here refers to the notion of the 'Dominant Processes Concept' (Blöeschl 2001) rather than trying to capture everything when upscaling point measurements to the dimension of the basin.

The special focus of this study is on the soil water resources evaluated by the Time Domain Reflectometry (TDR) technique in selected experimental sites of the small lowland basin of the Łasica River. It is located in central Poland (N 52°13' – N 52°26' and E 20°15' - E 20°57') as presented in Figure 1. The specific objectives were the following: (1) to provide an assessment of the soil moisture resources stored in the upper soil layers of a small basin, (2) to track temporal depletion and recharge patterns of the soil moisture conditions and dynamic groundwater storage and (3) to display the interactions between the subsurface water storage and discharge.

Soil water storage patterns refer to the changes in dynamic groundwater storage inferred from the monitoring system of groundwater levels as well as from the recession curve analysis of the discharge data. The experiment yields high-quality data on soil moisture linked to the dynamics of groundwater and discharge.

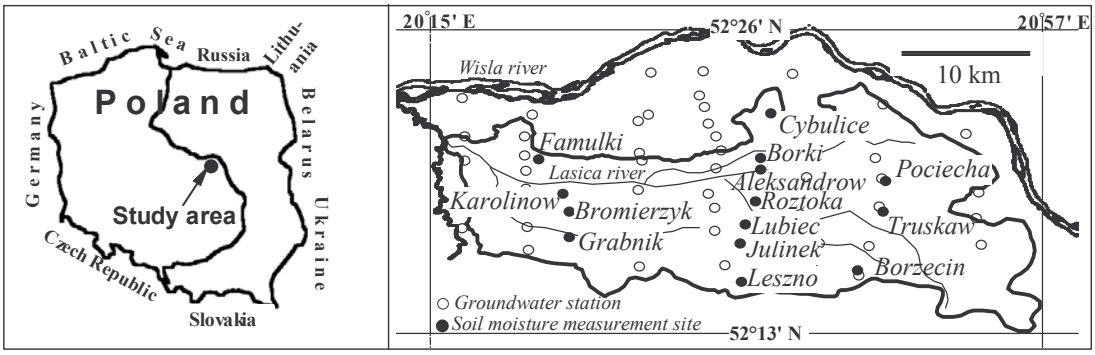

Fig 1: Location of the soil moisture measurement sites in the basin of Łasica River, central Poland.

EXPERIMENTAL DESIGN AND DATA

The experimental design of the study is based on point measurements of the volumetric soil moisture content along the soil depth down to the first saturated layer. Measurements were conducted from 1995 to 2004 in contrasting seasons of the year. A portable TDR meter (Easy Test) is applied to track the characteristic stages of the soil water storage of shallow soil layers in fourteen experimental sites. At each site the measurements of the soil moisture are taken at depths of 5 and 10 cm, and then with an increment of 20 cm.

In addition to the soil moisture data, groundwater and discharge data are used in this study. Groundwater records from the monitoring system of the Kampinos National Park represent groundwater elevation as well as the depth to the groundwater measured every two weeks. Daily discharge data of the Łasica River at Władysławów gauging station used in the recession curve analysis are supplied by the Institute of Meteorology and Water Management in Warsaw.

METHODS OF ANALYSIS

Interactions between soil water storage and dynamic groundwater storage are displayed in the form of simple regression functions. Observed stages of soil water storage derived from the field measurements are linked here with the groundwater levels, at a plot scale. Two different regimes of soil moisture patterns are distinguished; wet sites with very shallow groundwater levels are considered separately from dry sites with shallow groundwater levels. Drying and wetting patterns of the soil moisture profiles are displayed for selected reference sites. Soil water storage derived from a plot scale is then linked with dynamic groundwater storage retrieved from the recession curve analysis at the basin scale.

Based on the volumetric soil moisture values measured by the TDR field operating meter, soil water storage is calculated. Water storage W (mm) in the layer of depth $\Delta z = z_2 - z_1$ (cm) is obtained from the expression $W = (\theta \cdot \Delta z)/10$, where θ is volumetric moisture content (dimensionless). Thus water storage WS (mm) in the soil profile is expressed as a sum of water storage in particular soil layers W_i (mm) and is calculated as follows:

$$WS = \sum_{i=1}^{n} W_i = \sum_{i=1}^{n} \frac{\overline{\theta}_i \cdot \Delta z_i}{10} \qquad (1)$$

The value of $\overline{\theta}_i$ (dimensionless) represents the mean soil water content in i-layer and Δz_i is the depth of a particular soil layer. Taking into account the location of the TDR soil moisture probes installed at different depths, the soil profiles have been schematized in a number of soil layers. Thus water storage in the soil profiles at a depth of 100 cm is calculated according to the following expression:

$$WS_{100} = 0.75 \cdot \theta_5 + 0.75 \cdot \theta_{10} + 1 \cdot \theta_{20} + 1.5 \cdot \theta_{30} + 2 \cdot \theta_{50} + 2 \cdot \theta_{70} + 2 \cdot \theta_{90} \qquad (2)$$

The recession curve analysis of discharge data is applied here as an inverse tool for the evaluation of the volume of dynamic groundwater storage. Baseflow is considered to be an indicator of the current volume of dynamic groundwater storage (Tallaksen 1999). Master recession curves are derived here according to the theoretical framework proposed by Lamb and Beven using MRC Tool (1997). Then the results are coupled with the concept of nonlinear reservoir and analytical solutions proposed by Wittenberg (1999). The nonlinear storage-discharge relationship proposed by Wittenberg (1999) is applied in the form of the function: $S = aQ^b$, where a has the dimension $m^{3-3b}s^b$ for the value of S expressed in m^3, Q in m^3/s and b is dimensionless. Thus according to Wittenberg, the recession of baseflow can be described by the equation:

$$Q_t = Q_0 \left[1 + \frac{(1-b)Q_0^{1-b}}{ab} t \right]^{1/(b-1)} \qquad (3)$$

where b is a constant and a is approximated by the expression:

$$a = \frac{\sum (Q_{i-1} + Q_i)\Delta t}{2\sum (Q_{i-1}^b - Q_i^b)} \qquad (4)$$

with Q_i representing the discharge at time i of the observed flow recession. For practical purposes the exponent b is fixed as b=0.5 as suggested by Wittenberg and Sivapalan (1999). Using the proposed storage-discharge relation in form $S = aQ^b$, with Q approximated by equation (3), the changes in dynamic groundwater storage can be derived as follows:

$$\Delta S = a_{summer} \cdot Q_{\min,summer}^b - a_{spring} \cdot Q_{\max,spring}^b \qquad (5)$$

As a result, annual depletion of dynamic groundwater storage is retrieved, as a difference between the lowest value appearing in late summer or early autumn and the highest value of storage in spring (in the phase of discharge recession). For the period of soil moisture measurements, relative differences in soil water storage at a plot scale are linked to corresponding differences in dynamic groundwater storage at a basin scale.

RESULTS AND DISCUSSION

Depletion and recharge patterns of soil water storage

From the soil moisture data collected, volumetric soil moisture profiles have been derived for each measurement period. Selected profiles are presented in Figure 2. In all cases the evolution of vertical soil moisture profiles shows wetting and drying cycles. In spring, after the winter wetting season, the soil moisture content is relatively high. During the spring-summer period which is usually a drying season, the decrease in soil moisture content along the depth of the soil profile is observed. In wet sites (e.g. the Grabnik site) the highest volumetric soil moisture values are found at the surface and they decrease with depth. In surface soil layers a considerable decrease in soil moisture is usually observed during summer, with great water loss at the surface. Temporal fluctuations of water storage are displayed to represent two different regimes of the soil moisture patterns: wet sites with very shallow groundwater levels are considered separately from dry sites with shallow groundwater levels (Fig 3). The observed course of water storage confirms the thesis that in both cases fluctuations are formed by the wetting and drying cycles.

Extreme stages of soil water storage have been extracted (Fig 4a). Then the observed differences between extreme water storage values in each year were derived for both types of moisture sites (Fig 4b). The results obtained indicate that significant differences appear between different seasons within the hydrological year as well as between different years. The average difference in temporal water storage is calculated as a ten-year average. This value is 57 mm at sites with very shallow groundwater level and 115 mm at the remaining

sites. These average differences characterize the dynamics of soil water storage that are the result of site-specific characteristics and recharge by precipitation.

Interactions between soil water storage and groundwater

The interaction between soil water storage and groundwater is displayed by linking the change in soil water storage in 0–100 cm surface layer (ΔWS) with the change in depth of the groundwater table (Δh).

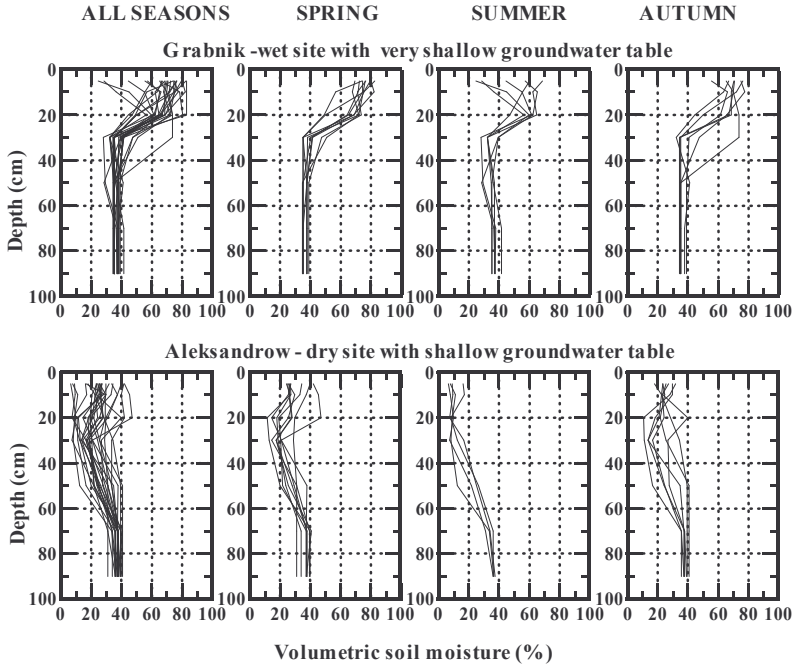

Fig 2: Volumetric soil moisture profiles at selected sites in the Łasica basin.

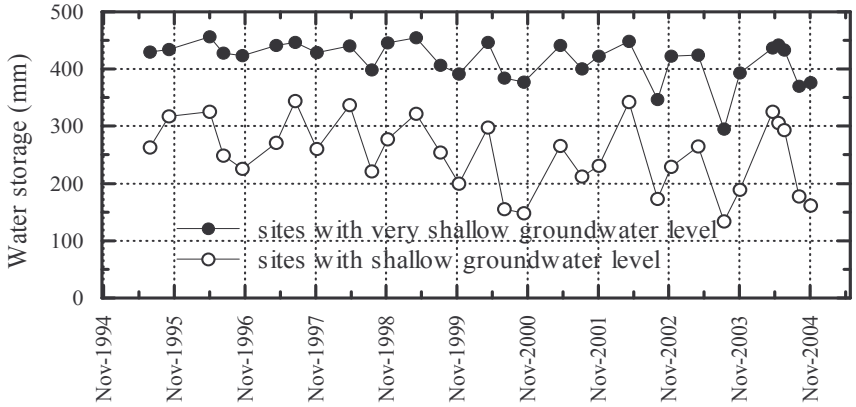

Fig 3: Temporal fluctuation of water storage in the 0-100 cm soil layer at sites with different soil water regime.

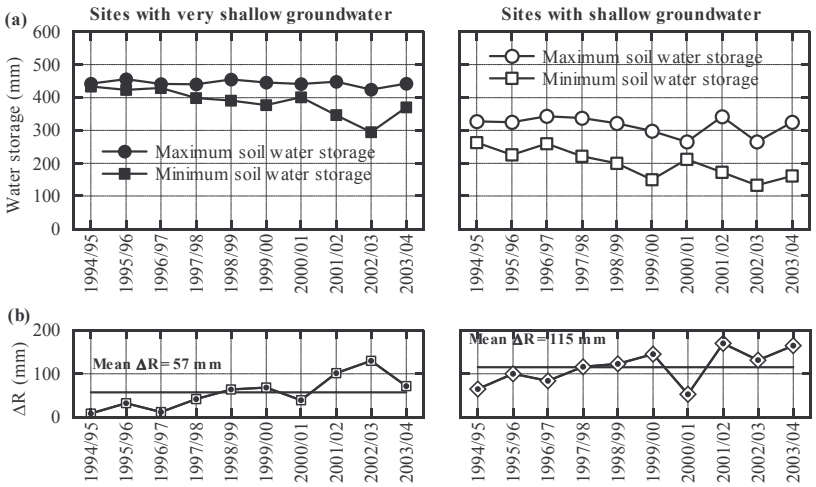

Fig 4: Extreme stages of soil water storage in the 0-100 cm layer (a) and annual differences in water storage (b). Both characteristics are displayed for two types of soil moisture regime.

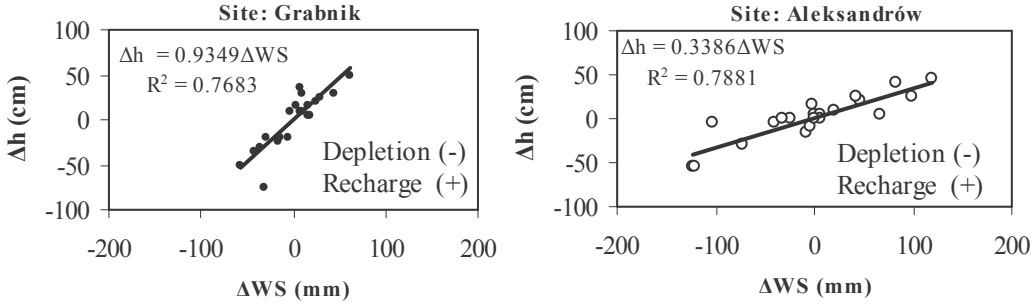

Fig 5: Change of soil water storage (ΔWS) linked to the groundwater level change (Δh) for selected sites.

Selected relationships are displayed in Figure 5. Depletion of soil water storage is represented by the negative values of ΔWS whereas positive values display the recharge.

Dynamic groundwater storage derived from discharge data

Long-term data of discharges for the period 1951-2002 are used in this analysis. Extracted curves comprise 137 recession curves for the spring months (March-April) and 392 recession curves for the months May-October. Such a split according to time of year is due to the seasonality of groundwater levels which represent maximum storage values in spring and then, usually when decreasing, they correspond to the depletion of groundwater resources. An automated method for the analysis of a large number of data proposed by Lamb and Beven (1997) is applied. A master recession curve is built based on the lowest "tails" of the recessions and sorting curves in decreasing order by use of MRC tool in Matlab 6.5. Fitting the Wittenberg function expressed in equation (3) to the master recession curves, the coefficient *a* is calculated according to equation (4). The value of parameter *a* for spring conditions is evaluated as 100.9 and for summer/autumn as 180.6.

Based on the relationship S = f(Q) with the fitted parameter values described above, the extreme values of dynamic groundwater storage are derived and then groundwater storage depletion is calculated. Figure 6a shows differences in extreme values of discharge values examined over a long-term period, namely the years 1951-2002. The range of yearly amplitude of discharges is 1-8m^3/s. The observed values of groundwater storage depletion vary between -34 mm and -112 mm, with the average value of ΔS=-68 mm. Relatively small storage depletion considered on a yearly basis can be associated with dry years, with low values of maximum discharges. The highest storage depletion is observed in years of considerable flooding in spring followed by low flows in summer.

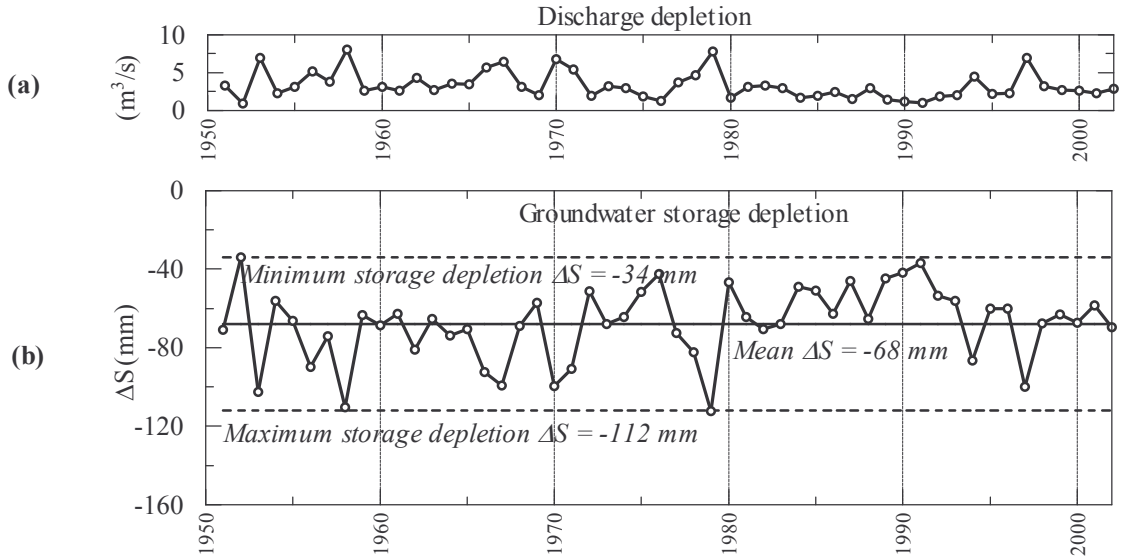

Fig 6: Annual differences in extreme discharge values (a) and annual depletion of dynamic groundwater storage in the basin inferred from recession curve analysis (b).

Interactions between soil water storage and dynamic groundwater storage

Relative changes in dynamic groundwater storage at the basin scale are coupled with the changes in soil water storage as displayed in Figure 7. The relationship ΔWS-ΔS is established separately for the two types of soil moisture site. Relative change of soil water storage at wet sites with a very shallow groundwater level is smaller than at dry sites with a shallow groundwater level if compared for the same change in dynamic groundwater storage. This is due to higher soil retention in wet sites than in dry sites, which is enhanced by a different slope of the established relationships.

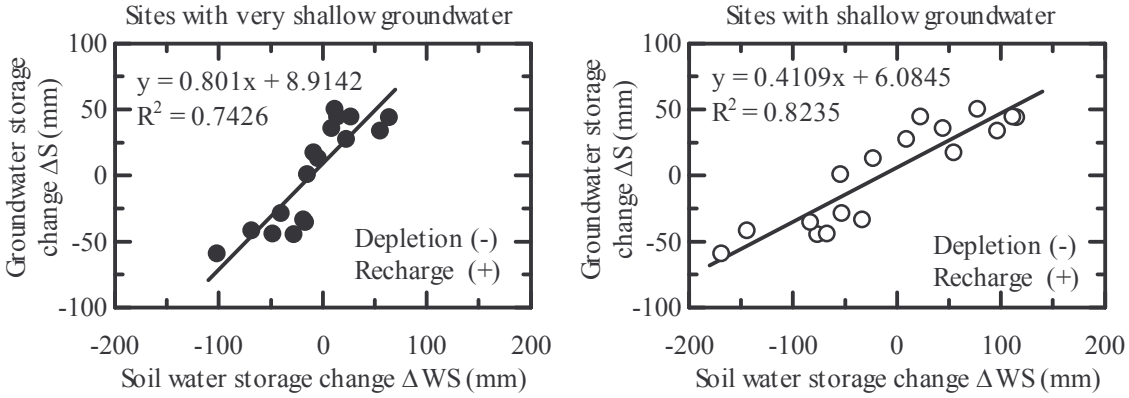

Fig 7: Dynamic groundwater storage change (ΔS) inferred from recession curve analysis at the basin scale as a function of soil water storage change (ΔWS).

CONCLUSIONS

The research provides information on soil water storage in the top soil layers inferred from TDR soil moisture measurements. The approach presented in this paper is intended to facilitate scale bridging of hydrological processes, specifically soil water storage and basin subsurface dynamic storage. The merging of soil water storage at a plot scale with discharge and dynamic groundwater storage at a basin scale helps bridge observational and modeling scales of the soil-water study. Enhanced understanding of quantitative relationships between characteristic stages of subsurface water storage and discharge is revealed through the consideration of depletion and recharge patterns of soil water storage. Investigated relationships reveal the substantial dynamics of the surface-subsurface interactions.

ACKNOWLEDGEMENTS

The soil moisture research has been supported by the Department of Environmental Sciences and Policy of the Central European University, Budapest by Grant No. 92-14. Additional funds have been awarded by the Ministry of Science, Committee for Scientific Research in Poland as Investment Grant No. 4441/IA/115/2003. The author wishes to thank Dr Robert Lamb from UK for making the MRC Tool available for research purposes and also for revising the program and providing helpful advice.

REFERENCES

Blöeschl, G. (2001) Scaling in hydrology. *Hydrological Processes*, 15, 709-711.

Lamb, R., Beven, K. (1997) Using interactive recession curve analysis to specify a general catchment storage model. *Hydrology and Earth System Sciences*, 1, 101-113.

Tallaksen, L. (1999) A review of baseflow recession analysis. *J. Hydrology*, 165, 349-370.

Wittenberg, H. (1999) Baseflow recession and recharge as nonlinear storage process. *Hydrological Processes*, 13, 715-726.

Wittenberg, H., Sivapalan, M. (1999) Watershed groundwater balance estimation using streamflow recession analysis and baseflow separation. *J. Hydrology*, 219, 20-33.

SOIL MOISTURE REGIME AT TWO SITES IN UHLÍŘSKÁ WATERSHED

P. Tachecí[1], M. Šanda[2] and A. Kulasová[3]

[1]*Faculty of Civil Engineering, Czech Technical University, and Water Research Institute T.G.M., (present address: DHI Hydroinform a.s.), Prague, Czech Republic*
[2]*Faculty of Civil Engineering, Czech Technical University, Prague, Czech Republic*
[3]*Czech Hydrometeorological Institute, Prague, Czech Republic*
e-mail Pavel Tachecí: p.tacheci@dhi.cz
e-mail Martin Šanda: martin.sanda@fsv.cvut.cz
e-mail Alena Kulasová: akulasova@chmi.cz

ABSTRACT

Intensive research focussing on the observation of subsurface flow and the soil moisture regime has been conducted since 1997 at the Uhlířská watershed, Central Europe at two parallel hillslope transects with different vegetation cover (young forest with grass and mature forest). The soil profile is formed by Dystric Cambisol on granite bedrock. Nesting of the instruments allows comparison of the soil moisture content using two independent methods: firstly, soil water suction measured at tensiometers installed in triplets (each in the different soil horizon) and utilizing retention curve for suction-moisture conversion and secondly, indirect soil moisture measurement by neutron probe using access tubes installed vertically in the soil profile. The set of 100 undisturbed soil samples was used for establishing 12 reference retention curves. During the 1998-2003 period, 41 routine measurements of soil water suction and soil moisture were taken. Recorded extreme moisture conditions (wet and dry) were selected for the comparison.
Although discrete values of moisture using both methods in the soil profile vary significantly, absolute differences between dry and wet conditions for particular soil depths are comparable. Averaged values of soil moisture gathered into three groups (four, four and three nests) were compared, representing plot/transect values. Approximate water retention capacity of the top 70 cm of the soil profile at forested transect B is about 172 mm. The soil profile of the top 60 cm at grassy transect A has a water retention capacity of approximately 80 mm. Results from the neutron probe measurements were about 12 – 29 mm higher than those determined from the soil water suction data.

Key words: soil water suction, soil moisture, tensiometer, neutron probe, field measurement, retention capacity Dystric Cambisol.

INTRODUCTION

Mountain areas on the borders of the Czech Republic are the source areas of large flood events which can cause severe damage in low-lying areas of the country (e.g. Šach et al., 2000). A detailed knowledge of the rainfall-runoff processes taking place in a source area is crucial for flood forecasting and the implementation of flood defence measures. The issue of the soil water regime determination is essential for all subsequent analyses of the runoff formation. Large areas of spruce forest in the Jizera Mountains heavily affected by air pollution were cleared between 1980 and 1993. A number of studies from all over the world make it clear that runoff response to rainfall for such vegetation cover change is highly dependent on the local conditions.
A comparison of the soil water regime of the cleared hillslope and that of the hillslope forested with a mature tree canopy is made. This provides the source information for the evaluation of the abrupt change in hydrological conditions in the watershed due to deforestation.

SITE AND METHODS

Uhlířská watershed description

The Czech Hydrometeorological Institute established a network of experimental watersheds in the Jizera mountains in the early 80s. The most fully examined watershed is Uhlířská (Černá Nisa river). The total area

of the watershed is 1.87 km^2, its average altitude is 822 m a. s. l., and the slope angle varies between 5 and 20 %. The average annual total of vertical precipitation is 1373 mm (1901-1950). The average annual discharge reaches 58 l/s (1982-1997) and the average annual air temperature is slightly above 4.4°C.

The bedrock consists of weathered and fractured granite. The slopes of the valley are formed by Dystric Cambisol (sandy loam) with peaty topsoil. It consists of 5 cm of humus, the black-brown Ah horizon is 20-25 cm thick and is followed by 20-25 cm of the brown Bv horizon and 20-50 cm of the light brown (to greyish or yellowish) C horizon with increasing amounts of solid particles. A 10-15 cm layer of litter can be found on the soil surface within the forest. Large amounts of roots, old branches and other tree debris were found in the soil profile (a consequence of clearance). Increasing amounts of boulders, bedrock particles and stones were detected in deeper layers of the soil profile. Tachecí and Šanda (2000) found a high variability in the pattern of surface infiltration velocities across the forested and deforested hill slopes, but the difference between average values for the two environments was not statistically significant.
The total area of the spruce forest decreased rapidly from 89% (1983) to 46.3% (1990) of the total watershed area. In 2000, the total area of the spruce forest reached over 90% (e.g. Tachecí, 2002).

Research focussing on the observation of the subsurface flow and the soil moisture regime has been conducted since 1997 with the co-operation of the Czech Technical University - Faculty of Civil Engineering, the T.G.M., Water Research Institute and the Czech Hydrometeorological Institute.

Soil moisture measurement

A network consisting of nested tensiometers, neutron probe access tubes and piezometers was set up at the two hillslope transects for the purpose of subsurface flow observation and the assessment of the soil moisture regime in 1998 (Šanda, 1999; Tachecí et al., 2000; Tachecí, 2002). The distance between the neutron probe access tube and the tensiometers in one nest is about 0.75 m, allowing comparison of soil moisture content using two independent methods. Both transects are parallel, but they differ in vegetation cover (Fig. 1). Transect A is located on the hillslope currently covered with young forest and grass. It was cleared in 1989 and reforested in the early 90s. A set of 9 neutron probe access tubes and 23 triplets of manually measured tensiometers is located along transect A. For the purposes of this study, measured data were ultimately grouped into two sets: the upper more level part of transect A and the lower, steeper part of the hillslope transect. Transect B is located in mature (approximately 40 years old) spruce forest. Measured values obtained at 5 locations measured by neutron probe and 13 locations measured by tensiometers were used as a single measurement group in this study.

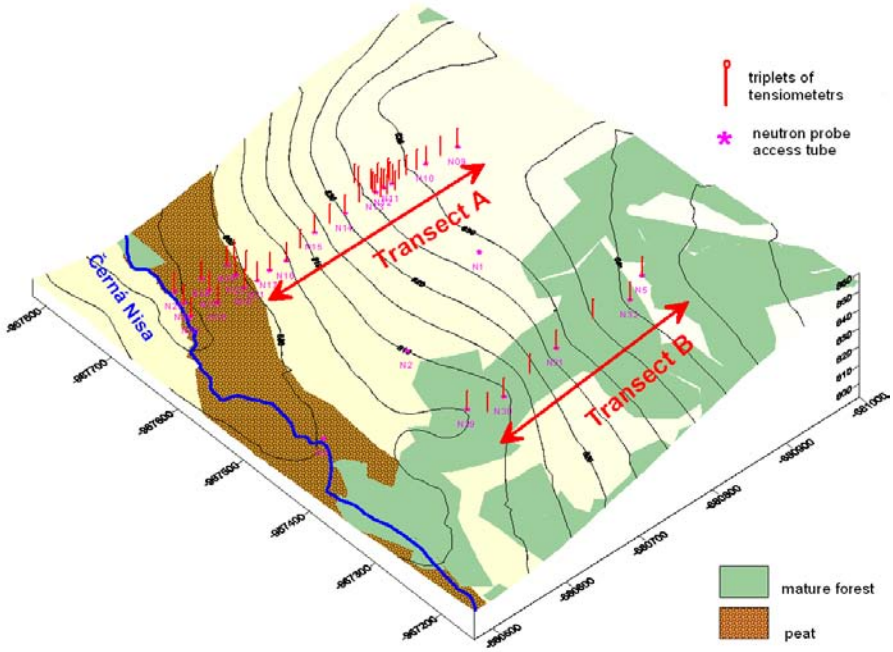

Fig. 1: Location map of the Uhlířská watershed hillslope measurement network.

A Didcot Instruments neutron probe was used for counting the relative number of thermalised neutrons. Volumetric moisture content was calculated using calibration coefficients based on the soil moisture determined gravimetrically. Measurement was conducted using aluminium access tubes driven into the soil profile to a depth of 50 – 70 cm (Fig. 2). The vertical increment of the measurement was 10 cm. The soil moisture content measured represents the average of the moisture from the spherical space (a diameter of approximately 20 cm). The number of field campaigns using a soil moisture neutron probe varied between 3 and 12 during the vegetation period (April-October) for the years 1998 to2003.

Fig. 2: Soil moisture measured by neutron probe.

For the manual reading of soil water suction in the tensiometers, a Soil Measurement Systems (SMS) Tensiometer™ was used. Suction is measured using the acrylic tube via the rubber septum cap and referenced to the location where the porous ceramic cup is installed in the soil profile. The tensiometers are installed in triplets, typically at depths of 20, 40 and 60 cm. The number of measurements taken during one vegetation period varied between 9 and 31 sets for 1998-2003.

Soil water pressure was transformed into soil moisture content using retention curves. The set of 100 undisturbed soil cores (100 cm^3) was taken from 4 pits along transect A and from one pit located in the upper part of transect B. A series of 7 points on the drainage branch of the retention curve with a maximum of 120 cm for the water column of the suction head was measured in the sand tank at the set of 52 soil cores. For 48 selected soil cores, a series of 11 points of the drainage branch of the retention curve was measured combining the sand tank (0-100 cm of suction head) and pressure plate extractor (Soil moisture Equipment for pressures of 100-3000 cm of the water column). A subset of 18 selected cores was examined at the maximum pressure of 15300 cm of the water column. Hysteresis of the retention curve was not considered due to the limit of the measurement.

Retention curves were fitted, grouped and scaled (Vogel and Císlerová, 1993) for 5 depths of the soil profile (15, 25, 35, 45 and 55 cm) in the case of transect A (divided into the upper and lower parts of the transect) and for three depths (19, 47 and 92 cm) in the case of transect B. Finally, 12 reference retention curves were established for the three groups of tensiometers. Two groups of retention curves for both transects are shown in Fig. 3. Based on the data measured, residual water content might be an inadequate extrapolation as a very sensitive result from the mathematical fit.

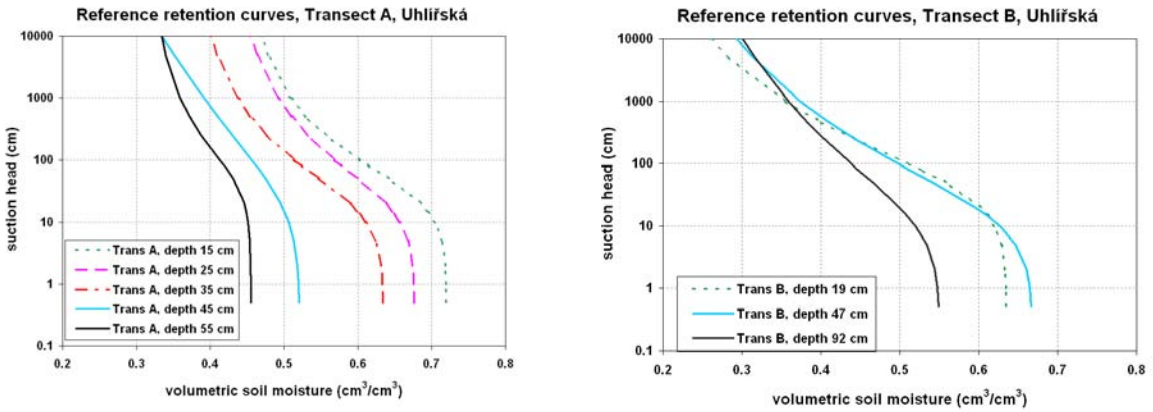

Fig. 3: Reference soil water retention curves for the upper part of transect A and for transect B.

Major differences between the retention curves constructed for corresponding depths in the soil profile make it necessary to use the interpolation of data along the vertical axis between the nearest reference soil layers where the retention curves are determined.

The data set of 41 routine measurements (performed on the same day) using tensiometers and the soil moisture neutron probe from the 1998-2003 period was established. This period included the extremely dry year of 2003, when only approximately 58% of the long-term average of the precipitation total during the vegetation season was observed. The annual precipitation total for 2003 was the minimum ever recorded since 1961 when hydrological monitoring began at the nearby Bedřichov CHMI station. The highest measured soil suction heads (30.8.2003) are close to 800 cm of water column at transect A and about 850 cm of the water column at transect B. During the 1998-2003 period, some measurements were taken in extremely wet periods (e.g. during high precipitation events and during fast snowmelt periods). It is believed that using the data from those events, saturated conditions of soil profile can be considered.

RESULTS

Soil water content variations

When extremely dry or wet conditions were reached the measurement campaigns for 11 selected nests were selected and compared. Vertical profiles of soil moisture change according to depth were constructed. Two examples of characteristic profiles (nest N11 located in the upper part of transect A and nest N5 located in the upper part of transect B) are selected in Fig. 4. Values represent extremely dry conditions (30.8.03), the rainfall event (17.7.00 and 10.9.01) and the snowmelt period (16.4.98). For extremely wet conditions, when pressure measurement is positive, saturated moisture content, determined gravimetrically, is instead used for comparison with the neutron probe data.

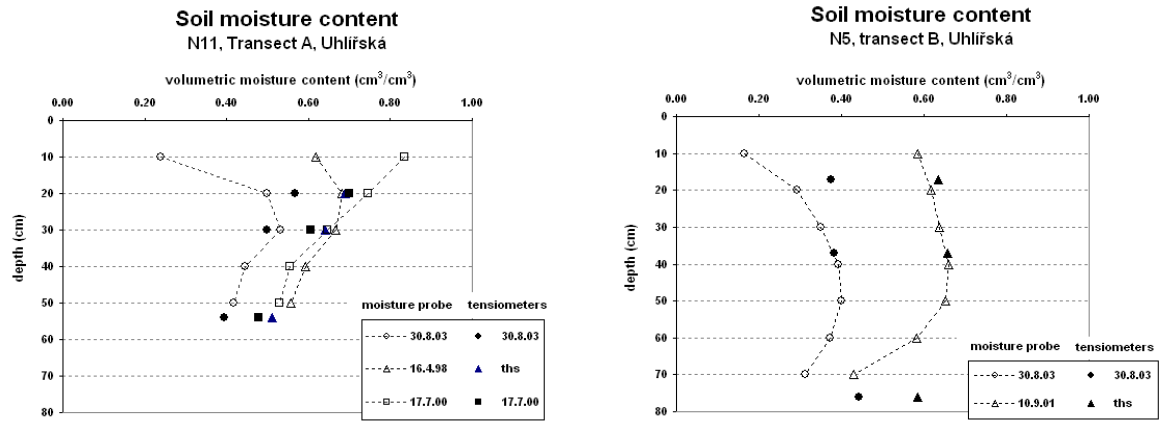

Fig. 4: The vertical profiles of the soil moisture values measured by neutron moisture probe (light) and calculated from the soil suction and retention curve (dark). Lines between points are drawn only for reasons of clarity.

A wide range of values at neutron probe depths of 10 and 20 cm may be caused by two factors: high content of peat and litter in the topsoil and systematic errors, resulting from the incorrect assumption that emitted neutrons travel in a sphere and bounce back to the detector. Here some of the particles may leave the soil environment, thus resulting in the error. Peaty topsoil of variable thickness is rich in organic matter, which also causes a bias in the neutron count (reference). The analysis of the soil moisture measurement by neutron probe in other parts of the Uhlířská watershed with a developed Histosol soil profile revealed that only the top 20 cm exhibits a variation in soil moisture, supporting the assumption that errors in measurement rather than an actual variation in soil water content are the cause of fluctuation in data acquisition.

It is clear that discrete values of soil moisture resulting from these two measurement methods are not equal. However, the general trend in soil moisture change is maintained. Total differences in soil moisture determined as a difference between dry and wet conditions is comparable for both methods.
Luxmoore et al (1981) compared measurements made by neutron probe and tensiometers at the isolated soil block of Fullerton silty loam (Walker Branch Watershed, eastern Tennessee) for a drainage period of 55 days

They found significant differences in the response times and spatial resolution of the tensiometers and the neutron probe. While the tensiometers give point values, the neutron probe averages spherical volume of about 15-20 cm diameter in soil profile.

Soil water retention capacity

Using the same assumptions, the retention capacity of the soil profile obtained from the differences in water content in extreme (wet and dry) conditions can be approximated. The comparison of the estimated retention capacity of the upper 60 cm of soil profile (transect A) and the upper 70 cm (transect B) respectively, is listed in Table 1. The values are averaged for the upper and lower parts of transect A and for the whole of transect B. The number of triplets of tensiometers and the number of soil moisture neutron probe access tubes used for the calculation are indicated as well.

The averaged values give a more general picture than particular discrete data representing soil moisture in the vertical profiles. Thus, the differences in total water contained in the profile can be established, firstly between the two transects (young forest and grass at transect A and mature forest at transect B), secondly, between the two parts of transect A (the upper, more level area and the lower, steeper part of the hillslope) and, finally, between the two methods used to examine retention capacity .

Table 1: Average water retention capacity of soil profile, transects A and B

Location	Depth of soil profile (cm)	Tensiometers		Neutron probe	
		number of nests	ret. capacity (mm)	number of places	ret. capacity (mm)
Transect A, upper	60	13	82	4	111
Transect A, lower	60	9	78	4	102
Transect B	70	13	172	3	184

Retention capacity of the soil profile is about 70 mm higher at transect B than at transect A. To analyse the source of this discrepancy, a comparison of measured soil suction values on 30.8.2003 is first carried out. The highest absolute values of suction head do not show a dramatic difference (850 and 800 cm of the water column of soil suction), but generally higher values of absolute suction head (about 150 cm of the water column) were measured at transect B in the whole data set. Then, volumetric soil moisture given by retention curves is compared for suction head corresponding to 800 cm and 0 cm (for two particular depths of 15 and 45 cm). The volumetric soil moisture is usually about 0.1 cm^3/cm^3 higher for transect B than for transect A in particular depths of soil profile. It can be concluded that a big difference in the retention capacity of the soil is caused by both the soil properties (represented by the retention curve) and higher drainage of water at transect B.

The difference in the retention capacity between the two parts of Transect A is very small, almost negligible. Both of the methods resulted in similar differences in water retention capacity between transects A and B. Measurement using the neutron probe gives higher values than calculations based on measured soil water pressure using tensiometers. Differences vary from 12 to 29 mm. It is presumed that this difference is mostly caused by measurement error when operating close to the soil surface with the neutron probe.

CONCLUSIONS

The extreme values (wet and dry conditions in the 1998-2003 period) based on measurements taken by tensiometers and using the soil moisture neutron probe were compared for soil moisture content values in the vertical profile (profile scale). Comparison of an approximated retention capacity in three groups of equipment nests (plot / hillslope scale) were examined.

Although point values differ significantly, total differences between the dry and wet conditions in given particular depths of soil profile resulting from both measurement methods are comparable.
Differences in the water retention capacity at plot scale calculated from both methods vary from 12 to 29 mm for the three groups. Nearly the same values were reported for the upper and the lower part of transect A. This transect can be taken as a whole for further comparison. Based on the measurements performed in 1998-2003, both methods give similar total ranges of moisture, here considered as practical water retention capacity. It is about 80 mm for transect A and about 172 mm for transect B. The difference is caused by the soil properties (represented here mostly by the retention curves), but higher absolute values of soil suction measured at transect B are also significant. It can be hypothesised that a) soil at clear-cut transect A was compacted during forestry operations b) that soil in the mature forest is drained to a higher extent than in the grassy areas.
For both transects, slightly higher values of water retention capacity were calculated from the neutron probe measurements. The explanation is that neutron probe error in measurements taken close to the surface (depths of 10 and 20 cm) can be expected as accuracy declines near the soil surface.

ACKNOWLEDGEMENTS

Subsurface water regime observation and measurement was supported by the grants IG ČVUT 3097416, IG ČVUT FSv 3097K1412 and IG ČVUT 309804201 (1997-1999). Further, they were granted by VÚV T.G.M. (Dr. Šárka Blažková) VaV/510/3/96 - DÚ 01, grant of Ministry of Education ČR No OK373 (Eurotas project, Dr. Šárka Blažková) and VÚV T.G.M. grant No. 1395 (Dr. Šárka Blažková). Data from CHMI regular network station Bedřichov were used for assessment of extremity of annual precipitation totals. We acknowledge the help of Ph.D. students from FCE CTU and Dr. Šárka Blažková from VÚV T.G.M. Prague.

REFERENCES

Luxmoore, R. J., Grizzard, T. and Patterson, M. R. (1981). Hydraulic properties of Fullerton cherty silt loam. Soil Sci. Soc. Am. Journ. 45: 692-698.

Šach, F., Kantor, P. and Černohous, V. (2000). Forest ecosystems, their management by man and floods in the Orlické hory Mts. in summer 1997 (in Slovak). Ekológia (Bratislava), 19/1, p. 72 - 91.

Šanda, M. (1999). Monitoring of the subsurface flow in the soil environment with the heterogeneous structure. Ph.D. thesis (in Czech) CTU FCE, Prague.

Šanda, M., Tachecí, P. and Kulasová, A. (2001). Evaluation of measurement of tensiometers, shallow ditch and lysimeters at research watersheds. 2001 Report. (in Czech) VÚV T.G.M., Praha.

Tachecí, P. and Šanda, M. (2000). Ponded infiltration experiments at Uhlířská watershed. Watershed hydrological and biochemical processes in changing environment. Proceedings of the Liblice Conference (22 – 24 September 1998). Edited by V. Elias and I.G. Littlewood, IHP – V, Technical Documents in Hydrology, No. 37, UNESCO, Paris, 2000, SC-2000/WS/38, p. 273 - 279.

Tachecí, P., Kulasová, A. and Šanda, M. (2000). Soil moisture measurement at deforested mountaneous watershed. (in Czech). Conf. “Hydrologic days 2000”, Plzeň, Czech Rep.

Tachecí, P., Kulasová, A. a Šanda, M. (2001). Soil moisture measurement by means of neutron probe and groundwater level observation. 2001 Report. (in Czech) VÚV T.G.M., Praha.

Tachecí, P. (2002). Hydrologic regime of small mountainous watershed and deforestation influence assessment. Ph.D. thesis (in Czech) CTU FCE, Prague.

Vogel, T. and Císlerová, M. (1993). A scaling-based interpretation of a field infiltration experiment. Journ. of Hydrol., 142: 337-347.

MONITORING THE IMPACTS OF URBANISATION ON ECOLOGICAL STATE OF RIVER WATER BODIES IN THE GRADASCICA CATCHMENT

M. Brilly[1], M. Toman[2] and S. Rusjan[1]

[1] *University of Ljubljana, Faculty of Civil and Geodetic Engineering*
[2] *University of Ljubljana, Biotechnical Faculty, Department of Biology*
e-mail Mitja Brilly: brilly@siol.net

ABSTRACT

The recent trend in water management is to improve the water environment in order to achieve a good water status. According to the EU Directive 2000/60/EC, evaluation of the ecological state of a specific water body calls for determination of the chemical and biological state, taking into account the characteristic living structures in water ecosystems. River rehabilitation is an important part of the process of achieving a good ecological water status. The complex partly urbanised Mali Graben, Mestna Gradascica and Glinscica watersheds in Slovenia of about 26 square kilometres in surface area were equipped with several rainfall stations, three Doppler velocity meters and a water quality multiprobe. In a short period of time, more than ten thunderstorm events were recorded and analysed. The project of monitoring the impacts of urbanisation on the ecological state of urban river water bodies includes the evaluation of water quality and the biological state of the Gradascica River and its tributaries in combination with hydrological conditions on the urbanized part of the watershed. The impacts of relatively simple rehabilitation measures in terms of improvement of living conditions for water organisms in the urban section of the Gradascica River (also called the Mali Graben), are also presented in the paper.

Key words: urban river, urbanized watershed, monitoring, river rehabilitation.

INTRODUCTION

The process of urbanisation has been accompanied by intensive changes in the hydrological characteristics of watersheds. The concept of the watershed in urban areas has become more complex and difficult to define because the natural topography is disturbed in the process. Thus, the water may be drained through storm drains and in some cases it may be diverted by drains into other basins (Riley, 1998). Therefore the area contributing to runoff may be completely different in an urbanised watershed than in its natural condition. As the land urbanises, which usually means that natural land is replaced by artificial paving in combination with vegetation clearing and compaction of the soil, the dynamics of hydrological processes change due to accelerated surface runoff and conveyance through drainage systems into the river channels. To assure the designed conveyance for floodwaters, these channels are usually heavily modified, closely regulated or even culverted. The ecological role of the channel is diminished to the minimum.

Commonly, the response of an urbanised watershed to rainfall is increased volume, peak flow and flood risk downstream, decreased low flows, increased pollution and degraded stream corridor habitats (Hall, 1984; Packmann, 1979). Although this generally applies, the reality may turn out to be otherwise due to the interacting nature of runoff processes involved. Another important aspect is the actual scale of the watershed area. Small-sized, densely urbanised river basins are more affected by the changed runoff pattern than large-sized rivers flowing through large urban areas, where the local urban runoff peaks contribute towards rather a small proportion of the entire river flow (Maksimovic et al., 2000). Stream channels are largely a product of the upland watershed area; the urbanisation affects not only the local runoff but also produces effects downstream, where flood peaks increase. Furthermore, higher nutrient levels are usually recorded in the streams of altered watersheds (DeAngelis, 1992). The surface water chemistry of a river at any point reflects several major influences, including the lithology of the watershed, atmospheric inputs, climatic conditions and anthropogenic inputs (Bricker and Jones, 1995).

STUDY AREA DESCRIPTION

The Gradascica River basin spreads through the transitional area from the Dinaric into the Alpine region of the central part of Slovenia. The headwater section flows through the varied mountain relief of the Dolomites, and comprises numerous ravines and valleys (Fig. 1). The Gradascica River basin covers an area of 154.4 km^2 reaching far into the Polhov Gradec Mountains.

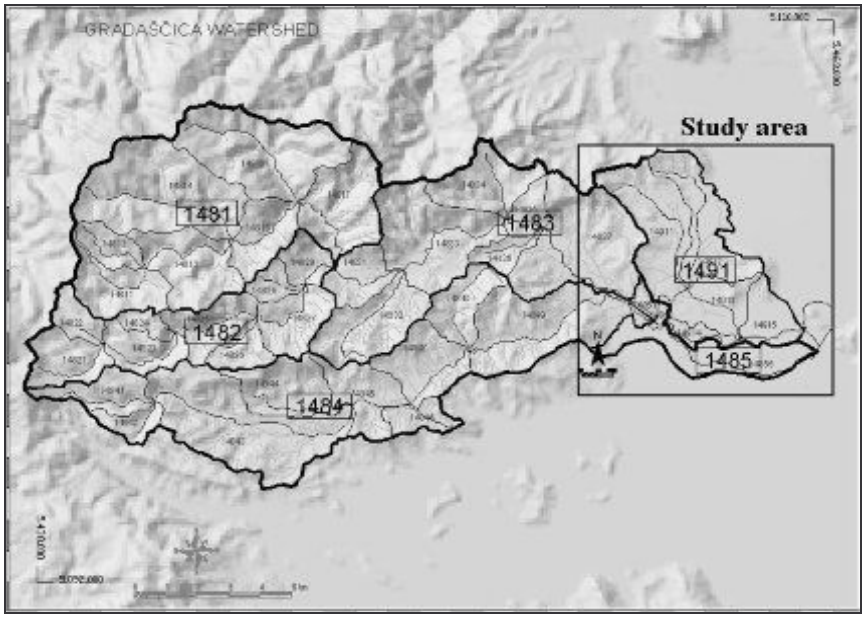

Fig. 1: The Gradascica River watershed.

Steep slopes, fairly high altitudes and abundant precipitation (average yearly quantity from 1600 to 1700 mm) result in a quick rise in the water level of the Gradascica. The plain area of the Ljubljana basin widens on the eastern part of the watershed. At the Bokalce dam, the Gradascica splits into two water bodies, the Mestna Gradascica and the Mali Graben, which flow into the Ljubljanica River (Fig. 2). The peak discharge of the secular high water wave in the profile above the Bokalce dam is up to 243 m^3/s. The Bokalce dam controls the discharge to the Mestna Gradascica stream and only about 10 % of the Gradascica River discharge diverts to the Mestna Gradascica stream. The Mali Graben carries in total about 90 % of the Gradascica River discharge.

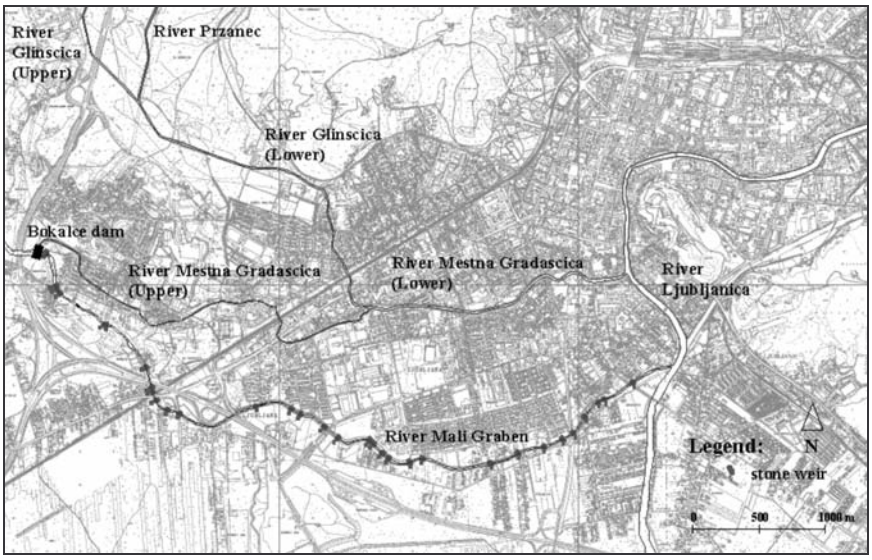

Fig. 2: The urbanized part of the Gradascica River watershed.

The study area is a sub-watershed of the water bodies of the Mali Graben, Mestna Gradascica and Glinscica, which is the tributary of the Mestna Gradascica stream. The Mestna Gradascica watershed is situated parallel

to the Mali Graben watershed. The area is close to the city centre and is heavily urbanised. The stream was heavily modified and regulated by concrete blocks. The Mestna Gradascica also divides into an upper and lower part at the confluence with the Glinscica. The Glinscica water body divides into the upper Glinscica, the Przanec tributary and the lower Glinscica (Fig. 2). Yearly precipitation in the study area is 1400 mm.

The former watershed area of the Glinscica stream comprised 16.7 km^2. The runoff within the urban area was determined by the removal of rainfall water by the sewerage system, and thus the orographic barrier failed to coincide with the actual Glinscica drainage area. The total drainage area of the Glinscica up to its outflow into the Mestna Gradascica stream is somewhat larger and comprises 19.3 km^2 of the watershed area, since the precipitation runoff from the area on the north-east part is diverted to the Glinscica watershed area via a storm water system. According to the CORINE database, urban areas account for 21 % of the study area and urban green areas 26 %, a total area of 12.2 km^2.

The land cover of the study area consists of continued and discontinued urban fabric, industrial units and roads; green urban areas, sports and leisure facilities; agricultural areas consist of non-irrigated arable land, pastures, complex cultivation patterns and land, principally occupied by agriculture, with large areas of natural vegetation; and forests include broad-leaved forest, coniferous forest and mixed forest.

METHODS

Data were collected from available databases and by monitoring. Maps and past water quality data were collected from the databases of the Agencies of the Ministry of the Environment, Spatial Planning and Energy of the Republic of Slovenia (ARSO), the land use data are taken from the CORINE database (Heymann, 1993).

The measuring equipment included a one-dimensional ultrasonic Doppler instrument, 2D/3D handheld Doppler velocimeter and water quality multiprobe. One-dimensional Doppler instruments, which were placed at the bottom of streams, continuously recorded the water level, water velocity and temperature. The multi-purpose instrument, designed for in-situ and flow-through applications, measures parameters simultaneously. It can be used for remote or attended monitoring of fresh, salt or polluted water in both surface and groundwater. The multiple parameters include: nitrate, temperature, conductivity, depth, dissolved oxygen, Oxidation Reduction Potential (ORP) and pH. Measurements by multi-purpose probe were carried out in different seasons in approximately 40 measuring cross sections along the streams Glinscica, Mestna Gradascica, Mali Graben and Przanec from July 2003 to July 2004 (Fig. 3). The continuous measurements of fluctuations of parameters in streams were also derived from the probe for 24 hours at a 15-minute sampling rate in 3 cross sections equipped with the Doppler instruments. Six rain gauge stations were used for rainfall measurement.

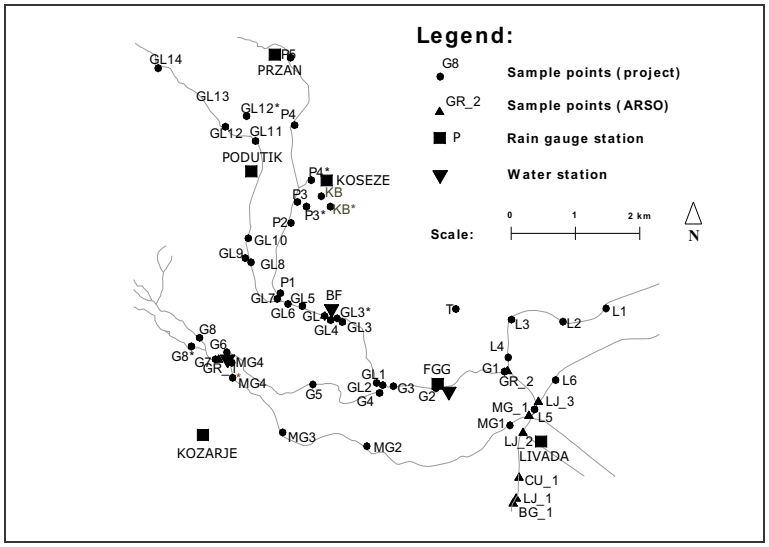

Fig. 3: Measuring cross sections, rain gauge stations and water stations.

In order to manage all the collected data, an information system has been established. It is based on a country-based watershed register (Šraj, 2001; Brilly, 2000). The system contains information thematic layers. Data for the information themes are organised as a file system managed with AutoCAD MAP 2004 GIS tool and prepared as vector or raster data, available for browsing on Internet.

RESULTS AND DISCUSSION

The measurements of parameters by the multi-purpose instrument were performed in four two-day campaigns in July, October 2003, and January, March, July 2004. The number of measuring points was reduced during each campaign because of the rather small scale of the studied area. Among the parameters measured, the measurements of dissolved oxygen and pH value are discussed in detail.

Dissolved oxygen

Dissolved oxygen is a basic requirement for healthy aquatic ecosystems (Wharton, 2000). Oxygen concentrations in the water column fluctuate under natural conditions, but oxygen can be severely depleted as a result of human activities. Urban runoff is often loaded with high concentrations of organic materials derived from a variety of sources (Klein, 1979).

The water in the streams was saturated with dissolved oxygen for more than 70 % of the time. The water was over-saturated in the summer time (Fig. 4).

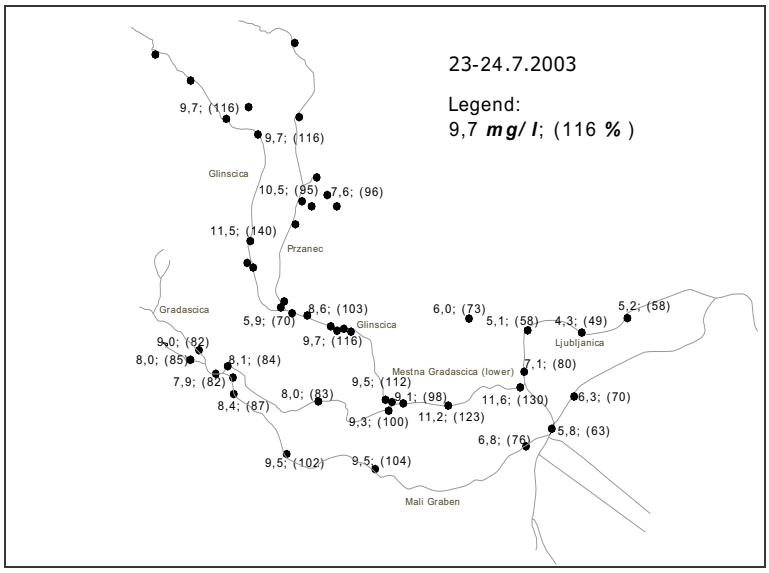

Fig. 4: Dissolved oxygen content in the summer time.

The over-saturation with dissolved oxygen was higher in the heavily modified concrete channels of the Mestna Gradascica and Glinscica streams than in the rehabilitated channel of the Mali Graben River. The concrete bottom and banks of the Mestna Gradascica and Glinscica streams are intensively overgrown with algae. As the concrete channel is mainly unshaded, photosynthetic activity is very intense. This is reflected in the high concentration of dissolved oxygen, which is oversaturated during the daytime in the summer.

pH

The pH of the stream water reflects the chemical characteristics of precipitation and land surface. Additional characteristics of pH in some poorly buffered waters is high daily variability in pH values attributable to biological processes that affect the carbonate buffering system (Jarvie et al., 2001). Levels of dissolved carbon dioxide in stream water reflect the balance between uptake of carbon dioxide by aquatic organisms

(for photosynthesis) and release of carbon dioxide (by respiration). On the other hand, the concentration of dissolved oxygen is increased by photosynthetic activity during the daytime and the dissolved oxygen can be depleted during the night by the respiration of water organisms. The product of the reaction of carbon dioxide with water is bicarbonate ion and hydrogen ion; an increased concentration of hydrogen ion means increased acidity and lowering of the pH (Chapra, 1997).

Continuous pH records reveal a wealth of detail on short-term variability and extremes in river water quality and have particular application for examining water quality signals which occur episodically and on shorter timescales.

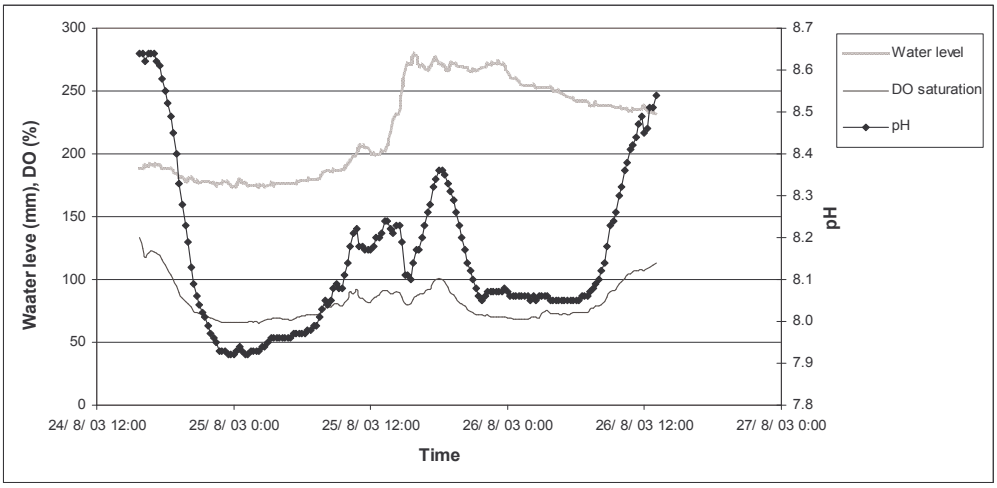

Fig. 5: Continuous measurements of water level, pH and dissolved oxygen saturation in the Mestna Gradascica River.

Continuous measurements of water level, pH and dissolved oxygen saturation in the Mestna Gradascica River are shown in Figure 5. The measurements were logged automatically at 15-minute intervals. The relation between the variations of pH and dissolved oxygen saturation is evident. Increased values of pH and dissolved oxygen saturation during the daytime are a result of diurnal photosynthetic activity in the water body. The temporal fluctuations of pH and dissolved oxygen saturation are also related to the increased water discharge during a small flood wave produced by 11 mm of rainfall.

Improvement of the aquatic habitat in the Mali Graben River

The revitalisation works in the Mali Graben River were carried out between 1984 and 1986, following the initiatives of fishing and angling clubs. There were several stone weirs built in the river channel (Fig. 2), however no concrete walls were built and the living conditions remained favourable.

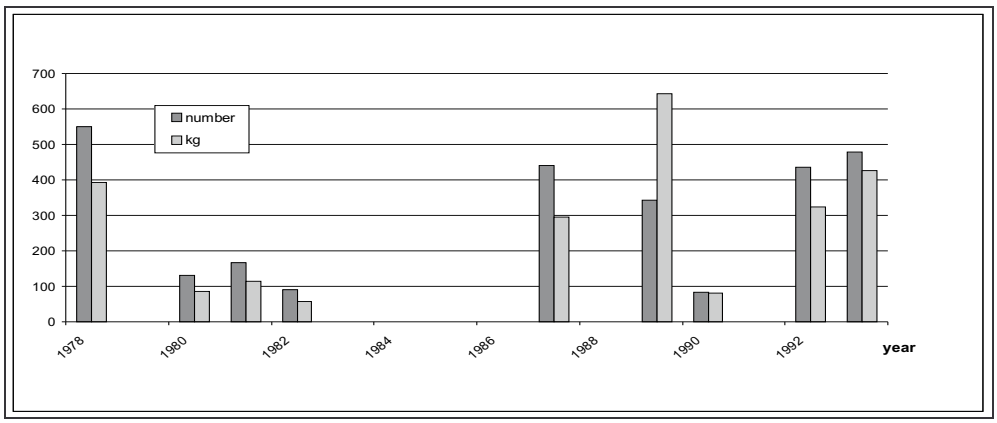

Fig. 6: Nase catches prior to and following restoration works in the Mali Graben River.

The weirs increased the water abundance in the channel during low flow conditions. The fish population has significantly increased after the introduction of stone weirs (Fig. 6). The measures represent good practice in urban river rehabilitation techniques.

CONCLUSION

The results of monitoring demonstrate a wide range of information that can be gained from continuous measurements of basic water quality parameters in connection with analysis of the hydrological regime of the urban environment. One of the major advantages of this type of monitoring is the possibility to quantify water quality extremes that cannot be detected by traditional spot measurements or sampling (Quinn, 2004). This leads to a better understanding of dynamic short term variability in stream water quality and a new insight concerning watershed and in-river processes. The understanding of the processes calls for many field measurements, modelling, data mining and analyses. The use of monitoring is the first research step to take and helps to understand the system and identify the key factors for modelling.

REFERENCES

Bricker, O.P., Jones, B.F., 1995, *Main factors affecting the composition of natural waters*, in: Salbu, B., Steinnes, E., editors, Trace elements in natural waters, Boca Raton: CRC Press, p. 1–5.

Brilly, M. 2000, *The Danube and its basin*, Follow-up Vol. 6, A hydrological monograph, Pt. 1, Danube river basin coding, Slovenian IHP Committee, Ljubljana, Slovenia, 99 pp.

Chapra, S. C., 1997, *Surface Water-Quality Modeling*, McGraw-Hill, New York, USA, 844 pp.

DeAngelis, D., L., 1992, *Dynamics of nutrient cycling and food webs*, Population and community biology, First edition, Chapmann & Hall, 270 pp.

Directive 2000/60/EC, 2000, *Directive of the European Parliament and of the Council of 23rd October 2000 establishing a framework for Community action in the field of water policy*, Official Journal of the European Communities, L 327/1.

Hall, M. J., 1979, *Urban Hydrology*, UK: Elsevier, 280 pp.

Heymann, Y., 1993, *CORINE land cover: Technical guide*, Environment, nuclear safety and civil protection series, Commission of the European Communities, Office for Official Publication of the EuropeanCommunities, Luxembourg. 144 pp.

Jarvie, H., P., Neal, C., Smart, R., Owen, R., Fraser, D., Forbes, I., Wade, A., 2001, *Use of continuous water quality records for hydrograph separation and to assess short-term variability and extremes in acidity and dissolved carbon dioxide for the river Dee, Scotland*, The science of total environment 265, 85–98.

Klein, R. D., 1979, *Urbanization and stream quality impairment*, Water Resources Bulletin, 15, 948–63.

Maksimovic, C., Sægrov, S., Milina, J., Thorolfsson, S. T., 2000 – *Urban drainage in specific climates, Vol. II: Urban drainage in cold climates*, IHP – V, Technical documents in hydrology, No. 40, Vol. II, UNESCO, Paris, 199 pp.

Packmann, J. L., 1979, *The effects of urbanisation on flood magnitude and frequency*, in: Hoollis G. E., editor, Man`s impact on the hydrological cycle, Norwich: Geo Books, p. 153–172.

Quinn, P., 2004, *Scale appropriate modelling: representing cause-and-effect relationships in nitrate pollution at the catchment scale for the purpose of catchment scale planning*, Journal of Hydrology, 291 (3–4), 197–217.

Riley, A. L., 1998, *Restoring streams in cities, A guide for planners, policymakers, and citizens*, Island Press, Washington, D.C., 445 pp.

Šraj, M., 2001, *Watershed Coding System of the Republic of Slovenia*, Acta hydrotechnica 19/30, Ljubljana, p. 3–24.

Wharton, G., 2000, *Managing river environments*, Cambridge, Cambridge University Press: 90 pp.

FOREST INFLUENCE ON FLOOD RUNOFF GENERATION STUDIED ON THE SPERBELGRABEN EXAMPLE

C. Hegg, A. Badoux, J. Witzig and P. Lüscher

WSL Swiss Federal Research Institute, Zürcherstrasse 111, CH-8903 Birmensdorf, Switzerland
e-mail Christoph Hegg: christoph.hegg@wsl.ch
e-mail Alexandre Badoux: alexandre.badoux@wsl.ch
e-mail Jonas Witzig: jonas.witzig@wsl.ch
e-mail Peter Lüscher: peter.luescher@wsl.ch

ABSTRACT

The general belief about forests reducing flood peak discharge is not supported by observations in three Swiss catchments with soil conditions that differ greatly from many other sites where forest influence on the flood runoff generation was studied. A detailed analysis was performed in the Sperbelgraben to investigate how forest influence on flood runoff generation differs with different soil conditions. The site was chosen since the influence of recent storm damage could be investigated at the same time. Soil profiles were analysed, plots of $1m^2$ artificially irrigated, 50 to 110 m^2 area surface runoff plots installed and runoffs in two neighbouring zero-order basins observed in a nested approach. The study showed that cover only slightly affects flood runoff generation in the Sperbelgraben forest, as soils are either very wet or very permeable. Storage capacity is too small to feature major influence on flood generation on wet sites, while water seeps deep into the ground even when the soil is still far from being saturated on permeable ones. The highest impact of forests on flood runoff generation is expected on soils showing a 20 to 60 cm deep reduced permeability layer.

Key words: runoff generation, forest influence, soil influence, flood generation.

INTRODUCTION

Scientists, politicians and practitioners have for many years shared the belief that forests reduce runoff in general and flood peak discharge especially (McCulloch and Robinson, 1993; Germann and Weingartner, 2003). Engler first described this finding in 1919, based on data collected in the Sperbel and Rappengraben. Studies in the Alptal (Burch et al., 1996) suggest that no influence of forest cover on flood peak discharge can be detected in certain circumstances, even though forests are clearly shown to affect water balance. Increased research activity in Switzerland on this topic leads to a differentiated approach on the forest influence on flood runoff generation described below.
Theoretical considerations explained in detail by Badoux et al. (2005a) show that forests cannot have an important influence on flood runoff generation on all soils. The major factor whereby forests can influence runoff generation is their soil storage capacity, which is often greater on a forest site than on arable land because of better soil properties, such as higher organic material content, less disturbed soil structure, deeper rooting depth and the like added to high-level evaporation from trees between rainfalls. The extent to which this storage capacity affects runoff generation during one event depends on its relationship with the amount of water involved. Floods are generally caused by large rainfall, during which the small storage capacity of shallow soils can only retain a small portion of rain. This influence on flood runoff generation can be so small as to be hardly detected, as occurs with interception retention. Such forest soils therefore have no major influence on flood runoff generation.

The finding that forest influence highly depends on the local situation requires a differentiated approach to identify whether forest management may affect flood runoff generation or not. The methodology used for this purpose should be simple and as cheap as possible. A methodology becomes cheap if it builds up on existing information or on investigations requiring completion anyhow. An ongoing Swiss mapping project for so-called forest site types was started to provide forest management with site-specific indications (Burger et al., 1996). A forest site type is the summary of features of similar forest sites grouped according to topographic and geomorphologic location, soil nature, flower composition and the like. This methodology was established based on the expertise of senior consultants and scientists without much field data.

One of the Lothar and mountain torrents project purposes was to support this methodology with field data if possible and to adapt it as required. The investigations and results carried out for this purpose and described below are explained in detail by Hegg et al. (2004).

STUDY SITE AND INSTRUMENTS

The main objective of the Lothar and mountain torrents project was to study the influence of damage caused by the storm Lothar on the water cycle in forested catchments. The study site was thus selected in a region where a damaged and an undamaged basin could be investigated close to each other. Such a situation was found in the Sperbelgraben catchment, studied from 1903 to 1958 by Engler (1919) and his successors (e.g. Burger, 1934; Casparis, 1959).

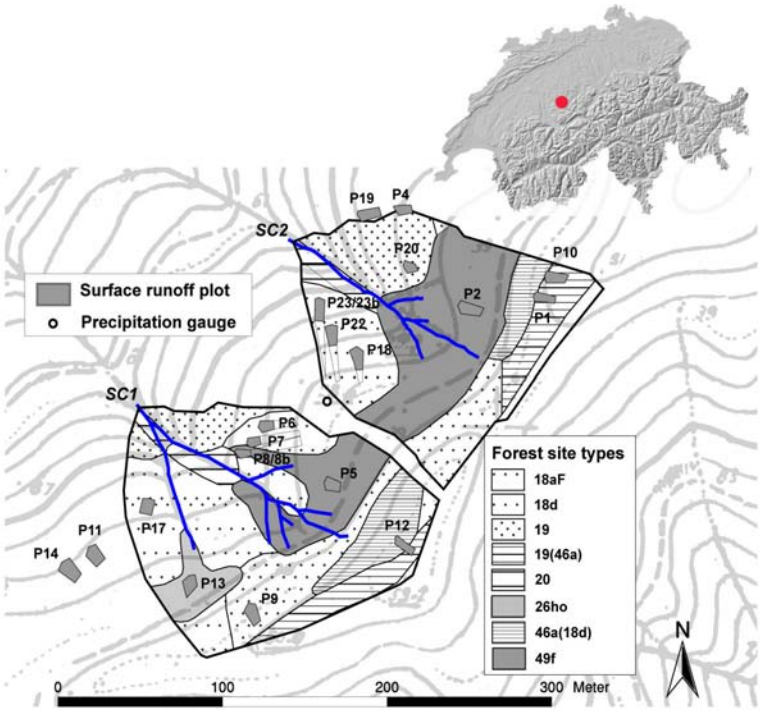

Fig. 1: Overview of the investigation area showing two sub-catchments, position of the 19 numbered surface runoff plots, forest site types, and rainfall gauge.

The small sub-catchments feature an area of 1.76 (SC 2 heavily damaged) and 2.03 (SC 1 lightly damaged) hectares located in the southeast zone of the Sperbelgraben catchment ridge at between 1075 and 1160 m a.s.l. (Fig. 1).
Apart from some soaked zones with close to impermeable Gleysols, the investigation area mostly features Cambisols with partly limited and unlimited permeability. The most important parameters of the two sub-catchments are listed in Table 1.

The ecologic properties of the forest site types influencing hydrologic behaviour are shown in Figure 2. Higher soil water content leads to a higher runoff coefficient. High soil acidity results in accumulating organic compounds on the surface as a litter layer due to lower decomposition rates. A hydrophobic litter layer may temporally reduce infiltration capacity and generate surface runoff under certain conditions. The driest and most acid soils in the investigated area were on forest site type 19. The wettest and least acid soils were on forest site type 49f. Some Cambisols feature a partly impermeable layer at some 70 to 80 cm depth.

Table 1: Some lightly damaged sub-catchment 1 and heavily damaged sub-catchment 2 parameters

		Sub-catchment 1	Sub-catchment 2
Area	[m^2]	20250	17620
Mean elevation	[m a.s.l.]	1130	1128
Circumference	[m]	550	540
Mean slope	[°]	25.3	25.7
Maximal slope	[°]	61.8	64.5
Channel density	[km km^{-2}]	17.3	11.0
Area with wet soils	[%]	22.8	36.7

Soil profiles were analysed and irrigation experiments performed on a 1 m^2 area just above the soil profiles on all major forest sites. Small surface runoff plots with an area of 50 to 110 m^2 were also operated close to soil profiles for two years. Two runoff-gauging stations were built at the outlet of both sub-catchments. Details of the technical installations are explained in Badoux et al. (2002a, 2002b).

The extent to which hydrologic properties as measured in the soil profiles correlate with observations made during irrigation experiments could be tested with this setting. How similar surface runoff plot reaction is to observations made with irrigation experiments on the same forest site types was also analysed. The forest site type map was used to measure slope runoff reactions in the study area. Comparing this extrapolation with the measurements at the two runoff gauging stations enabled identifying the extent to which slope runoff reaction can help explain sub-catchment runoff reactions.

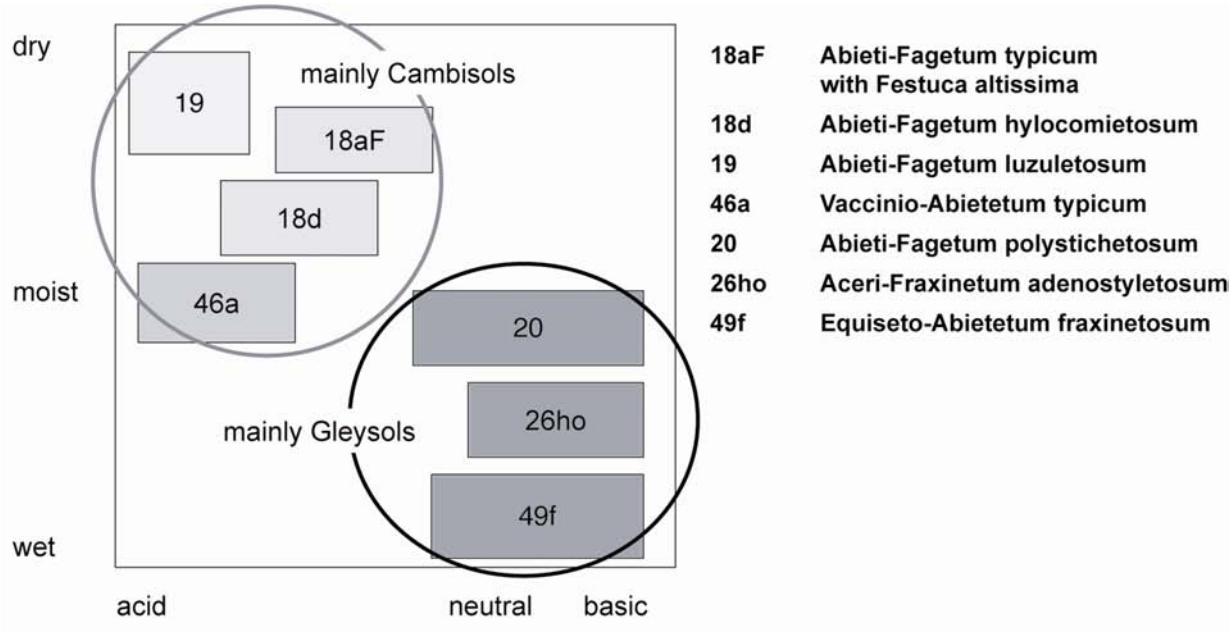

Fig. 2: Features of forest site types found in the Sperbelgraben (from Burger et al., 1996; modified).

The results of this work are described in detail by Hegg et al. (2004) and partly by Witzig et al. (2004), Badoux et al. (2005a, b). Some typical results and major conclusions are explained briefly hereunder.

SOME RESULTS

As described by Witzig et al. (2004), 1 h 60 mm irrigation experiments on $1m^2$ led to two very distinct reactions:

- Experiments on moist to wet forest site types produced high surface runoff amounts as saturation excess overland runoff. The wetter the soil, the higher the overland flow proportion.

- Either no or little surface runoff was measured on moist to dry forest site types. Surface runoff was observed on some sites just after irrigation start, but ceased as soon as the hydrophobic reaction inducing organic layer was wetted and became permeable. No saturation excess overland runoff could ever be observed, even in the presence of a poorly drained layer. TDR measurements showed that water percolated deep into the soil even when the soil upper part was still far from being saturated.

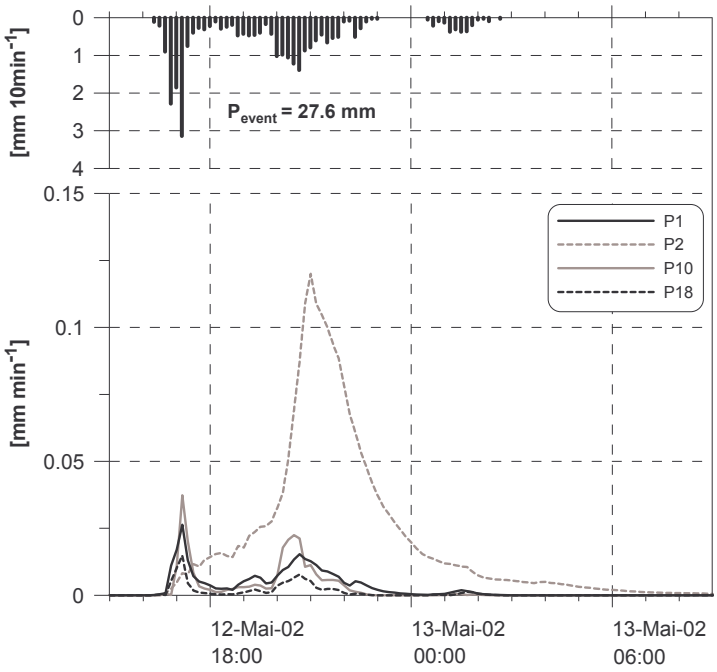

Fig. 3: Runoff and rainfall observed on four surface runoff plots in the Sperbelgraben during the May 12, 2002 event.

Figure 3 shows the runoff reaction of four typical surface runoff plots during a major rainfall. Two reaction types similar to those observed with irrigation experiments can also be identified on the plots. Plot P2 on forest site type 49f shows high surface runoff coefficients. Surface runoff increases with increasing rainfall intensity as soon as soil storage capacity is reached. This reaction is typical for saturation excess overland flow. Plots P1, P10 and P18 that rest on dry to moist forest site types show the highest surface runoff as soon as rainfall starts. This temporary infiltration excess overland flow ceases as soon as the organic layer is fully wetted. This layer does not always completely cover a plot area, so the hydrophobic reaction of a whole plot is normally less pronounced than observed during irrigation experiments.
Additional factors obviously play an important role when trying to explain sub-catchment runoff behaviour as a combination of different forest site types. Table 1 shows that sub catchment 2 features a higher proportion of wet soils and the proportion of damaged trees is three times higher. Faster reaction and higher runoff peaks would thus theoretically be expected for this heavily damaged sub-catchment.

As shown in a typical example of Figure 4, runoff reaction in the sub-catchments during floods is however more complex. At first rainfall, the lightly damaged sub-catchments yields higher runoff but behaviour of the heavily damaged sub-catchment can be explained at the second one only by considering additional factors such as drainage density or deep percolation as investigated in detail by Badoux et al. (2005b).

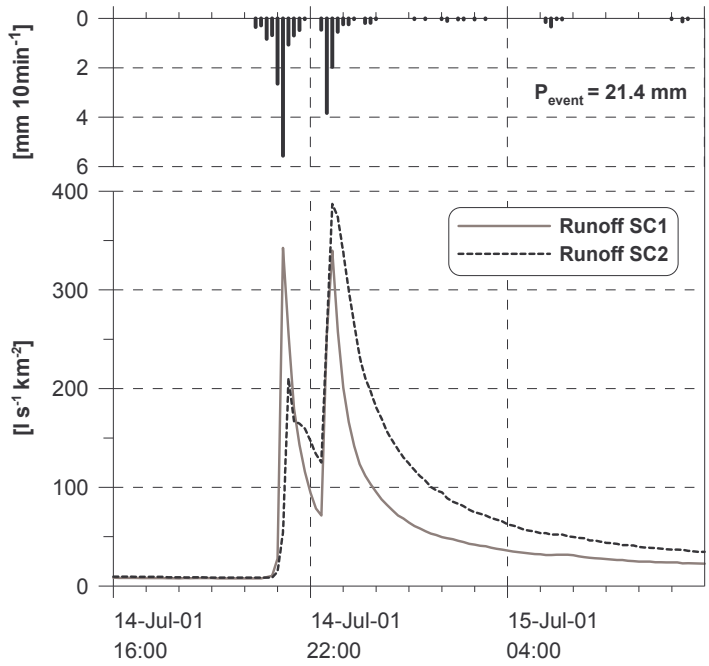

Fig. 4: Typical runoff reaction of the two Sperbelgraben sub-catchments during a July 2001 storm.

CONCLUSIONS

The forest site type map proved to be a suitable tool for extrapolating hydrologic properties from profile analysis to slopes in the Sperbelgraben. The hydrologic behaviour observed on surface runoff plots always corresponded reasonably well to expectations based on forest site type map and soil profile interpretation. Further up-scaling to the sub-catchment level was only partly successful as other still unexplained factors also had a major influence.
Forests have little influence on flood runoff generation in the Sperbelgraben. Either soils are so wet because of an impermeable underground that only little storage capacity is available and overland flow is the dominant process, or the underground is so permeable that water easily infiltrates deep into the ground even when soil storage capacity is still far from being saturated.

Different factors must be addressed when trying to estimate where forest influence on floods might be most important. The theoretical reflections explained by Badoux et al. (2005a) clearly show that such influence can be expected due to higher forest soil storage capacity. The observation of no saturation overland flow in the Sperbelgraben however limits the effect of soil high storage capacity on situations featuring limited in-depth percolation. The conclusion is that the influence of forests on flood runoff generation is the highest on soils featuring an impermeable layer at 20 to 60 cm depth (Hegg et al., 2004). The impermeable layer makes the soil saturate with intensive rainfall, the outcome being that overland flow can be postponed when additional storage capacity from better soil conditions under forests is available. When the impermeable layer is closer to the surface, storage capacity becomes too small to significantly affect storms capable of producing major floods. If this layer is much deeper, storage capacity is enough to also have a major influence on extraordinary rainfalls with or without a forest.

Additional irrigation experiments and plot studies are required in the near future to quantify the importance of the influence of forests on flood runoff generation under such conditions.

ACKNOWLEDGEMENTS

Parts of the results described in this paper were elaborated in a common project of WSL and the Berne University Institute of Geography sponsored by the Swiss Agency for forest, Environment and Landscape

described in detail by Hegg et al. (2004). The authors are grateful to all colleagues participating in this project and supporting the work required.

REFERENCES

Badoux A., Hegg C., Kienholz H., Weingartner R., 2002a. Investigations on the influence of storm caused damage on the runoff formation and erosion in small torrent catchments. - In: Spreafico, M. Weingartner, R. (eds) International Conference on Flood Estimation. March 6-8, 2002, Bern, Switzerland. Proceedings. Report no. II-17 of the International Commission for the Hydrology of the Rhine basin: 39-47.

Badoux A., Hegg C., Kienholz H., Weingartner R., 2002b. Investigations on the influence of storm caused damage on the runoff formation and erosion in small torrent catchments. - Proc. International Congress Interpraevent 2002 in the Pacific Rim - Matsumoto/Japan, vol. 2: 961-971.

Badoux A., Witzig J., Germann P., Kienholz H., Lüscher P., Weingartner R., Hegg C, 2005a. Investigation on the runoff generation at the profile and plot scale in the Sperbelgraben, Swiss Emmenthal. Hydrological Processes (submitted).

Badoux A., Jeisy M., Kienholz H., Lüscher P., Weingartner R., Witzig J., Hegg C., 2005b. Influence of storm damage on the runoff generation in two sub-catchments of the Sperbelgraben, Swiss Emmental. European Journal of Forest Reseach (submitted).

Burch H., Forster F., Schleppi P., 1996. Zum Einfluss des Waldes auf die Hydrologie der Flysch Einzugsgebiete des Alptals. Schweizerische Zeitschrift für Forstwesen 147(12): 925-937.

Burger H., 1934. Einfluss des Waldes auf den Stand der Gewässer; 2. Mitteilung; Der Wasserhaushalt im Sperbel- und Rappengraben von 1915/16 bis 1926/27. Mitteilungen der Schweizerischen Anstalt für das forstliche Versuchswesen 18. Band, 2. Heft: 311-416.

Burger T., Danner E., Kaufmann P., Lüscher P., Stocker R., 1996. Standortkundlicher Kartierungsschlüssel für die Wälder der Kantone Bern und Freiburg. ARGE Kaufmann + Partner/Burger + Stocker: Solothurn/Lenzburg.

Casparis E., 1959. 30 Jahre Wassermessstationen im Emmental. Mitteilungen der Schweizerischen Anstalt für das forstliche Versuchswesen 35. Band, 1. Heft: 179-224.

Engler A., 1919. Einfluss des Waldes auf den Stand der Gewässer. Mitteilungen der Schweizerischen Anstalt für das forstliche Versuchswesen 12. Band: 1-626.

Germann P.F., Weingartner R., 2003. Hochwasser und Wald - das forsthydrologische Paradigma. In: Jeanneret F, Wastl-Walter D, Wiesmann U, Schwyn M (eds), Welt der Alpen - Gebirge der Welt, Haupt Verlag, Bern, pp 127-141.

Hegg C., Thormann J.-J., Böll A., Germann P., Kienholz H., Lüscher P., Weingartner R., 2004. Lothar und Wildbäche. 79 p. Eidg. Forschungsanstalt WSL, Birmensdorf.

McCulloch J.S.G., Robinson M., 1993. History of forest hydrology. Journal of Hydrology. 150, 189-216.

Witzig J., Badoux A., Hegg C., Lüscher P., 2004. Waldwirkung und Hochwasserschutz - eine standörtlich differenzierte Betrachtung. Forst und Holz, 59. Jg, Nr. 10: 476 - 479.

INTERCEPTION IN PINE AND EUCALYPT FOREST IN CENTRAL PORTUGAL – INITIAL MEASUREMENT AND MODELLING RESULTS

J.J. Keizer[1], H.L. de Coninck[2], S.J.E. van Dijck[2], C.O.A. Coelho[1] and P.M.M. Warmerdam[2]

[1] *Centre for Environmental and Marine Studies (CESAM), University of Aveiro, 3810-193 Aveiro, Portugal*
[2] *Alterra-WUR, Wageningen, The Netherlands*
e-mail Jan Jacob Keizer: jkeiset@dao.ua.pt

ABSTRACT

This paper presents the initial results of an interception study in two open forest areas in the Serra do Caramulo of central Portugal. Limburg Soil Erosion Model interception module measurements tend to grossly underestimate interception estimates derived from gross rainfall, through-fall under tree canopies and in gaps and stem-flow, except for lighter rainfall. Better results were obtained with the sparse Gash model, especially for the pine site, but they first and foremost indication model's potential. Average rainfall for weekly periods reveals a strong tendency to be higher under canopies than in gaps, and are taken to suggest the prevalence of wind-driven non-vertical rainfall in the area.

Key words: below-canopy versus gap through-fall, LISEM, sparse Gash model.

INTRODUCTION

The event-based Limburg Soil Erosion Model (LISEM) (De Roo et al., 1995; De Roo & Jetten, 1999) has been and is being applied and tested for small experimental catchments located on the west flank of the Serra do Caramulo in central Portugal within EU-funded CLIMED project and nationally funded projects HIDRIA and MODAGUEDA. These projects differ in specific LISEM use objectives, but their common aim is to improve knowledge and understanding of factors and processes determining catchment runoff response and, in particular, to clarify the role of land use. The Serra do Caramulo west flank has undergone dramatically changed land cover/use over the past decades, partly induced by extensive forest wildfires between the mid 1980s and early 1990s (e.g. Walsh et al., 1992; Shakesby et al., 1996; Ferreira et al., 1997). The formerly prevailing stands of Maritime Pine (Pinus pinaster Ait.) have now been mostly replaced by commercial plantations of fast-growing eucalypt trees, Eucalyptus globulus Labill especially. Experimental catchments are accordingly dominated either by eucalypt stands of up to about 10-11 years old (i.e. a full rotation cycle), or by Maritime Pine stands that regenerate more or less spontaneously after the wildfires mentioned above.
Cumulative rainfall interception (I_{cum}) is modelled in LISEM with Aston's 1979 empirical equation, i.e.

$$I_{cum} = c_p * S_{max} * (1 - e^{-k * P_{cum} / S_{max}}),$$

where: c_p = vegetation cover fraction;
S_{max} = canopy storage capacity in millimetres;
k = vegetation density correction factor;
P_{cum} = cumulative rainfall in millimetres.

Canopy storage capacity and correction factor k are estimated in their turn from their empirical relationship with Leaf Area Index (LAI), i.e.

$S_{max} = 0.935 + 0.498 * LAI - 0.00575 * LAI^2$ (Von Hoyningen-Huenes 1981);

$k = 0.046 * LAI$.

Aston's equation is in fact a simplification of Merriam's 1960 equation, neglecting the evaporation term. Total interception in LISEM will therefore ultimately reach a plateau exclusively dependent on forest stand features, if the event lasts long enough. Aston's equation's applicability to the specific conditions of the present study area can also be questioned in a more general sense in view of its empirical nature. Also, its

substitution in LISEM with a physical model such the Gash and Rutter one (e.g. Valente et al., 1997) would be more in line with LISEM's overall model structure, which is firmly based on physical-process descriptions.
The main purpose of this study is to establish how well the LISEM interception module can represent interception in Serra do Caramulo forests, also in comparison to alternative interception models. Specific objectives are to:

1. identify interception in an eucalypt and a Maritime Pine stand from measurements of gross rainfall, through-fall and stem-flow;
2. evaluate the suitability of Aston's 1979 interception equation to model interception in these stands;
3. assess the performance of the Gash model sparse variant (Valente et al., 1997) to do the same.

MATERIAL AND METHODS

A Eucalyptus globulus Labill. stand of about 6 year old and a Pinus pinaster Ait. stand of about 10-year old were selected as being representative for the above-mentioned experimental catchments. The eucalypt stand is situated at an elevation of roughly 400 m above sea level on the upper northwest-facing slopes of the so-called Serra de Cima catchment (after the nearby village). An automated rainfall gauge already existed in the Serra de Cima village prior to this study and is used here for estimating gross rainfall, albeit in conjunction with a second automated rainfall gauge that was installed very close to the Maritime Pine stand within the first three months of this research. The Maritime Pine stand is located at a comparable elevation on the upper west-facing slopes of the nearby, so-called Lourizela catchment (again after the nearby village). The climate of the area is transitional between Atlantic and Mediterranean, with an annual rainfall varying from roughly 1500 to 2000 mm and a mostly pronounced wet season from November to March (e.g. Coelho et al., 2001).
In the two stands, a forest inventory plot of 20 x 20 m was laid out at a rather arbitrarily chosen location. For each tree within the plots, total height was measured using a 100LH Opti-Logic laser meter, and diameter at breast height (DBH) and aerial cover of the canopy were determined using ordinary measuring tape. The tree inventory data are resumed in Table 1. Table 1 also gives the stands' leaf area index (LAI) as derived from the empirical formulas of Pereira et al. (1997) and Porté et al. (2000), and their canopy cover fraction as estimated by photographic and visual means.

Table 1: Summary of tree inventory data and derived information for 20x20 m plots in a Eucalypt and a Maritime Pine stand

Stand	Tree individuals (nr.)	Tree height (m; average)	DBH (cm; average)	Aerial canopy cover (m^2; average)	LAI	Canopy cover fraction
Eucalypt	75	14	31	5	3.0	0.60
Pine	218	9	21	2	4.5	0.35

Unlike seems to be common practice in forest interception studies, here throughfall is not measured at randomly selected locations within the plots but at stratified-randomly selected locations, i.e. by stratifying the sampling space in below-canopy and gaps. The below-canopy sampling space, in turn, was divided in two classes on the basis of tree morphometry. In the case of the eucalypt plot, this involved the two most frequent classes of aerial canopy cover (i.e. 4-7 and 10-13 m^2), further referred to as small and big trees. From the neighbouring pairs of small and big trees, five pairs were randomly selected for placement of the following equipment, i.e. one rainfall gauge below the canopy of each tree and one rainfall gauge in the gap in-between. Each selected tree[1] was further equipped with a standard stemflow collar connected to a tank. In the case of the pine plot, a somewhat different experimental set-up was chosen since the two distinguishable classes of trees occurred in distinct parts of the plot. Therefore five small and five big trees were randomly selected and equipped with a rainfall gauge below their canopy and a standard stemflow collar connected to a tank. The five gap rainfall gauges were placed at the most open location in two randomly selected 2.5x2.5 m squares in the subplot with the small trees, and three randomly selected 5x5 m squares in the subplot with the

[1] One big tree was selected twice, so that stemflow is measured for nine trees in total.

big trees. At the two plots, from each of the three types of rainfall gauges (i.e. below-canopy small trees, below-canopy big trees, and in-gaps) one out of five gauges was randomly selected to be an automated device. Likewise, an automated stemflow measurement device was randomly assigned to one of the small trees and one of the big trees of each plot. The tipping-bucket rainfall gauges (Pronamic Professional Rain Gauge) have an orifice of 200 cm^2, and the totaliser rainfall gauges have an orifice of approximately 125 cm^2 and maximum storage capacity of nearly 185 mm. The automated stemflow measurement devices comprise balancing tipping buckets with a capacity of up to 650 ml per tip, and the tanks have a maximum storage capacity of 50 or 65 l. The rainfall and stemflow tipping buckets are linked up to ONSET Hobo Event Loggers. Field measurements of gross rainfall, throughfall and stemflow commenced on November 15 2002 and, in case of rainfall, are carried out at about weekly intervals.
The results for the sparse Gash model are obtained following Valente et al. (1997), including for derivation of the model parameters of canopy storage capacity (method of Leyton et al) as well as trunk storage capacity and stemflow partitioning coefficient (modified method of Gash and Morton). An exception are the mean evaporation estimates, which were obtained using the linear regression method between gross rainfall and interception for selected events (e.g. Llorens 1997).

RESULTS & DISCUSSION

Whilst rainfall, throughfall and stemflow data collection has just now completed its second year, the present paper focuses on the measurement results over the first year and in particular on the modelling results over the first three months. Table 2 summarizes the measurement results of these first three months. In the case of the eucalypt plot, the period from December 27 2002 to January 3 2003 could not be taken into consideration due to overflow of the totaliser rainfall gauges (i.e. throughfall exceeding 185 mm). In the case of the pine site, however, the inclusion of the data from this period has but a minor influence on the relative distribution of gross rainfall over the three forest components. In view of this limited influence (on the overall gross rainfall partitioning as well as on the other aspects presented here), the data from the 27/12/2002-03/01/2003 period were not either simply excluded from further analysis, or, alternatively, deemed candidate outliers as perhaps justified by the extreme gross rainfall value and the remarkably high interception value possibly reflecting an overestimation of gross rainfall. Not taken into consideration for Table 2 are further rainfall events (being defined as preceded and followed by a dry period of at least three hours) with a gross rainfall ≤0.4 mm as well as events that proved somehow doubtful (e.g. suspected failure of data logger or tipping-bucket equipment).

Table 2: Summary of rainfall and interception data from November 15, 2002 to February 21, 2003. For 20x20 m plots in a eucalypt and a Maritime Pine stand

Period	Gross rainfall	Throughfall		Stemflow		Interception	
Stand	(P_{gross}) (mm)	(mm)	(% P_{gross})	(mm)	(% P_{gross})	(mm)	(% P_{gross})
Period 1:							
15/11/2002 – 21/02/2003, excluding 27/12/2002 - 03/01/2003							
Eucalypt	1002	871	87	37	4	94	9
Pine	998	756	76	70	7	172	17
Period 2:							
15/11/2002 – 21/02/2003							
Pine	1243	922	74	92	7	229	19

The partitioning of gross rainfall in the eucalypt stand is remarkably similar to that reported by Valente et al (1997) for a Eucalyptus globulus stand in a more southern part of Portugal. The same is true in comparison to the eucalypt stand studied by Crockford and Richardson in southeastern Australia (Arnell, 2002). In the case of Pinus pinaster, the comparison with Valente et al. (1997) is somewhat less favourable. Whereas interception amounted to practically the same fraction of gross rainfall (16%) as reported here, stemflow was noticeably lower (<1 %). This difference in stemflow may well involve several factors including the rather distinct rainfall regimes and study durations (gross rainfall of 935 mm over a period of almost 2.5 years) as well as stand characteristics (e.g. tree age of 60 years, tree density per ha of 312). From the compilation in

Valente (1999) stemflow in pine stands would appear to be in general rather negligible (<2 % of the gross rainfall) but, according to Arnell (2002), in a Pinus radiata stand in southeastern Australia stemflow even exceeded that reported here (i.e. 9%).

The modelling results obtained using LISEM's interception module and the sparse variant of the Gash model are resumed in Table 3. LISEM noticeably underestimates overall interception for both stands. As is clear from Figure 1, underestimation of interception is particularly manifest for the larger rainfall events exceeding the interception plateaus that, as explained before, is inherent to Aston's equation. A single major rainfall event – i.e. that of January 2 2003, totalling nearly 200 mm - also helps explain the higher degree of underestimation in the case of the pine stand compared to the eucalypt stand, the event not being included in the eucalypt data set due to the already referred overflow of the rainfall gauges. The actual plateau values of 2.7 and 1.7 mm interception are earlier too high than too low. Valente et al. (1997) obtained canopy storage capacity estimates of 0.4 and 0.2 mm for their pine and eucalypt stands, respectively, and which compared well with the ranges of 0.25-1 and 0.2-0.8 mm the authors compiled from literature for pine and eucalypt forests.
The sparse Gash model gives remarkably good overall results for the pine plot in particular (Table 3). For the individual rainfall events, however, there is a definite tendency for the model to overestimate interception for the smaller rainfall events on the one hand and, on the other, to underestimate it for the larger events (Fig. 2). Underestimation for the larger events is even so less marked than in the case of LISEM. The preliminary nature of the sparse Gash results in particular must be stressed, though, and a more rigorous model assessment is being planned using, unlike is the case here, independent data sets for estimation of model parameters and for evaluation of modelling results.

Table 3: Summary of interception modelling results for the period from November 15, 2002 to February 21, 2003 for 20x20 m plots in a eucalypt and a Maritime Pine stand

Model	Measured	Modelled					
	Gross rainfall	Throughfall		Stemflow		Interception	
Stand	(P_{gross}) (mm)	(mm)	(% P_{gross})	(mm)	(% P_{gross})	(mm)	(% P_{gross})
LISEM							
Eucalypt [2]	1002	-	-	-	-	44	4
Pine	1243	-	-	-	-	78	6
Sparse Gash							
Eucalypt [2]	1002	831	83	11	1	160	16
Pine	1243	924	74	73	6	245	20

Quite unexpectedly, in the eucalypt as well as the pine stand total gap rainfall over the initial three months was roughly 10% lower than total below-canopy rainfall. In both stands, this difference was due to consistently lower averages of gap than below-canopy throughfall for the individual read-out periods of the totaliser rainfall gauges (n = 9-10). In fact, the overall difference of about 10% as well as the recurrent nature of this spatial pattern in throughfall also applies to the entire first year of data collection (i.e. November 15, 2002 to November 18, 2003) (Fig. 3). In the case of the pine stand, a mere two out of 29 read-out periods with over 10 mm of rainfall do not have a higher below-canopy than gap throughfall. In the case of the eucalypt stand, there is not even a single exception amongst of 32 read-out periods. A possible explanation for the systematic differences in gap and below-canopy throughfall is that rainfall in the study area is predominantly wind-driven, with rainfall striking the forest canopy at an angle creating lateral rain shadows. Apparently, the importance of non-vertical rainfall has been addressed in very few interception studies - exceptions being Herwitz and Slye (1995) and Levia and Frost (2003) - but is now becoming increasingly recognised. In the case of the eucalypt stand especially, also lateral movements of the tree canopies themselves due to the pronounced flexibility of the trunks may need to be taken into consideration. A simple solution for modelling interception under inclined rainfall conditions, using LISEM and the sparse Gash model, would seem to pass through temporal series of canopy photography, allowing dynamical estimates of crown cover. Even so, a next generation of rainfall gauges also recording the rainfall's energy and angle would seem to be crucial for a better knowledge and understanding of interception in forests in particular.

[2] Excluding the period from December 27 2002 to January 3 2003 (see Table 2 and accompanying text).

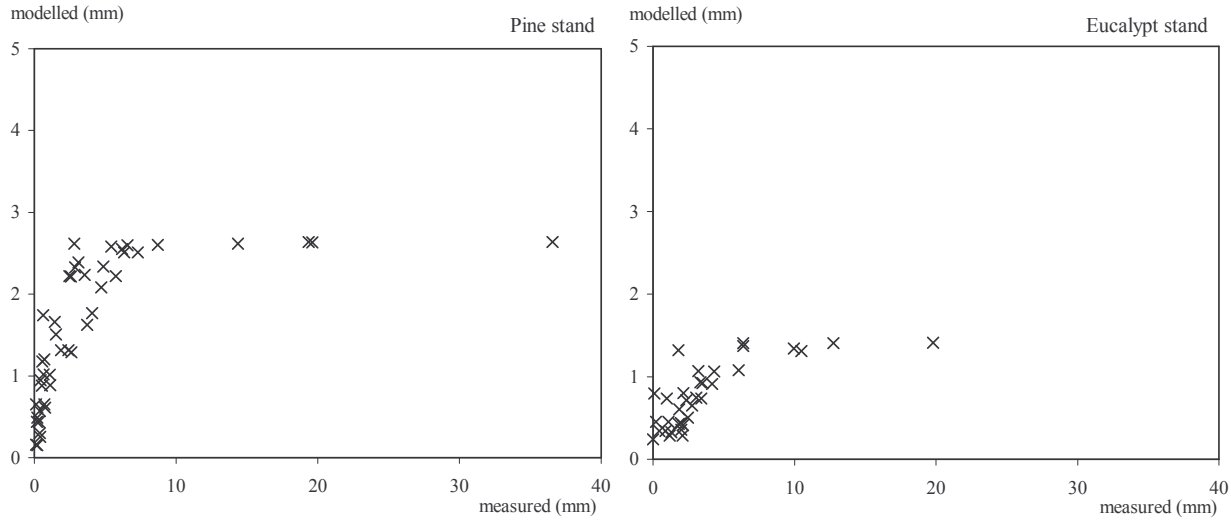

Fig 1: Interception measured and modelled, using LISEM, for individual rainfall events between November 15, 2002 and February 21, 2003 in a eucalypt and a Maritime Pine stand.

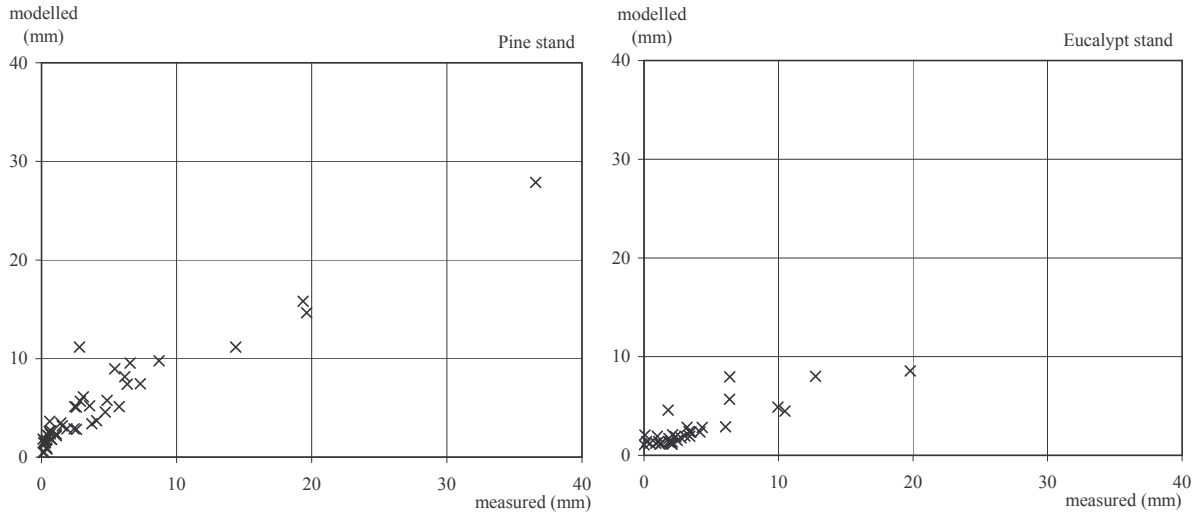

Fig 2: Interception measured and modelled, using the sparse Gash model, for individual rainfall events between November 15, 2002 and February 21, 2003 in a eucalypt and a Maritime Pine stand.

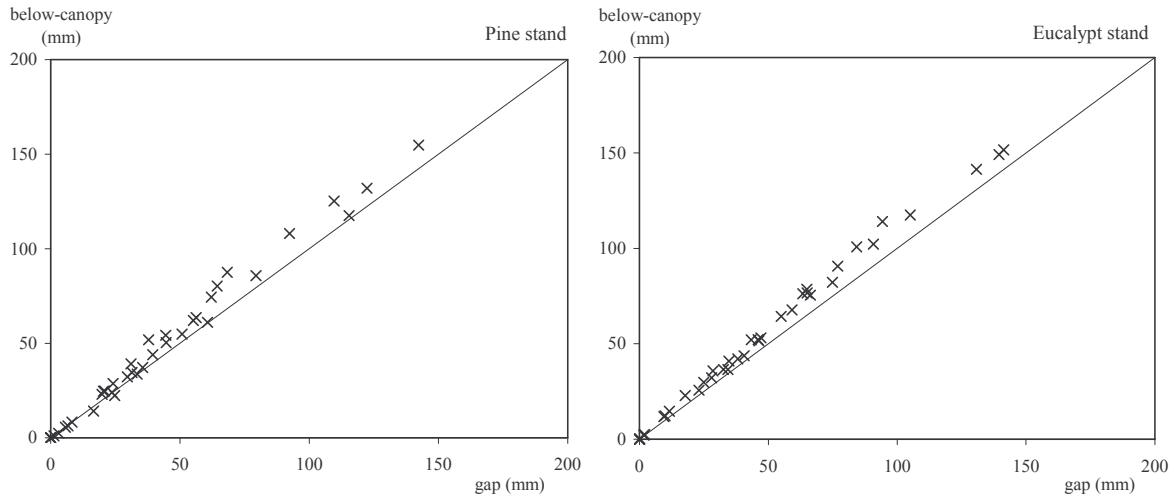

Fig 3: Average throughfall in gaps and below canopies for individual, about weekly read-out periods between November 15, 2002 and November 18, 2003 in a eucalypt and a Maritime Pine stand.

ACKNOWLEDGEMENTS

This work has been partially funded by the European Commission, under the contract ICA3-2000-30005, but does not necessarily reflect the Commission's view and in no way anticipated its future policy in this area. Also the funding by the Research Institute of the University of Aveiro and the Portuguese National Foundation for Science and Technology (FCT: SFRH/BPD/14608/2003), through post-graduate fellowships attributed to the first author, is gratefully acknowledged. Much appreciated is also the help from our colleagues Anne-Karine Boulet and António Ferreira as well as from our Erasmus trainees of the Hogeschool Zeeland, Jos Kruit, Niels van Eybergen, Robin Smallegange and Wouter Quist.

REFERENCES

N. Arnell (2002). Hydrology and global environmental change. Prentice Hall-Pearson Education, Harlow.

A.R. Aston (1979). Rainfall interception by eight small trees. *Journal of Hydrology* 42, 383-396.

C.O.A. Coelho, A.J.D. Ferreira, A.-K. Boulet and J.J. Keizer (2001). Impacto das mudanças nos usos do solo e da variabilidade da precipitação sobre a resposta hidrológica de pequenas bacias hidrográficas florestadas. *In*: Andresen, T., Coelho, C., Arroja, L. & Miranda, A.I. (eds.), *VII Conferência Nacional sobre a Qualidade do Ambiente,* pp. 251-265. (Grafigamelas, Aveiro).

A.P.J. De Roo and V.G. Jetten (1999). Calibrating and validating the LISEM model for two data sets from The Netherlands and South Africa. *Catena* 37, 3-4, 477-494.

A.P.J. Roo and V.G. Jetten, C.G.H. Wesseling and C.J. Ritsema (1995). LISEM: a physically-based hydrological and soil erosion catchment model. *In*: Boardman, J. & Favis-Mortlock, D. (eds.), *Modelling soil erosion by water*, NATO ASI Series, Ser. I, Global environmental change, Vol. 55, pg. 429-440 (Springer Verlag, Berlin Heidelberg).

A.J.D. Ferreira, C.O.A. Coelho, R.A. Shakesby and R.P.D. Walsh (1997). Sediment and solute yield in forested ecosystems affected by fire and rip-ploughing techniques - central Portugal: a plot and catchment analysis approach. *Physics and Chemistry of the Earth* 22, 3-4, 309-314.

S.R. Herwitz and R.E. Slye (1995). Three-dimensional modelling of canopy tree interception of wind-driven rainfall. *Journal of Hydrology* 168, 205-226.

J. Von Hoyningen-Huenes (1981). Die Interzeption des Niederschlags in Landwirtschaftlichen Pflanzenbeständen. Arbeitsbericht Deutscher Verband für Wasserwirtschaft und Kulturbau, DVWK, Braunschweig.

D.F. Levia and E.E. Frost (2003). A review and evaluation of stemflow literature in the hydrological and biogeochemical cycles of forested and agricultural ecosystems. *Journal of Hydrology* 274, 1-4, 1-29.

P Llorens (1997). Rainfall interception by a Pinus sylvestris forest patch overgrown in a Mediterranean mountainous abandoned area: II. Assessment of the applicability of Gash's analytical model. *Journal of Hydrology* 199, 346-359.

R.A. Merriam (1960). A note on the interception loss equation. *Journal Geophysical Research* 65: 3850-3851.

J.M.C. Pereira, M. Tomé, M.B. Carreiras, J.A. Tomé, J.S. Pereira, S. David and A.M.D. Fabião (1997). Leaf area estimation from tree allometrics in Eucalyptus globulus plantations. *Canadian Journal of Forest Research* 27, 166-173.

A. Porté, A. Bosch, I. Champion and D. Lousteau (2000). Estimating the foliage area of Maritime pine (Pinus pinaster Aït.) branches and crowns with application to modelling the foliage area distribution in the crown. *Annals of Forest Science* 57, 73-86.

R.A. Shakesby, D. Boakes, C.O.A. Coelho, J.B. Gonçalves and R.P.D. Walsh (1996). Limiting the Soil Degradational Impacts of Wildfire in Pine and Eucalyptus Forests in Portugal. *Applied Geography* 16, 4, 337-355.

F. Valente, J.S. David and J.H. Cash (1997). Modelling interception loss for two sparse eucalypt and pine forests in central Portugal using reformulated Rutter and Gash analytical models. *Journal of Hydrology* 190, 141-162.

F. Valente (1999). Intercepção da precipitação em povoamentos florestais esparsos. *PhD thesis*. Instituto Superior de Agronomia, Universidade Técnica de Lisboa, Lisboa.

R.P.D. Walsh, C.O.A. Coelho, R.A. Shakesby and J. Terry (1992). Effects of land use management practices and fire on soil erosion and water quality in the Águeda River Basin, Portugal. G*eoÖko Plus* 3,15-36.

A METHOD FOR DETERMINING FLOOD HYDROGRAPHS IN SMALL RIVER BASINS

P. Mita, C. Corbus and S. Matreata

National Institute of Hydrology and Water Managemen,t 97, Bucuresti-Ploiesti street – Bucharest – Romania
e-mail Pompiliu Mita: pompiliu.mita@hidro.ro
e-mail Ciprian Corbus: corbus@hidro.ro
e-mail Simona Matreata: simona.matreata@hidro.ro

ABSTRACT

The method proposed in this paper for determining flood hydrographs in small river basins is based on using certain relations between the main elements of the flood wave - maximum discharge, time of the rising limb and time of the recession limb of the hydrograph - and the characteristics of the rain that determines them. To determine the shape of the flood wave, the method used is based on the increase and decrease gradients of the rising and then falling limb of the hydrograph.
Such relations, which are the base of the method structure, were obtained for three representative basins: Iedut, Moneasa, Tinoasa - Ciurea, situated in different geographical areas, where there are considerable differences in the natural factors: soil, geology, relief, vegetation.
Simulations of some observed floods show that the method is viable and that the relational data for all these basins demonstrates a high degree of accuracy.

Key words: characteristics of flood hydrographs, characteristics of the rain, increase and decrease gradients.

INTRODUCTION

The method is based upon the relationships between the main characteristics of the flood hydrographs (maximum discharge, time of rising limb and time of recession limb) and the characteristics of the rain that determines the floods: quantity, duration and intensity of rain.

These relationships have been obtained for Iedut and Moneasa representative basins located in the western part of Romania and Tinoasa Ciurea representative basins located in the eastern part of Romania (Fig. 1).

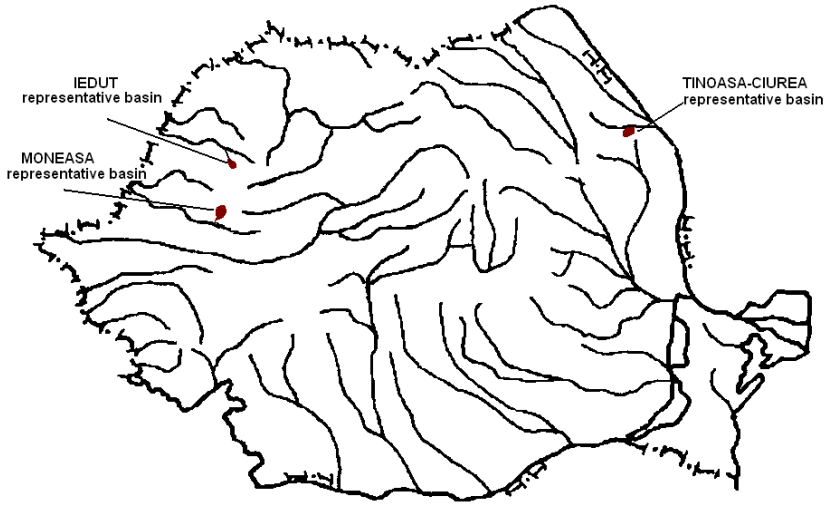

Fig. 1: The analyzed hydrographic areas.

In this paper, the method for determining flood hydrographs for the Iedut representative basin only is presented.

The Iedut representative basin is located in the Bihor Mountains of Romania and has the following morpho-hydrographic elements: area – 3.33 km^2; soil type – forest brown and brown-reddish; basin slope – 26%; forest cover – 23%. There are 3 gauging stations. The areas of the sub-basins are: 0.72 km^2, 2.41 km^2 and 3.33 km^2.

To analyse the dependence of the main characteristics of the flood waves on precipitation characteristics in the case of the Iedut River, more than 30 flood waves in the period 1975-2002 were processed. Some of these floods are characterized by their high maximum discharges. For example: on July 14, 1991, the maximum discharge was Q_{max} = 24.7 m^3/s for the 2.41 km^2 sub-basin (specific discharge q_{max} = 10,250 l/s km^2), in 1971, Q_{max} = 22.5 m^3/s (q_{max} = 9,340 l/s km^2). The discharge of July 14, 1991 was estimated at a 2-3% exceedence probability.

THE RELATIONS USED TO DETERMINE THE FLOOD WAVES CHARACTERISTICS AND CHARACTERISTIC MOMENTS

The flood wave and rainfall characteristics, which are used in the relations presented below, are shown in Figure 2.

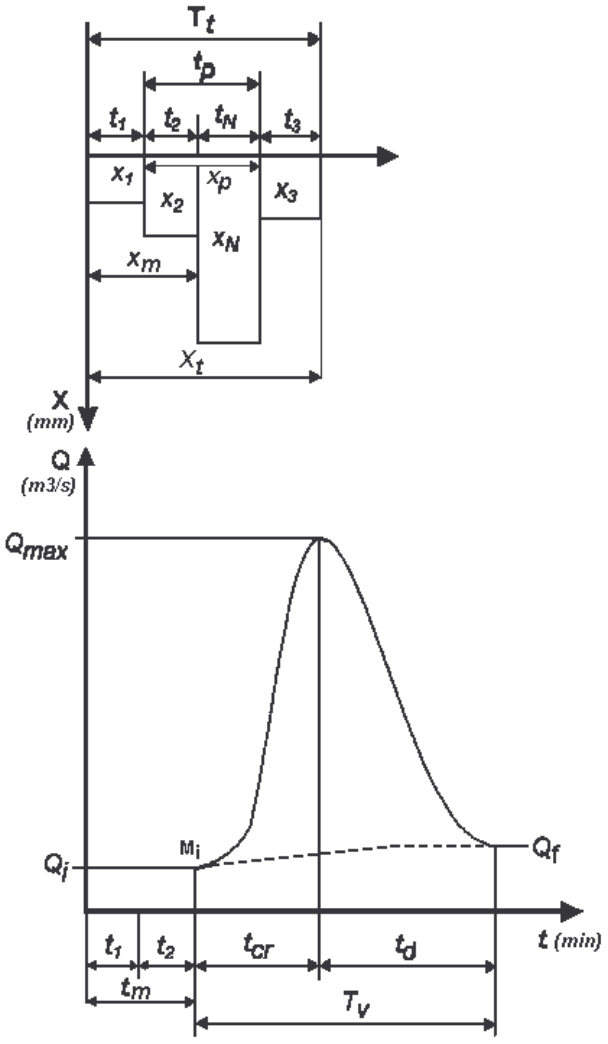

t_{cr}, t_d, T_v – time of rising limb, time of falling limb of the hydrograph and total duration of flood (min);
Q_{max} – the maximum discharge of the flood (m^3/s);
Q_i, Q_f – initial and final discharge (m^3/s);
M_i - the time the flood begins;
t_1 – the interval in which the total infiltration from the beginning of the rain is produced (min);
t_2 – the time interval between the end of the interval t_1 and the beginning of the flood event (min);
t_N – the duration of the rainfall nucleus (min);
t_3 – the time interval between the end of the rainfall nucleus and the end of the rainfall (min);
t_m – the time interval between the beginning of the rainfall and the beginning of the flood (min);
t_p - the interval between the end of the interval t_1 and the end of rainfall nucleus (min);
T_t – total duration of the rainfall (min);
x_1, x_2, x_N, x_3, x_m, x_p, X_t – amount of rain (mm) fallen during the intervals t_1, t_2, t_N, t_3, t_m, t_p, T_t. (min).

Fig. 2: Flood wave and rainfall characteristics.

The relations between the characteristics of the flood hydrograph and the characteristics of the rain, which are presented in this paper, were obtained for the Iedut River at Station 1 (area – 2.41 km^2).

To establish *the beginning moment of the flood, M_i*, the relation $t_m = f(i_m, API_{10})$ is used, where: t_m (min) is the interval between the beginning of the rainfall and the beginning of the flood, i_m (mm/min) – the intensity of the precipitation fallen in the t_m interval and API_{10} (mm) – the antecedent precipitation index of 10 days before, computed with an API model (Fig. 3).

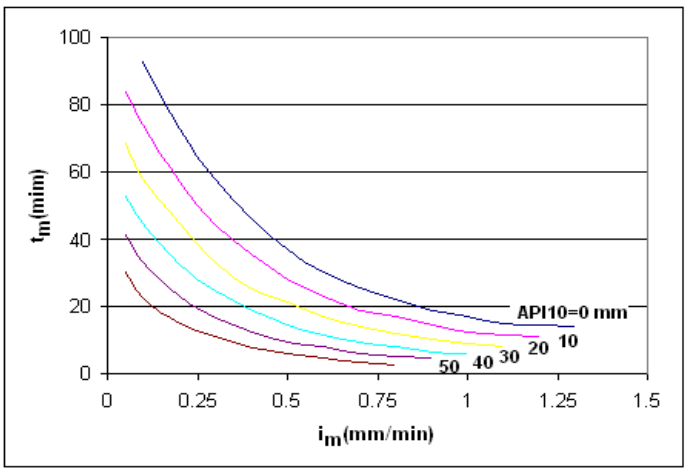

Fig. 3: Relation $t_m = f(i_m, API_{10})$ from the Iedut river, at station 1.

From this relation it can be seen that the flood begins faster as values of i_m (mm/min) and API_{10} (mm) are larger.

The *maximum discharge of the flood*, Q_{max} (m^3/s) is obtained from the relation $Q_{max} = f(i_p, t_p)$ (Fig. 4) where, i_p(mm/min) is the intensity of the x_p precipitation in the t_p time interval; $x_p = x_2 + x_N$ (Fig. 2).

The infiltration volumes, x_1, have been determined in one other study related to the antecedent precipitation, at the same time as the duration interval t_1(min) which they produced (Mita and Muscanu, 1986).

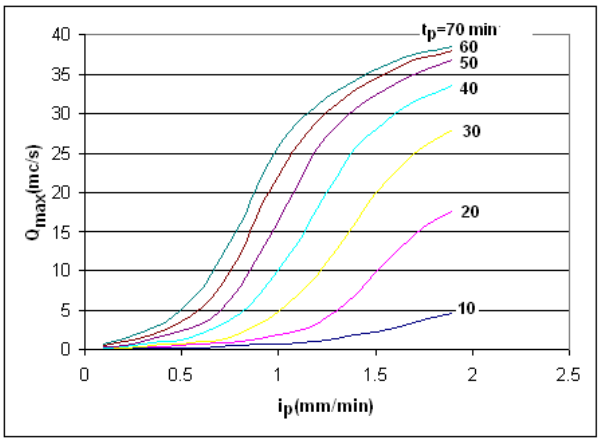

Fig. 4: Relation $Q_{max} = f(i_p, t_p)$.

From the relation presented in Figure 4, it can be seen that at equal values of i_p (mm/min) the discharge increases as the t_p interval increases. This increase is important until t_p = 40-45 min. The explanation is that this time interval corresponds with the time of concentration of the river basin. When t_p is of longer duration, the increase of discharge is less important.

In order to determine *the time of the rising limb of the hydrograph, t_{cr}*, relations have been derived between this characteristic t_{cr} and t_p duration (Fig. 5).

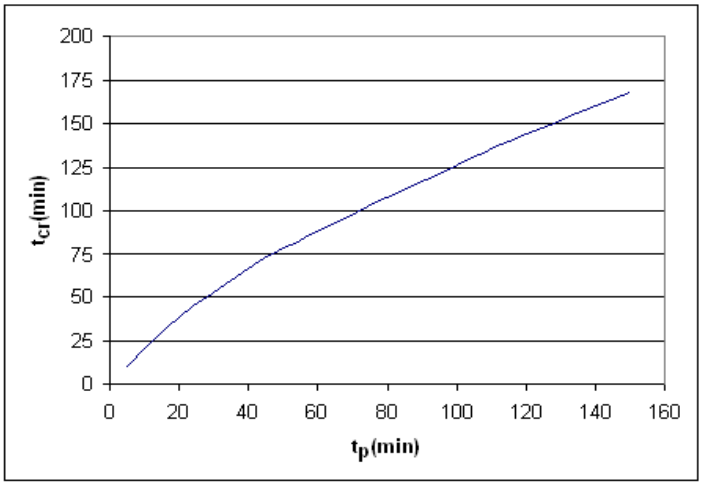

Fig. 5: Relation $t_{cr} = f(t_p)$.

From this relation it turns out that t_{cr} increases at longer t_p durations. The quantity of precipitation does not influence the t_{cr} duration (Mita and Corbus, 1996).

In order to determine *the shape of the rising limb of the hydrograph*, the increase gradient of the rising limb was determined, G_{cr} ($m^3/s/min$), using larger observed floods. The increase gradient, G_{cr}, of the interval between the beginning of the flood and Q_{max} has been computed as: $G_{cr} = (Q_t-Q_i)/t$ ($m^3/s/min$), where t is the time interval between the moment of beginning of the flood and a certain moment on the rising limb of the hydrograph.

Figure 6 shows the G_{cr} variation where the various values of i_p are determined for t_p = 40 min (when t_{cr} = 70 min – Fig. 5).

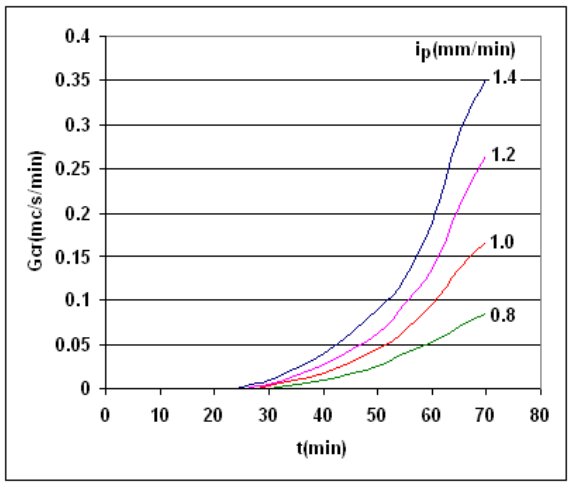

Fig. 6: Relation $G_{cr}(m^3/s/min) = f(t, i_p)$.

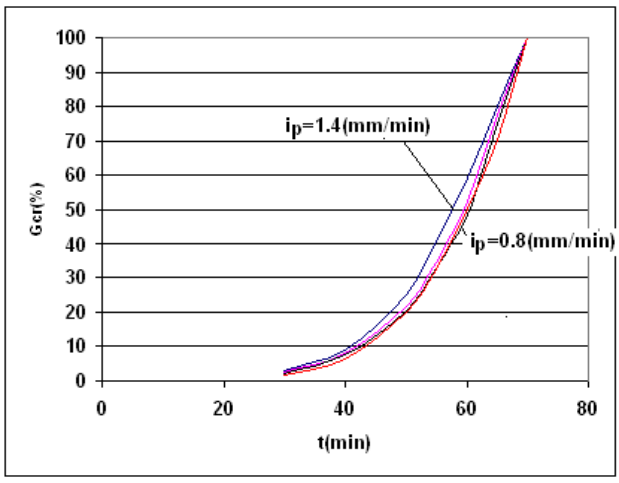

Fig. 7: Relation $G_{cr}(\%) = f(t, i_p)$.

This relation shows the increase of the G_{cr} values with the increase of the precipitation intensity, i_p.

To use these relations in practice, the gradient of increase of the discharges $G_{cr} = f(t, i_p)$ in Figure 6 was transformed to the relation $G_{cr}(\%) = f(t, i_p)$ as shown in Figure 7, where $G_{cr}(\%) = Q_t/Q_{max}*100$. This was done for the various i_p values, but the influence of i_p appears very small. By means of this relation it is possible to determine the discharge as a percentage of Q_{max}, which can be obtained after a certain time interval.

To determine *the time of the falling limb of the hydrograph from peak to final discharge (fig 2),* t_d, the relation $t_d = f(i_p, t_p)$ was obtained (Fig. 8).

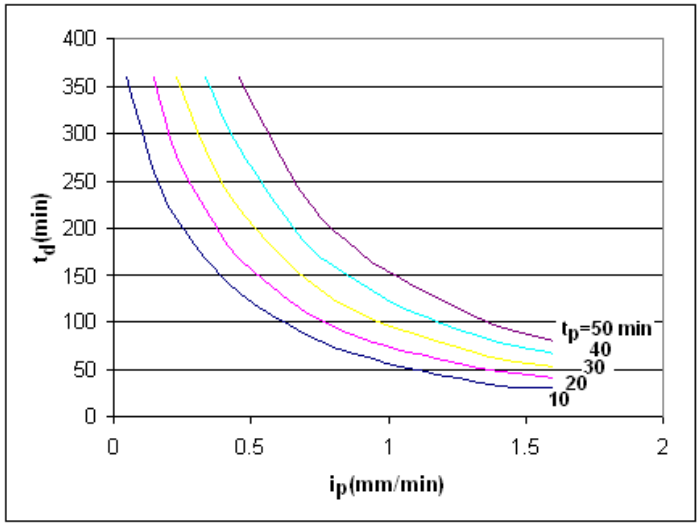

Fig. 8: Relation $t_d = f(i_p, t_p)$.

From this relation it turns out that the t_d values increase with the increase of the i_p and t_p values (Mita and Corbus, 1998).

To get a relation of *the shape of the falling limb of the hydrograph*, the gradient of decreasing discharge is computed, G_d ($m^3/s/min$) from the interval between the occurrence of maximum observed discharge and the end of the flood at time t_d. In Figure 9 the G_d variation is presented for the various i_p values of the t_p = 40 min curve. $G_d = (Q_{max}-Q_t)/t$ ($m^3/s/min$), where t is the time interval between the moment of the maximum discharge and a certain moment on the falling limb of the hydrograph.

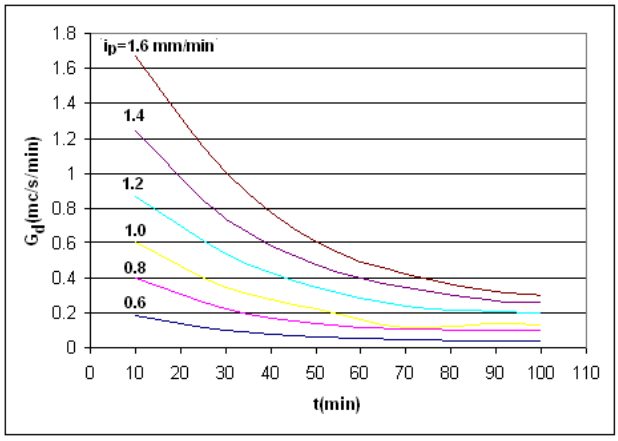

Fig. 9: Relation G_d ($m^3/s/min$)= $f(t, i_p)$.

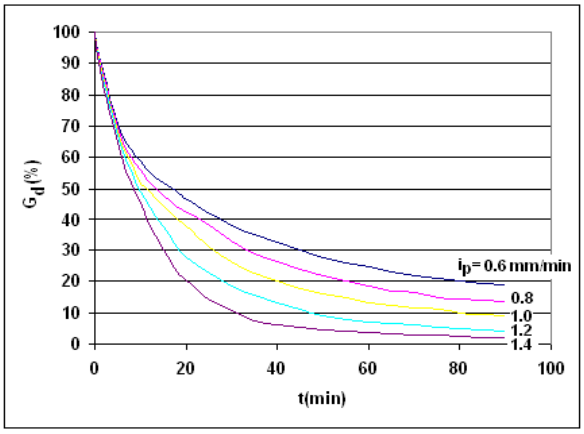

Fig. 10: Relation $G_d(\%) = f(t, i_p)$.

Furthermore, to make practical use of the relations obtained, from the decrease gradient of the discharges $G_d = f(t, i_p)$ in Figure 9, the relation $G_d(\%) = f(t, i_p)$ was computed as presented in Figure 10 - $G_d(\%) = (Q_t/Q_{max})*100$. This was also established for the various i_p values. By means of this relation it is possible to determine, as a percentage of Q_{max}, the discharge that can be obtained after a certain time interval.

APPLICATION

An example of a practical application of the proposed method is presented for the floods of July 14, 1991 and July 24, 1995 observed in the Iedut representative basin at Station 1.

The input data for both selected floods are: API_{10} = 5 mm, X_t = 66 mm, T_t = 64 min, i_m = 0.55 mm/min and API_{10} = 10 mm, X_t = 46 mm, T_t = 55 min, i_m = 1.2 mm/min. Given the rainfall characteristics and API_{10}, the elements that characterize the hydrographs corresponding to the surface runoff are computed. The computed values of these elements are: Q_{max} = 23.9 m^3/s, t_{cr} = 71 min, t_d = 102 min and Q_{max} = 14.5 m^3/s, t_{cr} = 54 min, t_d = 66 min.

Figure 11 shows the simulated and observed floods from July 14, 1991 and July 24, 1995.

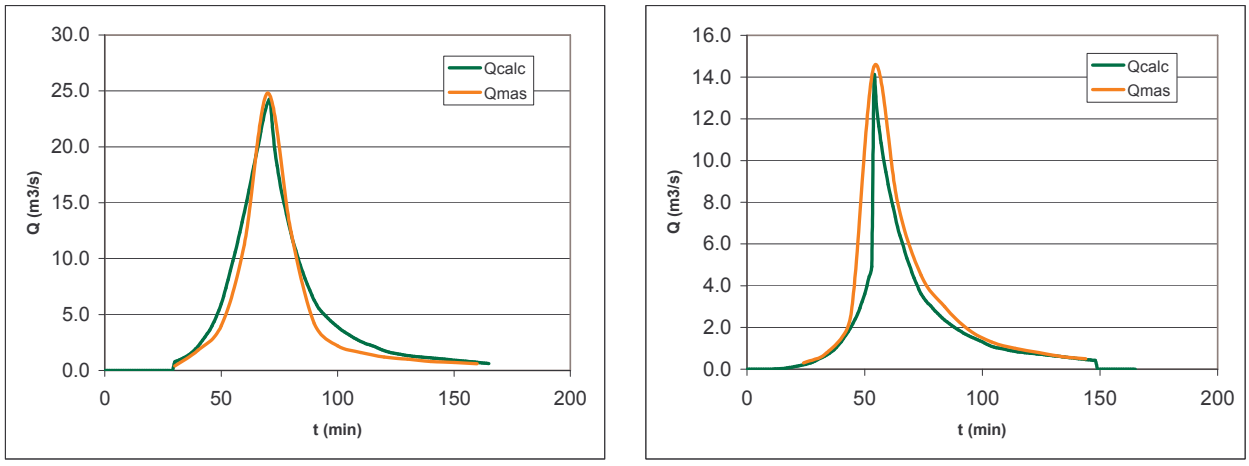

July14, 1991 July 24, 1995

Fig. 11: The simulated and observed floods.

The close correspondence of the characteristics of flood waves simulated with the recorded ones show that the proposed method was well chosen for computing flood waves in small basins.

CONCLUSIONS

- The high quality data from the representative basins led to close relations between the flood wave elements and the precipitation characteristics. The simulations carried out for some observed floods prove this and also the method's viability.
- The characteristics of the flood waves, obtained by means of the relations with the characteristics of the rain, could be useful for the elaboration of hydrological forecasts for large rivers by using rainfall-runoff models applied in small sub-basins as representative basins. Further, the elements of the flood waves obtained for selected representative basins could be used in water management practices.
- The relations between the flood elements and the precipitation characteristics obtained in the case of large basins areas (for example gauging stations of the Moneasa representative basins) proved the method's viability for areas up to 70 – 80 km^2 too.
- As is the case for any method of simulating hydrograph characteristics, accurate meteorological data plays a decisive role.

REFERENCES

Diaconu, C. (1976). Flood forecasting based on warning small basins. *Meteorology and Hydrology, no.* 1, Bucharest, Romania.

Mita, P., Muscanu, M. (1986). Runoff coefficients in small basins. *Studies and Research, Hydrology*, 53, NIMH, Bucharest, Romania.

Mita, P., Corbus, C. (1998). A model for determining flood waves in small basins up to 100 km^2. *Proceedings of seventh conference of the European Network of Experimental and Representative Basins,* Liblice, Czech Republic.

FORECASTING RUNOFF WITH ARTIFICIAL NEURAL NETWORKS

M. Neruda[1], R. Neruda[2] and P. Kudova[2]

[1]*Faculty of Environmental Studies, University of J. E. Purkyne in Usti nad Labem, Czech Republic*
[2]*Institute of Computer Science, Academy of Sciences of the Czech Republic, Prague*
e-mail Martin Neruda: neruda@fzp.ujep.cz

ABSTRACT

This paper presents the results of rainfall-runoff modelling with artificial neural networks. The Northern Bohemia River Ploucni was chosen as an experimental catchment for model calibration and evaluation. Two types of networks were used: multilayer perceptrons and radial basis function networks, with several architectures and training algorithms. Most networks could provide a reasonable model, the generalization capabilities of which were evaluated on previously unseen data. Multilayer perceptrons performed better, in general; the best results achieved were with a network with 3 hidden layers containing 5, 7, and 9 perceptrons.

Key words: artificial neural networks, rainfall-runoff modelling, multilayer perceptron, Radial Basis Functions (RBF).

INTRODUCTION

The River Ploucnice Valley from its origin to the town of Mimon was chosen to perform the modelling experiments described in this paper. The River Ploucnice originates from the southwest part of the Jested hill, at an altitude of 654 metres above sea level and flows into the River Elbe at the town of Decin at 122 metres above sea level (Farsky, 1999, 2001). Total catchment area is 1193.9 km^2, the area from river origin to Mimon being 267.9 km^2, and flow length 106.2 km. The above mentioned basin part was chosen because of the existence of a water stage recorder in the town of Mimon, as well as the availability of historical rainfall data for the region under review.

The following two tables illustrate the flow situation of the River Ploucnice. Table 1 presents *maximum annual flood flows (MAF)* for a given return period, and Table 2 daily flow duration curve (data are provided by the Czech Hydrometeorological Institute (CHMU) of Usti nad Labem). *MAF* values derive partly from empirical frequencies and partly from statistical probability fitting.

Table 1: The River Ploucnice at Mimon: Maximum annual flood flows (MAF) for given return period

Return period (in years)						
1	2	5	10	20	50	100
MAF (m^3s^{-1})						
21.7	31	45	57	70	88	103

Table 2: The River Ploucnice at Mimon: Daily flow duration curve

Duration (in days)												
30	60	90	120	150	180	210	240	270	300	330	355	364
Daily flow (m^3s^{-1})												
4.47	3.29	2.68	2.28	1.98	1.75	1.56	1.39	1.24	1.1	0.96	0.81	0.7

METHODOLOGY

Feed-forward artificial neural networks were used as the rainfall-runoff modelling tool. These networks represent a state-of-the-art approach for implementing an arbitrary input/output function. An important property of the neural network is its ability to learn the function from examples of input and desired output data, as its biological counterpart (Sima, Neruda, 1997). The use of neural networks in hydrology is not a new topic and an extensive overview of the subject is at Govindaraju R. S., Rao A. S., (2000). Together with other modern artificial intelligence techniques, such as genetic algorithms or fuzzy sets, they nevertheless still represent an alternative approach to hydrological modelling.

Two network architectures were used in this paper, namely a *multilayer perceptron (MLP)* network with perceptron units, and a *radial basis function (RBF) network* with local units (Neruda, 1995. Fig. 2). Neurons in the feed-forward network were arranged in synapsys-connected layers. Networks with one, two, or three perceptron (hidden) layers, and networks with one RBF unit layer were considered. These are typically trained by a flavour of a non-linear gradient optimization algorithm, called the error *back propagation* using either standard back propagation corresponding to a gradient descent optimization, or a back propagation enhanced with momentum term, or by the *three-step optimisation* algorithm or *regularization* as In the case of the RBF networks.

A perceptron unit as a mathematical model of a simplified neuron has $\boldsymbol{n}$ inputs and one y output (Minsky, Papert, 1969). Each i input represents a real value $\boldsymbol{x_i}$. Synaptic weight $\boldsymbol{w_i}$ is assigned to each input determining its permeability. The inner potential $\boldsymbol{\xi}$ of perceptron is then calculated as the weighted sum of its inputs. Perceptron input $\boldsymbol{y}$ is calculated from potential $\boldsymbol{\xi}$ by means of the so-called activation function σ: y=σ (ξ) (see Fig. 1a). The most common activation function is logistic sigmoid (1).

$$y = \sigma(\xi); \xi = \frac{1}{1+e^{-\xi}}; \xi = \sum_{i=1}^{n} w_i x_i \qquad (1)$$

An RBF unit computes its potential ζ by its distance from a centroid $\boldsymbol{c}$. Output y is then calculated from ζ by applying a radial function γ (Cf. Fig 1b). The most common γ function is Gaussian (2).

$$y = \gamma(\zeta); \gamma(\zeta) = e^{-\zeta^2}; \zeta = \sum_{i=1}^{n} \|x_i - c_i\| \qquad (2)$$

Two software systems were used for network training, namely the Stuttgart neural simulator SNNS 4.2, developed at Stuttgart and Tübingen University (SNNS, 2003) and the multi-agent computational intelligence system Bang developed at the Prague Institute of Computer Science (Bang, 2004).

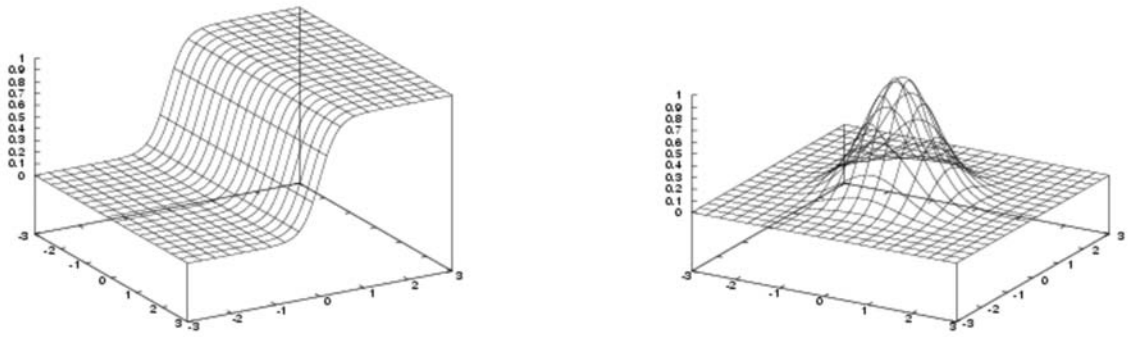

Fig. 1: a) Sigmoidal activation function of a perceptron. b) Gaussian activation function of a RBF unit.

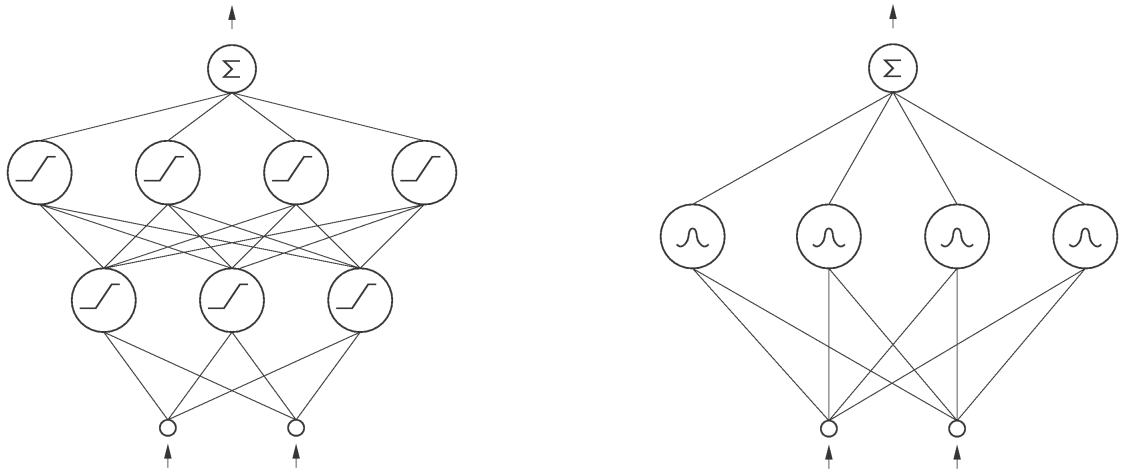

Fig. 2: a) Diagram of a 2-3-4-1 Multilayer perceptron network. b) Diagram of a 2-4-1 RBF network.

Historical data including daily flow and rainfall for the Ploucnice valley between November 1994 and April 2003 were collected. Average daily flows derive from continuous record. Next experiments are expected to use on-line forecast with 6-hours flow and rainfall data time steps. The data were been split into a *training set*, 1000 days between January 1999 and September 2001 and a *test set,* October 2001 to April 2003. Training data were used to set training network parameters and the testing set to verify network ability to model previously unseen data. The so-called *efficiency coefficient (EC)* was used for overall quantitative model performance**.**

$$EC = 1 - \frac{\sum (Q_m - Q_p)^2}{\sum (Q_m - \overline{Q})^2} \qquad (3)$$

Where Q_m … daily measured flows in water stage recorder (mm)
Q_p … daily computed flows by neural network (mm)
$\overline{Q}$ … average measured flow (mm)

EC can be in the interval between 0≤EC≤1; the bigger the value, the better the performance.

RESULTS AND DISCUSSION

Two series of experiments were completed with the MLP networks, the first one creating 1-day history models, and the second one operating with 2-day history ones. Predicting tomorrow's flow from today's values of rainfall amount and flow was attempted in the former, (Neruda M., Neruda R., 2002). This led to network architectures with 2 neurons in the input layer, 1 neuron in the output one, and possibly several hidden units with any number of neurons. These networks were denoted as: 2-5-7-1 (meaning input layer with 2 neurons, network with two hidden layers containing 5 and 7 units, and 1 output neuron), and 2-5-7-9-1 (meaning 3 hidden layers containing 5, 7 and 9 units). Rainfall and flows from two previous days were taken into consideration for 2-day history. Networks for these models were type 4-5-7-1 or 4-5-7-9-1. Experimental results are given at Table 3 and Figure 3a.

Table 3: Efficiency coefficient (EC) during MLP networks training and testing (BP is a back propagation algorithm and MBP a back propagation with a momentum term)

Architecture	Training	Testing	Architecture	Training	Testing
MLP 2-5-7-1 BP	0.87	0.86	MLP 4-5-7-1 BP	0.85	0.82
MLP 2-5-7-1 MBP	0.85	0.90	MLP 4-5-7-1 MBP	0.86	0.83
MLP 2-5-7-9-1 BP	0.89	0.92	MLP 4-5-7-9-1 BP	0.85	0.80
MLP2-5-7-9-1 MBP	0.93	0.93	MLP 4-5-7-9-1 MBP	0.86	0.79

Three RBF network types were used for RBF network experiments, namely the regular RBF, the Regularization network (RN) and the Product Kernel RN (Kudova P., Neruda R., 2005). 1-day and 2-day

history data were again considered. Rainfall for the predicted day was also considered among inputs (denoted as 1-day history+rainfall and 2-day history+rainfall, respectively in Table 4.) This value is expected to be set to reliable rainfall prediction in the case of real-time prediction. Experimental results are presented at Table 4 and Figure 3b.

Table 4: Efficiency coefficient (EC) and mean squared error in % (ERR) for RBF and RN networks

		RBF network		Regularization network (RN)		Product Kernel RN	
		training	**testing**	**training**	**testing**	**training**	**testing**
1-day history	EC	0.617	0.764	0.633	0.771	0.633	0.771
	ERR	0.059	0.049	0.057	0.048	0.057	0.048
1-day+rainfall	EC	0.609	0.756	0.834	0.579	0.633	0.771
	ERR	0.061	0.051	0.025	0.089	0.057	0.048
2-day history	EC	0.435	0.703	0.602	0.141	--	--
	ERR	0.088	0.062	0.062	0.182	--	--
2-day+rainfall	EC	0.362	0.565	0.608	0.211	--	--
	ERR	0.099	0.092	0.061	0.167	--	--

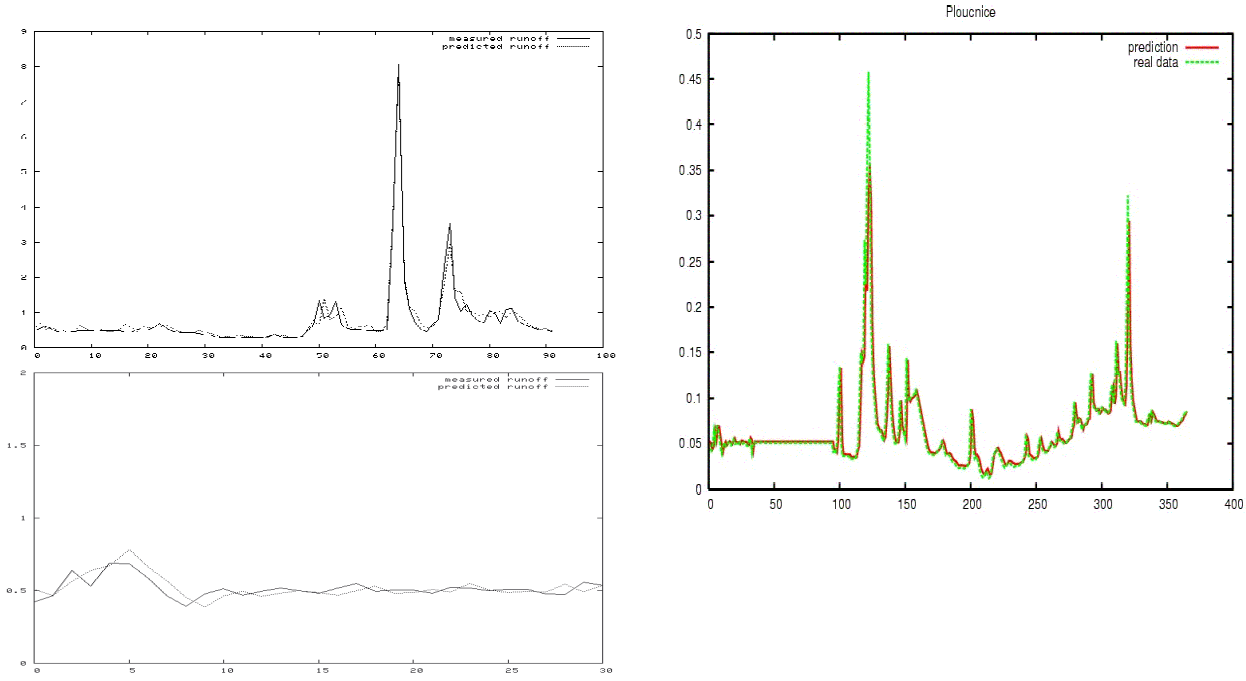

Fig. 3: A comparison of actual and predicted runoff: a) Training and testing results for the MLP network. b) Testing results for the RBF networks.

CONCLUSION

Both MLP and RBF neural networks have been shown to be used successfully for creating small rainfall-runoff models. Such models can be built from historical time series data with no previous knowledge of process underlying physics. The best results were obtained with the 2-5-7-9-1 perceptron network trained with the back propagation algorithm with a momentum term (Figure 3a) in the case under review. Two layers networks and three layers networks were more successful with the 1-day history models. Perceptron networks also achieved better general results than RBF networks. The reason for this is believed to be that networks with more free parameters tend to be over-trained more easily, thus achieving better training but

inferior testing error. Further experiments with three and more layer networks, as well as RBF networks should therefore be performed for testing different network architecture variants.

The choice of the particular architecture, including the number of hidden layers or their units is always a question of empirical knowledge combined with experiments. Conventional methods for setting free parameters values, such as full cross-validation are usually not feasible in the case in point, due to learning process complexity. The plan is to combine genetic algorithm searching for some parameters with the gradient learning of the network in the future.

Test models based on two days advance on-line forecast and more history data are also required for further experimentation. In cooperation with CHMU, the plan is to acquire data with finer steps (several hours) and make predictions based on those. Current work is with data from a smaller basin of the so-called Jestedsky potok creek, where a finer timescale is necessary.

ACKNOWLEDGEMENTS

This research work was supported by Grant Agency of the Czech Republic project 201/02/0428, and an internal grant of the Faculty of Environmental Studies, University of J.E. Purkyne in Usti nad Labem.

REFERENCES

Bang v.3.2 (2004). Home page http://www.cs.cas.cz/bang3.

Farsky I. in Mackovcin (1999). Protected areas CR, part 1. AOPK CR, Prague, pp. 26-34.

Farsky I. in Mackovcin (2001). Protected areas CR, part 3. AOPK CR, Prague, pp. 31-38.

Govindaraju R. S., Rao A. S. (eds.). Artificial Neural Networks in Hydrology, Kluwer Academic Publishers, Dordrecht, Holland, pp. 329, 2000.

Kudova P., Neruda R. (2005). Learning methods for RBF networks. Future Generation Computer Systems, Elsevier (in print).

Minsky M. L., Papert S. A. (1969). Perceptrons. MIT Press, Cambridge MA.

Neruda M., Neruda R. (2002). To contemplate quantitative and qualitative water features by neural networks method. *Plant production*, Volume 48, No. 7, ISSN 0370-663X.

Neruda R. (1995). Functional equivalence and genetic learning of RBF networks. In: Pearson D.W., Steele N.C., Albrecht R.F. (eds): Artificial neural nets and genetic algorithms. Proc. Int. Conf. Wien, Springer-Verlag: 53-56.

Sima J., Neruda R. (1997). Theoretical issues of neural networks. MatfyzPress, Charles University, Prague (in Czech).

SSNS - Stuttgart neural network simulator (2003). http://www-ra.informatik.uni-tuebingen.de/downloads/SNNS/

APPLICATION OF VARIOUS HYDROGRAPH SEPARATION TECHNIQUES IN A SANDSTONE MICRO-BASIN IN ORDER TO DETERMINE THE SPATIO-TEMPORAL ORIGIN OF STREAMWATER: PRELIMINARY RESULTS

L. Pfister[1], F. Barnich[1], L. Hoffmann[1], H. Hofmann[2], J.-F. Iffly[1], T. Kies[2], P. Matgen[1], M. Salvia[1], C. Tailliez[1] and Z. Tosheva[2]

[1]*Centre de Recherche Public – Gabriel Lippmann, 162a, av. de la Faïencerie, L-1511 Luxembourg*
[2]*Université de Luxembourg, 162a, ave. de la Faïencerie, L-1511 Luxembourg*
e-mail Laurent Pfister: pfister@lippmann.lu

ABSTRACT

Hydrograph separation techniques are suited for providing important information on the spatio-temporal variability of runoff producing processes in river basins. A very dense hydro-meteorological observation network was installed in the Huewelerbach micro-basin, located in the Grand-Duchy of Luxembourg (Europe). Recording streamgauges, piezographs, automatic samplers and conductimeters, as well as a meteorological station provide the input needed for this type of study.
In the sandstone dominated Huewelerbach micro-basin, baseflow is heavily influenced by the contributions of springs that are located at the contact line between sandstone and marls. Surface runoff, mainly on saturated areas close to the stream, largely contributes to total runoff during high flows. The contribution due to the alluvial groundwater body appeared to be relatively small during the observed events.

Key words: hydrograph separation.

INTRODUCTION

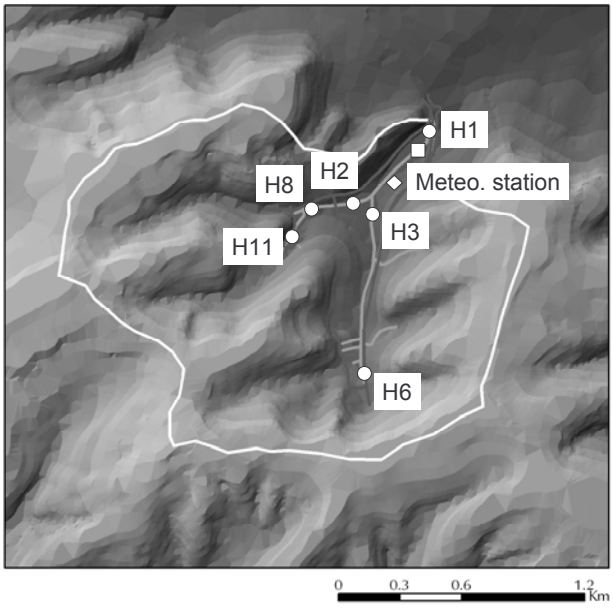

Fig. 1: Site map of the Huewelerbach basin with streamgauges and meteorological station.

Study area and objectives

The Huewelerbach micro-basin, extending over 2.7 km^2, is located in the Attert river basin, one of the major tributaries of the Alzette river (Grand-Duchy of Luxembourg, Europe). The Attert basin has been part of the ERB network since 2002. Currently, the Huewelerbach micro-basin is equipped with a permanent observation network that includes a meteorological station, three recording streamgauges located at the outlet of the basin and on both of its tributaries that are located in the upper half of the basin (Fig. 1). Three springs, located at the contact line between sandstone and marls, are equipped with recording streamgauges in the upstream part of the basin. During measurement campaigns, additional equipment consisting of automatic samplers and conductimeters are positioned near the recording streamgauges. Piezometric levels in the alluvial plain are measured via recording piezographs. Moreover, soil water samples are taken via suction cups and rainfall and throughfall are collected in raingauges. The recording time-steps vary between 5 to 60 minutes, according to the parameters that are measured.
An understanding of the origins of streamwater during a rainfall event is one of the main challenges of hillslope hydrology. Water originating from various parts of a river basin has specific chemical signals and it

contributes to streamflow through different flowpaths. Streamwater chemistry mainly depends on pathways through which water travels to the stream (Genereux et al., 1993). Knowledge of dominant flowpaths and the way they change during a rainfall event is crucial to the understanding and prediction of runoff generation and streamwater chemistry (Katsuyama, 2001). This paper presents the first results of approaches based on analytical hydrology (monitoring of surface and groundwater levels) on the one hand, and intensive hydrochemical observations on the other hand, in a sandstone micro-basin. The hydrochemical observations were analysed via the EMMA (End Member Mixing Analysis) technique, in order to quantitatively estimate the processes that control streamwater chemistry during a rainfall event.

METHODOLOGY

Hydrograph separation within the Huewelerbach micro-basin used several techniques characterised by a more or less high degree of complexity. These techniques basically consisted in:

a) Determination of the relative contributions from the two main tributaries of the Huewelerbach via the streamgauge recordings. This method is fully based on measurements made at three different locations of the stream network of the Huewelerbach and thus helps to indicate the respective amount of water coming from the two tributaries, as well as any other contribution that might occur between the three streamgauge stations.

b) Determination of the relative contribution of the various springs in the upstream area of the micro-basin. The measurements made on various springs help to evaluate their relative contribution to the runoff determined for the two major tributaries of the Huewelerbach.

c) Application of the Kliner-Knezek hydrograph separation method (Holko et al., 2002) in order to determine the contribution of the alluvial groundwater body. This method is based on the assumption that since there is a hydraulic connection between the river and its alluvial aquifer, a close relationship between groundwater and stream water levels can be expected. Groundwater runoff can thus be determined by plotting corresponding values of discharge against groundwater levels. In the resulting dotty plot, it is usually possible to draw an envelope line that actually represents the groundwater flow. This line can thus be used to determine the alluvial groundwater contribution to total streamflow, as a simple function of groundwater table levels. The envelope line is considered to consist of three different sections that represent different runoff components (i.e. alluvial groundwater, shallow groundwater and near-surface or overland flow).

d) The identification of stormflow sources and the estimation of their volumetric contributions to runoff were based on the End Member Mixing Analysis method (Christophersen et al., 1990; Hooper et al., 1990). The basic assumption of the model is that, at any given moment, the chemical composition of streamwater can be defined as the result of the linear mixing of runoff-contributing sources.
The analysed parameters comprised anions and cations (Cl^-, $NO3^-$, $SO4^{2-}$, Na^+, K^+, Mg^{2+}, Ca^{2+}), SiO_2, pH, alkalinity, UV-absorbance (254 nm), fluorescence emission and suspended solids. The component 'soil water' was characterised by analysing the water collected by suction cups. Rainfall and throughfall were collected in raingauges. Overland runoff was irregularly sampled in space and time. Spring water was both grab sampled at monthly intervals and automatically sampled during the analysed storms. Groundwater was also grab collected from a network of 21 piezometric tubes installed in the alluvial zone.

RESULTS

The preliminary results of a measurement campaign that took place from 30th April to 4th May 2003 are presented below. Total rainfall during this period amounted to 20.2 mm. Temperatures varied between 17.2 °C (day) and 1.7 °C (night) during this period.

The springs located in the Luxembourg sandstone in the upstream part of the basin showed no reaction at all to this rainfall event. Their contribution remained stable at 7 l s^{-1} (spring H8) and 0.9 l s^{-1} (spring H11). This behaviour can be considered as being quite representative of springs located in the Luxembourg sandstone, since the travel time of water through this aquifer is known to take up to several months. The recording streamgauge located some 50 meters downstream of a spring in the upstream part of the right-bank

tributary of the Huewelerbach (H6) showed a reaction to rainfall, with a rise of flow from 1.4 l s^{-1} to 4.3 l s^{-1}. Since this upstream part of the basin is characterised by soils that are always very wet, this reaction to rainfall is presumed to have been caused by surface runoff on saturated areas.

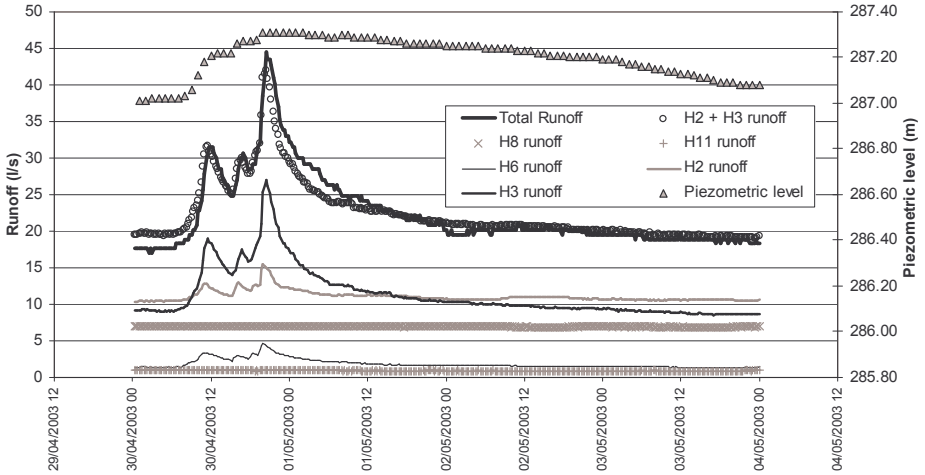

Fig. 2: Groundwater table fluctuations and contributions of tributaries (H2, H3) and springs (H6, H8, H11) to total runoff at the outlet of the Huewelerbach micro-basin.

When summed up, the contributions by tributaries H2 and H3 fit almost perfectly the total streamflow measured at the outlet of the Huewelerbach (Fig. 2). A closer analysis of the hydrographs shows that before the rainfall event, the combined contributions by the H2 and H3 tributaries are higher than the runoff measured at the basin outlet (H1). During the rainfall event, this situation is reversed, with higher runoff being observed at the outlet, compared to the combined contributions of H2 and H3. The lower part of the recession of the hydrograph indicates similar streamflow both at the outlet and by the cumulated tributaries.

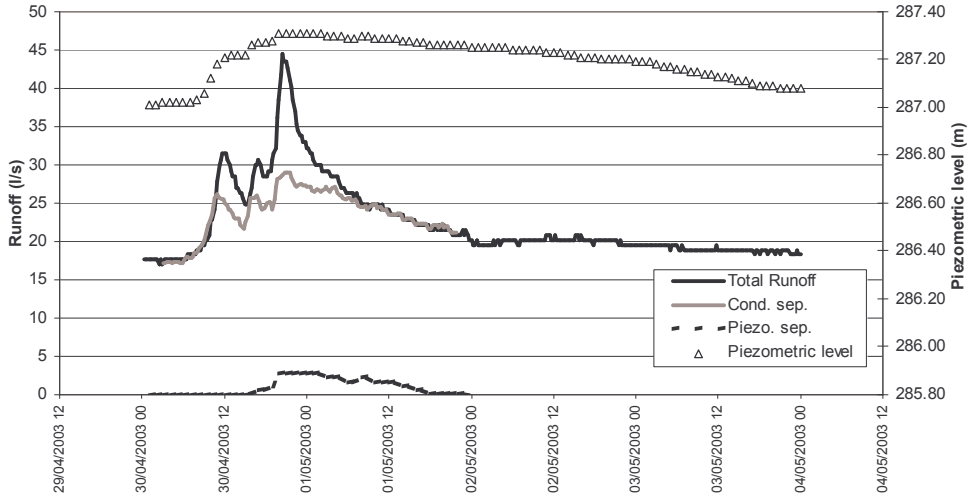

Fig. 3: Groundwater table fluctuations and contributions of new water/old water (according to EMMA) and alluvial groundwater (according to Kliner-Knezek method).

Both tributaries of the Huewelerbach, H2 and H3, reacted quite strongly to rainfall. However, it is clear that the streamflow increase is most significant in the rightbank tributary (H3). Here again, the saturation of the soils near the thalweg would seem to be the most obvious explanation. The use of electric conductivity measurements close to the basin outlet (H1) made it possible to use the End-Member-Mixing-Analysis method to determine the proportion of old water and new water in the hydrograph of the Huewlerbach. It

appeared that surface water contribution amounted to a maximum of 30% of total runoff at peak flow during this event (Fig. 3).

The analysis of piezometric levels in the alluvial plain of the Huewelerbach has shown that a threshold exists in the groundwater table fluctuations. Once this threshold is passed, either a loss of infiltration from the stream towards the alluvial groundwater body occurs, or there is an additional contribution by the groundwater body to the stream. For the piezograph located near the basin outlet, this threshold has been identified at 287.03 m.a.s.l.

The application of the Kliner-Knezek hydrograph separation indicates a contribution by the alluvial groundwater body of 174 m^3. This value is close to the positive difference of 143 m^3 between the total runoff at the outlet and the contribution of both tributaries H2 and H3. Compared to the contributions of all other processes within the basin, the alluvial groundwater appears to be the most variable in time.

CONCLUSION

The application of different hydrograph separation techniques has shown that the relative contributions of the various areas of the Huewelerbach micro-basin vary greatly in time. The alluvial groundwater body only played a minor contributing role during this event. Surface runoff proved to be an important process, as revealed by both the application of electric conductivity and the measurements made by the various recording streamgauges located on the stream network. The results obtained so far are currently being used to improve the internal consistency of conceptual rainfall-runoff models (see also Van den Bos et al. 2004).

ACKNOWLEDGEMENTS

This study was funded by the 'Fonds National de la Recherche' of the Grand-Duchy of Luxembourg. The authors also want to thank the anonymous reviewer for his helpful and constructive comments.

REFERENCES

Christophersen, N., Neal, C., Hooper, R.P., Vogt, R.D. and Anderson, S. (1990). Modelling streamwater chemistry as a mixture of soilwater end-members – a step towards second-generation acidification models. Journal of Hydrology 116, 307-320.

Holko, L., Uhlenbrook, S., Pfister, L. and Querner, E.P. (2002). Groundwater runoff separation – Test of applicability of a simple separation method under varying natural conditions. Proceedings of the 'FRIEND 2002: Fourth International Conference on FRIEND: Bridging the gap between Research and Practice'. Cape Town, South Africa. IAHS Red Book No. 274, 265-272.

Hooper, R.P., Christophersen, N. and Peters, N.E. (1990). Modelling streamwater chemistry as a mixture of soilwater end-members – an application to the Panola Mountain catchment, Georgia, U.S.A. Journal of Hydrology 116, 321-343.

Genereux, D.P., Hemond, H.F. and Mulholland, P.J. (1993). Use of Radon-222 abd calcium as tracers in a three-end-member mixing model for streamflow generation on the West Fork of the Walker Branch watershed. Journal of Hydrology 142, 167-211.

Katsuyama, M., Ohte, N. and Kobashi, S. (2001). A three-component end-member analysis of streamwater hydrochemistry in a small Japanese forested headwater catchment. Hydrological Processes 15, 249-260.

Salvia, M., Iffly, J.-F., Bouchet, A., Barnich, F., Hofmann, H., Kies, T., Tailliez, C., Tosheva, Z., Matgen, P. and Pfister L. (2004). Chemically based hydrograph separations in two experimental micro-basins of the Attert catchment. Proceedings of the 'ERB 2004 Conference: Progress in surface and subsurface water studies at the plot and small basin scale'. 172-175.

Van den Bos, R., Iffly, J.-F., Matgen, P., Salvia M., Hofmann, H., Tosheva, Z. , Kies, T. and Pfister, L. (2004). Constraining conceptual rainfall-runoff responses by incorporating imprecise tracer data information into the calibration process. Proceedings of the 'ERB 2004 Conference: Progress in surface and subsurface water studies at the plot and small basin scale'. 182-185.

EVALUATION OF UNCERTAINTY IN THE PARAMETERS OF A RAINFALL RUNOFF MODEL BY GENERALIZED KALMAN FILTERING

P. Torfs, R. Wójcik and P. Warmerdam

Wageningen University, Hydrology and Quantitative Water Management Group, Nieuwe Kanaal 11, 6709 PA, The Netherlands
e-mail Paul Torfs: Paul.Torfs@wur.nl

ABSTRACT

Fitting a rainfall runoff model to observational data never results in exact knowledge on the calibrated parameters. The best way to describe this limited knowledge is by a probability density and so-called Mixtures of Gaussians are very useful class of densities for achieving this purpose. To illustrate this, a simple linear reservoir model is fitted to the data from the small catchment of the Beerze in the Netherlands. It will be shown that new observations can be assimilated by taking conditional densities, and recursively updating parameters of the linear reservoir model by a general Kalman filtering technique. The Mixtures of Gaussians allow easy and efficient implementation of this data assimilation scheme.

Key words: uncertainty, rainfall-runoff model, non-Gaussian, Kalman filtering.

INTRODUCTION

As the rainfall runoff relation for any catchment is the result of many intrinsically complicated and not directly observable processes, our main source of knowledge of this relationship comes from fitting models to data of well observed experimental catchments. In this study, we use the data from the River Beerze in the south of the Netherlands. It is a small catchment, ≈ 240 km^2 , with 70% agricultural land, 25% forest and 5% urban area.
The average annual precipitation is about 800 mm, the average potential evapotranspiration about 500 mm. For this study, 19 years (January 1980 - December 1998) of data were available. All data were gathered on a daily scale. Both precipitation and discharge are expressed in mm/day. The top panel of Figure 1 shows the year 1998 as an example.

The model used in this study is a linear reservoir model:

$$S(n+1) = S(n) + r\,\Delta t\left(P(n) - Q(n)\right) \tag{1a}$$

$$Q(n) = \frac{1}{T} S(n) \tag{1b}$$

where $S(n)$ is the reservoir storage at the start of day n, and $P(n)$ and $Q(n)$ are precipitation and discharge rates respectively during that day and $\Delta t = 1$ day.

Although this model is extremely simple, it captures some of the most fundamental aspects of the rainfall runoff process: storage (S), reaction time (T) and runoff coefficient (r) (to calculate effective precipitation). But the model is clearly too simple: the middle panel of figure 1 shows the results of fitting one $S(0)$, T and r to one whole year of daily data. More complex (e.g. spatially distributed) models would produce better fits, this would require, however, many more parameters (1a, 1b).

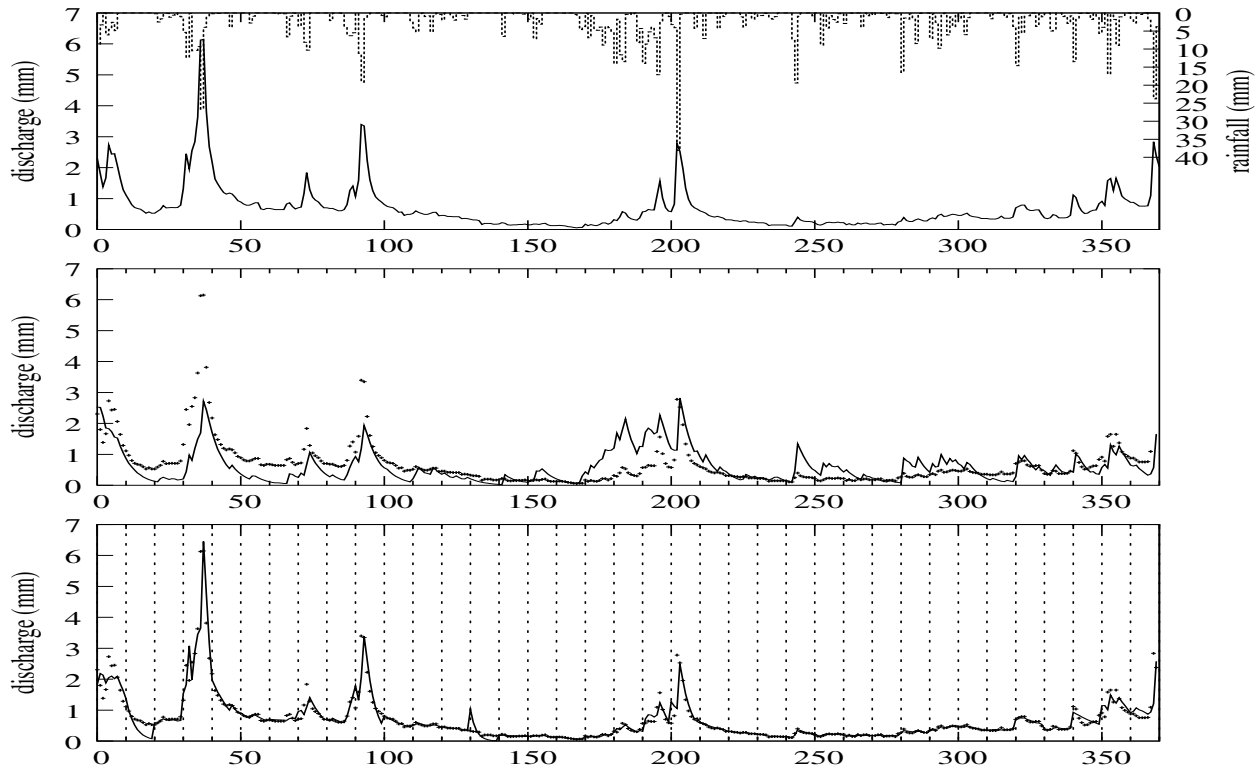

Fig. 1: Top: discharge (left y-axis) and precipitation (at ceiling, right y-axis). Middle: fitting one set of parameters to a whole year; bottom: fitting one set of parameters to each decade (points: measured, line: modeled).

ENSEMBLE OF PARAMETERS

Model (1) is however powerful enough to model shorter time periods: the bottom panel of Figure 1 shows the results of fitting the model to each decade for the year 1998.

Fitting the model to all the decades of the data set result in a large set of parameters which we call the *ensemble of parameters*:

$$\left\{\begin{matrix} P(i+0) & \cdots & P(i+9) \\ Q_{\text{obs}}(i+0) & \cdots & Q_{\text{obs}}(i+9) \end{matrix}\right\} \xrightarrow{\text{fitting model}} \left\{S_i(0), T_i, r_i\right\} \tag{2}$$

Without any other information or observations available, this ensemble summarizes our knowledge of the parameters for an unobserved decade.

Plotting such high dimensional ensembles is in general impossible, but one might gain some insight by looking at two dimensional projections, such as those in Figure 2.

This ensemble can be thought of as a discrete sample of the unknown "true" probability density, so that a kind of "smoothed histogram" of the ensemble would be a better presentation.

Looking at examples as presented in Figure 2, it is clear that simple parametric families of densities like Gaussians are not flexible enough to describe the geometry of the problem. For this reason, we introduce a more general class of densities in the next section.

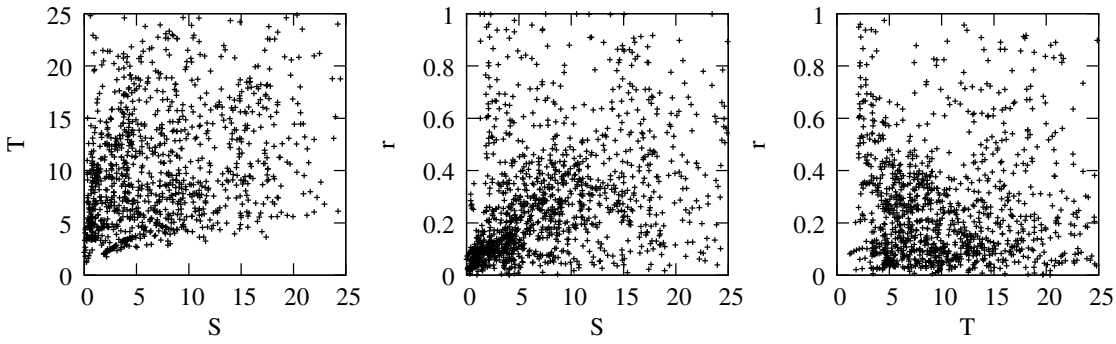

Fig. 2: Three projections giving an impression of the three dimensional ensemble of fitted parameters $\left(S_i(0), T_i, r_i\right)$.

MIXTURES OF GAUSSIANS

A more general and flexible class of densities are Mixtures of Gaussians (MG). They are formally defined as a weighted sum of Gaussian densities (see also Fig. 3), in formula:

$$f(x) = \sum_{i=1}^{N_c} w_i \, f_{(\mu_i, \Sigma_i)}(x)$$

$$f_{(\mu,\Sigma)}(\mathrm{x}) = \frac{1}{\sqrt{(2\pi)^N |\Sigma|}} \exp\left[-\frac{(\mathrm{x}-\mu)^{\mathrm{T}} \Sigma^{-1} (\mathrm{x}-\mu)}{2} \right] \tag{3}$$

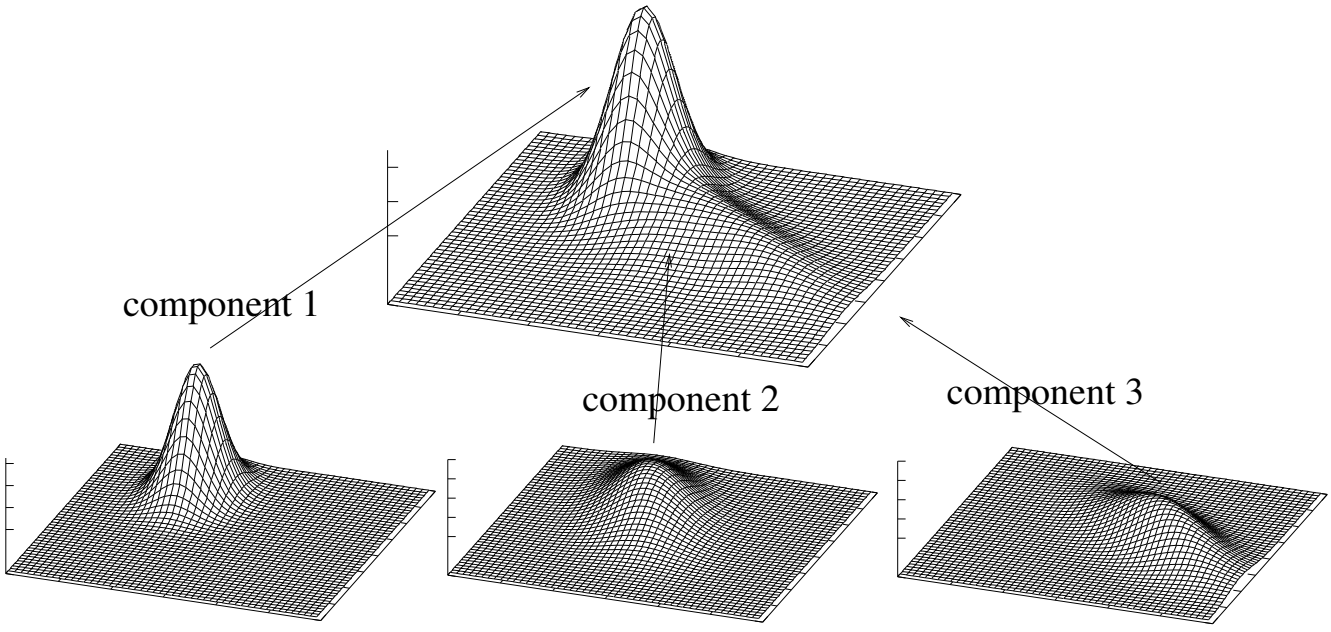

Fig. 3: A Mixture of Gaussians as the weighted sum of three Gaussian components, each with different mean and covariance.

Fitting an MG to an ensemble means fitting weights w, means μ and covariances Σ of components. For this, many implementations are available (e.g. Figueiredo and Jain, 2002), most based on maximum likelihood resulting in an E(xpectation)M(aximization)-type of algorithm (MacLachlan and Krishnan, 1997).

Densities of the MG type inherit a lot of good properties from their Gaussian components: calculation is easy and fast, marginal and conditional densities are again MGs and can be calculated analytically, (Monte Carlo) simulation is extremely easy and fast. For the rainfall runoff analysis, we fitted an MG to the ensemble of parameters:

$$\left\{S_i(0), T_i, r_i\right\} \xrightarrow{\text{MG-fit}} f(S,T,r) \tag{4}$$

While such a density is difficult to depict, the two dimensional marginals of Figure 4 reveal some of the structure of this MG. Comparing these probability densities to the discrete underlying ensembles of Figure 2, one sees that MG's are a smoothed continuous representation of the "density" of the underlying points. It is also clear from these examples that MG's can capture the particular local features of the ensemble while standard parametric densities (e.g. Gaussians) are unable to do this.

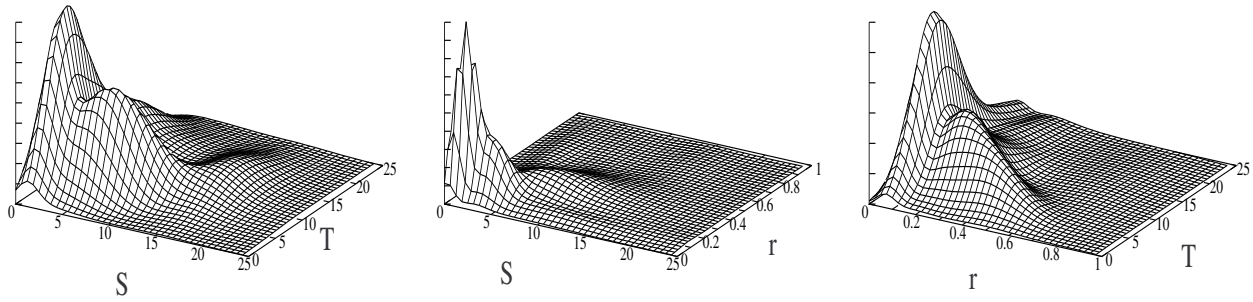

Fig. 4: Three marginals of the MG fitted to the ensemble of parameters (see also the corresponding ensembles of Figure 2).

ASSIMILATING OBSERVATIONS

The MG probability density discussed in the previous section summarized our knowledge of the parameters for a decade for which we have no observations. In most hydrological situations, some observations are available. They should be assimilated by taking conditional densities.

By way of example, we discuss here the problem where for a certain decade, the observed discharge - say $Q_{\text{obs}}(0)$ = 1 mm/day - is given. The algorithm to find the probability expressing our knowledge given this observation can be summarized as follows:

1. construct the ensemble of $\left(S(0), T, r, Q_{\text{mod}}(0)\right)$ by fitting the model

$$\begin{Bmatrix} P(i+0) & \cdots & P(i+9) \\ Q_{\text{obs}}(i+0) & \cdots & Q_{\text{obs}}(i+9) \end{Bmatrix} \xrightarrow{\text{fitting model}} \left\{S_i(0), T_i, r_i, Q_{\text{mod},i}(0)\right\}$$

2. fit an MG density on this ensemble:

$$\left\{S_i(0), T_i, r_i, Q_{\text{mod},i}(0)\right\} \xrightarrow{\text{MG-fit}} f(S,T,r,Q)$$

3. the answer to the problem stated above is given by the conditional density:

$$f\left(S,T,r\middle|Q=1\right)=\frac{f\left(S,T,r,1\right)}{\iiint f\left(S,T,r,1\right)\,dS\;dT\;dr} \tag{5}$$

Figure 5 shows the as such calculated density for the parameters (S (0), T) (again, densities of points in dimensions higher than 2 are difficult to plot). Comparing this density to the left of Figure 4 shows that assimilating observations results in narrower probability densities, reflecting our gain in knowledge.

Calculating conditionals is a step that cannot be performed on the ensemble, as it will generally not contain a point with $Q(0)$ = 1 mm/day exactly, making the evaluation of the denominator of formula (5) impossible. Calculating conditionals and marginals for MGs can be done analytically and thus very fast.

RECURSIVE ASSIMILATION: KALMAN FILTERING

Observations are usually gathered on a regular basis, leading to recursive assimilation. The best known recursive assimilation technique is Kalman filtering (Wood and Crow, 2003). The classical version of this applies to linear models and Gaussian uncertainties. The use of MGs allows non-Gaussian and non-linear extensions (e.g. Anderson and Anderson, 1999; Torfs et al., 2002).

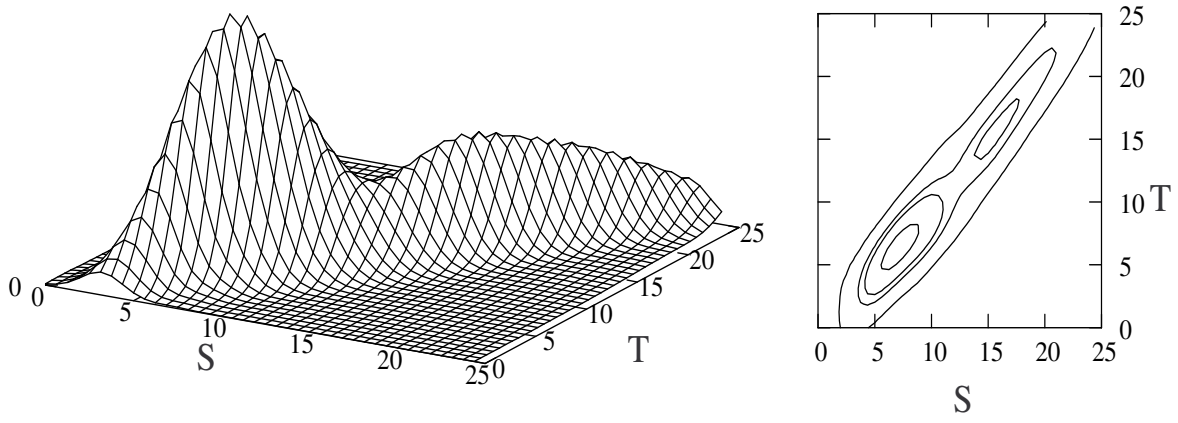

Fig. 5: The conditional density of (S, T) given Q = 1 mm/day. Right: the corresponding contours.

We illustrate this for the data in this study by discussing the example where the precipitation P (i) is known for each day i, but the discharge is only available for the beginning of each decade: Q_{obs} (k * 10). For the first decade, the problem is solved by the theory of the previous section. One may however expect that the parameters S, T , r of two consecutive decades are not completely independent and that there is some statistical relationship between them.
There should for example even be a strong relationship between the reservoir content S_{end} calculated for the end of a decade (by using the parameters S (0), T , r and the observed precipitation for that decade) and the best initial reservoir content (the $S'(0)$ parameter) of the following decade. Combining these statistical relationships with the observation of the beginning discharge of that next decade $Q'_{\text{obs}}(0)$ is the key to all Kalman filtering algorithms.

These statistical relationships can be modeled by fitting an MG:

$$\left\{S_{\text{end}},T,r,S'(0),T',r',Q'_{\text{obs}}(0)\right\}\xrightarrow{\text{MG-fit}}\phi\left(S,T,r,S',T',r',Q'\right)$$

A typical step in the recursive algorithm can now be described as follows:

1. Our knowledge at the beginning of the algorithm is given by an MG density: f_{ini} (S, T , r) From this density, we simulate a representative ensemble of parameter values:

$$f_{\text{ini}}\left(S,T,r\right)\xrightarrow{\text{MG-sim}}\left\{S_i(0),T_i,r_i\right\}$$

2. Combine each of these parameter values with the given precipitation to calculate -using the model- the value at the end of the decade: $S_{\text{end},i}$. Note that these calculations do not impose any restrictions (e.g. linearity) on the model.

3. *prediction step*: use the ensemble thus obtained and the statistical knowledge present in the MG ϕ to simulate results for the next decade, and fit an MG density to it:

$$\phi\left(S',T',r',Q'\middle|S_{\text{end},i},T_i,r_i\right)\xrightarrow{\text{MG-sim}}\left(S_i',T_i',r_i',Q_i'\right)\xrightarrow{\text{MG-fit}}f_{\text{pred}}\left(S',T',r',Q'\right)$$

4. *correction step*: calculate the conditional density with respect to the observations

$$f_{\text{cor}}\left(S,T,r\right)=f_{\text{pred}}\left(S,T,r\middle|Q=Q_{\text{obs}}\right)$$

   This f_{cor} will be the f_{ini} of the next recursive step.

Note that in this procedure, we did not impose any restrictions (e.g. Gaussianity) on the occurring probability densities.

Figure 6 illustrates a typical result obtained by applying the algorithm above. On any given day, our knowledge of the state of the system is a probability density which changes from day to day. In the figure, only the modeled discharge is plotted, and its density is represented by an ensemble of points simulated from this density. The skewness (and thus non-Gaussianity) of some of these ensembles is clearly visible looking at the outliers (e.g. for days 272 and 273). Sometimes the system gets out of phase with reality, but then the updating brings it back to reality, as can be seen at day 320, for example.

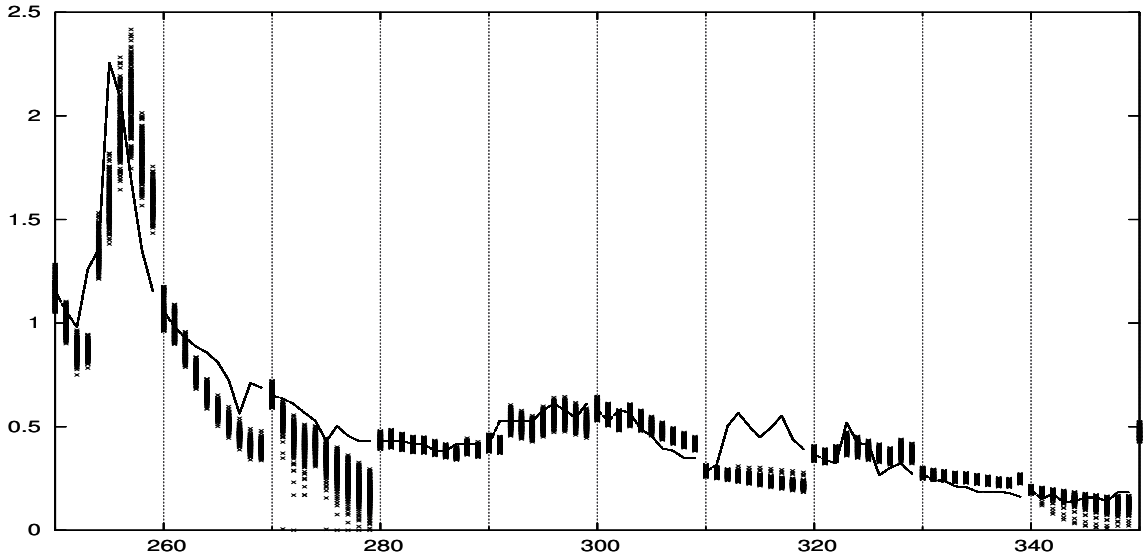

Fig. 6: Discharge (y-axis) obtained by Kalman filtering depicted by an ensemble for each day (x-axis). The solid line is the true discharge.

CONCLUSIONS

From the example above, one may draw the following conclusions:

- modeling uncertainty even in simple cases like the one in this study generates many non-Gaussian ensembles which can be effectively modeled by MG;
- MGs are efficient in calculating conditionals, marginals and making simulations;
- as modeling is handling uncertainty, good modeling requires the systematic use of probability densities as a description of knowledge.

REFERENCES

J. Anderson and S. Anderson. A Monte Carlo implementation of nonlinear filtering problem to produce ensemble assimilations and forecasts. *Mon. Weather Rev*., 128:1971-1981, 1999.

P. Torfs, E. van Loon, R. Wójcik and P.A. Troch. Data assimilation by non parametric density estimation. In: W. Gray, G. Pinder, S. Hassaninzadeh, R. Schotting, editors, *Computational Methods in Water Resources*, 1355-1362. Elesevier, Amsterdam, 2002.

M. Figueiredo and A. Jain. Unsupervised learning of finite mixture models. *IEEE T. Pattern Ana.*, 23(3):381-396, 2002.

G.J. McLachlan and T. Krishnan. The EM Algorithm and Extensions. *New York: Wiley*, 1997.

E. Wood and W.T. Crow. The assimilation of remotely sensed soil brightness temperature imagery into a land surface model using Ensemble Kalman filtering: a case study based on ESTAR measurements during SGP97. *Adv. Water Res.*, 26:137-149, 2003.

SPRING AND SUMMER TRANSPIRATION FROM WATER STREAM BANKS AND DAILY STREAM FLOW FLUCTUATIONS IN A SMALL ALPINE CATCHMENT

C. Vezzani and C. Gregoretti

Padua University Department of the Territory and Agro-Forestry Systems
e-mail Claudia Vezzani: claudia.vezzani@adbpo.it
e-mail Carlo Gregoretti: carlo.gregoretti@unipd.it

ABSTRACT

Daily spring and summer stream flow fluctuations were observed in the 1.9 km² Rio Vauz catchment in Italy's eastern Dolomite Mountain range. Maximum water removal from the stream occurs in daytime, so evapo-transpiration from riverbank areas and stream surface water was considered the main controlling factor. Computing missing volumes from observed daily fluctuations and evapo-transpiration by the well-known Penman combined equation was used to estimate basin area percentage affecting stream flow variation by evapo-transpiration. This area was thought to spread on bank areas along the stream net. Hydrological quantities present in Penman equation were measured at meteorological stations close to the catchment. Two different approaches were assessed to analyse the phenomenon and use it in model applications.

Key words: evapotranspiration, diurnal fluctuations, mountainous catchments.

INTRODUCTION

Troxell (1936) observed River Santa Ana daily stream and ground water flow fluctuations in hot summers. He explained them with daytime evapo-transpiration in the bank areas lowering the water table and affecting stream discharge, followed by nighttime recharge.
Tschinkel (1963) compared daily stream flow fluctuations with evaporation data with a black pan evaporation meter. He noted that the highest and lowest stream flow discharges occurred respectively at forenoon and the early evening and that amplitude dropped abruptly on low evaporation days.
Kobayashi et al. (1990) noted daytime stream flow discharge variations in a boreal watershed and found that stream flow decrease was due to evapo-transpiration from the forest along the stream channel and not to surface water evaporation. Kobayashi et al. (1995) also noted decreased amplitude as the season advanced and attributed it to decreased soil water availability affecting evapo-transpiration.
Bren (1997) compared observations of daily water table level fluctuations in bank zones before and after slope vegetation removal (bank areas excluded) in a mountain stream and argued that daytime fluctuations were only due to bank area transpiration.
Constanz (1998) observed greater daytime fluctuations in losing than in gaining reaches and explained them as caused by temperature-induced streambed permeability changes (higher temperature increases hydraulic conductivity and bed seepage loss).
Bond et al. (2002) analysed the relationship between stream flow patterns and transpirations in a 100 hectare forested basin. They compared tree sap and stream flow data and recorded short-time high correlation between sap and stream flow; they stated that stream flow decrease was due to the evapo-transpiration of a narrow area along the river.

Daily fluctuations in a small alpine stream discharge occurring in June and July 2003 were observed in this study. Such fluctuations were explained by ground water level fluctuations due to evapo-transpiration. Assuming water discharge as affected by water contained in the two bank strips along both sides of the water stream, a rough estimate of the extension of bank area influencing the water stream discharge was presented with a coefficient to apply to the Penman equation for estimating seasonal evapo-transpiration.

THE CATCHMENT AND OBSERVED DATA

Daily fluctuations were noted in the stream discharge of a small 1.9 km^2 alpine basin of the eastern Dolomites, called the Rio Vauz catchment, ranging in altitude from 1835 to 3152 metres a.s.l. The basin is completely undisturbed by human activity and entirely covered by natural pasturelands with extensive short, smooth and mown grass except for large areas of bedrock outcrops in the upper part. The basin features a typical alpine climate, with a mean annual rainfall of some 1100 mm. Precipitation is mostly snow from November to April. The runoff is dominated by snowmelt until end May and rainfall from June/July to October. The stream net consists of a main stream, the Rio Vauz, which starts from a spring at about 2350 metres altitude, and flows to the basin outlet, laying at 1835 metres, covering a distance of some 1.9 km. At 1940 metres altitude a small tributary joins the main stream. Average monthly discharge at the outlet ranges from 0.3 m^3/s in the early summer, when snowmelt runoff prevails, to 0.05 m^3/s during the summer and autumn. Maximum peak discharges were observed during the autumn and spring, and exceeded 1 m^3/s. Water discharge was measured at the outlet and in an upstream cross-section (200 m higher) along the Rio Vauz, using triangular weirs and pressure-transducers water level loggers (Fig. 1).

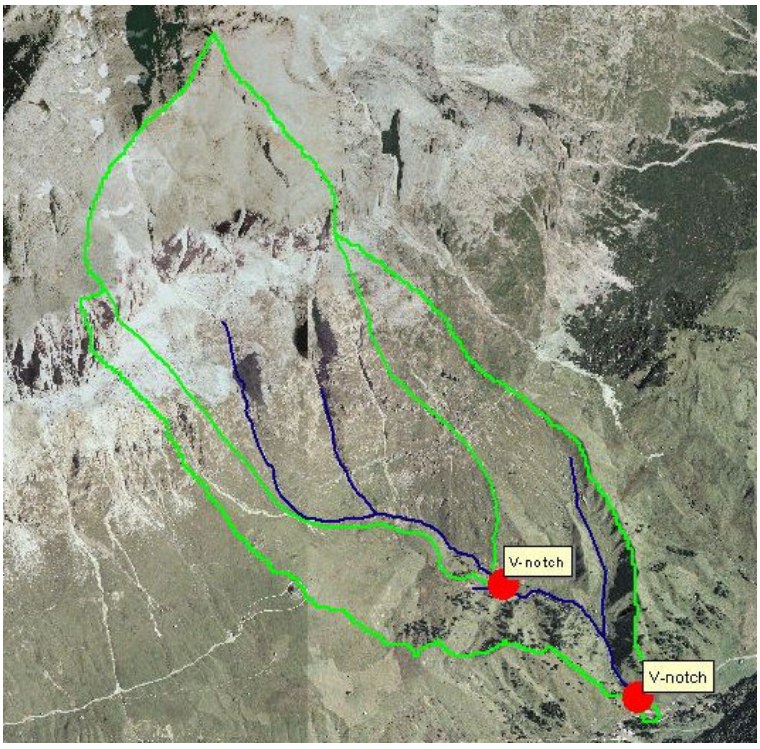

Fig. 1: Locations of V-notches for discharge measurements in the Rio Vauz catchment.

V-notches stage-discharge relationships were measured by fitting theoretical discharge coefficients to local flow measurement data. Discharge was measured continuously with a 10 min recording interval from June to September. Higher station data, corresponding to the smaller sub-catchment (Fig. 1) were used in this study. Hourly series of total solar radiation, wind speed, air temperature and air humidity were provided by the Passo Pordoi meteorological station, managed by the Arabba Centro Valanghe, located at 2000 metre planar distance from the catchment area barycentre and at the same altitude. Net solar radiation data were obtained by using a linear total to net radiation ratio, a 3-year record series from a net radiometer set up on an alpine grassland at 2000 metres altitude in a Cinque Torri station closed area (Fig. 2). Local air pressure was obtained from hourly data measured at the nearby San Vito di Cadore station, at 1107 metres altitude, with a temperature-based altitude correction ratio. Basin and stream net were geometrically and topographically measured with a 10x10 m DEM.

Daily discharge fluctuations were noted during the whole recording period and assumed to be due to evapo-transpiration from near-stream bank areas (Bren, 1997; Bond et al., 2002). Maximum discharges occurred around midnight while minimum discharges were noted around midday in early summer (June).

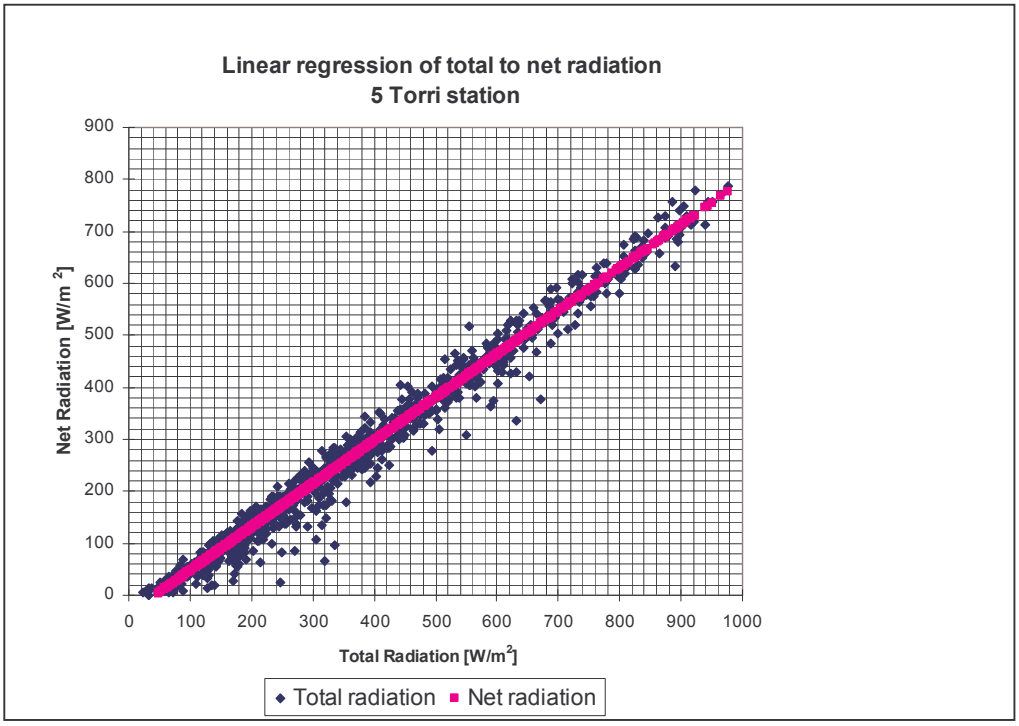

Fig. 2: Regression between total and net radiation on alpine grassland.

Minimum and maximum data delayed as the season advanced and the basin started drying up. A straight line connecting two consecutive maximum discharge points identifying the evapo-transpiration day was assumed to be the theoretical flow in the absence of evapo-transpiration. The underlying missing volume was assumed to be the daily observed amount of evapo-transpiration from bank areas and stream water surface (the latter mostly negligible). Some rainfall produced noise over the discharge signal during the whole period, and only 13 days (4 consecutive days from June 19 to 22 and 9 consecutive days from July 7 to 15) were considered reliable for calculating stream discharge volume at each evapo-transpiration-day.

As shown in Figure 3 a, b, the wave shape varies from June to July. It can be stated that great water availability in June provided by previous monthly snowmelts was enough to supplying all plant water needs for transpiration during the day and for recharging subsurface flow to the initial level of water table during hours of low or zero evapo-transpiration. In other words, no limitation to soil moisture conditions exists, in that water filling the basin just after the end of the snowmelt process compensated for evapo-transpiration induced losses, by recharging the water table in the area close to the stream. Conversely, soil water content clearly decreased in July with no rainfall recovering: wave shape and is likely to be cut by a nearly exponential recession limb, representing base flow discharge recession as the basin dries up.
Bren (1997) showed how average slope over some days with no rainfall of the falling tail of base flow hydrograph is steeper when transpiration occurs versus zero transpiration. Volume calculations show the absence of temporal trends in daily amounts in June, marked by water abundance, whereas discharge fluctuation amplitude decreases with time during the nine days of July, as daily maximum discharge and related daily missing volume. The estimated missing volumes of the four days in June oscillate around a nearly median value (Fig. 4 a) whereas the estimated missing volumes of the nine-days period of July decrease exponentially (Fig. 4 b).

BANK AREA CONTRIBUTION TO STREAM DISCHARGE

Stream discharge in an alpine environment is supplied by rainfall runoff, late spring and early summer snowmelt and subsurface flow from the surrounding soil. Lateral subsurface flow velocity and discharge are affected by soil moisture content; the higher the water table level, the higher the water discharge supplied by

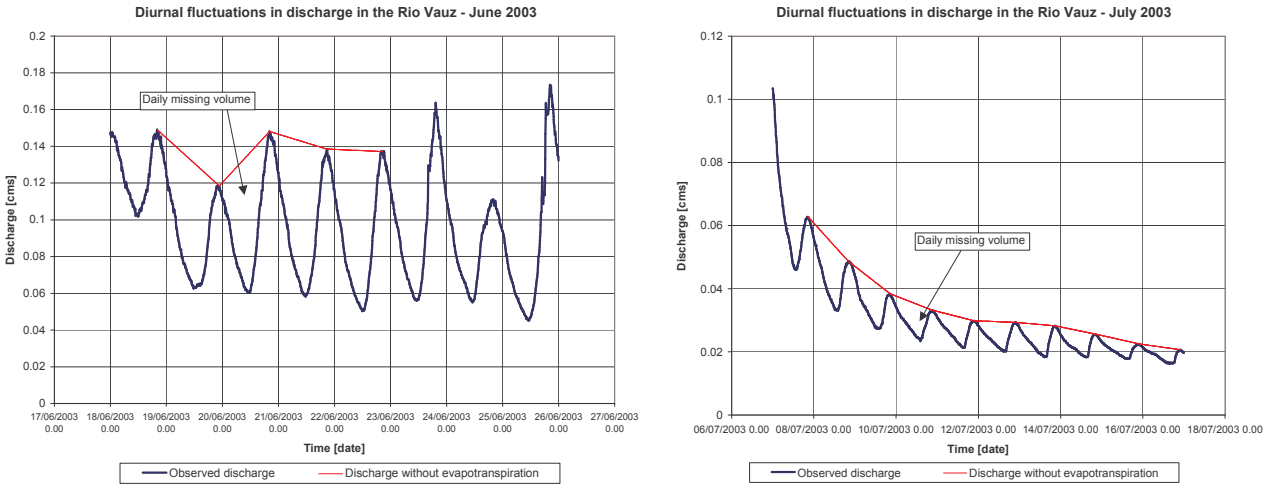

Fig. 3: Observed daytime fluctuations in the Rio Vauz: a) June, wet period; b) July, dry period.

subsurface flow to the stream, and the daily bank area extension contributing to stream discharge. The water table level is controlled by the evapo-transpiration rate in dry periods: the higher the latter, the lower the former. So both evapo-transpiration rate and soil moisture content control the bank area contributing to stream flow and stream water discharge. On the other hand, the groundwater table level also affects plant stomata activity, as the stomata react with lower transpiration in reduced soil moisture conditions, thereby affecting the evapo-transpiration rate itself.

Two opposite approaches are proposed to represent the process. The first assumes a potential evapo-transpiration rate and decreasing subsurface lateral velocity as the basin is drying up, with an increasingly narrower bank area strip contributing to stream discharge during the growing season. Soil drying induced physiological stresses on canopy evapo-transpiration are neglected. The second approach assumes a constant bank strip area contributing to stream discharge and only takes into account evapo-transpiration reduction due to soil drying induced physiological stresses. Daily evapo-transpiration is obtained from the first derivation of Penman equation in either case:

$$E = \frac{\Delta}{\Delta + \gamma} \cdot E_r + \frac{\gamma}{\gamma + \Delta} \cdot E_a \tag{1}$$

Where γ (Pa/° C) is the (Priestley and Taylor, 1972) psychometric constant defined as:

$$\gamma = {de_s}/{dT} \tag{2}$$

T being temperature in ° C and e_s saturation vapour pressure Pa:

$$e_s = 611 \cdot e^{\left(\frac{17.27T}{237.3+T}\right)} \tag{3}$$

and Δ the gradient of the saturated vapour pressure curve at air temperature, estimated by:

$$\Delta = \frac{4098 \cdot e_s}{(237.3 + T)^2} \tag{4}$$

E_r and E_a are respectively evapo-transpiration computed from net radiation rate and aerodynamic computed evapo-transpiration rate (Thornthwaite and Holzman, 1939).
Being a first attempt, the use of a purely environmental formulation for evapo-transpiration was accepted for uniform extensive grassland featuring a high decoupling surface vapour holding capacity to free air stream coefficient (Jones, 1992), assuming incident radiation as the main controlling factor for leaf stomata activity. Future use of biological formulations is however also considered necessary to better understand this issue.

RESULTS

Coefficient K = 0.9 was used with the first approach to reduce pan evapo-transpiration E_{day} obtained from Penman equation (1) in June with wet conditions, while a lower reduction coefficient K = 0.7 was used in July with dry conditions (Jones, 1992). Bank area extension A_{day} contributing to stream discharge was computed daily as follows:

$$A_{day} = \frac{V_{day}}{K \cdot E_{day}} \tag{5}$$

V_{day} being the daily missing volume calculated from stream discharge, A_{day} bank area extension and E_{day} daily evapo-transpiration. Hypothetical bank area width W_{day} is obtained by dividing area A_{day} by net upstream measured length L:

$$W_{day} = A_{day} / L \tag{6}$$

Mean bank strip width was 255 metres (35.5 % catchment area) in June, versus 50 m (7 % catchment area) in July (Fig. 4). These monthly bank belt extensions could be used with the Penman equation to compute daily missing volume from stream in no rainfall periods.

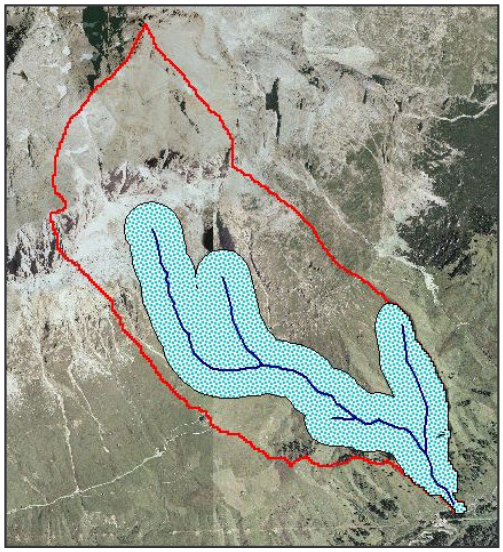

Fig. 4: Mean bank area strip width in the Rio Vauz: June, wet period (line); July, dry period (area).

With the second approach, riparian area A_0, assumed to be the maximum potential referred to water limitless condition, was calculated by dividing the mean value of daily-volumes missing from the stream over the four days of June, by evapo-transpiration height averaged over the same period. Reduction coefficient K_{calc} to estimate the evapo-transpiration rate by the potential one was then computed with the following equation:

$$K_{calc} = \frac{V_{day}}{A_o \cdot E_{day}} \tag{7}$$

Reduction coefficients obtained range from a 0.9 maximum in June corresponding to wet conditions to less than 0.1 in July, these differences being explained not only by radiation and wind availability changes. A theoretical trend of K versus time can be obtained by fitting K_{calc} computed values of consecutive July 7 to 15 rainless days according to Equation 7, with an exponential curve:

$$K_{calc} = a \cdot e^{b \cdot t} \tag{8}$$

Decreasing coefficient b, related to the case of no rain, is 0.0066 (Fig. 5).

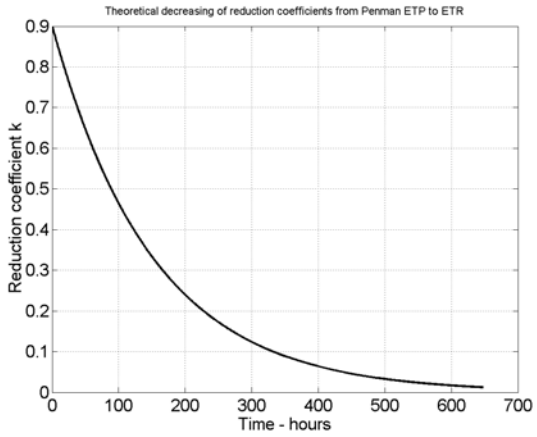

Fig. 5: Reduction coefficient from ETP to ETR versus time, during summer without rainfalls.

ACKNOWLEDGMENT

The Authors wish to thank Professor Tommaso Anfodillo for his useful suggestions and courtesy.

REFERENCES

B.J. Bond, J.A. Jones, N. Phillips, D. Post and, J.J. McDonnel (2002) *The Zone Vegetation Influence on Base Flow Revealed by Patterns of Stream Flow and Vegetation Water Use in a Headwater Basin*. Hydrological Processes, Volume 16, pages 1671-1677.

L.J. Bren, (1997) *Effects of slope Vegetation Removal on the Diurnal Variations of a Small Mountain Stream*. Water Resources Research Volume 33, Nr. 2, pages 321-331.

J. Constantz, (1998) *Interaction between Stream Temperature, Stream Flow and Groundwater Exchanges in Alpine Streams*. Water Resources Research Volume 34, Nr. 7, pages 1609-1615.

H.G. Jones (1992) *Plants and Microclimate*. Cambridge University Press, Cambridge.

D. Kobayashi, K. Suzuki and M. Nomura (1990) *Diurnal Fluctuations in Stream Flow and in Specific Electric Conductance during Drought Periods*. Journal of Hydrology Volume 115, pages 105-114.

D. Kobayashi, Y. Kodama, Y. Ishii, Y. Tanaka and K. Suzuki (1995) *Hydrological Processes,* Volume 9, pages 833-841.

C.H.B. Priestley, R.J. Taylor, (1972) *On the assessment of surface heat flux and evaporation using large-scale parameters.* Monthly weather rev., Volume 100, pages 81-92.

C. W. Thornthwaite, B. Holzman (1939), *The determination of evaporation from land and water surfaces*, Monthly Weather Rev., Volume 67, pages 4-11.

H.M. Tschinkel (1963) *Short-term fluctuation in stream flow as related to evaporation and transpiration*. Journal of Geophysical Research, Volume 68, Nr.24, pages 6459-6469.

H.C. Troxell (1936) *The diurnal fluctuation in the ground-water flow of the Santa Ana River and its meaning*. Transaction American Geophysical Union, Part 2, pages 496-504.

GENERATION OF DELAYED PEAK FLOWS IN THE SMALL STRENGBACH CATCHMENT (VOSGES MASSIF, FRANCE)

D. Viville and S. Gaumel

EOST-Centre de Géochimie de la Surface (UMR 7517-CNRS/StrasbourgI), 1, rue Blessig, F-67084 Strasbourg Cedex, France
e-mail Daniel Viville: dviville@illite.u-strasbg.fr

ABSTRACT

The present work discusses the generation of delayed peak flows in relation to the water table in the granitic Strengbach catchment. These peak flows occur during major rain events and are linked to lateral flow coming from the upper parts of the slopes. There is a downslope movement of water over distances of up to several thousand meters. A threshold beyond which the delayed peaks occur has been clearly identified. This threshold approximately corresponds to a 180 mm water storage in the basin (sum of groundwater and soil storage).

Key words: runoff generation, delayed flood, subsurface stormflow, threshold, small mountainous catchment.

INTRODUCTION

In small catchments, the response of the stream to rainfall is rapid, but, in some cases delayed responses (hours to days after precipitations) are observed (Burt and Butcher, 1985; 1986; Onda et al., 2001). The quick flow peak can be attributed to the saturation–excess overland flow originating from the permanently saturated area of the valley bottom and the delayed discharge peak is due to the convergence of soil water into hillslope hollows (Burt and Butcher, 1986). Such delayed responses of the stream are observed in the Strengbach catchment (Vosges mountains, North Eastern France) and the present work discusses their generation in relation to water table movements.

STUDY AREA AND METHODOLOGY

The forested Strengbach catchment is located on the eastern side of the Vosges massif (north-eastern France). This small catchment (0.8 km²) ranges from 883 m to 1146 m (a.s.l.) and mainly lies on a base-poor granitic bedrock. Podzolic and brown acidic soils overlie coarse-textured tills developed to a thickness ranging from 1 to 9 m. This catchment is forested mainly with Norway spruce (65% of the area); mixed beech and silver fir take up the rest of the area. The climate is temperate oceanic-mountainous; mean annual precipitation is of 1400 mm regularly spread throughout the year and mean annual runoff is of 850 mm with high flow rates during the cold season and low flow rates at the end of summer.
A variable saturated area (up to 3% of the catchment area for a 128 $l.s^{-1}$ discharge), close to the outlet, is connected to the stream (Fig. 1) and is mainly located on the southern slope. This location of the water table can be explained by the higher storage capacity of the southern side which is longer, less inclined and covered by thicker superficial formations than the northern side.

The Strengbach main brook is gauged at the outlet (RS) and also upstream at site RAZS which defines a 0.55 km² subcatchment. From 1996 to 1999, water level fluctuations were continuously recorded in piezometers (A, C, D and G) located on the southern side at a 30 minute time step. The equipment in the basin also includes an automatic weather station located at the top of the basin.

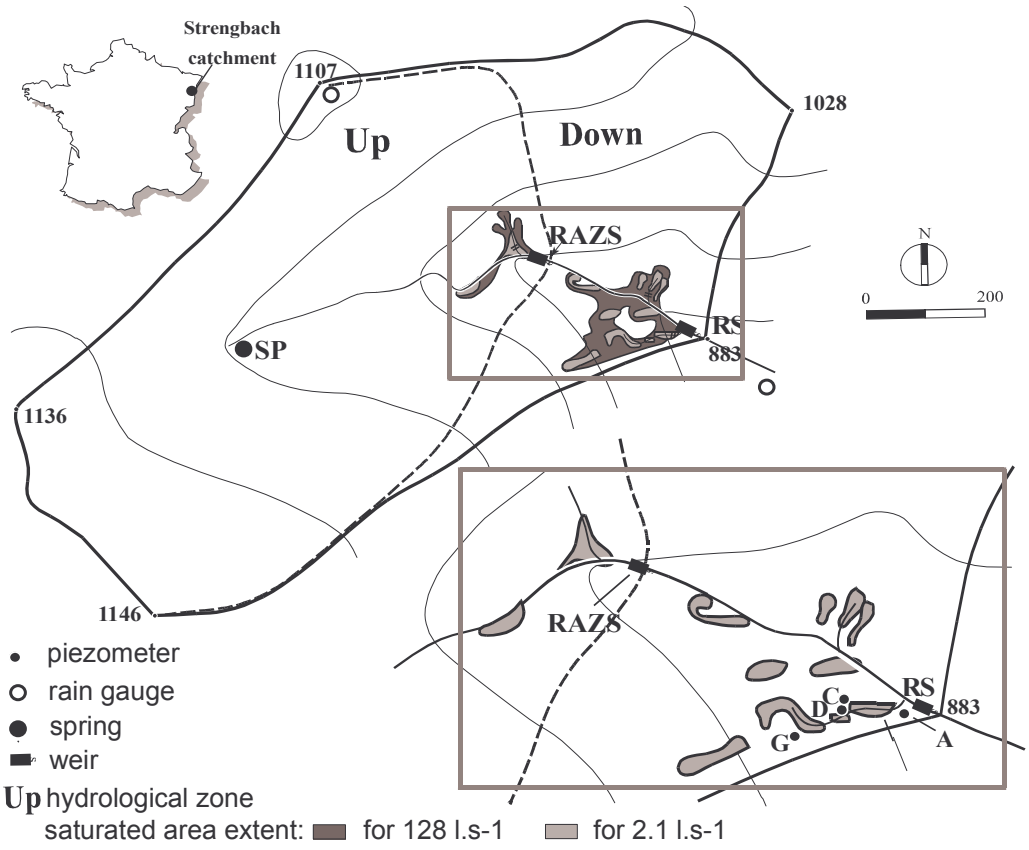

Fig. 1: Location and measurement network of the Strengbach catchment.

During the period from May 1996 to October 1999, 15 major hydrological events caused by rainfall events greater than 60 mm were studied and 11 delayed floods were generated during these events (Gaumel, 2003). In order to know if the delayed floods occur when a defined amount of water stored in the catchment is reached, it is necessary to determine the initial hydric conditions of the basin. This catchment water storage corresponds to the sum of the soil water content and of the groundwater reservoir which is the stream supply. The soil water content is determined with a water soil balance model and the groundwater reserve is deducted from the stream recession curve; the integral of this 2nd order hyperbolic function gives an estimation of the volume of this well drained aquifer. The initial conditions are determined at a daily time step.

RESULTS

Among the 15 studied events, 4 have been selected to show the influence of the initial conditions and of the rainfall on the responses of the Strengbach brook. The events of May and July 1996 occur in initially humid conditions, while in June 1996 and October 1997 the basin was relatively dry.

Before the July 1996 event, the hydrological conditions are humid; the discharge is of 8 $l.s^{-1}$ on 30 June and the total water storage in the catchment is of 97 mm (Fig 2a, b, c).
A succession of rain showers occurs mainly between 5 and 12 July for a total amount of 110 mm of rainfall. These rainfall events produce corresponding discharge peak flows until 8 July. These peak flows are due to the rapid response of the groundwater table located in the lower part of the catchment (Fig 2b and 2c). On 8 July, the rainfall ceases for thirty hours and the discharge increases from 25 to 40 $l.s^{-1}$ whereas the water level in the piezometers falls, then later on, remains at a high level until 16 July.
This 9 July delayed flood is produced when the amount of water (storage plus rain) reaches a 184 mm value. This peak flow is due to the continuous supply of the groundwater table (see piezometer G) by subsurface flow coming from the upper part of the slope; this process certainly also occurs in the upper catchment and explains the increased contribution of the upper subcatchment to the total discharge (Fig. 2c).

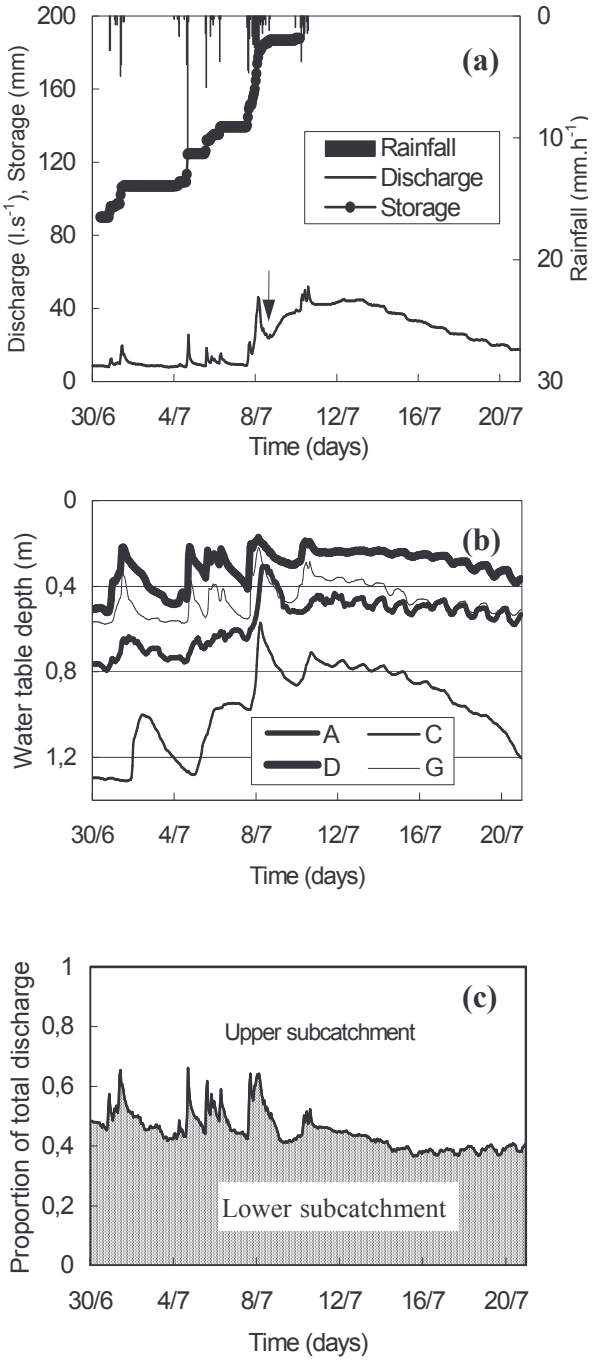

Fig. 2: July 1996 event: (a) rainfall, discharge and total water storage; (b) water table variations; (c) contribution of subcatchments to the discharge.

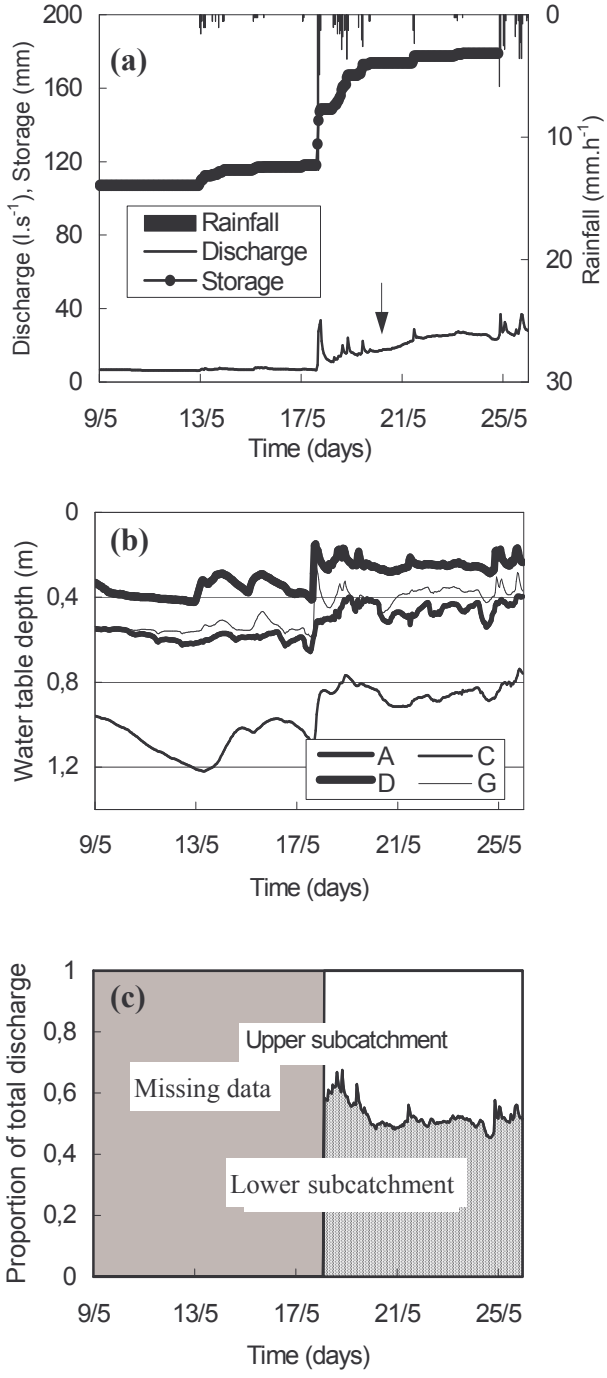

Fig. 3: May 1996 event: (a) rainfall, discharge and total water storage; (b) water table variations; (c) contribution of subcatchments to the discharge.

In May 1996, the initial hydrological conditions are humid; the water table is relatively high, the discharge is of 6,5 $l.s^{-1}$ and the total water storage in the catchment is of 107 mm (Fig. 3a, b). Some minor rainfall events occur on 13 May, but the 17 to 19 May major rainfall event induces a rapid response of the stream; the latter is due to an important contribution of the lower part of the basin (Fig. 3c). Later on, when the rainfall ceases on 20 May, the discharge increases slowly but continuously till 23 May.
The rising of the discharge occurs once the total amount of water stored in the catchment equals 174 mm.
As for the July 1996 event, the delayed peak is due to the arrival of water coming from the upper part of the slope (see piezometer G on 21 May) and to the increasing contribution of the upper subcatchment.

The antecedent hydrological conditions are relatively dry in October 1997; the water table level is low, the discharge is of 3 $l.s^{-1}$ and the total water storage in the catchment is of 84 mm (Fig 4a, b). An important rainfall event (110 mm) occurs between 9 and 12 October 1997, generating a 50 $l.s^{-1}$ peak flow due to a general rise in the water table.
Between the 12 and 13 October, the water table decreases but remains at a high level and the discharge increases regularly; this rise in the discharge occurs for a total water storage of 183 mm.
Later on, until 17 October, the discharge and the water table do not vary a lot. From 17 to 19 October, there is a general fall in the water table in this lower part of the catchment, whereas the discharge remains constant; during this period, the contribution of the upper subcatchment to the discharge is probably very important.
Some time after 19 October, the discharge rises slightly again and a peak is also noticed on 22 October.
This second delayed peak is due to the 21-22 October water level rising; it must be noticed that there has been no rainfall since 17 October. This delayed water level corresponds to the arrival of a downwards subsurface flow wave propagation generated in the upper part of this slope and far from the outlet of the catchment.

In June 1996 the initial hydrological conditions are relatively dry; the water table level is low, the discharge is of 7,9 $l.s^{-1}$ and the total water storage in the catchment is of 71 mm (Fig 5a, b). The successive rainfall showers which occur between 20 and 23 June 1996 produce successive peak flows due to the rise in the groundwater table.
When the rainfall stops, the water table falls and no delayed peak flow occurs. The total water storage in the catchment is only of 131 mm.

DISCUSSION AND CONCLUSIONS

In the Strengbach catchment, the storm runoff appears in the stream as soon as rain falls. The hydrographs show extremely rapid responses to rainfall with steep recessions and the stream hydrograph declines rapidly several hours at most after the end of the storm. This quickflow is related to saturation excess overland flow from the permanently saturated area in the valley bottom.

The use of chemical and stable isotopic tracers has shown that, during these rapid peak flows, a rapid infiltration of a significant amount of rain via preferential pathways explains the groundwater ridging in this saturated area. This sharp rise in the water table can induce superficial runoff due to groundwater exfiltration (Ladouche et al., 2001; Viville et al., 2003). In these cases, the water comes mainly from the superficial layers of the saturated area.

Later, a second delayed peak can appear several days after rainfall input. This delayed flood is associated with the arrival of subsurface flow from the upper part of the slopes -as can be seen in October 1997- which are far from the outlet.
The piezometric level successively begins to rise in G, D, A and then C; there is a downslope movement of water over distances of up to several thousand meters. The increasing contribution of the upper subcatchment to the total discharge also reflects the role played by water coming from zones far from the outlet of the catchment. The use of tracers in previous studies has shown that this water comes from the deeper layers of the upper parts of the catchment.

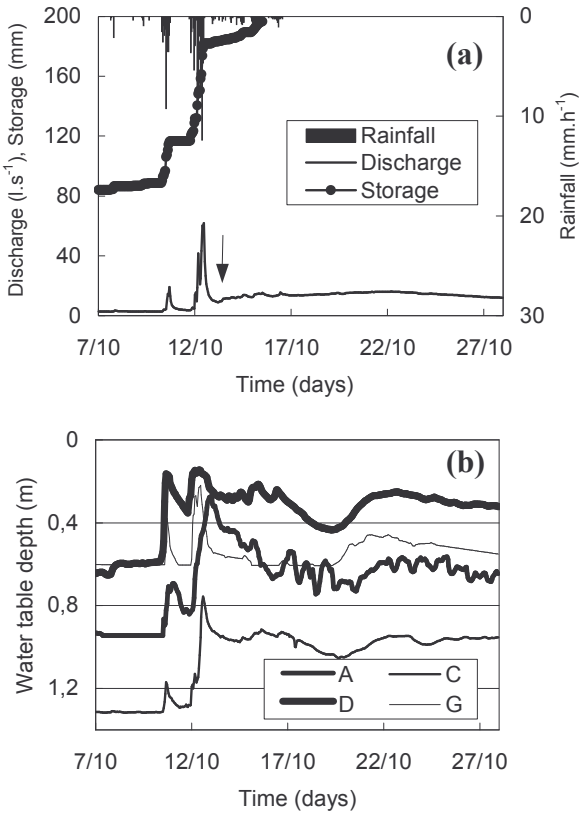

Fig. 4: October 1997 event: (a) rainfall, discharge and total water storage; (b) water table variations.

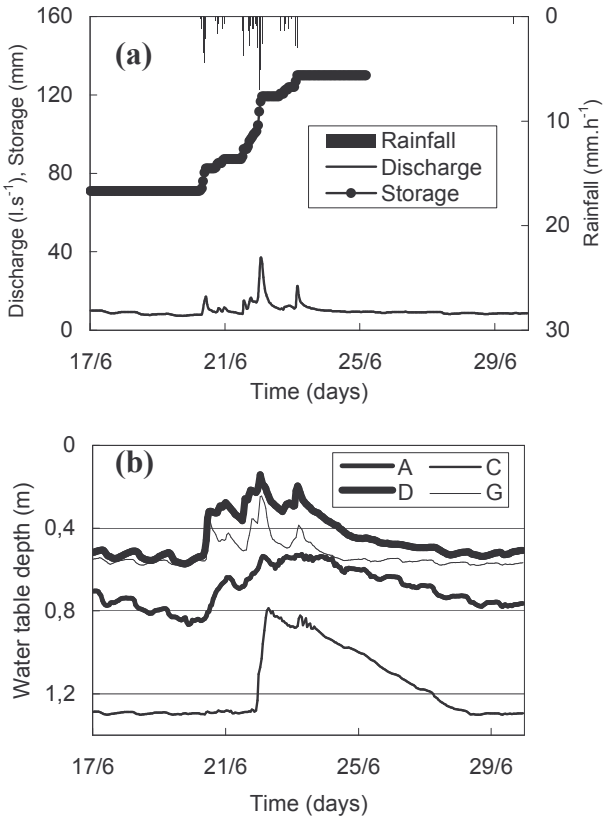

Fig. 5: June 1996 event: (a) rainfall, discharge and total water storage; (b) water table variations.

The occurrence of the delayed peaks depends on the total amount of water (storage + rain) in the catchment. Such delayed floods occur when a threshold water storage - indicated by an arrow on the figures - of about 180 mm is reached.

For example, this threshold is reached in May, July and October but not in June. Indeed, we can see that for the same amount of rainfall (70 mm in May and 60 mm in June), but for very different initial conditions (107 mm and 71 mm respectively), a delayed peak is observed in May when the threshold is reached for an amount of 177 mm and no peak occurs in June when the total storage is only of 131 mm.

Depending on the events, the major role can be played by the rainfall (July and October) or by the initial conditions (May). The existence of thresholds has already been defined in small catchments to explain the overflowing of temporary water tables (Cosandey and Didon-Lescot, 1990), or complex flood events (Kostka and Holko, 2003) and set up the problem of non linearity of basin responses to rainfall events.

REFERENCES

Burt, T.P. and Butcher, D.P. (1985). On the generation of delayed peaks in stream discharge. *J. of Hydrology*, Vol. 78, pp. 361-378.

Burt, T.P. and Butcher, D.P. (1986). Development of topographic indices for use in semi-distributed hillslope runoff models. *Zeitschrift für Geomorphologie*, Suppl.-Bd. 58, pp. 1-19.

Cosandey, C. and Didon-Lescot, J.-F. (1990). Etude des crues cévenoles : conditions d'apparition dans un petit bassin forestier sur le versant sud du Mont Lozère, France. *IAHS Publ. n° 191;* Proceedings of the Ljubljana Symp., pp. 103-115.

Gaumel, S. (2003). Rôle de la nappe de fond de vallon dans les écoulements à l'exutoire. Bassin versant du Strengbach (Hautes-Vosges), *Mémoire de Maîtrise, Faculté de Géographie et d'Aménagement, Université Louis Pasteur, Strasbourg,* 138 p.+ ann.

Kostka, Z. and Holko, L. (2003). Analysis of rainfall-runoff events in a mountain catchment. In *Technical Documents in Hydrology*, n° 67, UNESCO, Holko L. and Miklánek P., (eds), Interdisciplinary approaches in small catchment hydrology : monitoring and research, pp. 19-25.

Ladouche, B., Probst, A., Viville, D., Idir, S., Baqué, D., Loubet, M., Probst, J.-L. and Bariac, T. (2001). Hydrograph separation using isotopic, chemical and hydrological approaches (Strengbach catchment, France). *J. of Hydrology*, Vol. 242, pp. 255-274.

Onda, Y., Komatsu, Y., Tsujimura, M. and Fujihara, J.-I. (2001). The role of subsurface runoff through bedrock on storm flow generation., *Hydrological Processes*, Vol. 15, pp. 1693-1706.

Viville, D., Probst, A., Ladouche, B., Idir, S., Probst, J.-L. and Bariac, T. (2003). Stormflow component determination using hydrological, isotopic and chemical approaches in the small forested Strengbach catchment (granitic Vosges massif, France). In *Technical Documents in Hydrology*, n° 67, UNESCO, Holko, L. and Miklánek P., (eds), Interdisciplinary approaches in small catchment hydrology : monitoring and research, pp. 13-18.

SELECTED UHLÍŘSKÁ BASIN WATER QUALITY INDICATOR 1982/2004 MONITORING RESULTS

A. Kulasová[1], L. Bubeníčková[2], R. Hancvencl[1] and J.Hlaváček[3]

[1]*Czech Hydrometeorological Institute, Želivského 5, 466 05 Jablonec nad Nisou, Czech Republic*
[2] *Czech Hydrometeorological Institute, Na Šabatce 17, 143 06 Praha 4 - Komořany, Czech Republic*
[3] *Waterworks Joint-Stock Company, Soběšická 151, 638 01 Brno, Czech Republic*
e-mail Alena Kulasová: kulasova@iol.cz

ABSTRACT

The natural environment of experimental basin Uhlířská in the Jizera Mountains of the Euro-region NISA Black Triangle was badly affected by air pollution between 1970 and 1990. Atmospheric deposition diminished after steps taken to prevent uncontrolled waste material emission from thermal power plants into the air. Periodical water quality monitoring in the Uhlířská basin closing profile 1982-2004 responded first to high air pollution reflected in low water pH and washed-out basic elements added to increased concentration of nitrates, sulphates, aluminium and the like. Water quality improved later on. Automatic devices took frequent water samples to study water quality regime of selected elements in relationship to runoff during several increased run-off episodes caused by snow fall or thaw. Water conductivity, temperature, pH, Cl and $N\text{-}NO_3^-$ and redox potential were monitored automatically with a YSI 6920 every ten minutes since December 2003 for more detailed study of their regime versus run-off changes.

Key words: experimental basin, atmospheric pollution, water quality response, water quality monitoring, runoff episodes.

INTRODUCTION

The natural environment in the Czech Republic, Jizera Mountains of the Nisa Euro-region Black Triangle was badly affected by air pollution between 1970 and 1990. The spruce monoculture vegetation cover started to dry and was clear-cut to a large extent. The impact of air pollution impact also negatively affected stream water quality. After the 1990 measures, taken to prevent the uncontrolled impact of thermal power plant waste materials, atmospheric deposition decreased considerably.

The paper presents the water quality monitoring results of selected indicators: acidity, sulphates, nitrates and aluminium in the Uhlířská basin 1.87 km^2 area closing profile, obtained by the Czech Hydrometeorological Institute jointly with the Prague Research Water Resources Institute T.G.M. and the Brno Waterworks J-S Company in 1982 to 2004. The presentation contains analytical results of water samples in monthly steps, in increased run-off episodes and in 10-minute time intervals by automatic measuring probe YSI 6920 MDS.

WATER QUALITY IN EPISODIC SURFACE WATER SAMPLES

The samples of water for quality analysis were taken irregularly from 1982 to 2004 at a rate of 5 to 15 samplings yearly until 1993 (Mach et al., 1982-1993), and later in regular monthly intervals (Kulasová et al., 1989-2003). Results obtained in the first half of the monitoring period responded to high atmospheric pollution reflected in soil washed-out basic elements, low pH water, and increased concentrations of nitrates, sulphates, aluminium and other heavy metals. Water quality improvement was observed in the last period of 1994 to 2004.

Samples were analysed in several laboratories during the first 1982/1993 period and at that time the spruce monoculture vegetation cover affected by acid rains experienced drastic changes. Trees dried and 70 % of forested area was cleared. In the second 1994 to 2004 period, clear-cutting had already finished and basin reforestation started. Only one laboratory had been authorized to perform water analyses since 1994. Water analyses results were divided into two periods: 1982 to 1993 and 1994 to 2004 following on these changed

conditions. Results are presented in Figures 1 and 2. Water quality analysis results only respond to a limited part of discharge proportions measured at the Uhlířská gauging station as sampling was haphazard and sampling discharges predominantly corresponded to lower random values. Average discharge value at sampling time in the second period was 0.100 to 0.054 $m^3.s^{-1}$, slightly lower than in the first one. Water was less acidic with average pH increased from 4.8 to 5.4, but individual pH data were more scattered (Fig. 1). The reason is probably the accidental character of samples, as pH is very sensitive to several factors such as the amount of humic acid in water, melting snow water quality, acid rains and the like. The content of nitrates, sulphates and aluminium (Fig. 2) were considerably lower in the last period.

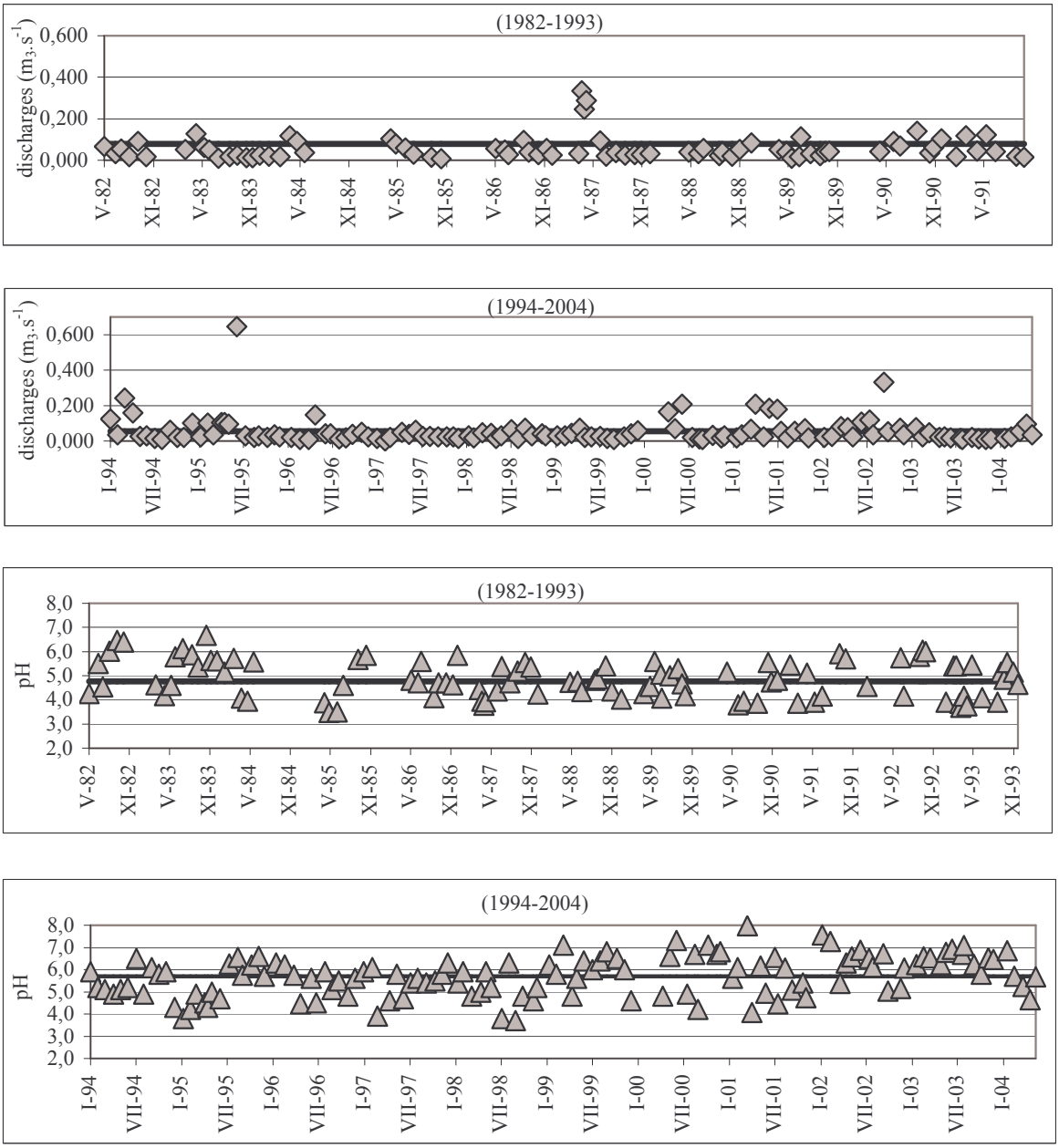

Fig. 1: Comparison of discharge and water acidity in Uhlířská station surface water samples in 1982 to 1993 and 1994 to2004.

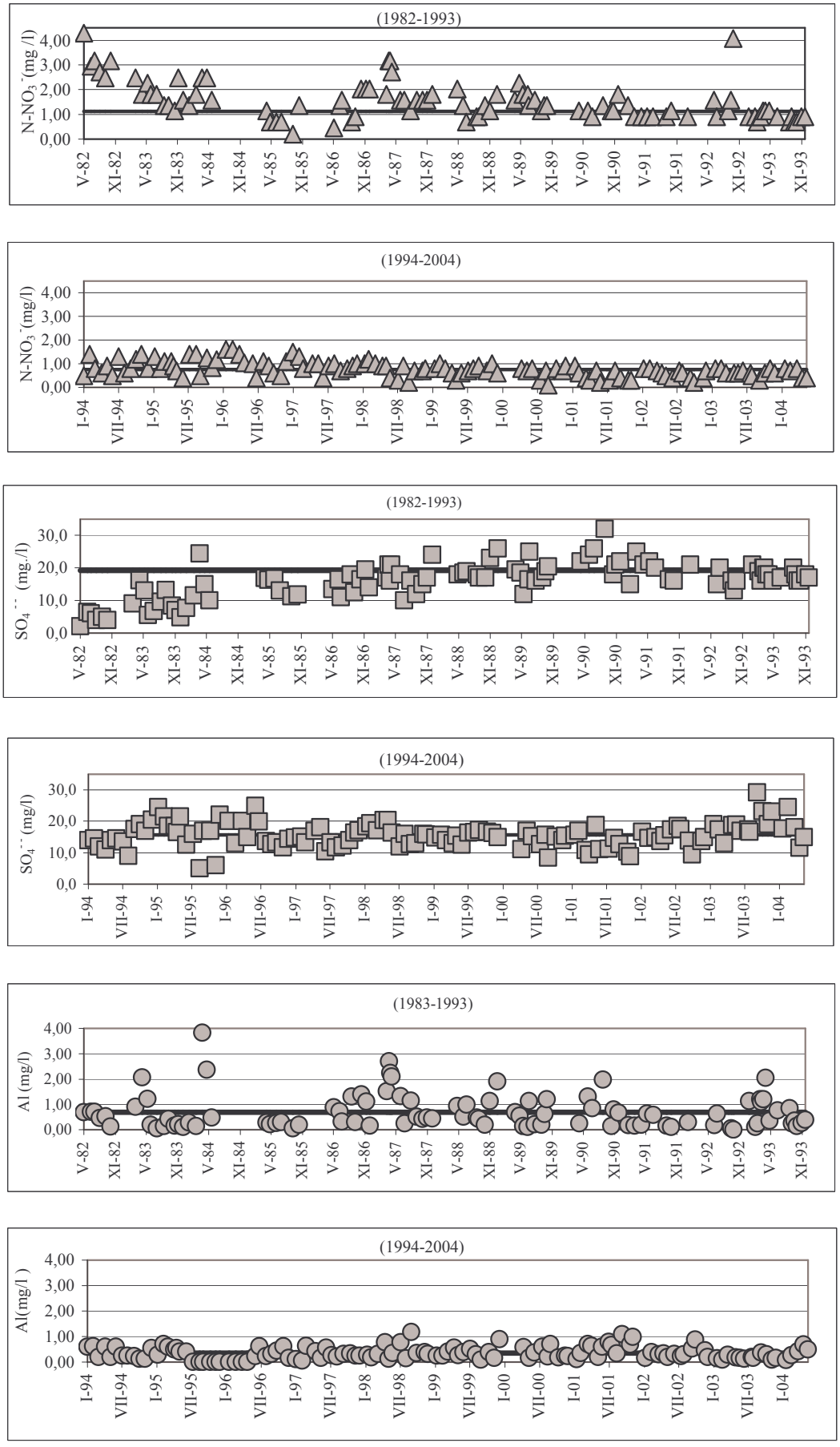

Fig. 2: Comparison of NO_3^-, SO_4^- and Al concentrations of Uhlířská station surface water samples between 1982 and-1993 and from 1994 to-2004.

WATER QUALITY INCREASED RUNOFFS

Sample randomisation gave no data on river flow water acidity to monitored material concentration ratio, but PHARE Project EC/WAT/28 automatic samplers enabled studying water quality (pH, $N\text{-}NO_3^-$, SO_4, Ca, Mg, Na, K, A, Fe, Mn, Pb, Cd, Cu, Ni) of some selected components during increased discharges when water sampling was at 4-hour intervals (Vilímec, Hancvencl, 1997, 1998).

Figure 3 gives summer 1997 and 1998 pH, nitrate nitrogen and aluminium data. The data on pH decreased with increasing discharges during the summer single wave (June 11 to 16, 1998) and pH soon increased again after the discharge peak was reached. Return to initial values before the event was slower than decrease rate. The values of pH on July 18 and 19, 1997 also decreased with increasing discharges, but did not decrease further and remained at the same level during the increase of the following second wave. Return of pH to initial values before the episode was delayed. Nitrate nitrogen concentrations were the same as pH. Increasing discharge aluminium reached its maximum during the discharge peak.

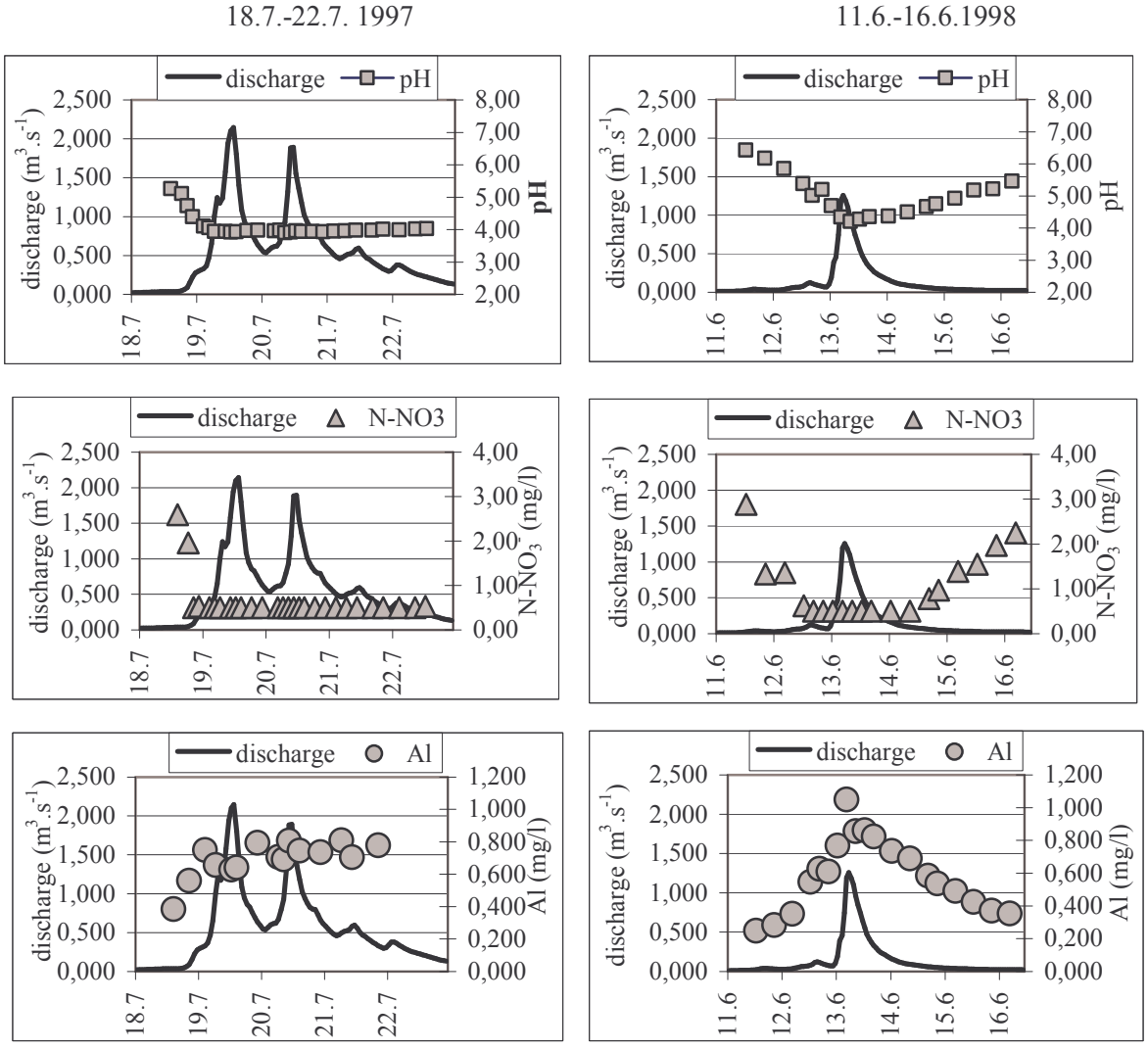

Fig 3: Regime of pH, Al and $N\text{-}NO_3$ during summer precipitation-run-off episodes in years 1997 and 1998.

AUTOMATIC MEASURING PROBE MONITORING RESULTS

Continuous water temperature and $N\text{-}NO_3^-$, pH, chlorides, conductivity and redox potential monitoring with Yellow Springs, Ohio, USA automatic measuring probe YS 6920 MDS began in December 2003 in the

general context of Project Labe IV (VaV/650/5/03). Monitoring was every 10 minutes to enable more detailed regime versus runoff change studies. Figure 4 shows the results of measured values of water temperature, nitrate nitrogen and pH during winter runoff from the snowmelt of March 19 to 23 2004. As opposed to summer episodes originated from rainfall-runoff, the values of $N\text{-}NO_3^-$ increased with increasing discharges peaks reached just after maximum discharge. This was due to runoff of polluting materials accumulated in the snow cover. This increased nitrate nitrogen concentration after snowmelt identical to the event measured in the winter of 1998.

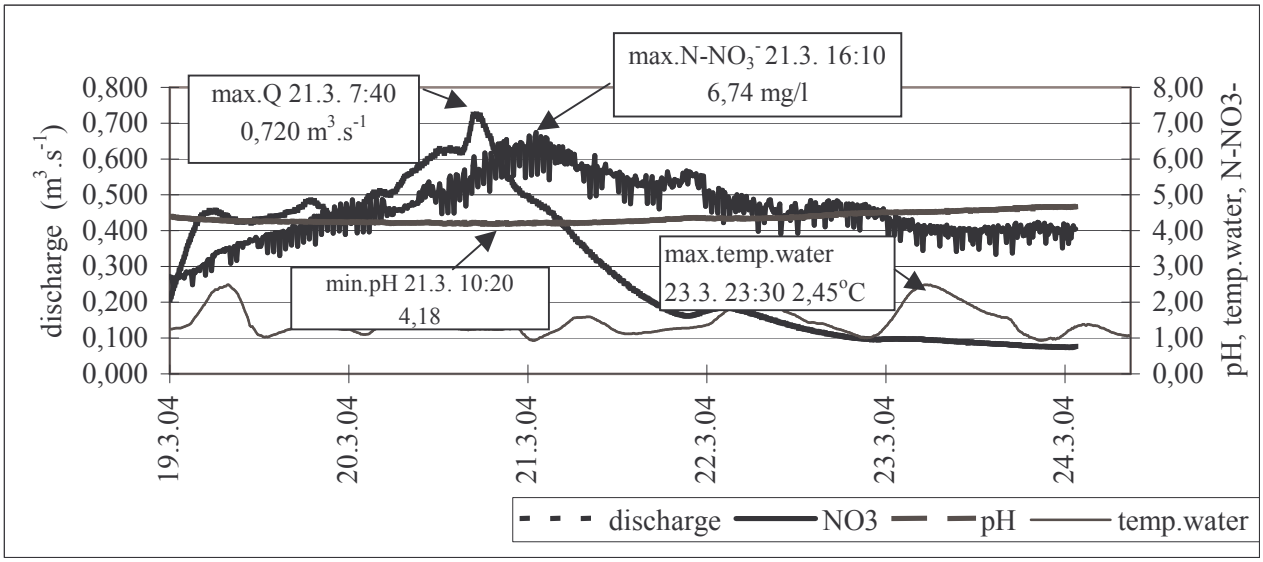

Fig. 4: Discharges, pH, nitrate nitrogen and water temperature during the runoff from the March 2004 snow melt.

MEASURED EXTREMES IN THE PERIOD 1982-2004

The Table shows maximum extreme values of acidity, nitrate nitrogen, sulphate and aluminium measured in monthly water samples from 1982 to 2004, those of acidity, nitrate nitrogen and aluminium in water samples taken in the runoffs of 1997-1998 and April 2004 and pH and nitrate nitrogen measured with probes from December 2003 to September 2004.

The minimum value of pH (3.5) was measured in 1985 and (3.7) in 1998. Other maximum values were between 3.9 and 4.4. Water acidity was higher than allowed drinking water levels. Maximum aluminium concentration was measured in April 1984 (3.82). Concentration was lower in 1985 to 2004, though still much above the drinking water limit. Nitrate nitrogen exceeded recommended drinking water limits in May 1982, March and May 1997 and March 2004 (6,74). Sulphate values satisfied limits set.

CONCLUSIONS

Frequent rainfall in the Jizera Mountains carry increased amounts of dangerous air pollution material. Pollutants accumulate in the snow cover during the winter and are released at snowmelt.
The spruce vegetation cover and soil itself also affect water quality. Water is acidic and its high aluminium concentration exceeds the limits set by the Health Ministry Statement on drinking water quality standards. The random character of monthly water sampling gives no data on monitored material dependence on river flow, an important issue in greater water periods. The Jizera Mountains streams supply two reservoirs used for drinking water supplied to 300,000 inhabitants of the towns and villages below the mountains. Knowledge of continuous courses of material concentration and pH is thus all-important for water quality forecasting in extreme meteorological situations. Testing water quality with a monitoring probe in the Uhlířská basin gave the best results. Extending such monitoring to the other streams flowing into the reservoirs is recommended. Results obtained could differ due to differing physical and geographical

conditions, vegetation cover and local climate conditions. The instrument is expensive and its maintenance time consuming, so waterworks institutions are to be contacted for cost sharing negotiation.

Table: Extreme measured values from 1982 to 2004

Parameters	pH		$N\text{-}NO_3^-$ mg/l		SO_4^{--} mg/l		Al mg/l	
Monthly water samples								
1982-1993	11.5.1985	3,5	18.5.1982	4,29	11.9.1990	32,0	9.4.1984	3,82
	17.6.1985	3,5						
1994-2004	7.9.1998	3,7	23.1.1996	1,06	15.9.2003	29,1	7.9.1998	1,17
			27.2.1996	1,06				
Runoff water samples								
	16.3.1997	4,2	16.3.1997	4,6	13.3.1997	15,0	16.3.1997	1,05
	1.5.1997	4,0	1.5.1997	4,01	28.4.1997	15,0	1.5.1997	0,84
	20.7.1997	3,9	18.7.1997	2,59	18.7.1997	12,6	21.7.1997	0,81
	13.6.1998	4,2	11.6.1998	2,89	15.6.1998	15,2	13.6.1998	1,05
	4.4.2004	3,9	29.3.2004	0,80	29.3.2004	17,7	2.4.2004	0,84
Measuring probe YSI 6920								
	6.2.2004	4,2	7.2.2004	3,12				
	21.3.2004	4,2	21.3.2004	6,74				
	24.7.2004	4,4	2.6.2004	2,33				

252 Health Ministry Statement dated April 22 2004 on drinking water quality standards

Parameters	pH	$N\text{-}NO_3^-$ mg/l	SO_4^{--} mg/l	Al mg/l
limit values	6.5-9.5	Recommended less than 3.39	250	0.2

REFERENCES

A. Kulasová, J. Pobříslová (1994/2004). Hydrological Yearbooks (1989/2003). Experimental Catchment Jizera Mountains. *CHMI Reports*, page 70, Jablonec.

M. Mach, A. Grünwald. (1982/1993). Research and Monitoring of Qualitative Indicators of Water Quality in the Region of the Jizera Mountains. *ČVÚT, FS, Reports of Chair of Health Engineering,* pages 20-100, Prague.

J. Vilímec, R. Hancvencl (1997,1998). Water Quality Analysis in a Stream Showing Rainfall-Runoff Episodes. *Research Report VaV/510/3, T.G.M. RWRI,* pages 40, 20*,* Prague.

DIURNAL FLUCTUATIONS IN STREAM-WATER CHEMICAL COMPOSITION IN SMALL CATCHMENTS IN THE CARPATHIAN FOOTHILLS (SOUTHERN POLAND)

J. Raczak and M. Zelazny

Jagiellonian University, Institute of Geography and Spatial Management, Department of Hydrology
31-044 KrakÛw, ul. Grodzka 64, Poland
e-mail Joanna Raczak: j.raczak@geo.uj.edu pl

ABSTRACT

The aim of the study was to understand the diurnal fluctuations of stream-water chemical composition in small catchments in the Carpathian Foothills with different dominant types of land-use. During 2002-2004, twelve 24-hour sampling series were performed at 2-hour intervals in three streams. During April-September periods, at the time of low-flow conditions, the stream flows displayed considerable diurnal fluctuations, as a result of differences in daytime and night time evapotranspiration rates.
The most distinct chemical patterns were observed in catchments with a strong anthropogenic impact, i.e. the Kubaleniec and Stara Rzeka. The average ionic concentration and its diurnal changes in Kubaleniec and Stara Rzeka were greater in summer than in winter. In the forested catchment of Lesny Potok there was no difference in the range of diurnal streamwater chemical composition changes between wintertime and summertime.

Key words: diurnal fluctuations, water quality, nutrients, Carpathian Foothills.

INTRODUCTION

Little research has been done into diurnal patterns of river chemistry fluctuations occurring during low-water periods. While American researchers started investigating diurnal changes in low-water river discharge as early as the first half of the 20th century (Godwin 1931, Troxell 1936, Dunford and Fletcher 1947), the corresponding chemical changes came into focus only recently. North American researchers come to the fore with the highest number of publications mostly concerned with the dynamics of heavy metals (Ortiz and Stronger 2001, Nimick et al. 2003) and iron concentration (McKnight and Bencala 1989, 1990, Sullivan et al. 1998, Sullivan and Drever 2001).
So far, however, no satisfactory explanations of what causes changes in the chemical composition have been provided using the available cases of such variation patterns, which were documented as both material and as displaying a trend.
Therefore, further studies are needed to reduce the high degree of uncertainty related to desirable sample timing and to how representative samples taken at various times of the day can be. This paper aims to probe the diurnal chemistry changes in small watercourses draining catchments with various land uses, and to identify the causes.

STUDY AREA

The research was conducted in the catchment of the Stara Rzeka River and two of its subcatchments, the streams of Kubaleniec and Lesny Potok (Fig. 1).
Located at between 200 and 360 m above sea level the Stara Rzeka catchment (22 km^2) spans two mantle units, Slaska and Podslaska, consisting of Cretaceous and Tertiary (Miocene) flysch formations. These are topped with a thick layer of loess-like formations. The Slaska unit consists primarily of sandstone, shale and claystone, while the Podslaska unit comprises claystone and marly clays, as well as some of the Bochenska salt series (Olewicz 1973, Poborski 1952). The Stara Rzeka catchment features a complex land use structure with 41 percent forest, 38 percent arable land, and 13.5 percent meadow and pasture. The rest consists of village development areas.

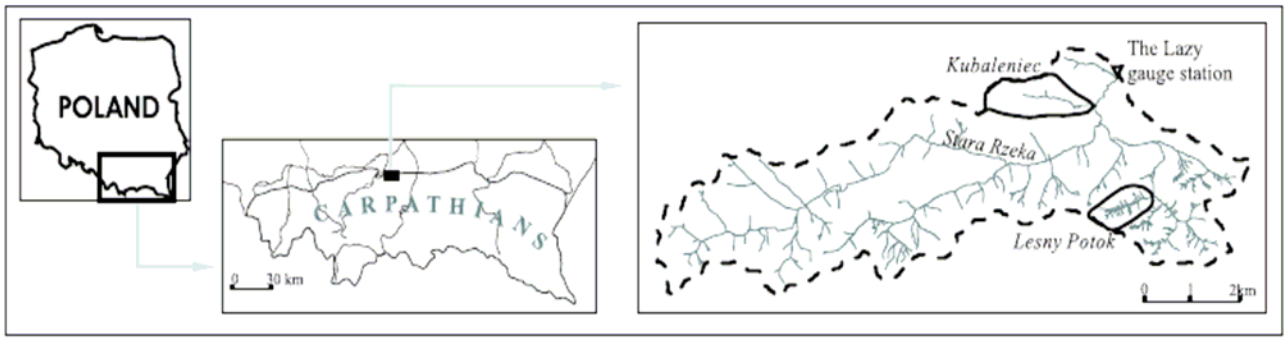

Fig. 1: The study area.

The Kubaleniec catchment (ca. 1 km^2), contained within the Podslaska unit, is a typical agricultural area (with 65 percent arable land, 23 percent meadow and pasture, and 12.5 percent village development), with a dense pattern of roads and field terraces running along the slopes, a typical Foothill feature.
The dominant slope gradient is 3 to 6°. The upper and middle sections of the river are alimented by springwater and shallow alluvial water in the flat-bedded valley, while the lower section of the river draws from deeper-level alluvial waters. The Lesny Potok catchment (ca. 0.6 km^2), entirely within the Slaska unit, has a dominant slope gradient of 10 to 15° (Swiechowicz 2002), and is almost 100 percent covered with forest (beech and fir).

METHOD

During 2002-2004, there were twelve 24-hour sampling sessions with samples taken at two-hour intervals. Field measurements included water temperature, pH and electrical conductivity (EC, at +25°C), using a multifunctional measuring device ELMETRON CX-401. During 19-20 September 2003, in an experiment carried out at Kubaleniec and Stara Rzeka oxygen was additionally measured using a JENWAY 9071DO2 Meter. Laboratory tests included a secondary pH and conductivity measurements. Samples were also filtered (0.45µm) and tested for macroelements (Ca^{2+}, Mg^{2+}, Na^{+}, K^{+}, HCO_3^{-}, SO_4^{2-}, Cl^{-}), nutrients (NH_4^{+}, NO_2^{-}, NO_3^{-}, PO_4^{3-}),and total Fe. The Mg^{2+}, SO_4^{2-}, NH_4^{+}, NO_2^{-}, NO_3^{-}, PO_4^{3-} and Fe, concentration was measured using spectrophotometry (Merck SQ 118), Ca^{2+}, Na^{+}, K^{+} were measured with flame photometry (PFP7 JENWAY), and HCO_3^{-} and Cl^{-} using acidimetric and argentometric methods respectively.

Water level was gauged continuously, initially with a floating limnigraph and then, from June 2003 on, with an automatic recorder (RC-10 TRAX) and water level detectors (Aplisens SG-25 and Peltron PLH27). The meteorological data came from a meteorological post at the Lazy Research Station of the Institute of Geography and Spatial Management, Jagiellonian University, Cracow, located in the Stara Rzeka catchment. Groundwater level was measured with piezometers located near the sampling sites at Lesny Potok (2 piezometers) and Kubaleniec (3 piezometers).

RESULTS AND DISCUSSION

Flow changes within 24-hour periods

Outside flood events, river discharge diminished each day after the event as groundwater resources became depleted. During April-September, there was a clear diurnal pattern of flow fluctuations on the hydrograph, while there were no such rhythmic changes during the winter months.

Clear differences in the diurnal hydrograph shape at all three streams (Figure 2).

At Lesny Potok, the daytime drying limb was short and steep while the discharge increase limb at night was elongated and gradual. The discharge dropped directly after sunrise and increased after sunset. This shape, according to Lundquist and Cayan (2002), is characteristic of evapotranspiration (evaporation directly from the channel and soil and transpiration), as the process driving the diurnal flow cycle.

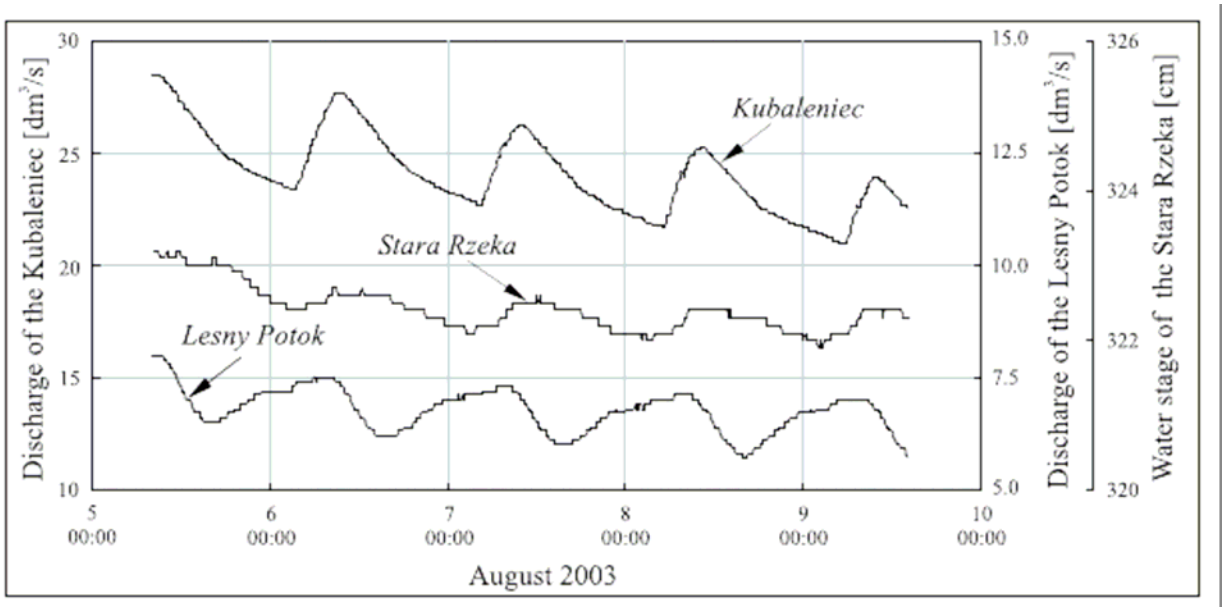

Fig. 2: Water stage of the Stara Rzeka River and discharge of Kubaleniec and Lesny Potok during low flow conditions (5-9 August 2003).

This hypothesis is confirmed by diurnal fluctuations amounting to a few centimetres of the (alluvial) groundwater table in the Lesny Potok catchment.

At Kubaleniec, the diurnal hydrogram was different than at Lesny Potok; the drying curve was long and gradual, while the discharge increase curve was short and very steep. Again, evapotranspiration was the prime driver of this pattern, but its effect on the agricultural catchment with limited water resources was different. During daytime, as a result of increased evapotranspiration, spring water tended to dry out quickly a short distance from the spring or, during particularly hot summer days, disappeared altogether despite a constant discharge into the springs. During the same period, the shallow (alluvial) groundwater table dropped by a dozen centimetres or more. At that time, Kubaleniec was mostly alimented by deeper circulation groundwater. After sunset, despite a drop in evapotranspiration, any increase in discharge at the water gauge was only observed late at night or early in the morning. Before it reached the water gauge, the spring water was used to wet the dry stream channel.

The diurnal hydrograph of Stara Rzeka was similar to that at Kubaleniec, as a major part of the Stara Rzeka catchment displayed similar properties both geologically and in land use, as that of Kubaleniec. Since the beginning of the 20-century, hydrologists have discussed discharge fluctuations occurring within 24-hour periods. Kobayashi et al. (1990), when investigating such changes in a small catchment on Hokkaido excluded the possibility of direct loss of water through evaporation from the stream channel; the stream water was colder then the dewpoint. In the Stara Rzeka catchment, during the experiments, evaporation occurred at various intensities during the day, as evidenced by the relative humidity (Fig. 3).

According to Dunford and Fletcher (1947) and Bren (1997), diurnal changes in stream discharge depended mainly on the wooded stream banks, which increased transpiration. In the Kubaleniec catchment, the banks are not uniformly wooded and yet there were more than a dozen centimetre fluctuations in the shallow alluvial water tables during 24-hour periods in summertime. This would attest to an important role being played by evapotranspiration as the driver of the diurnal hydrograph also in non-wooded catchments.

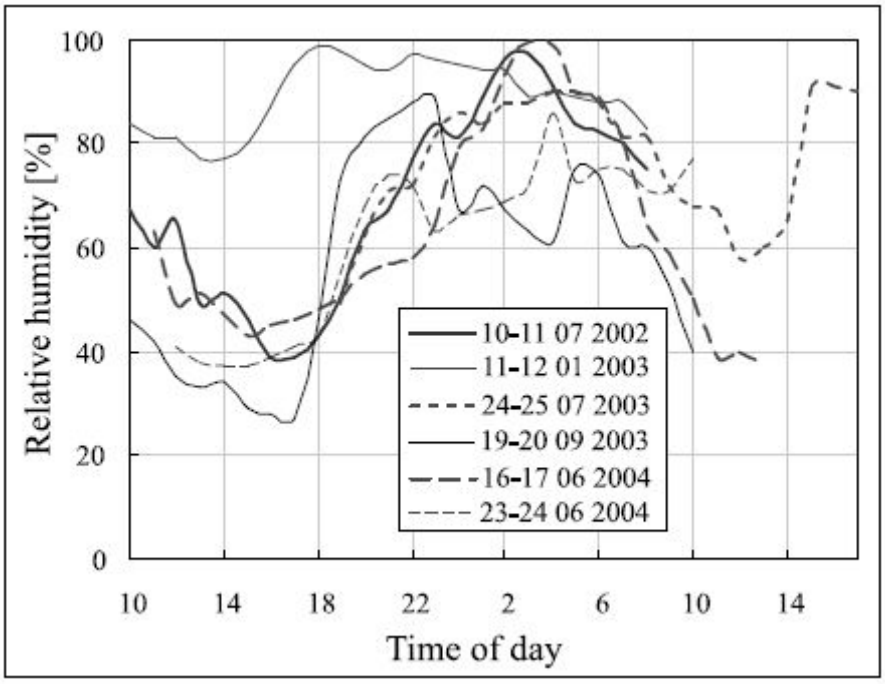

Fig. 3: Relative humidity at the Lazy meteorological station during 24-hour sampling periods.

Water chemistry changes within 24-hour periods

The changing diurnal discharge was accompanied by chemical changes. During summertime, the greatest conductivity at Lesny Potok was recorded during the lowest flows, i.e. in the afternoon or evening; conversely, the lowest conductivity was measured during the greatest discharge periods, i.e. in the early morning hours (Fig. 4). Changes to the conductivity clearly coincided with the discharge changes. This was due to a greater ionic density during daytime as a result of evapotranspiration, as compared to night time. Differences in conductivity were not great and ranged from several to more than a dozen µS/cm. Slight concentration changes in macroelements were recorded (Ca^{2+}, Mg^{2+}, Na^{+}, K^{+}, HCO_3^{-}, SO_4^{2-}, Cl^{-}), as was a clear alternating pattern in nutrient concentration, such as ammonia ions, nitrites, nitrates and orthophosphates.

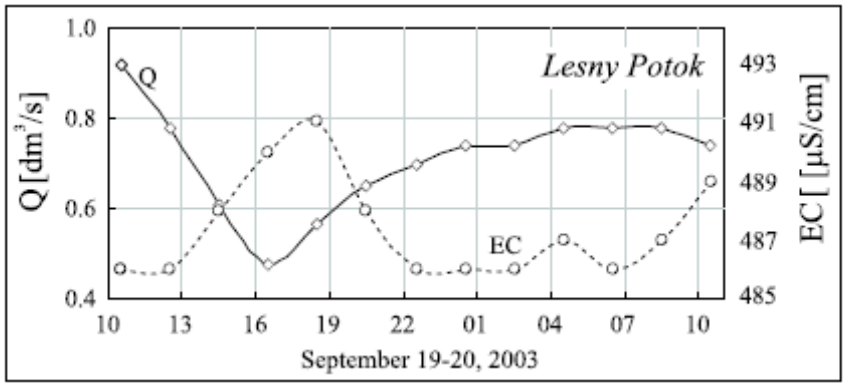

Fig 4: Diurnal fluctuation of discharge (Q) and electrical conductivity (EC) of Lesny Potok during 24-hour experiment (19-20 September 2003).

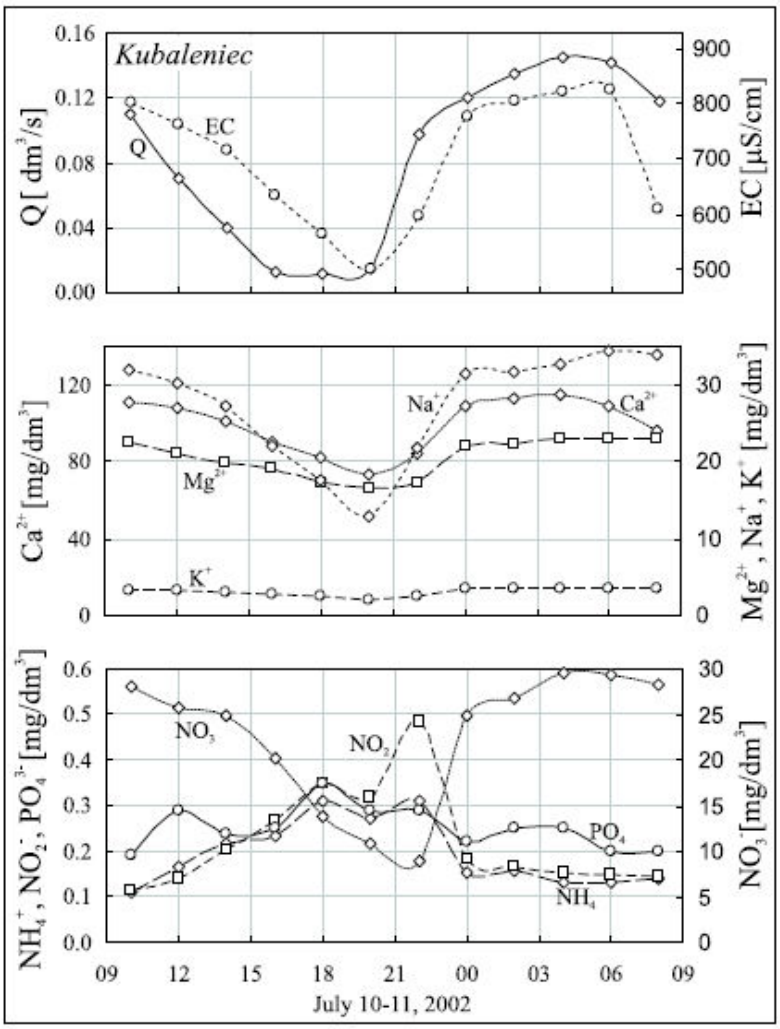

Fig 5: Diurnal fluctuation of discharge (Q), electrical conductivity (EC), cations and nutrients content in the Kubaleniec streamwater during 24-hour experiment (10-11 July 2002).

A completely different pattern of chemical changes was discovered at Kubaleniec. As the discharge dropped during the day, so did conductivity and macroelements and nitrates, but other nutrient compounds increased (NH_4^+, NO_2^- and PO_4^{3-}) (Fig 5). Those changes were very clear, such as with conductivity ranging from 500 µS/cm in the evening to 826 µS/cm in the early morning hours (10-11 July 2002). They had been caused by the changing water supply mechanism as a result of the changing intensity of evapotranspiration.
When the discharge increased at night and in the early morning hours, more of the Kubaleniec water came from shallow alluvial water and water from various types of effluents, including springs and seepages in the mid and upper part of the catchment.
As a result of extensive organic fertilisation the shallow alluvial water of the Kubaleniec catchment was highly polluted and water from effluents in the right-bank catchment often transported household sewage discharged from farms located on the watershed at Brzeznica village. During the daytime decrease in the Kubaleniec flow caused by intense evaporation, the proportion of polluted waters in the supply to the stream diminished. Kubaleniec was alimented primarily with deeper circulation alluvial waters, characterised by lower conductivity and macro-ion concentration.

A similar mechanism of the diurnal water chemistry fluctuation, i.e. the changing supply of polluted water, had been observed by Bourg and Bertin (1996) in France and by Nimick et al. (2003) in the US. The chemical composition of the Stara Rzeka water during a summertime precipitation-less 24-hour period varied widely; sometimes it was close to that in Lesny Potok and on other occasions, to that of Kubaleniec.

Changes to the nutrient concentration in the streams also depended on the biological activity of microorganisms and vegetation in the catchment and the watercourse itself, i.e. the decay of organic matter, transformation of the mineral forms of nitrogen and the diurnal consumption of such nutrients. The dynamics of nitrogen mineral forms depended on the nitrification/denitrification process, as attested to by the varying proportions of ammonia, nitrite and nitrate ions during the 24-hour period (Fig. 6).
The role of the individual factors driving the change of the nutrient content is difficult to discern, as pointed out by Bourg and Bertin (1996). Further interdisciplinary research would be needed if this issue were to be solved.

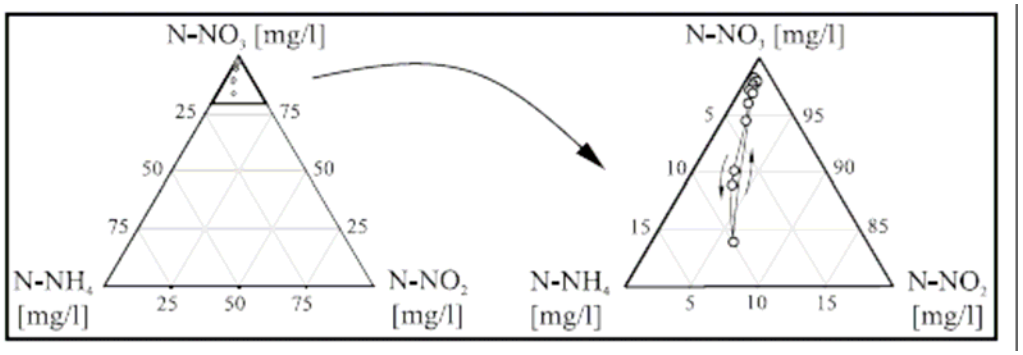

Fig 6: Changes of proportions of ammonia, nitrite and nitrate ions in the Kubaleniec streamwater during 24-hour experiment (10-11July 2002).

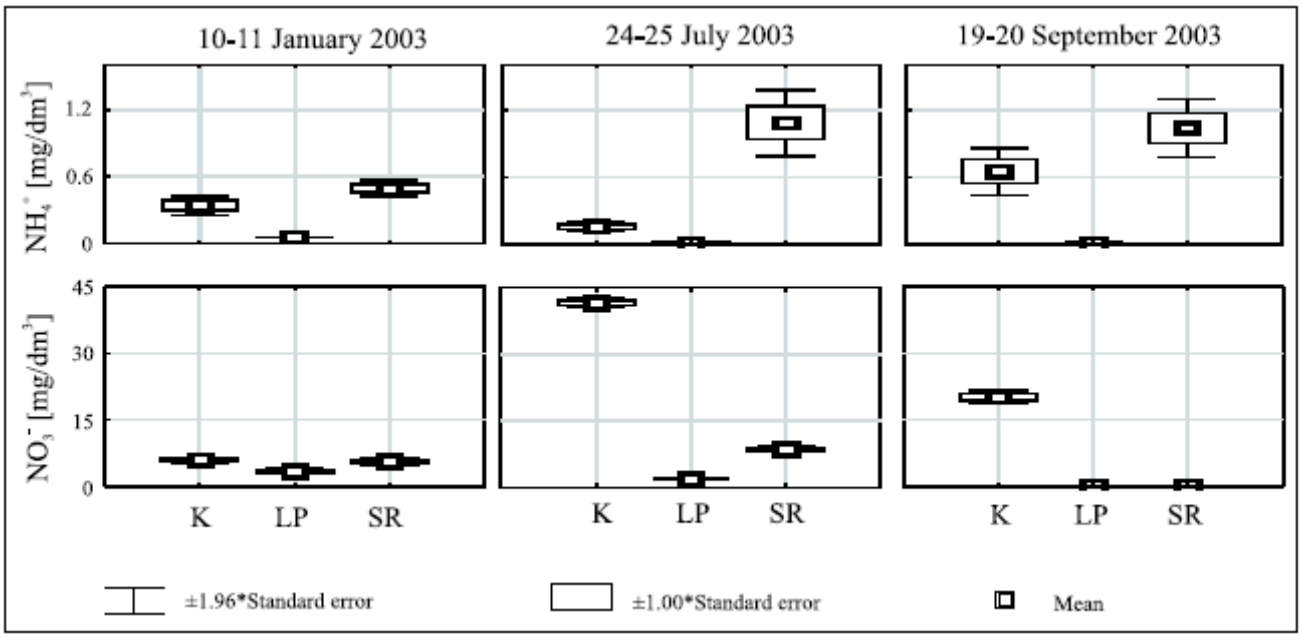

Fig 7: The mean concentration of ammonia and nitrate and its changes in Kubaleniec (K), Lesny Potok (LP) and Stara Rzeka (SR) streamwater during 24-hour experiments.

An analogous programme was carried out in wintertime at air temperatures below -10°C. Similar conductivity changes were recorded on all three watercourses with an increase at night and decrease during the day. The daytime conductivity reduction was caused by an increased supply to the channel of low-mineralisation water from snow and ice melting in the sunshine.

The average ionic concentration and its changes in anthropogenic catchments (Kubaleniec and Stara Rzeka) was lower in wintertime than in summertime. In the wooded catchment of Lesny Potok the average ionic concentration and its diurnal changes were similar both in winter and in summertime (Fig. 7).

CONCLUSIONS

During summertime, clear changes in flow intensity were recorded in small foothill watercourses within 24-hour periods. The changes were caused by evapotranspiration which, however, had different effects on the 24-hour hydrograph depending on land use. The diurnal changes in water flow intensity were accompanied by patterns of water chemistry changes. The most distinct chemical changes were observed in catchments with a strong anthropogenic impact, i.e. the Kubaleniec and Stara Rzeka catchment.
The average ionic concentration and its diurnal changes in Kubaleniec and Stara Rzeka were greater in the summer than in the winter. Similar levels of ion concentration and diurnal changes were observed in the wooded Lesny Potok catchment.
The documented water chemistry changes measured within 24-hour periods outside flood events lead to a great deal of uncertainty as to the desirable timing of water sampling in order to get results which are representative for particular days. There is no mention of such sampling timing in any of the methodologies of river water chemistry research with respect to low flow periods.

ACKNOWLEDGEMENTS

The research project was funded by the Polish Committee for Scientific Research (Project 3 P04G 050 22).

REFERENCES

Bourg, A.C. and Bertin, C. (1996). Diurnal variations in the water chemistry of a river contaminated by heavy metals: natural biological cycling and anthropic influence. *Water, Air and Soil Pollution*, 86.
Bren, L.J. (1997). Effects of slope vegetation removal on the diurnal variations of a small mountain stream. *Water Resources Research,* vol. 33, no. 2.
Dunford, E.G. and Fletcher, P.W. (1947). Effect of removal of stream bank vegetation upon water yield, Transactions. *AmericanGeophysical Union*, Vol. 28, no. 1.
Godwin, H. (1931). Studies in the ecology of Wicken fen, 1, The groundwater level of the fen. *J. Ecol*., 19.
Kobayashi, D., Suzuki, K. and Nomura, M. (1990). Diurnal fluctuaction in stream flow and in specific electric conductance during drought periods. *J. Hydrol.,* 115.
McKnight, D.M. and Bencala, K.E. (1989). Reactive iron transport in an acidic mountain stream in Summit County. Colorado: a hydrologic perspective. *Geochimica et Cosmochimica Acta*, vol. 53.
McKnight, D.M. and Bencala, K.E. (1990). The chemistry of iron, aluminum, and dissolved organic material in three acidic, metal-enriched, mountain streams, as controlled by watershed and in-stream processes. *Water Resources Research*, vol. 26, no. 12.
Nimick, D.A., Gammons, Ch.H., Cleacby, T.E., Madison, J.P., Skaar, D. and Brick Ch.M. (2003). Diel cycles in dissolved metal concentrations in streams: occurrence and possible causes. *Water Resources Research*, vol. 39, no. 9.
Lundquist, J. D. and Cayan D. R. (2002). Seasonal and spatial patterns in diurnal cycles in streamflow in the western United States. *J. Hydrometeorol.*, vol. 3.
Olewicz, Z.R. (1973). Geologia przedkarpackiego obszaru miedzy Wieliczka a Bochnia*, Pr. Inst. Naft., Wyd. ÑSlaskî,* Katowice, 52.
Ortiz, R.F. and Stogner, R.W. (2001). Diurnal variations in metal concentrations in the Alamosa River and Wightman Fork, Southwestern Colorado, 1995-97. *U.S.Geological Survey, Water-Resources Investigations Report 00-4160*. Denver, Colorado.
Poborski, J. (1952). Zloze solne Bochni na tle geologi okolicy. Biul. 78, PIG, Warszawa.
Sullivan, A.B., Drever, J. I. and McKnight, D. M. (1998). Diel variation in element concentrations, Peru Creek, Summit County, Colorado. *Journal of Geochemical Exploration*, 64.

Sullivan, A.B. and Drever, J. I. (2001). Spatiotemporal variability in stream chemistry in a high-elevation catchment affected by mine drainage. *J. Hydrol.*, 252.

Swiechowicz, J. (2002). Wspoldzialanie procesow stokowych i fluwialnych w odprowadzaniu materialu rozpuszczonego i zawiesiny ze zlewni pogorskiej. w: *Przemiany srodowiska na Pogorzu Karpackim*. t. 3. IGiGP UJ, Krakow.

Troxell, H.C. (1936). The diurnal fluctuactions in the groundwater and flow in the Santa Ana River and its meaning, *Eos Trans. AGU*, 17.

THE HYDROLOGIC AND NITRATE REGIME OF KOPANINSKÝ TOK RESEARCH WATERSHED

P. Tachecí[1] and T. Kvítek[2]

[1]DHI Hydroinform a.s., Prague, Czech Republic, [2]Research Institute for Soil and Water Conservation, Prague – Zbraslav, Czech Republic
e-mail Pavel Tachecí: p.tacheci@dhi.cz
e-mail Tomáš Kvítek: tomas kvitek@vumop.cz

ABSTRACT

Kopaninský tok research area data (1982-2002) were used for a modelling study on hydrologic and nitrate regime, serving as a basis for the comparison of the influence of expected agricultural management changes on the water quality and quantity in a perennial stream. A complex water movement model was built using the MIKE SHE WM model, while nitrate concentrations in water percolating below the unsaturated zone were simulated using the DAISY GIS model for 20 individual agricultural management units. Movement of the nitrate pollution in the unsaturated and saturated zones and in the stream was simulated using the MIKE SHE AD module. Discharge at 6 stream gauges was simulated quite well in calibration (2000-2002) and validation (1982-2000) periods, however in most cases, nitrate concentrations do not fit the field sampling points satisfactorily. Using the Doležal and Kvítek (2004) hypothesis of two main sources of nitrate pollution in the Kopaninský stream, it is expected that the model simulates base flow (the second source) much better than interflow (the first source).

Key words: distributed hydrological modelling, water balance, regime of nutrients, agricultural catchments, MIKE SHE model, DAISY GIS model.

INTRODUCTION

The Czech Republic, as well as some other Central European countries, is facing the problem of surface and subsurface water pollution from agricultural sources. Large amounts of (mostly inorganic) fertilizers were used during the second half of the 20th century. After 1990 those amounts rapidly decreased, but the response of the average concentration of nitrates in the groundwater and surface water was not as adequate as might have been expected. For a more precise insight into the local and regional application of changes of agricultural rules and their impacts, the National Agricultural Research Agency founded the "The application of the alternative management system for soil and water conservation in the landscape" research project with The Research Institute for Soil and Water Conservation, Prague – Zbraslav (VUMOP) acting as its project co-ordinator. This project consists of a number of particular studies. This contribution focuses on the modelling study using deterministic mathematical modelling systems only. Models of the current conditions form a basis for further assessment of the influence of expected agricultural management changes to the water quality and quantity. Three particular areas with different climatic and hydrogeological conditions were studied in the project framework. Here, attention is only paid to the Kopaninský tok area, which forms the research watershed.

KOPANINSKÝ TOK RESEARCH WATERSHED

This research area has been operated by VUMOP since the beginning of the 1980s as a source of data for different types of research studies. Basic data of the area are: average latitude 49^{o} 28' N, average longitude 15^{o} 17' E, height above sea level: min 467, max 578 m a. s. l. Total area is about 8.6 km^2 of which arable land covers 52 %, grassland 14 % and forest (spruce prevails) 30 %. Average annual precipitation total is about 665 mm, average annual air temperature 7.0 °C (meteorological station Humpolec, 1901-50). The bedrock consists of partly weathered and fractured paragneiss, the soil cover is formed mainly by Dystric Cambisol. The depth of the soil profile varies around 100 cm. The area of interest is hilly (Bohemo-Moravian Highland). A large part of the area was systematically drained using tile drainage dug mostly to

about 15 meters in length and lying at a depth of 1 m below the soil surface (e.g. Kvítek and Doležal, 2003; Lexa and Kvítek, 2003).

Since 1992, discharge and water quality have been measured regularly twice a month at the main perennial stream (Kopaninský tok) and some tributaries. Different land cover conditions and agricultural practices take place at those sub-watersheds. Since 2000 some of the measuring devices have been automated. In this paper we focus on the upper part of the whole watershed only, closed by stream gauge no. T7 (located upstream of Velký Rybník settlement, see Fig. 1). The total area of the modelled part of the watershed is 6.7 km^2, of which 51 % is covered by arable land, 12 % by grass, 35 % by forest, and the remaining 2 % consists of water bodies and urban areas. About 20% of the area is drained artificially.

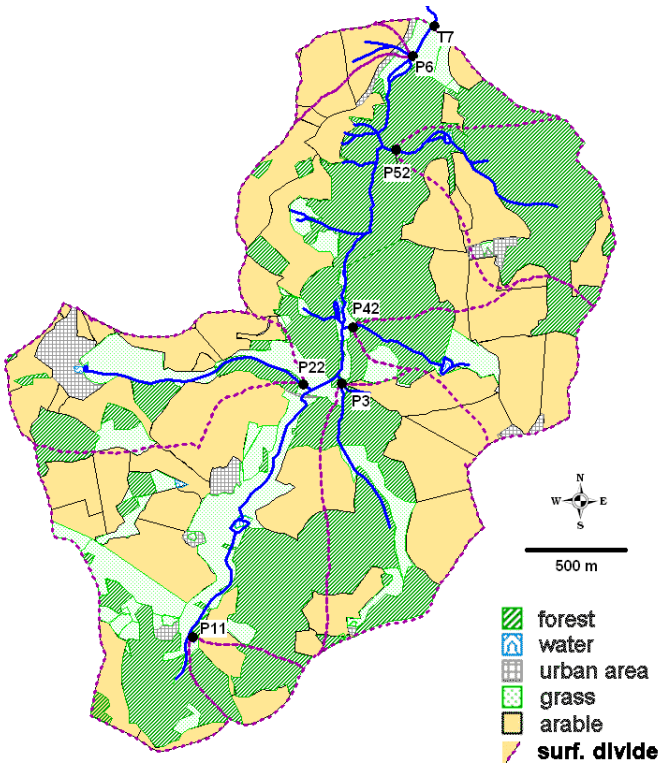

Fig. 1: The upper part of Kopaninský tok watershed modelled area. Agricultural management units, land use categories, stream network, stream gauges and sub-watersheds divides are visible.

Doležal and Kvítek (2004) conducted an analysis of the 1992-2000 data. They identify three zones in the watershed: the recharge zone (hill tops), the transient zone (middle and lower parts of slopes) and the discharge zone (flat strips around perennial streams). They hypothesise that the recharge zones are the main sources of nitrate contamination of the groundwater. Furthermore, based on data analysis they conclude that interflow probably acts as the main polluter of stream water, followed by baseflow.

DATA USED

Two types of data inputs were used for modelling: spatially distributed maps and time series of point measurements. A digital terrain model was generated from a contour line map. Land use and vegetation cover maps were established for the 1982 – 2002 period using historical data from farmers and combined with 1:10 000 maps of the area. Twenty three spatial agricultural management units were delineated. The soil types map was aggregated using the VUMOP databank (based on a dense historical field measurement campaign). For our purposes the whole area of interest is considered to be covered by one soil type. Total depth of the soil profile for modelling purposes was estimated at 1.2 m. The hydraulic characteristics were obtained using measured points of retention curves at 70 soil cores taken from 10 pits dug across the watershed. Measured retention curves points were fitted to a van Genuchten-Mualem type of relationship and

scaled to three reference retention curves for particular soil profile horizons (Vogel, 1990). Saturated hydraulic conductivity was approximated using surface infiltration experiments and other studies (e.g. Hejnák, 1994). The other physical parameters were set using physical and granular analyses of the soil samples. The map of the soil substrates, as well as the map of depth of soil substrates, were created using Hejnák's data (2000). Final values of the saturated hydraulic conductivity and other hydraulic parameters of the saturated zone layers were calibrated. The map of drained areas was created using historical drainage project data. Drainage runoff coefficients were calibrated. A simple schematised 1D hydrodynamic (kinematic wave) model of flow in the stream and main tributaries was created (total length of the modelled main stream is about 5.9 km).

Daily time series (1982-2002) of the precipitation, air temperature and potential evapotranspiration (computed using Penman-Monteith equation) from the Křešín – Kramolín station were used. This station (operated as a part of the regular Czech Hydrometeorological Institute network) is situated at a distance of about 20 km, but it is still considered to be representative of the area of interest. For calibration and validation purposes, time series of the measured discharge in 6 stream gauges operated by VUMOP (1993-2002 period) were used.

The time series of nutrient inputs have to be estimated for every delineated agricultural management unit. For this purpose, average annual NO_3 and NH_4 atmospheric deposition amounts were approximated using Czech Geological Survey network data. The majority of nutrients within the soil results from agriculture. Field research focussing on agricultural practices was conducted by VUMOP. Unfortunately, the farmers did not provide any historical data of crop types and fertilisers used for the largest part of the watershed (61% of the area). Estimated average values have to be used instead of the more accurate records of crops, agricultural management operations and fertilizer amounts available for the remaining 39% of the area. A unique historical time series of agricultural operations was created for all 20 agricultural management units of the arable soil, covering the 1982-2002 period. The remaining three units were identified as forest, grassy areas and urban areas.

MODELLING TOOLS USED

Two types of spatially distributed models were used. MIKE SHE is a comprehensive mathematical modelling system distributed by DHI Water and Environment (Denmark). The Water Movement (WM) and Advection – Dispersion (AD) modules of the 2003c version were used in this study. The WM module allows the simulation of the water flow at terrain surface (overland flow and river channel hydrodynamical 1D model). In the unsaturated zone, the Richards equation approximation was used, while the layered 2D solution of the Boussinesq equation was used for the saturated zone. The actual evapotranspiration rate was computed by the implemented Kristensen – Jensen routine, using as input potential evapotranspiration time series. A more detailed description can be found at www.MIKESHE.com and in Abbott and Refsgaard's book (1996).

The DAISY GIS tool is an application of the well known Danish Royal Veterinary and Agricultural University model DAISY (e.g. Hansen et al., 1990; Hansen et al., 1991; Abrahamsen and Hansen, 1999) running in the ESRI ArcView 3.2 environment. The GIS-based graphical user interface enhances the use of the DAISY model for spatially distributed cases of water and nutrient regime simulation in a soil profile. The Danish version of 2003 was used for the purposes of this study. More about DAISY GIS can be found at www.mikeshe.com/daisygis.

MODELLING SET-UP, CALIBRATION AND VALIDATION

The whole area of interest was covered by regular grid elements (30x30 m) for MIKE SHE model purposes. The DAISY GIS model works with irregular polygon areas, having a unique combination of soil, land use and climatic conditions directly in ArcView shape layer file format. The parameters, time series and spatially distributed data were put into both models. Vegetation data for all agricultural management units were processed and put into the MIKE SHE model (leaf area index and root depth parameter time series) and into the DAISY GIS model (agricultural management operations and types of crop in particular periods).

The spatially distributed simulation of the hydrologic and nitrate regime was carried out in the following way. First, a water movement and moisture regime model of the area was established using the MIKE SHE WM modelling system. Components for modelling of surface runoff, river flow, unsaturated zone, saturated zone, evapotranspiration and snow melt were used (see example in Fig. 2).

The daily average values of the discharge into the main stream (stream gauge No T7, closing profile of watershed) for the 2000-2002 period were used for the calibration of the WM model. Bi-weekly instantaneously measured values of discharge at 6 stream gauges (period 1993-2002) were used for the validation of the model. Model performance to predict discharge was evaluated by using a split-sample type of test for the T7stream gauge. The spatial distribution of parameters was validated against instantaneously measured discharge data at five stream gauges (where no calibration was carried out). A summary of results is presented in table 1. The water balance for the entire 1982-2003 period was established successfully. All of the validation tests proved the model as a whole was performing well. Runoff response at stream gauges of sub watersheds is expected to be well simulated too.

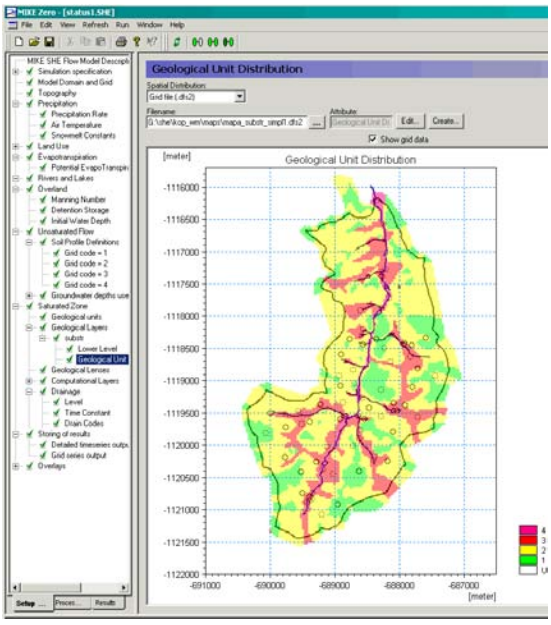

Fig. 2: Example of the MIKE SHE WM model set-up; distribution of saturated hydraulic conductivity across the area (SZ).

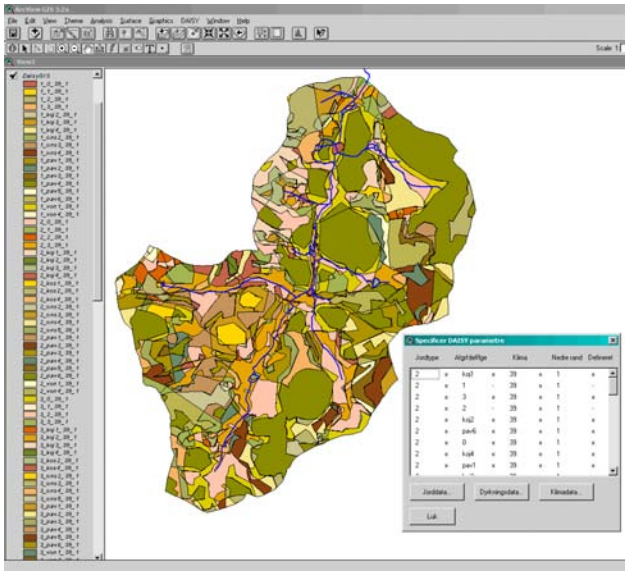

Fig. 3: Map of polygons with unique soil and field management conditions as an input for the DAISY GIS model.

Tab. 1: Summary of the calibration and validation performance of the WM model

Gauge Station	Q avg (l/s)	Time period	No of measured values	Correlation coeff. R	Nash – Sutcliffe efficiency coeff.	Notes
T7	34.3	2000-2002	962*	0.776	0.57	calibration
T7	27.2	1993-2000	164	0.751	0.50	validation
P22	5.1	1993-2002	258	0.831	0.49	validation
P3	4.3	1993-2002	258	0.832	0.52	validation
P42	2.5	1993-2002	258	0.784	0.39	validation
P52	3.6	1993-2002	258	0.758	0.27	validation
P6	0.6	1993-2002	258	0.683	0.33	validation

* daily average data

A detailed soil moisture and nitrate regime model for the unsaturated zone was built using the DAISY GIS tool, as well as spatially distributed parameters and data (see Fig. 3). Twenty three unique daily time series of

nitrate concentrations in water percolating to the saturated zone were obtained as spatially distributed results of the DAISY GIS model. They were used as input for the MIKE SHE AD model, based on MIKE SHE WM results. This model was able to simulate the movement of nitrate pollution through the unsaturated and saturated zones to the stream. The main parameters (dispersivities of particular zones and porosity) were calibrated. Computed time series of nitrate concentrations in the individual stream gauges at Kopaninský stream and its tributaries were compared with measured data.

Then, several scenarios of changes in agricultural management were simulated (the partial conversion of arable areas to grassy areas, conversion of the whole arable area, closing of the drainage system). Changes in nitrate concentrations in streams were compared.

RESULTS AND DISCUSSION

The example of the obtained results (stream gauge No P52, period 2.1.1996-1.1.2001) is presented in Fig.4. The area of sub-watershed 5 is about 0.65 km^2; 67% is covered by forest and 33% by arable land.

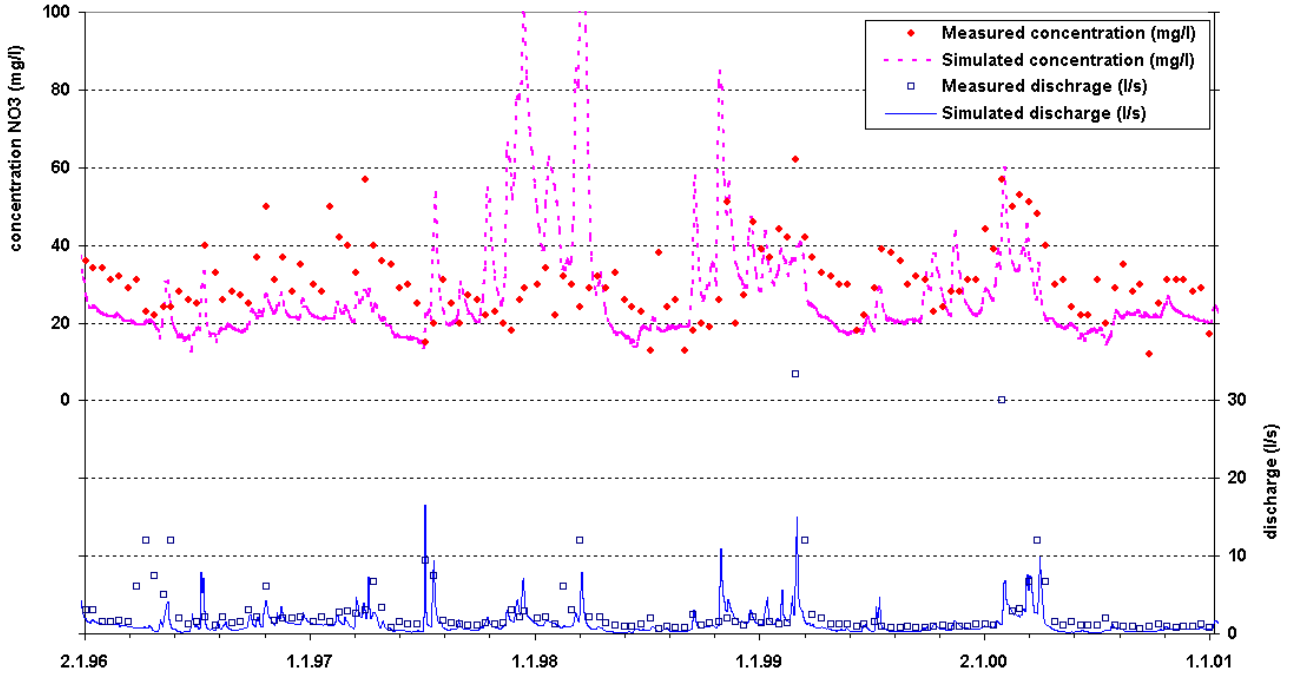

Fig. 4: Example of results (stream gauge No P52, period 2.1.96-1.1.01). Comparison of measured and simulated NO_3 concentrations (upper part) and discharges (lower part).

It is observed that higher concentrations of nitrates (up to 60 mg/l) are reached mainly during the spring season, when high discharges occur too. The model is able to follow this trend quite successfully sometimes (spring 1999, 2000), but on occasion simulated concentrations are too high (1998) or do not respond (1997) at all. Lower concentrations during the rest of the season are slightly underestimated by the model. Discharge values are simulated quite successfully, but some of the peak values during the snow melt period are underestimated. The MIKE SHE model uses a simple Degree-day routine for snowmelt and it was not explicitly calibrated for snow parameters. From this simple analysis it is clear that the model is generally able to simulate leaching of nitrates during high-flow conditions (especially during spring), but it is not able to predict observed concentration values. A similar level of agreement of the simulated and measured values was found in another sampling point (P42). Higher values were simulated in some other gauges (T3, P3, P22), as well as lower values (T7, P6). A general overview of the simulated and measured values in all other stream gauges and across the whole period supports the hypothesis that the model most probably simulates the baseflow source of nitrate pollution rather well, but is not able to cope properly with interflow (using the concept of nitrate sources at the watershed formulated by Doležal and Kvítek, 2004).

Examining the reasons for the poor correlation of the model simulation result with measured data, two major sources of error can be suspected. First, a particular problem caused by the rather general schematisation of the agricultural management operations in most parts of the watershed, where farmers did not provide historical data on crop type and fertilisers used. Estimated average values following agricultural management guide rules and recommendations were used instead.

Second, one has to think about model structure and scale issues. The model is not explicitly built as a hillslope flow model, but as a combination of the surface runoff component, a vertical 1D unsaturated flow component and a 2D saturated zone flow component with a drainage option. Thus interflow cannot be simulated directly at grid scale (30m). On the other hand, the discharge is rather well simulated. However, the recession limbs of hydrographs are slightly steeper for most flood waves. At this scale of rather small watersheds (units of km^2) we are already above the scale of a hillslope or a valley (the Kopaninský stream has several perennial streams as tributaries with their own subwatersheds), but we are not at the scale of large landscape units, where the influence of one particular agricultural management unit on transformation and transport processes cannot be investigated.

Despite all of these problems, this model still serves as a good tool for the comparison of long-term influences of possible changes in agricultural management on nitrate concentrations. Differences in the simulated long term time series of nitrate concentrations (between current status and proposed variants) were statistically evaluated.

ACKNOWLEDGEMENTS

This paper reports the results obtained in project no. QC 0242, financed by the National Agricultural Research Agency (Ministry of Agriculture of the Czech Republic). Project co-ordinator is the Research Institute for Soil and Water Conservation, Prague – Zbraslav (VUMOP). The authors thank Dr. František Doležal, (VUMOP) for useful comments.

REFERENCES

Abbott, M. B. and Refgaard, J.C. (1996). Distributed hydrological modelling. Kluwer Academic, Dordecht Abrahamsen, P. and Hansen, S. (1999). Daisy: An open soil-crop-atmosphere model. Submitted to Environmental Modelling and Software.

Doležal, F. and Kvítek, T. (2004). The role of recharge zones, discharge zones, springs and tile drainage systems in peneplains of Central European highlands with regard to water quality generation process. Physics and Chemistry of the Earth 29 (2004) 775-785.

Hansen, S., Jensen, H.E., Nielsen, N. E. and Svendsen, H. (1990). DAISY: Soil Plant Atmosphere System Model. NPO Report No. A 10. The National Agency for Environmental Protection, Copenhagen, 272 pp.

Hansen, S., Jensen, H.E., Nielsen, N. E. and Svendsen, H., (1991). Simulation of nitrogen dynamics and biomass production in winter wheat using the Danish simulation model Daisy. Fert. Res. 27, 245-259.

Hejnák, J. (1994). Geological survey for agricultural management of Švihov reservoir watershed (in Czech). Final research report of project MŽP GA/379/93.

Hejnák, J. (2000). Hydrogeological maps and parameters of Kopaninský tok watershed area. Unpublished part of research report of project NAZV QC0242.

Kvítek, T. and Doležal, F. (2003). Hydrologic and nutrient regime of Kopaninský tok area at Bohemo-Moravian highland (in Czech). Acta hydrologica slovaca, 2003, vol. 4, no. 2, p. 255-264. ISSN 1335-6291.

Lexa, M., Kvítek, T. (2003). Analysis of concentration of nitrate in streams of catchment of dribling water reservoir Zelivka in the Czech republic. European Geophysical Society 2003, Geophysical Abstracts,Vol. 5, 10649.

Vogel, T. (1990). Numerical modelling of soil water movement in non homogeneous soil profile, Doctoral Thesis, CTU Prague. (in Czech).

EFFECT OF SOIL MANAGEMENT TECHNIQUES ON RUNOFF AND SURFACE EROSION IN HILLSIDE VINEYARDS

A. Ferrero and L. Lisa

National Research Council (CNR) Institute for Agricultural and Earth Moving Machines (IMAMOTER), Strada delle Cacce, 73 – 10135 - Turin, Italy
e-mail Aldo Ferrero: a.ferrero@ima.to.cnr.it

ABSTRACT

In two sites in N.W. Italy, multi-year controls of rainfall, runoff, soil and nutrient losses from hillside vineyards, with different soil management of the inter-rows, were carried out. In a hillside catchment (450 m a.s.l.), two vineyard plots were hydraulically isolated and supplied with runoff measurement devices. Both plots have rows running across the slope (15-35%), and conventional tillage (T) and controlled grass cover (GC) have been compared over the last six years. On the other site the plots were in a vineyard with rows running down the slope (22-25%). Normal rainfall (max. intensity < 10 mm h^{-1}), rainstorms and long lasting rainfall were examined separately. Some of the physical-hydrological properties of the topsoil on transects transversal to inter-rows were monitored. On the first site, as an average over seven years, top soil loss resulted in 2.4 t ha^{-1} per year from the T plot and 0.5 t ha^{-1} from the GC plot. Soil loss was greater during rainstorms, accounting for 92% of the total in T plot and 84 % in the GC plot. In the vineyard, with the downward-running rows , as an average over four years, annual soil loss resulted in 14.2 t ha^{-1} from the T plot and 2.9 t ha^{-1} from the GC plot. The long lasting rains produced the greatest amount of runoff: respectively 682.4 Kl ha^{-1} and 401.3 Kl ha^{-1}. The GC management considerably increased the organic matter content and the aggregate stability of the upper soil, compared with T plot.

Key words: hillside catchment, soil erosion, sloping vineyard, tillage, grass cover.

INTRODUCTION

Viticulture represents the main cash crop of the hillside agriculture of Piedmont (N.W. Italy). High quality vineyards are mainly located on steep hillslopes (gradient 20-40%); traditionally they are cultivated with deep and surface tillage to keep the soil bare of vegetation. This technique can lead to deterioration of the soil's physical properties, surface erosion and nutrient leaching. Tillage decreases the aggregate stability and creates soil conditions leading to runoff due to surface sealing (Lal, 1993). Increasingly, to make full mechanization easier, new vineyards are planted with rows running down the slope, instead of the traditional contour planted rows, a technique that helps to break runoff. Moreover in these areas, soil erosion is much higher than in comparable European sites (Tropeano, 1984). In Southern Italy a multi-year comparison of the ploughing and tillage techniques across or down the slope in hilly plots, with the same crop sequence, has shown mean yearly soil losses of 1.45 t/ha from those with contour soil working and of 3.16 t/ha from the ones worked down the slope (Basso et al., 2000).
Controlled grass cover of the inter-rows has proved to prevent structural degradation of the soil (Pagliai et al., 1995) and, by increasing soil water absorption during high intensity rainstorms, to reduce soil erosion (Sicher and Venturelli, 1989). After some years of grass cover management of the vineyard, we have found the formation of a compact "pan" in the tractor's tracks and vigour decrease of the vines, particularly in dry years. (Lisa et al., 1999). To ascertain the efficiency of this type of vineyard management in containing runoff and soil erosion, a multi-year experiment has been conducted at two sites in Piedmont, representative of hillside viticulture: the rainfall, runoff and soil losses from vineyard plots with tillage and grass cover managements were monitored.

METHODS

The climate of the two sites is similar consisting of cold winters with snow and dry summers with rainstorms including a drought period from the beginning of July to the middle of August (Fig. 1). The experimental

catchment of Vezzolano (Northern Monferrato) situated at 450 m a.s.l., has a mean annual rainfall of 841 mm and clay loam soil (28% clay) over marls of the Baldissero Formation (Middle Miocene). The vine rows run across the slope (15-35%) and are arranged in bands with a slight longitudinal slope (2-10%) and terracing at the head. Measurements were carried out here from 1992 to 1998. Two plots, some 0.56 ha each, with conventional tillage (T) (autumn ploughing, two tillings) and with controlled grass cover (GC) (mowing and chopping three times per year) were hydraulically isolated by an inter-row with uphill counter slope, and supplied with water capture outlet, measurement devices and slowing decantation tanks. The runoff gauge consists of two balancing buckets, developed from an IRPI design (Tropeano, 1984) equipped with click counter and recording system (Fig. 2), and of an overflow meter to measure any overflow from the tanks. The weather station at the farm equipped with a pluviograph (0.2 mm resolution) supplied the meteorological inputs.

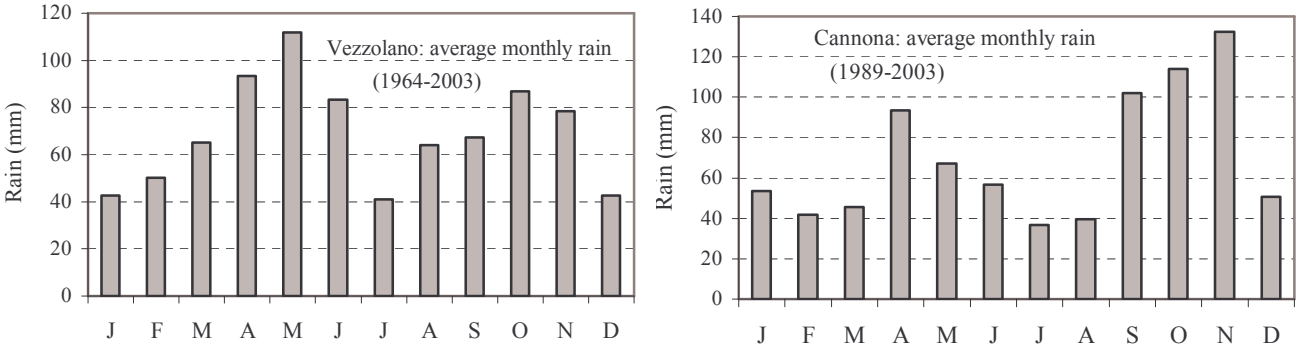

Fig. 1: Average monthly rain at the two experimental sites.

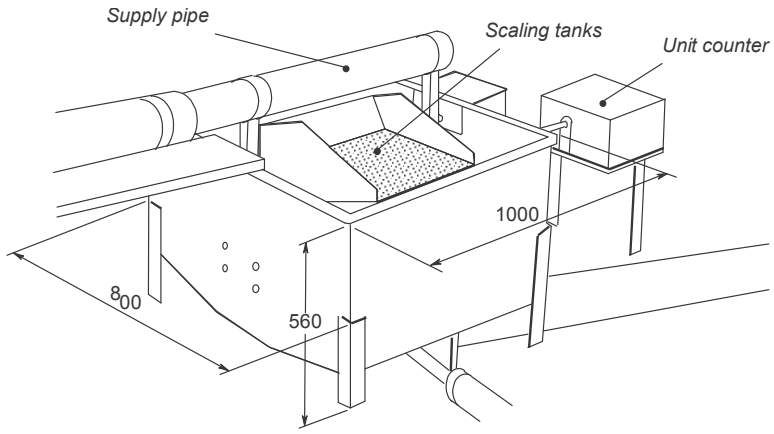

Fig. 2: Schematic of the measurement device for the water runoff from the vineyard plots, fitted with scaling tanks and counter.

Surveys have been carried out since 1999 at the Cannona regional experimental farm, near Carpeneto, (S.W. Piedmont). This farm is at 310 m a.s.l. with a mean annual rainfall of 852 mm and lies on clay soil (38% clay), resting on clays of the Lugagnano Formation (Middle Pliocene). Two plots measuring some 0.13 ha and with rows running down the slope (22-25%) spaced at 2.75 m intervals, were hydraulically isolated by uphill counter slope and by ditches. They were supplied with a water capture outlet, measurement devices and decantation tanks. The water measurement units are the same as at the Vezzolano site. The weather station at the farm and a pluviograph installed at the monitored vineyard are used for comparing the water runoff in light of the rainfall trends.

At both sites, samples of the muddy water were taken and subjected to analysis for soil and nutrient content. Soil deposits in the sedimentation tank, before the gauge unit, were also measured.

Some soil characteristics in three layers down to a depth of 30 cm were determined. Bulk density, water content at saturation and at field capacity were measured on undisturbed soil cores using a method developed at our Institute (Ferrero, 1991).

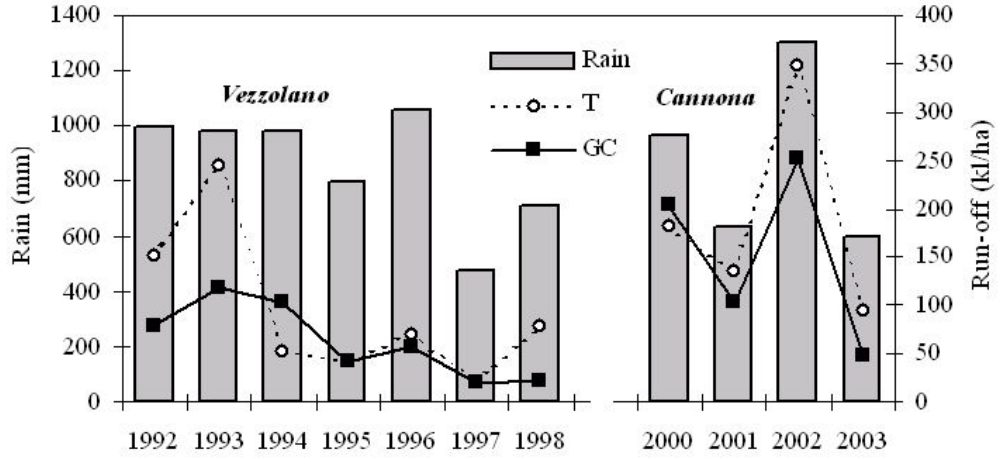

Fig. 3: Total annual rainfall and runoff trends at tilled (T) and grass covered (GC) vineyard plots at Vezzolano and Cannona.

Monitoring of soil water content by sampling and resistance to penetration using a penetrometer with crank advance was carried out over the growing season. The water aggregate stability index (W.A.S.) was determined according to the procedure described by Pagliai et al., (1997). The vegetative and productive characteristics of the vine plants were also monitored in the two plots.

RESULTS

All the rainfall episodes were taken into account when their runoff exceeded 300 l ha^{-1}. Normal rainfall (maximum intensity < 10 mm h^{-1}) was examined separately from rainstorms and autumnal rains (long lasting rainfalls).

At the Vezzolano site 101 events were considered from 1992 to 1998. The mean duration was 47 h, with mean intensity 1.9, 11.2 and 1.5 mm h^{-1} for normal, rainstorm and autumnal events. In 1993 the runoff was very high in relation to rain depth, especially from T plots, as a result of two high intensity rainstorms. In 1994 the runoff was higher at the GC plot as a result of heavy autumnal rainfall (Fig. 3). In Table 1 the features of each event type are reported.. The runoff coefficient was twice as high at the T plot as at the GC plot during rainstorms, conversely it was much higher at the GC plot during autumnal rains. Moderate annual soil losses were detected during normal rainfall: 21 and 18 kg ha^{-1} at the T and GC plots; during rainstorms they rose to 2390 kg ha^{-1} at the T plot and only 459 kg ha^{-1} at the GC plot (Fig. 4).

At the Cannona farm 69 events were examined, having a mean duration of 96.3 h and a mean rain depth of 58.4 mm. The mean intensity was 1.82, 7.37 and 1.47 mm ha^{-1} for normal, rainstorm and autumnal rainfall events. The yearly amount of runoff versus rain depth showed a tendency to be much higher than at the Vezzolano site, especially during autumnal events, the mean runoffs being 41.7 mm and 31.9 mm respectively from the T and the GC plot. In 2000 the runoff was higher from GC plots as a result of heavy autumnal rains giving rise to prolonged runoff from the surface and the deep soil.

The runoff coefficient was much higher at the T plot than at the GC plot during rainstorms (Table 1), during normal events differences narrowed. The mean annual soil losses were higher than in Vezzolano; during rainstorms they rose to 8089 kg ha^{-1} and 1842 kg ha^{-1} respectively at the T and GC plots. Significant losses

were also detected during autumnal events: they were six times higher at the T plot (3020 kg ha^{-1}) than at the GC plot.

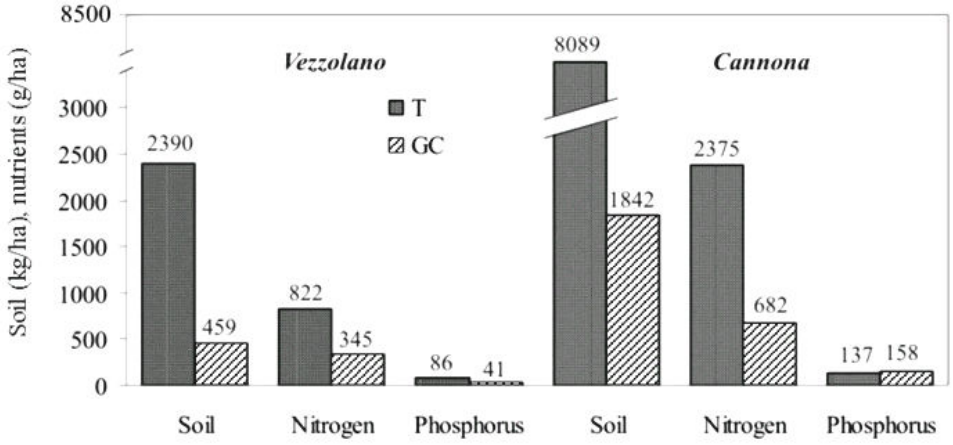

Fig. 4: Average annual soil and nutrient losses during the monitored rainstorm events from tilled (T) and grass covered (GC) vineyard-plots, for the period 1992-1998 at the Vezzolano site and for 2000-2003 at Cannona.

Table 1: Mean features over the years of the recorded rainfall events, runoff coefficient and soil losses from tilled or grass covered vineyard plots at the two experimental sites

Sites		***Vezzolano***			***Cannona***		
Features		Events			Events		
		Normal *[57]	Rainstorm [39]	Autumnal [5]	Normal [30]	Rainstorm [24]	Autumnal [15]
Duration	(h)	62.2	25.0	63.2	53.2	24.8	211.0
Rainfall	(mm)	44.4	36.0	60.7	37.4	45.5	85.5
Max. intensity	(mm h^{-1})	6.2	31.6	4.1	4.6	18.4	4.8
Runoff coeff.	%						
- Tilled		0.72	2.66	1.44	4.78	10.2	37.8
- Grass covered		0.47	1.27	2.82	4.95	6.1	31.4
Soil loss	(kg ha^{-1})						
- Tilled		3.1	500.6	1.9	360.0	1170.2	2485.6
- Grass covered		2.4	99.2	1.3	82.1	247.7	461.3

* in brackets the number of events considered

At both sites the measurements of the soil characteristics indicated a considerable increase in organic matter in the upper soil of the GC plot (Table 2), and of the aggregate stability (WAS). The bulk density was always higher in the GC soil, the highest value being found in the areas of the tractor tracks; this behaviour was more evident at Vezzolano. At both sites the water content at field capacity proved to be higher in the first two layers of the GC plot.

Grass cover notably increased the penetration resistance of the soil, the highest values (up to +0.5 MPa) in the tractor tracks were detected in the vineyard arranged with rows running across the slope. The biggest differences were found at the end of winter. In the vineyard, with rows running down the slope, the differences of penetration resistance between tracked and untracked areas and between the two types of soil

management were lower than at the Vezzolano site. In both plots a compact "pan" appeared in the areas occupied by the tractor tracks and thicker in the GC plot, down to a soil depth of 8-15 cm.

The productive and qualitative measurements highlighted lower plant vigour (less pruning wood) and grape production in the GC treated plots. The effect of soil management appeared to be highly influenced by the weather conditions, especially by low rainfall depth during the fruit growth. The reduced yield tends to recover in the years featuring more rainfall (Fig. 5).

Table 2: Selected soil characteristics (upper 20 cm), in hillside vineyards traditionally tilled or grass covered at the Vezzolano and Cannona sites

Soil characteristics	*Vezzolano*				*Cannona*			
	Tilled soil		Grass cover		Tilled soil		Grass cover	
Parameter	Depth, (cm)				Depth, (cm)			
	0-10	10-20	0-10	10-20	0-10	10-20	0-10	10-20
Organic matter (%w/w)	2.1	2.5	3.9	3.2	1.6	1.9	2.8	2.4
Bulk density ($Mg\ m^{-3}$)	1.19	1.22	1.22	1.28	1.26	1.32	1.30	1.37
Satur. capacity (%v/v)	53.2	49.8	54.2	51.3	48.6	47.5	50.2	48.8
Field capacity (%v/v)	36.1	34.2	38.5	37.6	34.5	33.6	37.6	36.5
Penet. resistance (MPa)	1.7	2.3	2.2	2.9	1.4	2.1	1.8	2.7
Water-stable aggregate Index, W.A.S.	6.1	5.5	20.9	26.2	5.8	6.3	16.6	19.8

Moreover, the qualitative characteristics showed a trend towards higher sugar content in the grapes from GC plots. The differences in grape yield were greater at the Cannona site: mean production over four years and the standard deviation resulted in 4.41 ± 0.48 kg/plant and 3.19 ± 0.57 kg/plant respectively in the T and GC plots.

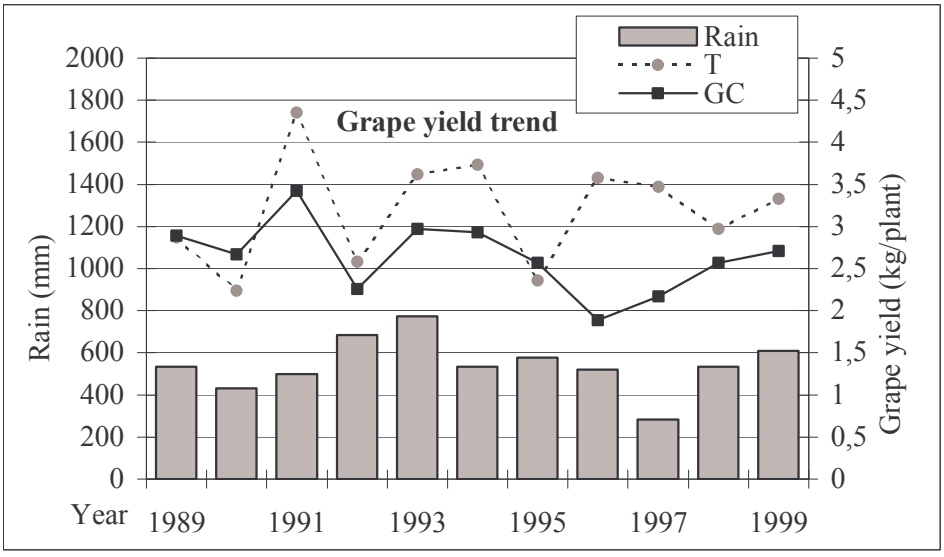

Fig. 5: Total annual rain during the growing period and trend of grape production (Barbera variety) from 1989 to 1999 in the grass covered (GC) and traditionally tilled (T) plots (Vezzolano site).

CONCLUSIONS

At the two experimental sites, the practice of controlled grass cover of the vineyard inter-rows has proved to be effective in reducing runoff and soil erosion. The mean values over seven years at the Vezzolano site,

indicate a top soil loss of 2.41 t ha^{-1} from the T plot and only 0.48 t ha^{-1} from the grass covered one. At the Cannona farm the mean soil losses, over four years, accounted for 9.40 and 1.73 from the T and GC plots. The soil losses at Vezzolano are less than in a similar experiment in central Italy, this may be due to the specific arrangement of the rows in bands with a gentle longitudinal slope.

The trend of greater runoff during autumnal rain (long lasting rains) from the GC plots (more evident at the Vezzolano site) can be induced by a higher bulk density of the grass covered soil, whereas in the tilled soil, the roughness effect prevails producing a greater hydraulic gradient (Burk et al., 1999).

The positive effect of the practice is enhanced during rainstorms: the annual runoff values reach 56.5 mm from the T plot and only 26.4 mm from the GC plot at Vezzolano; at the Cannona site the difference is less marked. Moreover the runoff is more immediate and the soil losses are much greater than at Vezzolano. This behaviour can be explained by the arrangement of the vineyard with rows running down the slope. During high intensity short lived rainstorms, the plant cover and the mulching action of the herbage residues slow down the rain flow and increase the water retention of the top soil, thus reducing soil erosion and nutrient washing (Foti et al., 2000).

The difference in soil erosion depending on the practice followed would also be clarified by the physical properties of the soil, which indicate a considerable increase in organic matter and stability in water of the aggregates in the GC topsoil: both these properties greatly influence soil detachability and transportability (Lal et al., 1994).

Nevertheless, these improvements in soil erosion and soil properties were counteracted by some decrease in grape production in the GC plots, though the grapes were of better quality.

ACKNOWLEDGEMENTS

The research was supported by the Agricultural Agency of the Regione Piemonte. We thank Dr. G. Bonifacino and M. Rabino of the Cannona Regional Experimental Farm and G. Benvegnù of the Vezzolano farm for their technical assistance and R. Massobrio of the IRPI (CNR) for the textural analyses.

REFERENCES

Basso, F., De Franchi, A.S., Pisante, M., Basso B. and Landi, G. (2000). Influence of tillage methods on soil erosion and yield in Southern hilly crop system. *Riv. Agron.*, 34, p. 296-305.

Burk, A. R., Chanasyk, D.S. and Mapfumo, E. (1999). Influences of land disturbance and management regime on infiltration and runoff. *Canadian Agric. Eng.,* 41, p. 127-132.

Ferrero, A. (1991). Effect of compaction simulating cattle trampling on soil physical characteristics in woodland. *Soil Tillage Research*, 19, p. 319-329.

Foti, S., Cosentino, S.L. and Mantineo, M. (2000). Crops and soil erosion. Preliminary results on research in the internal hill of Sicily. *Riv. Agron.,* 34 (4), p.425-434.

Lal, R. (1993). Tillage effects on soil degradation, soil resilience, soil quality and sustainability. *Soil Till. Res.*, 27, p. 1-8.

Lisa, Laura, Parena, S. and Lisa, L. (1999). Comparison between grass cover and soil working techniques in Piedmont region: vine growing aspects. *11èmes Journées d'Etudes GESCO. Palermo (Italy), 6-12 June*, vol. 2, p. 891-895.

Pagliai, M., Raglione, M., Panini, T., Maletta, M. and La Marca, M. (1995). The structure of two alluvial soils in Italy after 10 years of conventional and minimum tillage. *Soil Till. Res*., 34, p. 209-223.

Pagliai, M., Torri, D. and Patruno, A. (1997). Aggregate stability and size distribution (in Italian). Methods of soil physical analysis. *FrancoAngeli, Milano, Italia*, Part V, 1, p. 7-13.

Sicher, L. and Venturelli, M.B. (1989). Controlled grass cover in vineyard. *Informatore Agrario*, 11, p. 45-48.

Tropeano, D. (1984). Rate of soil erosion process on vineyards in Central Piedmont. *Earth surface process and landforms*, 9, p. 253-266.

QUANTIFICATION OF NEAR-SURFACE PROCESSES IN A MICROSCALE CATCHMENT BY COMBINING PEDOLOGY, HYDROLOGY AND HYPER-SPECTRUM DATA

M. Kuhnert[1], S. Haubrock[2], C. Lemmnitz[3], H. Thoss[1], O. Bens[3], S. Chabrillat[2] and A. Güntner[1]

[1]*GeoForschungsZentrum Potsdam (GFZ), Germany, Section 5.4 Engineering Hydrology*
[2]*GeoForschungsZentrum Potsdam (GFZ), Germany, Section 1.4 Remote Sensing*
[3]*Brandenburg University of Technology Cottbus, Germany, Soil Protection and Re-cultivation*
e-mail Matthias Kuhnert: kuhnert@gfz-potsdam.de

ABSTRACT

Runoff and erosion are complex processes influenced by a number of interdependent boundary conditions and processes. The purpose of this study is to better understand these processes in a re-cultivated lignite mining area in southeastern Germany featuring fairly dry climatic conditions. The paper gives initial results of remote sensing measurements as well as pedology and hydrology studies. Hydrology monitoring covers rainfall, runoff, erosion and soil water content. Pedology studies include changing soil water repellence characterization. Hyper-spectrum remote sensing measurements enable spatially distributed soil water content measurement. Results show different soil substrate behaviour in terms of rainfall-runoff ratio, which is also influenced by soil water repellence, affected by soil water content and organic carbon amount in its turn. The expected cross-linked investigation surplus value is given.

Key words: erosion, soil water repellence, hyper-spectrum measurements, hydrology.

INTRODUCTION AND OBJECTIVES

Water erosion is caused by raindrop impact and surface runoff and is governed by several processes at or near the soil surface. Different spatial scales must be considered to assess erosion and sediment fluxes in river basins. These various processes require many different complementary measurement and monitoring approaches, often implying the need to evaluate different inter-correlated techniques, such as ground-based measurements and remote sensing from smaller to larger spatial scales.

The purpose of this study is quantifying water-induced soil erosion and assessing its influencing factors and processes on dry land condition uncultivated areas. Cross-linking hydrology, soil science and remote sensing are therefore an essential to observe processes from different points of view and compare different techniques. Classical measurement techniques can be used to validate novel techniques applied in the field. In addition to soil water content and runoff hydrology monitoring at different scales and climatic monitoring, this study is directed at soil water repellence, hyper-spectrum analysis and laser scans. These techniques measure major parameters governing water-induced soil erosion such as infiltration rate, initial soil water content, soil surface roughness and water repellence. Standard pedology measurements define climatic conditions and soil physical properties such as texture and porosity.

Hydrophobicity influences water infiltration and runoff (Shakesby, 2000). Independent investigations on soil water repellence and runoff and their influencing factors enable identifying process interdependence. The influence of organic materials such as compost and peat as well as geogenic materials such as lignite and xylite added to the influence of quantities on soil wetting behaviour are studied. Laboratory tests, microscopy and chemical analysis supplement field investigations for more detailed water repellence cause-and-effect chain identification. Water balance with infiltration and water retention tests is also investigated.

The crucial role that remote sensing techniques can play in monitoring environmental processes is widely accepted (Baumgardner and Silva, 1985; Chabrillat et al., 2002), but the complex infiltration and runoff issue is difficult to derive directly from remotely sensed images. Many factors requiring separate detailed

investigation in fact apply to infiltration rate. Many quantitative surface geophysical and chemical parameters, such as soil moisture (Weidong et al., 2001), organic matter (Baumgardner and Silva, 1985), mineralogical content (Baumgardner and Silva, 1985), crust development (Goldschleger et al., 2002), and surface roughness (Sole-Benet et al., 1997) can potentially be derived with the innovative remote sensing technique of hyper-spectrum imagery. A comparison of the spectra with FDR measurements enables quantifying initial soil water content. The combination of super-spectrum remote sensing data and small-scale pedology studies is applied to quantify several soil surface features, such as physicochemical properties and organic matter content. The results enable measuring the parameters influencing soil water repellence and infiltration rate. Field investigations are supplemented by laboratory analyses, including soil wetting behaviour and spectrum reflectance measurements.

PROJECT AREA

The investigated catchment is 40,000 m^2 in size, located in a former surface lignite area in the Lower Liusatia mining district southeast of Berlin.

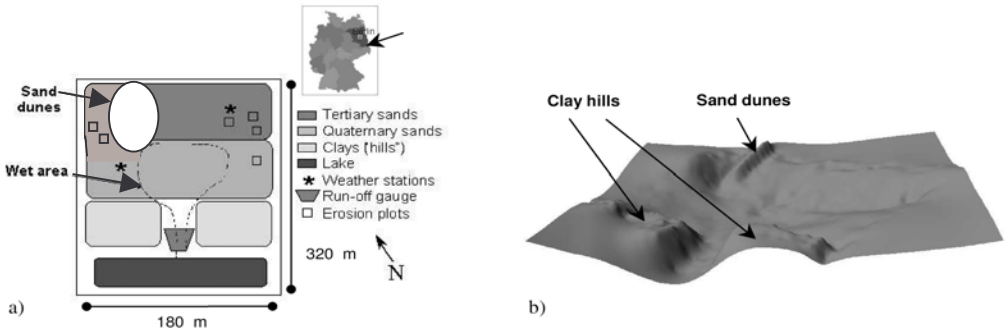

Fig. 1: a) Diagram of the test site, b) DEM of the area 10 times vertically exaggerated.

The project area was artificially re-filled in 2001 with different origin and property sediments, such as quaternary and tertiary sand, sand dunes and clay deposits (Fig. 1). Considerably more heterogeneity presents between substrates than inside each one. A 30 cm thick clay layer aquiclude is located at about 2 m depth. Test site elevation ranges from 129.4 to 135.6 m. Ground water level is about 0.5 to 1.5 m below the surface. Mean slope gradient is 4.9%, with a maximum of around 14 % (Fig. 1b). The study is focused on the tertiary and quaternary substrates. The 90 % S, 5 % U, 5 % T tertiary sand is more prone to develop crusts than the 80 % S, 15 % U, 5 % T quaternary sand. Young soil age entails scarcely vegetated land surface.

Low annual rainfall and comparatively high evaporative demand (mean for the 1961/1990 period (Wendling, 1999): fall 563 mm a^{-1}; potential evapo-transpiration 600 – 650 mm a^{-1}) provide climatic conditions of dry land areas. Rainfall seasonality with dry summer periods also entails droughts that may affect soil surface physical and hydraulic properties and the erosion process as a consequence.

Intermittent surface runoff occurs on mainly vegetation-free crusted sandy soil surfaces, which leads to high erosion rates and the formation of a complex network of rills within a short period. These conditions, together with low annual rainfall, make the test site a valuable pilot study area for developing monitoring approaches to assess erosion and land degradation processes in dry land areas.

METHODS

Remote sensing

Field soil sample spectra are measured with spectrum radiometers in laboratory conditions and correlated with involved pedology or hydrology parameters. Conventional methods, such as soil moisture in a drying chamber for instance, are used for parameter determination and a model is built and tested for transferability to other samples, by correlating these quantities to certain spectrum data.

Radiometers are then also taken to the field to measure the same parameters in natural conditions (spatial scale ~50 cm) and monitor seasonal surface reflectance changes. The stronger water absorption bands are masked due to atmospheric absorption for field measurements with the sun used as the light source, so laboratory methods must take into account that certain spectrum areas around 1.4 and 1.9 μm cannot be used in natural conditions. Spectrum radiometer measured parameters are again quantified with conventional methods or by sampling and subsequent laboratory analyses.

Hydrology and erosion

Surface runoff and erosion are measured at two different spatial scales, namely at the large scale of the entire 4-hectare study area and on four $1m^2$ plots for the micro scale. The plots are placed in areas without rill erosion in the tertiary and quaternary substrate to assess inter-rill erosion separately. Runoff is measured with a gauging weir at the outlet of the entire area and with tipping buckets on the plots. Sediment delivery is measured by estimating the volume of sediments deposited at the weir.

A monitoring network records weather conditions, soil moisture and groundwater levels with high temporal resolution. Soil moisture is measured at different locations and depths with FDR devices, with 0-to 50 cm close to surface measurements below the runoff/erosion plots and in the main drainage channel, and at 1 m maximum depth at selected tertiary and quaternary deposit sites. Spatial distribution of near-surface soil water content for the entire area is also measured by seasonal surveys with hand-held FDR probes (one during the winter and two during the summer).

Soil water repellence

The surface of the different overburden materials in the project area is investigated in detail every month. The uppermost topsoil is divided into five sections of one centimetre each. Parts were analysed afterwards for actual and potential water repellence, soil moisture, organic carbon content and water absorption. Actual and potential water repellence was identified by measuring contact angle with an OCA 5 Data Physics goniometer. Under 2 mm size soil particles were fixed on a microscope slide with two-faced adhesive tape. Twenty contact angles were measured on ten droplets of deionised water placed on the soil.

Different carbon sources, such as lignite, xylite, peat and compost, were mixed for laboratory tests with silica sand to obtain 1, 3 and 5 % C_{org} content. Mixtures were respectively adjusted to 8 and 15 % water content and substrates were subsequently dried at 20, 25 and 30 °C to constant dry weight and analysed for soil water repellence.

RESULTS AND DISCUSSION

Preliminary results show that the features of the two different substrates mostly influence runoff volumes. The influence of other factors, such as varying slope gradients, is secondary and not discussed in detail here. Figure 2 shows runoff coefficients for a number of varying intensity rainfalls. The magnitude of the quaternary substrate runoff coefficient is of the same order as the entire area, whereas tertiary substrate runoff coefficients tend to be higher. In particular, tertiary plots produce high runoff at low rainfall intensity. There are two possible reasons for this behaviour: firstly, the quaternary substrate predominates on the project area and its behaviour thus dictates the study area overall response; secondly, the tertiary substrate is

in the northern upstream part of the area (Fig. 1). Surface runoff generated in the tertiary substrate has to pass for a long distance through the quaternary substrate before reaching the weir and may in this passage be subject to infiltration-induced transmission losses, causing reduced overall runoff at the outlet and no smaller ones.

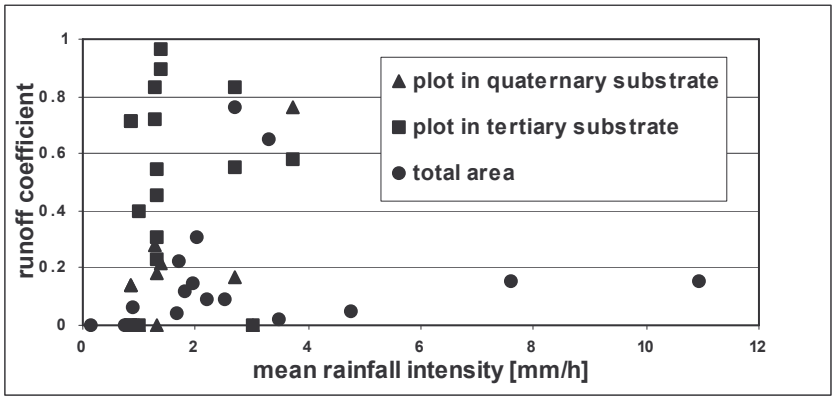

Fig. 2: Runoff coefficients for several rainfall events at different intensity (measurements for plots and total area are not always for the same rainfall).

So far (May 24 2004 to November-3 2004), sediment delivery of the entire study area has been measured for 130 days. Sediment delivery rate was 0.19 t ha^{-1} $month^{-1}$ during this period with a mean monthly rainfall of 49.4 mm. This value is small considering high tertiary substrate runoff and the distinct erosion observed. Lower erosion can be expected for the quaternary substrates together with marked sedimentation of material transported from the tertiary areas on the long distance to the gauging station, as observed in the field, can be offered as a similar explanation to runoff behaviour.

Surface soil water content spatial distribution mainly depends on substrates. The two clay hills and a wet zone in the small central dell that enables clay and silt deposition show some 20 to 40% volume higher average soil water content in time than the 5 to 10% volume for quaternary sand and less than 5% volume for the tertiary.
Seasonal effects are increased wet zone size in winter and decreased in summer. The seasonal changes are shown in Figure 3 for two different points on tertiary substrate, which are not identical to micro plots. Apart from soil water content, soil temperature is the second influencing factor on soil water repellence that changes during the year (Table 1).
Greater in-depth investigation is required to separate between the parallel effects of temperature and soil water content on water repellence.

Different substrates on the soil top layer presented various wetting behaviour. Clay deposits and quaternary sandy materials were always easily wet, while tertiary sandy materials showed a variable behaviour from easy wettability to a remarkable highly persistent water repellence. Although measured mean contact angles of tertiary sand do not indicate high water repellence of >90 degrees, a remarkable effect on infiltration rate can be recognised.
Differentiation is made between hydrophilic quaternary sand and hydrophobic tertiary sand to underscore the difference between the two dominating substrates on the study site. Initial laboratory test results showed that contact angles depended strongly on organic carbon.
Figure 4 shows contact angle increase at increasing amounts of organic carbon regardless of soil temperature. Initial water content was also seen to influence contact angles. Higher initial water content tended to cause lower contact angles (Fig.4).

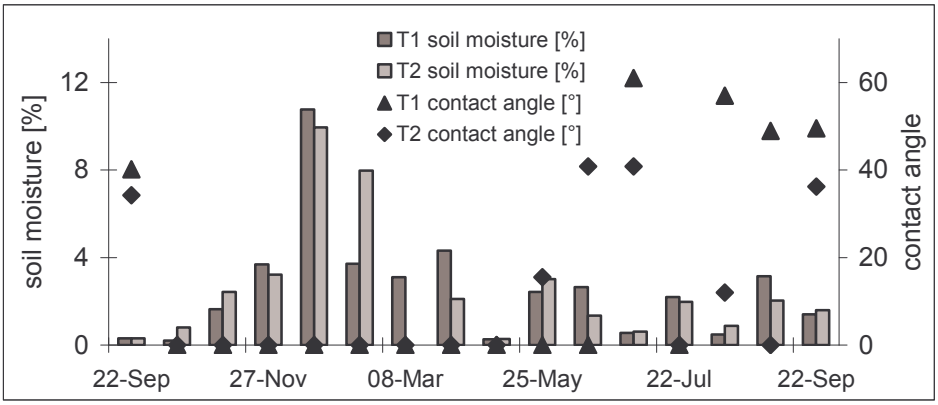

Fig. 3: Soil moisture and median contact angles on tertiary substrate during one year.

Table 1: Contact angles for weathered lignite dried at different temperature

Depth	0-1	1-2	2-3	3-4	4-5	**0-5**
Temperature						
20 °C	90.0	78.0	86.0	91.5	95.5	**88.2**
25 °C	79.5	90.5	88.5	98.5	95.5	**90.5**
30 °C	78.5	90.5	88.0	101.5	99.0	**91.5**

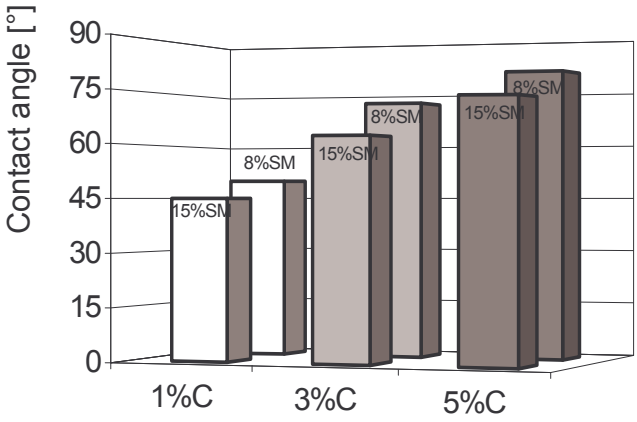

Fig. 4: Contact angles of weathered lignite mixed with silica sand on a % organic carbon content and % soil moisture drying temperature of 20 °C, n=10.

Detecting soil water content by remote sensing requires calibrating the techniques used with classical hydrology methods. Laboratory investigations using spectrum reflectance measurements enables calibration by gravimetry soil moisture measurements. Results as shown in Figure 5 are smooth spectrum curves, due to the absence of laboratory atmospheric noise. The deep absorption bands around 1.4 and 1.9 µm are due to absorption by H_2O and OH and thus potentially promising regions to quantify soil moisture. Reflectance cannot be measured directly in the centre of these bands, however, due to atmospheric absorption in natural conditions. Conversely, absorption band boundaries proved to be appropriate for quantifying soil moisture. Initial analysis results show that certain band ratios in this region can be correlated to soil moisture with correlation coefficients as high as 0.95 for each soil type.

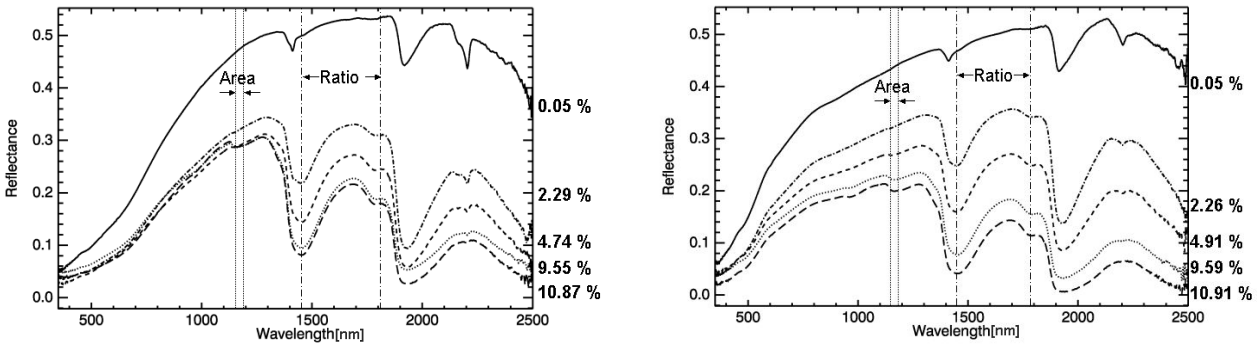

Fig. 5: Laboratory spectra of soil samples with different moisture percentages: left) tertiary sand and b) quaternary sand.

CONCLUSIONS

Soil water repellence is particularly high in dry initial soil conditions with high organic carbon content. These conditions are relevant in the selected study area with lignite material and dry climatic conditions. Hydrology investigations show high runoff for the tertiary substrate and a comparatively small runoff response at the entire area. Further investigation will have to focus on separating the different substrate runoff and erosion features. Hyper-spectrum measurements give the opportunity to quantify soil water content at the surface in a spatially distributed way. As they are directly linked to soil water repellence, which in turn affects surface runoff generation and erosion, these cross-linkages should give an improved picture of the factors affecting near-surface processes in dry land areas.

ACKNOWLEDGEMENT

We would like to thank the Company Vattenfall Mining Europe for admitting our research.

REFERENCES

M.F. Baumgardner, L.F. Silva (1985): *Reflectance properties of soils*, Advances in Agronomy, 1-44.

S Chabrillat, A.F.H. Goetz, L. Krosley, H.W. Olsen (2002): *Use of hyper-spectrum images in the identification and mapping of expansive clay soils and the role of spatial resolution*, in: Remote Sensing of Environment 82, pages 431-445.

N. Goldschleger, E. Ben-Dor, Y. Benyamini, D. Blumberg, M. Agassi (2002): *Spectral properties and hydraulic conductance of soil crusts formed by raindrop impact*, in: International Journal of Remote Sensing, 19, pages 431-445.

R.A. Shakesby, S.H. Doerr, R.P.D. Walsh (2000): *The erosive impact of soil hydrophobicity: current problems and future research directions*, Journal of Hydrology, Vol. 231-232, pages 178-191.

A. Sole-Benet, A., Calvo, A. Cerda, R. Lazaro, R. Pini, J. Barbero (1997): *Influence of micro-relief patterns and plant cover on runoff related processes in badlands from Tabernas (SE Spain)*, Catena, Vol. 31, pages 23-38.

L. Weidong, F. Baret, G. Xingfa, T. Qingxi, Z. Lanfen, Z. Bing (2001): *Relating soil surface moisture to reflectance*, in: Remote Sensing of Environment 81 pages 238-246.

U. Wendling, G. Fuchs, G. Müller-Westermeier (1999): *Mittlere jährliche potentielle Verdunstungshöhe als Gras-Referenzverdunstung. Hydrologischer Atlas von Deutschland*, Bundesministerium für Umwelt, Naturschutz und Reaktorsicherheit, Karte 2.12.

SEASONAL RHYTHMS OF SEDIMENT DEPOSITION AND SCOURING IN THE LAVAL AND MOULIN CHANNEL NETWORK (DRAIX EXPERIMENTAL BASIN, FRANCE)

N. Mathys[1], M. Esteves[2] and J.M. Grésillon[3]

[1]*Cemagref Grenoble, ETNA, BP 76, 38402 Saint Martin d'Hères, France*
[2]*LTHE Grenoble, LTHE, BP 53, 38 041 Grenoble cedex 9*
[3]*Cemagref, 3bis Quai Chauveau, 69336 Lyon Cedex 09*
e-mail Nicolle Mathys: nicolle.mathys@grenoble.cemagref.fr

ABSTRACT

Located in the Alps of south-eastern France on very erodible black marl substratum, the experimental site known as Draix was created in 1983-1984. Its aim was principally to study mountain erosion processes. On three small basins with scarce vegetation cover, the analysis of the available data showed highly nonlinear responses to rainfall events in terms of sediment yield. Different types of runoff and erosion situations and a seasonal rhythm of the phenomena were identified. At the event scale, the erosion response involved erosion processes on the slopes as well as deposition and scouring processes in the channel network. In order to analyse these phenomena, a field study was conducted over the 12 months of the year 2002 in the Laval (86 ha) and Moulin (8 ha) basins. Several representative reaches were selected in the two basins with the measurement of cross-sections after each significant rainfall event. At the same time, morphometric observations of the basin networks were conducted and completed by a photographic survey. Four types of behaviour during floods were identified, two of them bringing downstream particularly heavily loaded floods: i) late spring or summer storms, characterized by high erosion on the slopes, high storage of sediment in the drainage network and medium to high sediment exportation; and ii) moderately high but long-lasting autumn events inducing low erosion on slopes, scouring and massive de-stocking in the reaches and very high sediment yield at the outlet.

Key words: debris flow monitoring, precipitation thresholds, debris flow routing.

INTRODUCTION

In the southern French Alps, the Black Marl formation, a very erodible outcrop, covers a large area where freezing in winter and high-intensity rainfall in summer produce both a badlands topography and high levels of solid transport during floods. The Draix experimental basins have been monitored since 1984 in order to study the erosion process in this kind of mountain basins (Richard and Mathys, 1999). Many studies that have been done in badlands terrain in southern Europe, such as Tabernas (Canton et al., 2001) and Valcebre in Spain (Gallart et al., 2002), and "calanchi" in Tuscany, Italy (Torri et al., 1999), demonstrated the variability of this terrain's erosional response to a rainfall event. But most of these studies at the plot or micro-catchment scale relate this variability to rainfall characteristics or local initial soil surface conditions. In Draix basins, previous analysis at the small basin scale brought out the effect of the deposition and scouring processes in the channel network. In order to analyse how the sediments are stocked or destocked in the channel network, a field study was conducted throughout the year 2002 in the Laval (86 ha) and Moulin (8 ha) basins. This paper analyses the field observations and collates them to the rainfall, runoff and sediment supplies at the outlet.

STUDY SITE AND METHODS

The experimental basins of Draix are located 200 km south of Grenoble, on Jurassic marine black marls that are very sensitive to weathering and erosion. They present a characteristic badlands morphology with V-shape gullies. The mean annual rainfall is 900 mm. Summers are dry with the odd short yet severe storm. Because of the frequent freeze and thaw cycles in winter, the degradation processes are very active and produce a thick layer of weathered material at the end of winter. During winter, marl platelets fall due to

gravity and constitute stocks at the bottom of the slopes. On steep slopes, small landslides and mudflows also supply sediments to the stream channels. In summer and early autumn, severe storms provide material by concentrated runoff on the slopes. In the main channel, when the liquid discharge coming from the slopes contains only a small amount of solid sediment, the flood is highly erosive and erodes the deposits of the previous floods. On the other hand, when there is too much sediment from the slopes, there is deposition. This alternate deposition-aggradation phenomenon is a determining factor of the sediment yield of the flood events and needed to be investigated in greater detail. This study was carried out on the Moulin (8 ha) and Laval (86 ha) Draix site basins, with scarce vegetation cover (46% and 32%, respectively). The Laval is composed of several sub-catchments draining into the main channel about 1.5 km in length with a slope gradient ranging from 8% to 4%. Data and observations on a small monitored gully, the Roubine gully (0.13 ha, 21% vegetation), are used as a reference of the processes occurring at the scale of an elementary gully unit. The Moulin basin is a smaller basin whose main stream, 300 m long, has a 4% slope. Pluviographs and a set of devices at the outlet of each catchment measure rainfall, liquid discharge and sediment transport (Richard and Mathys, 1999).
For the field survey, several representative reaches were selected in the two basins with the measurement of cross-sections after each rainfall event of some importance (eight surveys). In the main channel, reference stakes were installed in stable parts of the banks and a cable with a constant tension was tightened and used as a level reference (Photo 1). In secondary channels or gully bottoms, metal poles were hammered into the valley bottom and the length of the part sticking out of the deposits was measured (Photo 2). For each survey the measurements were completed by a qualitative description of the fillings in the gully bottoms of the Moulin basin and by photographic survey of the reaches and remarkable points in the Laval basin (photo 3).

Photo 1 : transect measurement

Photo 2 : pole measurement

Photo 3 : photographic survey

RESULTS

Autumn 2001 was especially dry within a year 2001 slightly under the average for rainfall depth (14% of the annual depth versus 29% on average). No major runoff events occurred after summer, so, in both the Laval and Moulin catchments, the channel networks were filled with sediments at the beginning of the monitoring period.
On the Moulin basin, the first notable flood, in May, dug a channel in the colluvial deposits formed at the bottom of the slopes during the winter (Photo 4). At the end of May, the main channel was notably refilled with many deposits formed in the tributaries and larger gully bottoms. A short and intense storm at the end of July both brought a great amount of sediments at the outlet (15.5 m3) and scoured the steep upstream gullies down to the parent material (Photo 5). The other summer storms filled the lower part of the main channel while the intermediate section deposits were eroded. A large amount of sediment was transported to the outlet during the events of October (38.5 m^3) and the bedrock began to be visible in many sections of the intermediate network. A long-lasting flood event in November related to a high rainfall depth (97 mm) scoured most of the available material, and even in the reaches which were not emptied, the bedrock was visible on a part of the valley bottom. For example, Photo 6 shows how the downstream reach of the torrent, which was filled with a smooth and thick layer of sediments at the end of July (Photo 1) was scoured after this flood. The following event, at the end of November, with a rainfall input of 58 mm and a higher peak yielded no sediments in the trap (less than 1 m^3) : the "flush" effect of the previous flood exhausted most of the available stock of material.

Figure 1 collates the volumes measured in the sediment trap with the characteristics of the rainfall-runoff events and illustrates these processes. The sediment stock variations explain most of the scattering of the points. The short and violent summer storms (01/08) have a high peak discharge but the yield at the outlet is limited by their short duration and low volume. We observed that these events added a great amount of sediments in the network stocks. The autumn events (September and October) yielded more than expected considering the rainfall depth or peak discharge. The high and long-lasting November flood, with its high volume and succession of several peak flows, was able to scour in the great amount of available material and was therefore highly productive at the outlet. The following event, occurring with no or little available stock, yielded an exceptionally low amount of sediments.

Photo 4: erosion of winter foot slope deposits in May

Photo 5: "Cleaning" of the upstream gullies by a summer storm

Photo 6: scouring by the November flood in the main reach

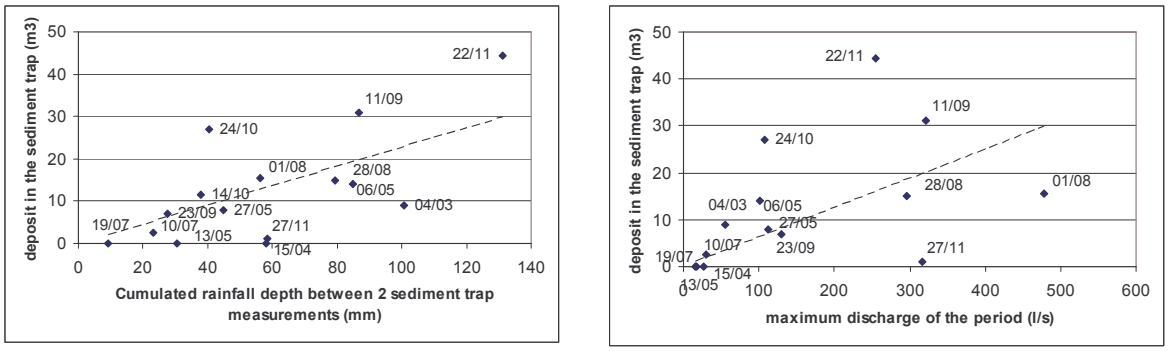

Fig. 1: Relationship between trap deposit of the Moulin basin and the rainfall depth or peak discharge.

On the Laval basin, the reaches were particularly loaded with sediments at the end of 2001 because of the dry conditions in autumn 2001. Few moderate floods yielded at the outlet only 163 m^3, whereas on average, the deposits during this season are 900 m^3 and can reach 2000 m^3. The transect measurements conducted in a reach 95 m long and 5 m wide, located 700 m upstream from the sediment trap, illustrate the deposition and aggradation cycles in the Laval stream (Fig. 2).

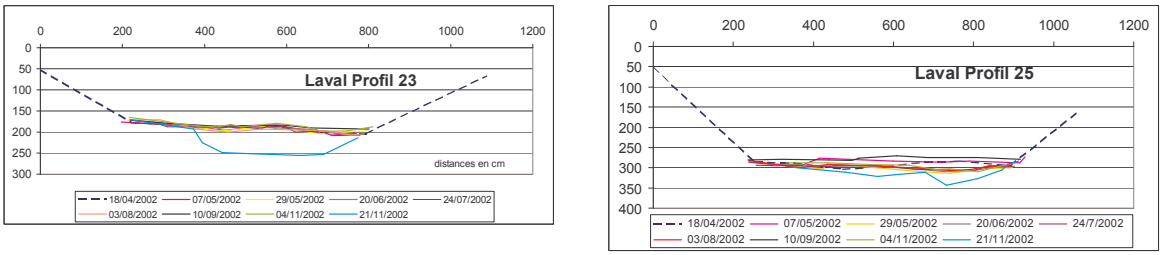

Fig. 2: Transect measurement in one of the Laval reaches.

The hydrological characteristics of the events recorded during the year 2002 in this basin are shown in Table 1. The layer of 30–70 cm of sediments present is April was slightly increased by the first flood of May. The stock in this reach can be estimated at 150 m^3 at this period. A short flash flood on July 30th (duration 45 min, with a rising time of only 7 min) brought a great deal of sediment to the outlet (400 m^3)

and increased the stocks all along the channel. In the Roubine gully, the sediment yield of this event was the highest of the year (Figure 3). This shows that the storm was highly erosive on the slopes and that the runoff in the steep gullies had a high transport capacity. The storms at the end of August and beginning of September emptied the upstream reaches while the medium and downstream reaches were still reloaded (+ 70 m^3 in the described reach). The rainfall events in October yielded 169 and 189 m^3 in the trap, although the peak flows and runoff volumes were low (Table 1). The photographical survey of the network shows that globally the stocks were reduced by these two events (Photo 7, 8). In the reach described here, the stocks decreased about 40 m^3. Therefore we can assess that the sediment supply from the slopes was limited and that the flow constituted its load mainly from the available deposits. As for the Moulin basin, the November 16th flood massively scoured all the stocks and deposited 790 m^3 in the trap while it scoured all the material remaining in this reach (- 160 m^3). In nearly all the network, the bedrock was visible (Photo 9). The following flood of November 24th, devoid of available material, only yielded one-tenth the material (75 m^3), even though the rainfall depth and rainfall kinetic energy were only twice as low.

Table 1: rainfall, runoff and deposit data on the Moulin and Laval basins

Flood event date	Rain depth	Run-off	Max int. in 5 min	Max int. in 60 min	Kinetic energy	Laval peak flow	Date of trap survey	Laval trap vol.	Moulin trap volume
	mm	mm	mm/h	mm/h	j/m²	l/s		m^3	m^3
06/02	15.8	2.0	7.2	4.8	256	25	07/02	1	0
15/02	5.6	7.2	12.0	3.2	65	280	04/03	30	9.0
02/05	81.0	19.5	19.2	9.4	1459	1460	06/05	369	14.0
10/05	23.6	9.1	12.0	7.4	387	190	16/05	24	0.1
23/05	32.0	11.1	26.4	12.0	659	2140	27/05	162	7.9
05/06	21.0	1.3	16.8	7.2	396	190	05/06	1	0
06/06	10.6	3.2	7.2	4.6	182	380	07/06	0	0
06/07	12.8	0.5	33.6	4.2	246	195	10/07	77	2.5
28/07	11.2	0.1	57.6	11.2	272	60			
30/07	25.4	6.8	120.0	23.8	668	6980	01/08	403	15.5
31/07	4.2	0.6	43.2	7.4	93	670			
01/08	14.4	2.3	43.2	7.4	292	360	12/08	0	0
24/08	22.2	3.7	67.2	19.6	541	3260			
26/08	8.4	3.6	31.2	6.8	178	275	28/08	115	15.0
30/08	11.8	2.8	14.4	4.4	208	1550			
31/08	8.4	0.7	45.6	7.6	190	45			
02/09	4.4	1.3	7.2	1.6	54	235	02/09	70	nd
04/09	10.6	2.5	12.0	5.8	185	290			
05/09	25.0	9.8	40.8	12.2	505	1385			
07/09	6.6	0.7	36.0	6.6	151	190			
09/09	13.2	2.3	26.4	6.8	227	550	11/09	169	31.0
21/09	20.4	1.3	60.0	15.2	445	190	23/09	1	7.0
10/10	32.4	10.3	14.4	9.8	607	1260	14/10	189	11.5
17/10	10.6	0.8	33.6	4.4	200	135	18/10	1	0
21/10	13.8	2.6	67.2	10.0	326	1730	24/10	195	27.0
22/10	11.4	3.5	31.2	6.4	245	1540			
16/11	97.4	78.3	20.0	11.4	1784	2880			
21/11	24.8	8.2	14.4	6.4	432	475	22/11	793	44.5
24/11	58.4	15.3	43.2	8.8	914	1350	27/11	75	1.0

nd : no data

Figure 3 shows the rainfall and runoff data on the Laval basin, completed by the data from the sediment traps of the three basins. The triangles represent the dates of the network surveys and the specific values of the deposits are plotted in order to make the results comparable.

Photo 7,8,9: filling and emptying of the surveyed reach in the Laval channel

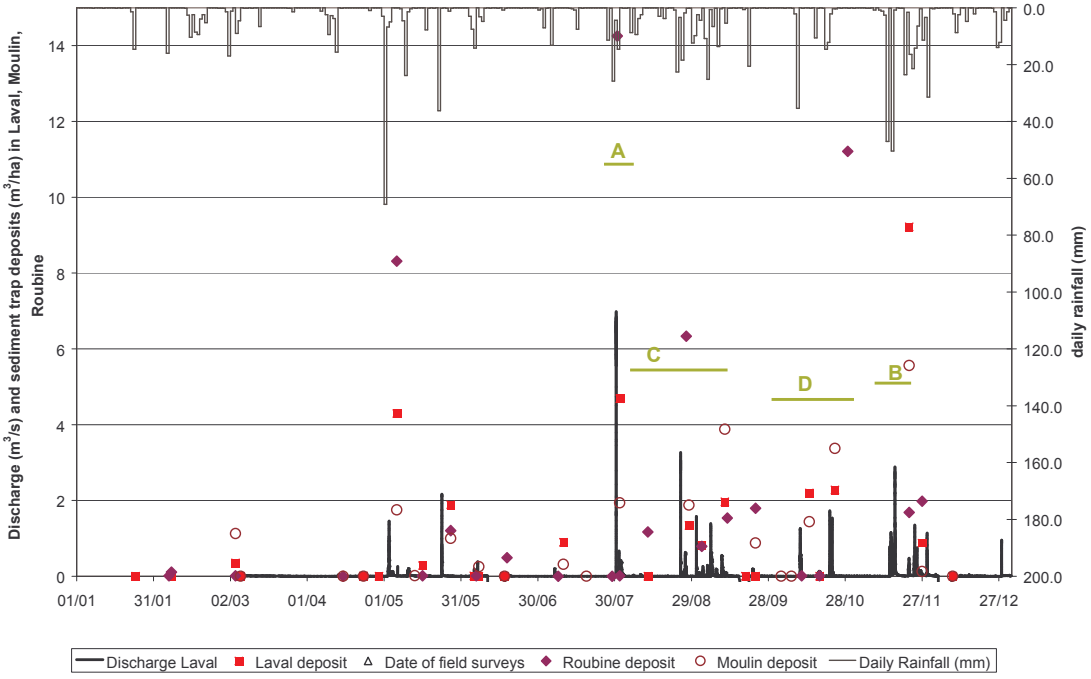

Fig. 3: Rainfall, runoff and deposit sequence on the Roubine, Moulin and Laval basins. Letters refer to the types of events discussed below.

DISCUSSION AND CONCLUSION

This study identified four main types of rainfall-erosion situations (see letters in Figure 3):
- a violent summer storm (A). It was the most significant event of the year in terms of rainfall intensity and peak flow. It was the most erosive event in the Roubine basin, where it brought 28% of the total yield for the year 2002. The high discharge transported a great deal of material at the Laval outlet (17% of the annual yield), but, as the sediment supply from slopes was high and the flood short, a large amount of material was also stored in the reaches. The high intensity of the rainfall generated a high level of runoff in the steep headwater gullies, whose bottoms were cleaned of deposits after this shower. The flood was less erosive in the Moulin catchment and less steep. *In conclusion, this situation was characterized by high erosion on slopes, high storage in the channels and medium to high yield at the outlet*.
- a long and high flood in autumn (B). This event with the highest cumulated rainfall depth and highest total runoff was not erosive on the slopes and yielded a small amount of sediment in the Roubine trap (3% of the annual amount). On the other hand, it carried downstream most of the sediments available in the streams of the Laval (30% of the total) and Moulin (22%) networks. This massive scouring of the stocks left no material to be transported by the next flowing, long and high flood. Despite high peak flow and runoff volume, this next event represented less than 3% of the annual yield of the Laval basin (less than 1% for the Moulin basin). *In conclusion, this situation was characterized by low erosion on slopes, high scouring in the deposits and very high yield at the outlet*.

- a succession of summer storms in August and the beginning of September (C). These storms both highly eroded the slopes (see the high trap volume in Roubine for the 24/8 event) and increased the sediment stocks in the channels. However, the sediment yield at the outlet of the Moulin basin was high (23% of the total) and consistent with the fact that in Laval the upstream reaches were empty: the upstream supplies decreased and the stocks were transported downstream. *In conclusion, this situation was characterized by moderate erosion on the slopes, high storage in the lower part of the network and medium to high yield at the outlet.*
- a succession of early autumn storms (D). Despite moderate discharges and runoff volumes, the flow brought a large amount of sediment in the Laval and Moulin traps (20% and 38%, respectively, by four events between September 10th and October 25th). These materials came mainly from the scouring of the previous stocks. Therefore, one of these floods (October 21st) was highly productive in the Roubine network (22% of the annual yield). This confirms that high intensity over a short duration induces erosion on slopes and explains the deposits observed at this period in the upstream steep gullies in the Moulin basin. *In conclusion, this situation was characterized by medium erosion on slopes, moderate scouring in reaches and moderate yield at the outlet.*

The spring period was not monitored in the Laval network. The observations in the Moulin basin show that the previous stocks were eroded by the first floods in spring. The first event in May was productive both in the Roubine (8.3 m^3/ha) and the Laval (4.3 m^3/ha) areas. The high sediment load of the first intense event of the spring is frequently observed in the Roubine basin. It is caused by the mobilization of the winter colluvial deposits accumulated at the foot slopes after winter (Photo 4; Robert et al., 2003; Descroix and Mathys, 2003).

The effect of exhausting stocks, obvious for the November 16th event, was quite frequent and seems to have been active also at the Roubine gully, for example with the succession of events on May 2nd and 23rd , August 24th and 30th, October 21st and November 16th, where the second events in each pair were considerably less erosive than the first. Of course, other parameters such as intensity and duration of the shower, and peak flow of runoff also played a role, but it seems that the first event dug the rills down to the unweathered marl and that the following one could only erode the banks of the rills. The sheet erosion between the rills appears less involved in the sediment supply than the rill erosion (Klotz et al., 2003).

These results on the seasonal behaviour of the sediment yield processes suggest the rainfall-runoff-erosion ETC model should be adapted (Mathys et al., 2003) and the present simulation at the event scale should be replaced with a continuous model or at least modelling a succession of events and using parameters varying with the season.

REFERENCES

Canton, Y., Domingo, F., Sole-Benet, A. and Puigdefabregas, J., 2001. Hydrological and erosion response of a badlands system in semiarid SE Spain. Journal of Hydrology, 252(1-4): 65-84.

Descroix, L. and Mathys, N., 2003. Processes, spatio-temporal factors and measurements of current erosion in the French southern Alps: A review. Earth Surface Processes and Landforms, 28(9): 993-1011.

Gallart, F., Llorens, P., Latron, J. and Regues, D., 2002. Hydrological processes and their seasonal controls in a small Mediterranean mountain catchment in the Pyrenees. Hydrology and Earth System Sciences, 6(3): 527-537.

Klotz S., Mathys N., Maquaire O., M. and Olivier J.E, 2003. Evolution of sediment stocks in a small gully catchment : the Roubine (Draix experimental basins, South Alps, France). Conférence : Gully erosion in Mountain Areas, Digne, 15-17 octobre 2003

Mathys, N., Brochot, S., Meunier, M. and Richard, D., 2003. Erosion quantification in the small marly experimental catchments of Draix (Alpes de Haute Provence, France). Calibration of the ETC rainfall-runoff-erosion model. CATENA, 50(2-4): 527-548.

Richard, D. and Mathys, N., 1999. History, technical and scientific context of the experimental basins of Draix. Characteristics, avalaible data and main results after ten years of monitoring. In: Cemagref Grenoble Etgr (Editor), actes du séminaire, Draix Le Brusquet Digne, 22-24 octobre 1997. Cemagref Editions, Antony, pp. 11-28.

Robert, Y., Corona, C., Arques, S. and Rovera, G., 2003. Cycles érosifs et bilans sédimentaires dans les ravines marneuses des Alpes de Haute Provence (bassins de Draix). Modélisation et régionalisation selon différentes unités géodynamiques, Gully erosion in Mountain Areas: Processes, Measurement, Modelling and Regionalization, pp. 139 - 143.

Torri, D., Regues, D., Pellegrini, S. and Bazzoffi, P., 1999. Within-storm soil surface dynamics and erosive effects of rainstorms. CATENA, 38(2): 131-150.

SUSPENDED SEDIMENT YIELD AND HYSTERETIC LOOPS IN TWO SMALL BASINS (VALLCEBRE, EASTERN PYRENEES)

M. Soler and F. Gallart

Institute of Earth Sciences "Jaume Almera", CSIC. Lluis Solé i Sabarís s/n, 08028 Barcelona
e-mail Montserrat Soler: msoler@ija.csic.es

ABSTRACT

The aim of this work is to investigate the sediment suspended transport and the relationship between discharge and sediment concentration in two small catchments in the Eastern Pyrenees with a different land cover during a period of four years. Ca l'Isard is mainly covered by forest but with some severely eroded areas (badlands). In contrast, these areas are not present in Can Vila, which is characterised by the presence of meadows on abandoned agricultural terraces. Discharge, turbidity and transported solid content data have been obtained by means of automatic samplers and sensors located in gauging stations at the outlets of both catchments. Sediment transport was higher in Ca l'Isard due to the contribution from badland areas, but runoff was lower because of deep percolation through limestone. Positive, negative and eight-shaped sediment concentration hysteresis loops were observed in both catchments. The most frequent in both catchments were positive loops during the wet season (spring and autumn), whereas the eight-shaped were noticeably less frequent in the catchment without badlands (Can Vila).

Key words: sediment transport, suspended solid concentration, land cover, badlands, hysteresis loops.

INTRODUCTION

The continuous monitoring of discharge (Q) and suspended sediment concentrations (SSC) in streams allows not only the improved estimation of sediment yield (Walling and Webb, 1988), but it may also provide some help for understanding the runoff and sediment production processes active in the catchment (e.g. Williams, 1989; Sammori et al., 2004). Climates with strong seasonal contrasts, like the Mediterranean one, induce marked annual variations in stream discharge and the hydrological functioning of catchments depending on both precipitation characteristics and antecedent conditions (Gallart et al., 2002; Latron, 2003; Seeger et al., 2004).

The purpose of this paper is the study of suspended sediment yield and discharge-concentration relationships from two adjacent small catchments with different land cover during a period of four years (2000-2003).

STUDY AREA AND METHODS

The Vallcebre experimental catchments (Fig. 1) were set up in 1990 for studying hydrological and erosion processes (Gallart et al., 2002; Latron, 2003). They are tributaries of the Llobregat River and located at 1,100 m a.s.l. in the Catalan Pyrenees. The bedrock consists mainly of red clayey mudstones with some gypsum and sandstone layers, and an intermediate limestone thick bed. Annual precipitation is about 925 mm and mean annual temperature is about 9ºC. Sediment yield from these catchments is very high, as most of the sediments come from heavily eroded clayey outcrops (badlands) whose activity is closely related to freezing in winter and intense rainstorms in summer (Regüés 1995, Regüés et al., 2000).

The Ca l'Isard sub-basin (1.32 km^2) is mostly forested (70%), whilst scattered vegetation and meadows on old agricultural areas cover 10% of the area, and badlands represent 4.5%. Moderately karstified limestones are the bedrock on one-half of the catchment area (54%), although bare rocky outcrops represent a much smaller part (7.1 %) (Latron, 2003). The gauging station is equipped with a concrete rectangular flume, water level and temperature sensors, an automatic ISCO 2700 water sampler, and an OBS-3 D&A infra-red backscattering turbidity sensor, as well as a Mobrey MSM 40 ultrasonic beam attenuation suspended

sediment sensor, which allows the continuous recording of sediment concentrations up to 240 gl^{-1}. A DT Data Electronics data-logger is used to record the readings as well as triggering the water sampler during events.

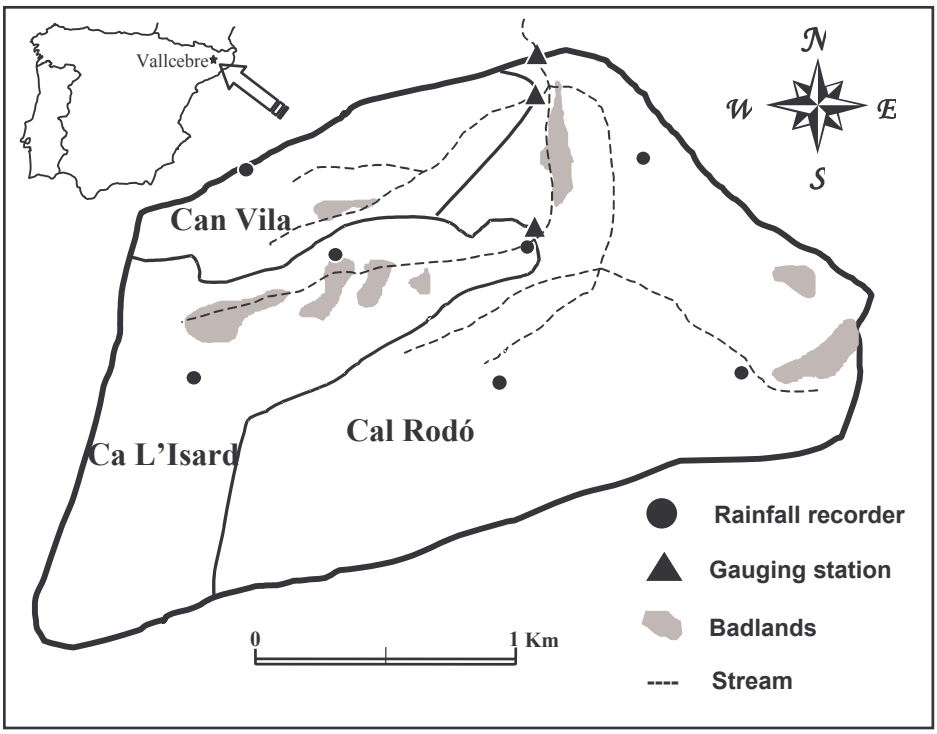

Fig. 1: Map of the Vallcebre catchments, showing the location and the instruments.

The Can Vila sub-basin (0.56 km^2) is mainly covered by meadows on old fields (52%), whereas forest is the second land cover (33%), limestone bedrock outcrops only in scarce bare rocky areas (3%), and eroded landscapes are much less important than at Ca l'Isard (0.9%). The gauging station is provided with a V-notch control (as sediment transport is not a limiting factor), with similar instrumentation as described for Ca l'Isard, except the ultra-sonic equipment that is not necessary here due to the limited sediment concentrations.

The analysis of the Q-SSC relationships was made using the hysteretic patterns described by Williams (1989).

RESULTS

The main runoff and sediment transport events may be observed in Figure 2. Winter is the season with the least precipitation and during summer runoff is limited but sediment transport is relevant because of the high intensity of rainstorms. Sediment concentrations were irregular, as shown by the varying transport-runoff ratios. On the longer run, most of the sediment transport occurs during autumn (Gallart et al., 2002), but during the period analysed, there were no large autumn events; however, there was an exceptional event on 26th February 2003 that transported 44% of the sediment yield for the whole period at Can Vila. At Ca l'Isard, the catchment with a greater badlands area, 5 events transported more than 100 Mg km^{-2} yielding 52% of the total transport in the four years.

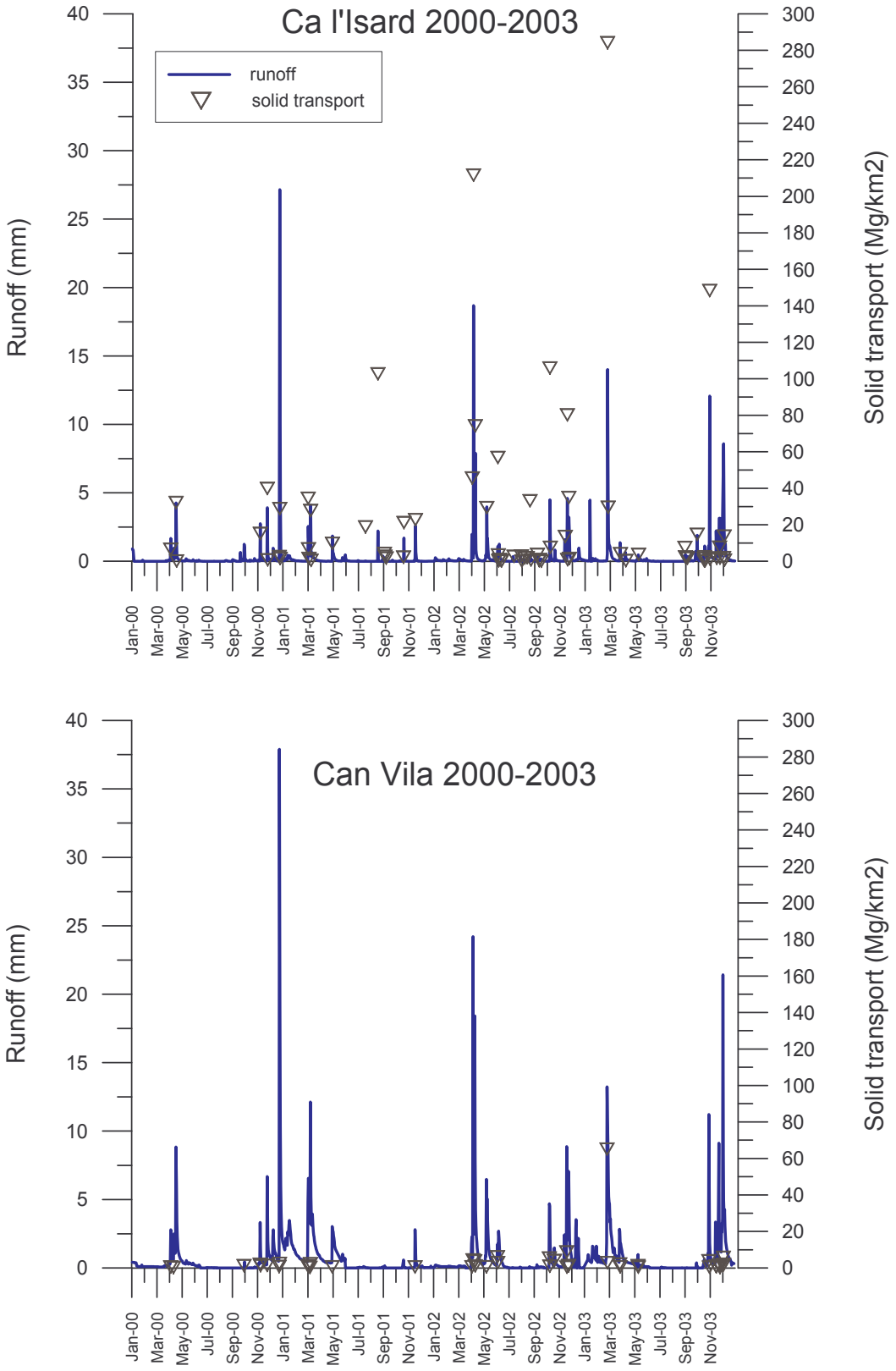

Fig 2: Daily runoff and sediment transport for the four years of the study.

Ca l'Isard

During the study period, mean annual runoff from the Ca l'Isard sub-basin was 81.5 mm, mean runoff coefficient was 0.096, suspended sediment yield was 4.8 Mg ha^{-1} $year^{-1}$, and dissolved sediment yield was about 1 Mg ha^{-1} $year^{-1}$. The maximum suspended sediment concentration, observed in July 2002, was 175 g l^{-1}. Event peak discharge was well correlated with event sediment transport ($r=0.618$, $p<0.01$) and event mean sediment concentration ($r=0.658$, $p<0.01$).

Positive (clockwise) hysteresis loops (Fig. 3, left) were observed during 20 from the total 51 events analysed (39%). These patterns occurred during the wet seasons (spring and autumn) when baseflow was significant and peak discharges were the most important of the whole year. Mean event duration was about 4 hours longer than the annual average (27 hrs). Sediment concentrations usually exceeded the mean annual value (15 g l^{-1}) and also showed the coarser grain sizes (Soler et al., 2003).

Eight-shaped hysteresis loops with positive tendency (Fig. 3, centre) were observed during 18 events (35%), throughout the year but more frequently during the transition between dry and wet periods. Baseflow had a wide range (0-24 l s^{-1}) as well as sediment concentrations (0.05-34 g l^{-1}) which were higher in November. The duration of the events was average.

Negative (counter-clockwise) hysteresis loops were observed only during 13 events (25%). Most of them (10) occurred during dry periods when base flow was smaller than 3 l s^{-1}. Sediment concentrations showed a wide range, although most of the values were smaller than the annual average; sediment deposition on the stream bed was frequently observed after these events. The mean duration of the events was about 7 hours below the annual average.

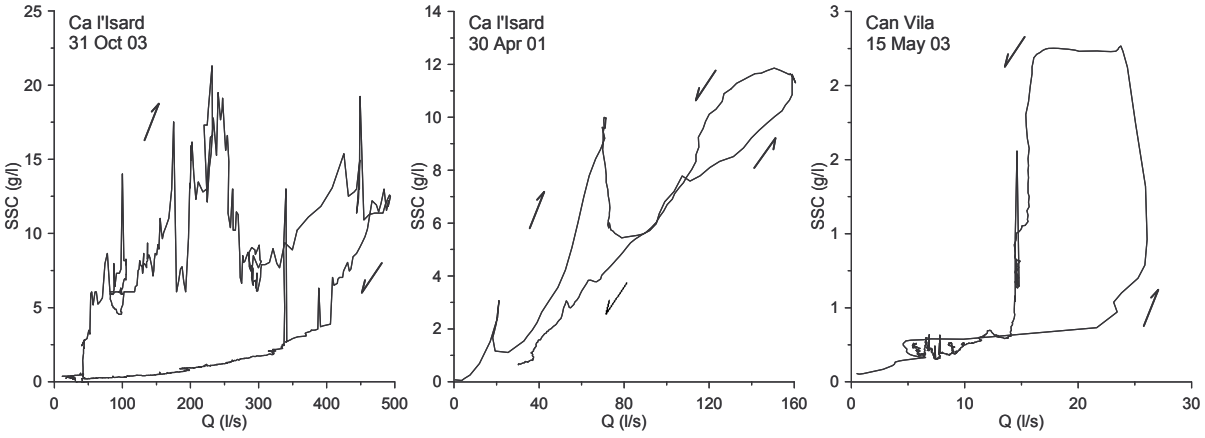

Fig. 3: Examples of positive (left), eight-shaped (centre), and negative (right) hysteresis loops observed in the catchments during the study period.

Can Vila

During the study period, mean annual runoff from the Can Vila sub-basin was 235.6 mm, mean runoff coefficient was 28.6%, suspended sediment yield was 0.4 Mg ha^{-1} $year^{-1}$, and dissolved sediment yield was about 2.9 Mg ha^{-1} $year^{-1}$. The maximum suspended sediment concentration, observed in October 2002, was 7.2 g l^{-1}. Event peak discharge was very well correlated with event sediment transport ($r=0.904$, $p<0.01$) and event mean sediment concentration ($r=0.505$, $p<0.01$).

As in Ca l'Isard, most of the events showed relationships between discharge and sediment concentrations with positive hysteresis loops (61%), although here the eight-shaped loops were noticeably less frequent (10%) than the negative ones (29%). Positive loops were observed during the wet periods, when base flow

was greater than 1 l s^{-1}, but sediment concentrations did not show any clear arrangement and event duration was 5 hours longer than the annual average (27 hours). Negative loops were well marked in this catchment (Fig. 3, right), and these occurred during dry periods when baseflow was smaller than 1 l s^{-1}; sediment concentrations were rather irregular, and event duration was on average 13 hours shorter than the average.

DISCUSSION AND CONCLUSIONS

The above results demonstrate a much lower runoff from the Ca l'Isard catchment, as well as a smaller dissolved transport and much greater suspended sediment concentrations and yield when compared to those from the Can Vila catchment. The first two differences are the result of the deep percolation through the moderately karstified limestone bedrock areas in the Ca l'Isard catchment (Balasch, 1998; Latron, 2003), whereas the third is caused by the much larger extension of badlands in that catchment.

Runoff generation in these catchments is dominated by saturation mechanisms, whereas Hortonian mechanisms are active only on bare areas during high intensity rainstorms in summer (Gallart et al. 2000, Latron, 2003). Yet, the erodible regolith is formed on badland surfaces in winter due to physical weathering, and is eroded mainly in summer due to the high intensity rainstorms.

Positive hysteresis loops occurred during wet periods, when the vegetated hillslopes contributed to runoff by saturation mechanisms, whereas the rainfall intensity was too low to produce significant runoff and erosion from badland surfaces. The increasing discharge caused the erosion of the sediments previously deposited on the stream bed, whereas the recession limb of the hydrograph typically showed very low sediment concentrations due to sediment exhaustion.

Eight-shaped loops started with the mobilisation of fine sediments previously deposited on the stream bed, whereas the later part of the event showed more of an increase in sediment concentration coming from the remote badland areas than a decrease caused by dilution or sediment exhaustion. Fine sediment deposition on the stream bed may occur at the end of these events because of the sustained high concentration-discharge ratio. The larger badland area in the Ca l'Isard catchment may explain the more frequent occurrence of these loops in it.

Finally, negative loops occurred during dry periods, when the stream bed was relatively clean and most of the sediment was produced on the badland surfaces, located far from the catchment outlets (Latron, 2003). These are typically sediment-laden events.

ACKNOWLEDGEMENTS

This research was carried out with the support of the PROHISEM (REN2001-2268/HID), PIRIHEROS (REN2003-08678/HID), TEMPQSIM (EVK1-CT-2002-00112 projects) and the CSIC-DGCONA (RESEL) Agreement. The authors are indebted particularly to D. Regüés, J. Latron and X. Huguet for their assistance.

REFERENCES

Balasch, J.C. (1998). *Resposta hidrològica i sedimentària d'una petita conca de muntanya analitzades a diferent escala temporal*. Tesis doctoral, Facultat de Geologia, Universidad de Barcelona, 372 pp.

Gallart, F., Llorens, P., Latron, J., Regüés, D. (2002). *Hydrological processes and their seasonal controls in a small Mediterranean mountain catchment in the Pyrenees.* Hydrol. and Earth Syst. Sci., 6(3), 527-537.

Latron, J. (2003). *Estudio del funcionamiento hidrológico de una cuenca mediterránea de montaña*. Tesis doctoral. Facultat de Geologia. Universitat de Barcelona. 269 pp.

Regüés, D. (1995). *Meteorización física en relación con los procesos de producción y transporte de sedimentos en un área acarcavada*. Tesis doctoral, Facultat de Geologia. Universidad de Barcelona, Barcelona, 302 pp.

Regüés, D., Balasch, C., Castelltort, X., Soler, M., Gallart, F. (2000). *Relación entre las tendencias temporales de producción y transporte de sedimento y las condiciones climáticas en una pequeña cuenca de montaña mediterránea (Vallcebre, Pirineos Orientales)*. Cuadernos de Investigación Geográfica, 26, 41 - 65.

Sammori, T., Yusop, Z., Kasran, B., Noguchi, S., Tani, M. (2004). *Suspended solids discharge from a small forested basin in the humid tropics*. Hydrol. Process. 18, 721-738.

Seeger, M., Errea, M.P., Beguería, S., Arnáez, J., Martí, C., García-Ruiz, J.M. (2004). *Catchment soil moisture and rainfall characteristics as determinant factors for discharge/suspended sediment hysteretic loops in a small headwater catchment in the Spanish Pyrenees*. J. Hidrol., 288, 299-311.

Soler, M., Regüés, D., Gallart, F. (2003). *Estudio del tamaño de las partículas en suspensión en relación con el caudal y la concentración de sedimento en una cuenca de montaña*. Rev. Cuaternario y Geomorfología, 17 (3-4), 69-77.

Walling, D.E., Webb, B.W. (1988). *The reliability of rating curve estimates of suspended sediment yield: some further comments*. IAHS Pub. No. 174, 337-350.

Williams, GP. (1989). *Sediment concentration versus water discharge during single hydrologic events in rivers*. J. Hydrol., 111, 89-106.

SUSPENDED SEDIMENT YIELD CONTINUOUS MONITORING IN TWO BASQUE COUNTRY CATCHMENTS PRELIMINARY RESULTS

A. Zabaleta, M. Martínez and I. Antigüedad

Hydrogeology Group, University of the Basque Country, 48940 Leioa, Bizkaia, Basque Country (Spain)
e-mail Ane Zabaleta: gpbzaloa@lg.ehu.es

ABSTRACT

Turbidity as a surrogate of suspended sediment concentration (SSC) has been continuously monitored since October 2003 in two mountainous rivers, the Aixola and Añarbe, of the Gipuzkoa County in the Basque Country. Relationships between the two parameters of turbidity and SSC were established in the laboratory; considerable variability was found in turbidity for a given concentration following on to sediment size changes caused by stream flow and sediment source variations. Event to event exploration of turbidity/discharge evolution was also analysed and three types of hysteretic loops were found dependant on event features and previous basin conditions. Preliminary results of the study are presented here.

Key words: continuous monitoring, turbidity, sediment yield, Aixola and Añarbe catchments (Basque Country).

INTRODUCTION

Optical sensors are commonly used for measuring turbidity as their advantage over conventional water sampling is the provision of continuous time series. This parameter can be used for efficient continuous suspended sediment discharge estimation when the turbidity to suspended sediment concentration ratio is calibrated frequently (Lewis, 1996). Setting a reliable relationship between SSC and turbidity requires a sound sediment-sampling programme with extensive data collection at short time intervals and a data set used for interpolation rather than extrapolation (Sun et al., 2001). Use of a turbidity meter can be an efficient means for sediment yield estimation with this approach.

Several data sets derived from flow events between October 2003 and August 2004 were used in this study to develop turbidity and suspended sediment ratio for the River Aixola and Añarbe catchments separately. These relationships were then used first to estimate continuous suspended sediment concentration and suspended sediment yields for each event later. SSC-discharge evolutions were also analysed and the different hysteresis types of the SSC-discharge relationships of single flood events identified as well as the relationships between hysteresis types and runoff generation conditions.

STUDY AREA

The River Aixola is located in the west of the Gipuzkoa County and drains a 4.8 km^2 headwater catchment into the Aixola water reservoir. The main basin bedrock is Upper Cretaceous Calcareous Flysch with alternating marl and sandy limestone layers. Average annual rainfall in the area is about 1200 mm well distributed throughout the year. The highest peak is at 750 m a.s.l., the outlet at about 340 m a.s.l. and mean elevation is 511 m a.s.l. The river runs from south to north, building up a valley with gentle slopes facing east and west. This basin is mostly (90%) reforested for industrial use with *Pinus radiata* trees. Here, mature trees grow up together with small ones planted after an important tree felling operation completed in the basin in the spring of 2002.

The River Añarbe, located in the eastern part of the County drains a 48 km^2 headwater catchment into the Añarbe water reservoir. Main bedrock is Devonian-Carboniferous alternating layers of shale and grauvacke, granitic materials from the Aiako Harria Stock and metamorphic materials. Average annual rainfall is around 2250 mm, the area being the highest rainfall one of the Basque Country. Mean elevation is 532 m a.s.l., with

the highest peak at 1035 m a.s.l. and the outlet gauging station at 200 m a.s.l. This high elevation range explains the very steep basin slopes. Most of the catchment is covered with reforested and mature *Pinus nigra* (also for industrial use) in the lower half of the basin and autochthonous vegetation as *Quercus robur* and *Fagus sylvatica* in the upper half.

MATERIALS AND METHODS

Turbidity (NTU units; Solitax-DrLange device), discharge and rainfall were measured every 10 minutes at both catchment outlets. Additionally, automatic water samplers were installed in both stations and programmed to take water samples at Aixola turbidity decrease or Añarbe turbidity rise. Samples taken were used to develop turbidity (NTU) and suspended sediment concentration (mg/l) relationships for each catchment. SSC values can thus be derived from turbidity observations.

Turbidity and SSC ratios were usually site and occasionally time specific and a unique relationship was normal for a particular catchment within a particular period of time (Gippel, 1989). This is why this study developed turbidity and SSC relationships for each catchment, taking account of as many events as possible.

Since suspended sediment grain size is markedly influential on turbidity records, this turbidity to suspended sediment concentration (SSC) ratio can change in time. When sediment grain size changes as a consequence of stream flow or material source changes concentration varies for a given turbidity record. If stream flow is the cause of sediment coarsening, the relation between SSC and turbidity is curvilinear, but if sediment sources change this relation can differ markedly from one moment to the next (Lewis, 2003).

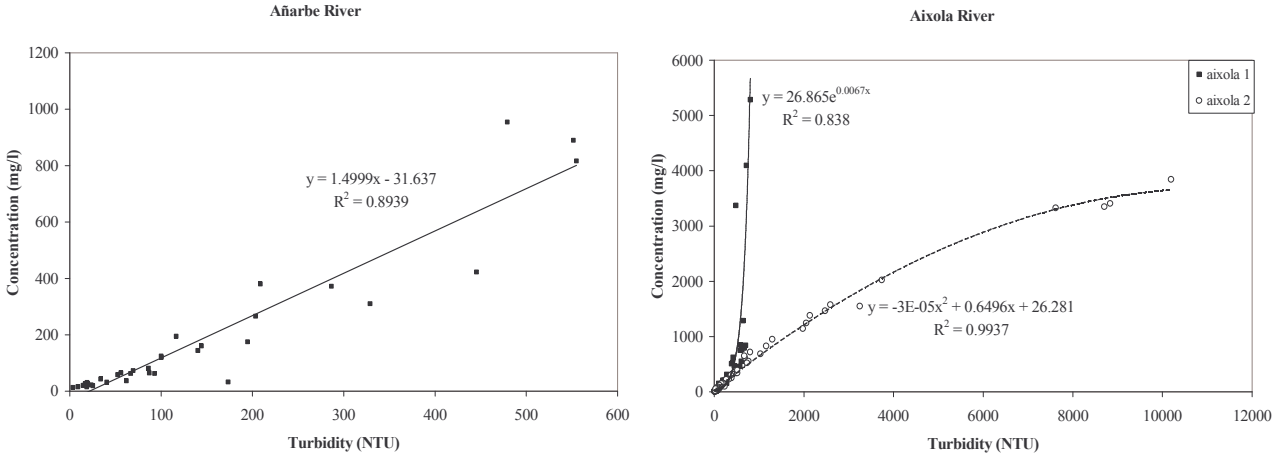

Fig. 1: Ratio of suspended sediment concentration (mg/l) to turbidity (NTU) in samples taken in River Añarbe and Aixola outlets.

The turbidity-to SSC ratio can be defined by a straight line for the River Añarbe (Fig. 1), which means there is no important variation to suspended sediment size and concentration for a given turbidity record consequently does not vary much. For the River Aixola, however, this ratio is more complicated due to the high dispersion shown in the SSC-turbidity graph, suggesting that more than one sediment source exists. Samples taken before March 15, 2004 (aixola 1) describe a unique non-linear relation, associated to transported sediment coarsening with stream flow. From that date onwards, the SSC to turbidity ratio changed drastically and some of the samples taken not only do not fit to aixola 1 but describe a different ratio (aixola 2), with a convex curvature, suggesting that the proportion of fine sediments increases with discharge. This kind of sample appears at the same time as land filling is performed in an area close to the river up-stream the catchment, so new and different material is provided to the river for transport. From this moment onwards, the ratio between these two parameters changes depending on the proportion of sediment provided from each source area to stream flow at each moment.

This is why event SSC calibration will be required to estimate suspended sediment loads in the Aixola catchment. The event of June 8 is shown in Figure 2 as an example. One can see that the first samples adjust to the aixola 1 relationship, prior to land filling, the next are located between aixola 1 and aixola 2, suggesting sediment source mixing, and the last adjust to aixola 2, which that appeared as a consequence of the land filling.

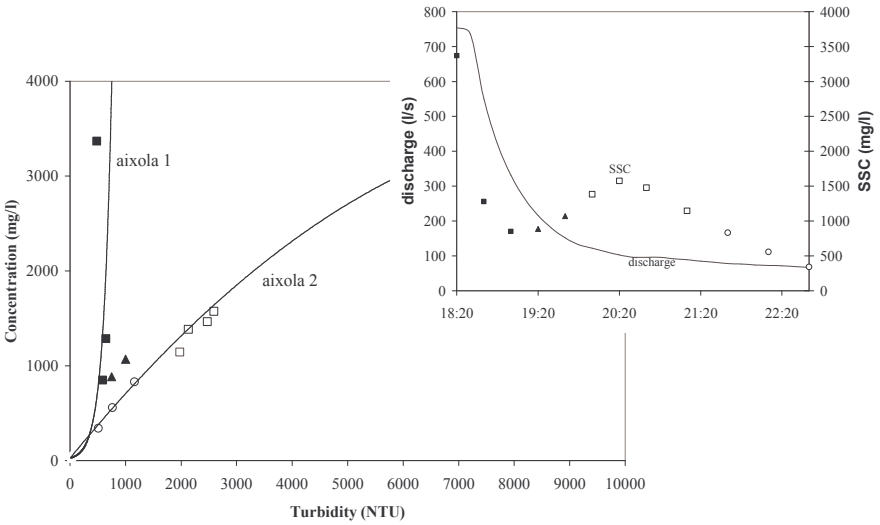

Fig. 2: Relation of suspended sediment concentration (mg/l) to turbidity (NTU) in samples taken in the outlet of the River Aixola on June 8 2004 and the corresponding hydrograph and sedimentograph.

RESULTS AND DISCUSSION

As is common in some rivers (Regués et al., 2000; Lewis, 2003), most annual suspended sediment in the River Añarbe is delivered from the basin during a few large runoffs (Fig. 3), so one single event can change overall yearly sediment yield. In contrast, suspended material in the Aixola basin is delivered the whole year long and all events have associated important suspended sediment yield.

This difference can be related to basin area and river morphology. Sediment sources in the Aixola (4.8 km^2) are relatively close to the catchment outlet with fast water and solid basin to outlet transit. Conversely, sediment sources are farther from the outlet in the River Añarbe, because of its larger area (48 km^2), and channel morphology facilitates sediment deposition, and suspended material only can reach the outlet in large storm flows.

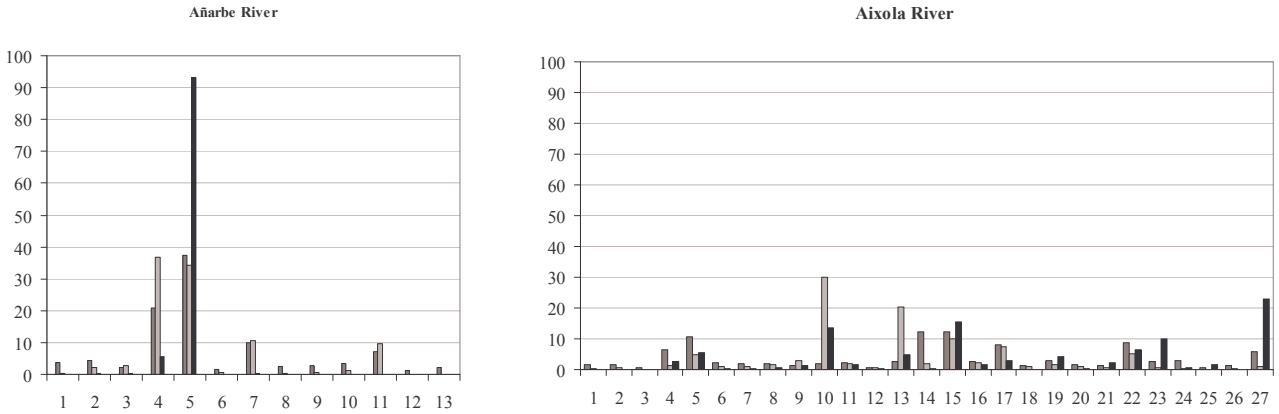

Fig. 3: Rainfall ■, discharge ■ suspended sediment yield ■ percentages for events recorded from October 2003 to July 2004, separately in the Rivers Añarbe and Aixola.

Analysis of those individual events shows that discharge and turbidity peaks are out of phase. This hysteresis is observed commonly and has been explained by a number of sediment delivery mechanisms and processes. As Williams (1989) concluded by systematically exploring possible SSC-Q relationships, five common classes of hysteretic loops can be distinguished: single valued, clockwise, counter-clockwise, single valued plus a loop and eight shaped. SSC-Q graphs were drawn to classify events recorded in the monitoring time using this kind of approach. Linear axes were used for both variables, with discharge in l/s in x-axis and suspended sediment concentration in mg/l in y-axis. Three hysteretic loop types were identified for the Aixola and Añarbe catchments, each related to different flood types and previous catchment conditions.

Floods were recorded in the River Aixola 27. Twelve were classified as counter-clockwise, nine as clockwise and the remaining six as 8-shaped. A main component analysis was made with rainfall (total, maximum 30 minute and previous 12 hour and 7 day), discharge (average discharge of the event, maximum 30 minute discharge and difference between discharge peak and base discharge) and suspended sediment concentration (sediment yield of the event (kg)) typical of these 27 events. The factorial planes shown in Figure 4 reflect the most important information, with factor I in the horizontal axis featuring average and maximum discharge (l/s) and suspended sediment yield (kg) and in the vertical, factor II featuring rainfall intensity and factor IV by the previous 7 days data. Factor III, featuring porevious12 hours rainfall, is not shown in these figures as being both feature prior conditions; Factor IV gives a visually clearer explanation to the loop patterns.

Figure 4a shows that clockwise hysteretic loop flow events are related to high discharge and suspended sediment concentration records and feature very intense rainfall and low prior rainfall records. In these cases, depletion of sediment available for transport occurs before water discharge reaches its maximum. Counter-clockwise and 8-shaped flow events occur in not very intense rainfalls and with lower discharge and SSC records than the ones mentioned above.

In Figure 4b counter-clockwise and 8- shaped events can be distinguished better. While in the latter pre-event rainfall is important and there is rapid sediment availability depletion once SSC peak is reached, in counter-clockwise events there is no important rainfall before the event and SSC depletion happens slower. In this last case, Brasington and Richards (2000) suggested that sediment is derived predominantly from hill slopes rather than from bank or channel erosion.

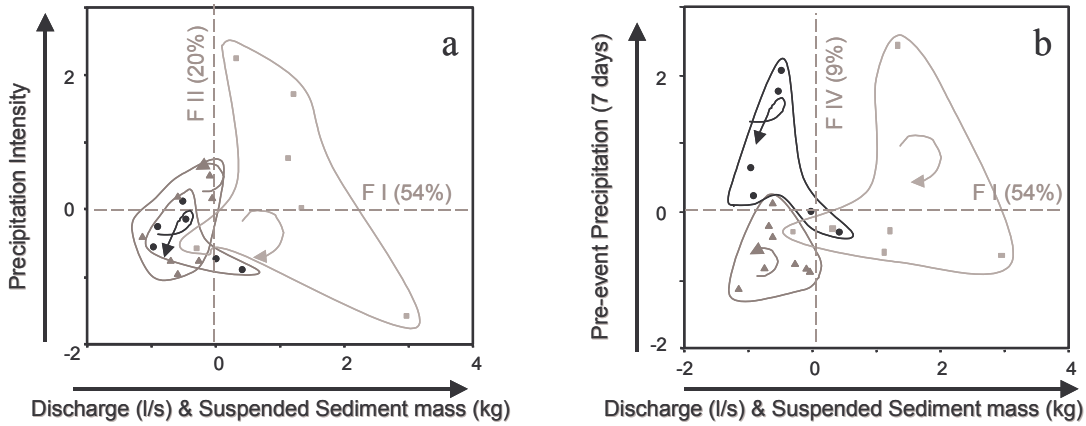

Fig. 4: Factorial planes showing relations between SSC-Q hysteretic loop patterns and event and pre-event features in the River Aixola: discharge (average and maximum (l/s)), rainfall (intensity and previous 7 days) and suspended sediment yield (kg). ■ represents events where relations between SSC and Q are described by a clockwise hysteretic loop, ▲ events with counter-clockwise loops and ● events with 8- shaped loops.

The thirteen flow events recorded in the River Añarbe show a general clockwise trend, even though mostly broken by high suspended sediment concentration peaks. In this case, and considering the large basin surface

and river channel width, fast increase of suspended sediment concentration at flood beginning can be explained by rapid displacement of sediment deposited near the channel (Regüés et al., 2000).

CONCLUSIONS

Results analysed show that some meaningful differences related to catchment features exist between suspended sediment dynamics in these two catchments. Firstly, suspended sediment delivery from the catchment occurs in a very different way in each case (Fig. 3). While in the River Añarbe, 93% of suspended sediments in are delivered from the catchment in a single event, the River Aixola delivers suspended sediments in a more continuous way, the highest sediment yield of a single event being much lower (23%). This difference is mainly related to drainage basin area and channel morphology.

Secondly, event variables correlated with suspended sediment yield also differ. As Table 1 shows, sediment discharge in the River Aixola is positively correlated (n=27) with total rainfall (mm) and average discharge (l/s) as well as with total prior 12-hour fall. Conversely, previous rainfall in the River Añarbe (n=13) is not correlated with sediment discharge and suspended sediment yield depends on total fall and event discharge.

Table 1: Pearson correlation between total suspended sediment yield (kg) in each event and total rainfall (Pt) and average discharge (Qav) of the event and previous 12 hour fall (P12h) for the Rivers Aixola (n=27) and Añarbe (n=13). Correlation is significant at the 0.01 level for bold numbers and 0.05 for italics

		Pt	P12h	Qav
Aixola	Sediment yield (kg)	*0.45*	*0.56*	**0.78**
Añarbe	Sediment yield (kg)	**0.94**	-0.18	*0.70*

Lastly, sediment dynamics in the Aixola also differs from that the Añarbe. In the former catchment three hysteretic patterns were found influenced by event discharge and fall features, and pre-event fall amount: clockwise hysteretic loops, with high discharge and sediment yield, counter-clockwise loops, where discharge, sediment delivery and previous rainfall are low and eight shaped loops with low discharge and sediment delivery but high previous rainfall So, as specified by Seeger *et al.* (2004), not only event conditions but also previous conditions are an important factor in this case, controlling sediment transport processes and a significant factor differentiating all hysteresis loop types.

Channel dynamics are more relevant in the River Añarbe, due to its larger area. Behaviour is fast depletion of sediment due to the scarce sediment available for transport in the riverbed and near the channel. That is why only clockwise pattern hysteretic loops were found in this catchment.

The data presented are the preliminary results of a study that started in October 2003 and is still in progress in the framework of a long-term investigation, so that new data are constantly being included. The next step will be to analyse annual suspended sediment dynamics and calculate sediment yield for hydrological year 2003-2004 in both catchments.

ACKNOWLEDGMENTS

The authors wish to thank the Sustainable Development Department of Gipuzkoa Provincial Council, the Spanish Ministry of Science and Technology (REN2002-01705/HID) and the University of the Basque Country for supporting this investigation.

REFERENCES

J. Brasington, K. Richards, (2000) Turbidity and Suspended Sediment Dynamics in Small Catchments in the Nepal Middle Hills. *Hydrological Processes*, 14. 2559-2574.

C.J. Gippel, (1989) The Use of Turbidity Instruments to Measure Stream Water Suspended Sediment Concentration. *Monograph series no. 4 Department of Geography and Oceanography, University College, The University of New South Wales and Australian Defence Force Academy* 204p.

J. Lewis, (1996) Turbidity-Controlled Suspended Sediment Sampling for Runoff-Event Load Estimation. *Water Resources Research*, 32. 2299-2310.

J. Lewis,. (2003) Turbidity Controlled Sampling for Suspended Sediment Load Estimation in: Erosion and Sediment Transport Measurement in Rivers: Technological and Methodological Advances (ed. By J. Bogen, T. Fergus & D.E. Walling) (Proceedings of the Oslo Workshop, June 2002) *IAHS Publ. 283*; pages 13-20.

G.P. Williams, (1989) Sediment Concentration Versus Water Discharge During Single Hydrologic Events in Rivers. *Journal of Hydrology*, 111. 89-106.

M. Seeger, M. P. Errea, S. Beguería, J. Arnáez, C. Martí, J.M. García Ruiz, (2004) Catchment Soil Moisture and Rainfall Characteristics as Determinant Factors for Discharge/Suspended Sediment Hysteretic Loops in a Small Headwater Catchment in the Spanish Pyrenees. *Journal of Hydrology*, 288. 299-311.

D. Regües, J.C. Balasch, X, Castelltort, M. Soler, F. Gallart, (2000) Relación entre las tendencias temporales de producción y transporte de sedimentos y las condiciones climáticas en una pequeña cuenca de montaña mediterránea (Vallcebre, Pirineos Orientales). *Cuadernos de Investigación Geográfica*, 26. 41-45.

H. Sun, P.S. Cornish, T.M. Daniell, (2001) Turbidity-based Erosion Estimation in a Catchment in South Australia. *Journal of Hydrology*, 253. 227-238.

THE RECHARGE-DISCHARGE PROCESS IN BOSSEA CAVE GROUNDWATER BASIN (NW ITALY)

M. Civita[1], M. Gandolfo[2], G. Peano[3] and B. Vigna[4]

[1]*Department of Land, Environment and Geo-Engineering - Polytechnic of Turin*
[2]*Department of Land, Environment and Geo-Engineering - Polytechnic of Turin*
[3] *External consultant*
[4]*Department of Land, Environment and Geo-Engineering - Polytechnic of Turin*
e-mail Bartolomeo Vigna: bartolomeo.vigna@polito.it

ABSTRACT

The Bossea groundwater basin is located in the southern part of the Piedmont region, in the Ligurian Alps. The basin has been studied since the early 1980s, in order to gain new information about the hydrodynamic and geochemical behaviour of a karstic system. In particular, the goal of the hydrogeological research, carried out by the Cuneo branch of the Italian Alpine Organization (CAI), in collaboration with Turin Polytechnic and the support of various local environmental agencies, is twofold: firstly, the study of the recharge-discharge processes that characterize the behaviour of the main aquifer system feeding the main drain; and secondly, the dynamic process of water in the unsaturated zone above the cave. The results from the Bossea groundwater basin study show the importance of hydraulic pressure transmission and piston flow phenomena in the aquifer network behaviour.

Key words: groundwater basin, karst system, gauging station, floods, unsaturated zone.

INTRODUCTION

The Bossea groundwater basin has been studied since the early 1980s via a scientific Station set up within the Bossea cave. This station is specially equipped to monitor the most significant hydrodynamic and geochemical parameters of the system. It is run by the Cuneo branch of the Italian Alpine Organization (CAI), in collaboration with Turin Polytechnic and the support of various local environmental agencies.

The Bossea groundwater basin is located in the southern part of the Piedmont region, in the Ligurian Alps between 800 and 1700 meters a.s.l. (Fig. 1).
The recharge area is located in both Corsaglia and Maudagna Valleys, predominantly consisting of karstic limestone, which is partially covered by eluvio-colluvial deposits. The hydrographic network consists of some secondary streams (Rio di Roccia Bianca, Rio Bertino) characterized by a scarce run-off that varies depending on weather conditions.
The main springs fed by the system are located near the Corsaglia riverbed, close to the town of Bossea, 800 meters a.s.l. The stream flowing throughout the Bossea cave, and feeding the above-mentioned springs, is also the main water drain of the system.

The first section of the cave is E-W oriented, right on the boundary between the impermeable basement and the carbonate complex and has a series of large drop-off rooms ranging from 826 meters to approximately 940 meters a.s.l. It then continues into a large horizontal gorge, that has developed along a series of tectonic discontinuities running E-W and terminates into a number of conduits in the saturated zone (Fig. 2). These have been explored down to 70 meters below the surface and are located 1500 meters from the entrance. The main drain gains a series of secondary tributaries all along the cave.

GEOLOGICAL AND HYDRO-GEOLOGICAL CONFIGURATION

The Bossea groundwater basin has a total dimension of 2.8 km^2 and consists of a narrow (about 700 m wide) layer of limestone and dolomite limestone of the Middle Triassic and Cretaceous periods. The carbonate

structure is laterally limited by the pre-triassic metamorphic basement (quartzite and porphyroids) through a series of sub-vertical tectonic contacts oriented E-W. The western boundaries of the basin are located next to a deep tectonic-karstic depression (polje), near Prato Nevoso, in Val Maudagna (Fig. 2). This structure is characterized by a series of fictile and rigid deformations, which consequently result in a high fracture state of the different lithologies. The carbonate complex is characterized by extensive superficial and deep karstic phenomena, resulting in a high secondary permeability.

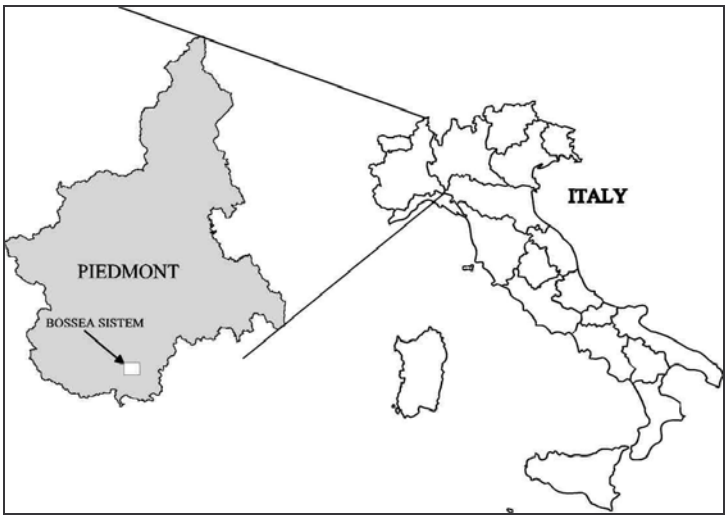

Fig. 1: The Bossea Cave system location.

The recharge area of the cave system also includes a series of secondary torrential rivers. These secondary order rivers, which are incised up to the impermeable Pre-Triassic rock, feed the aquifer through a series of sinkholes, located next to the point of contact with the carbonate rocks. Consequently, the supply of the cave system originates from the direct recharge (caused by precipitation and snowmelt) and from the ingestion of surface stream run-off (Civita et Al. 1984, 1987).

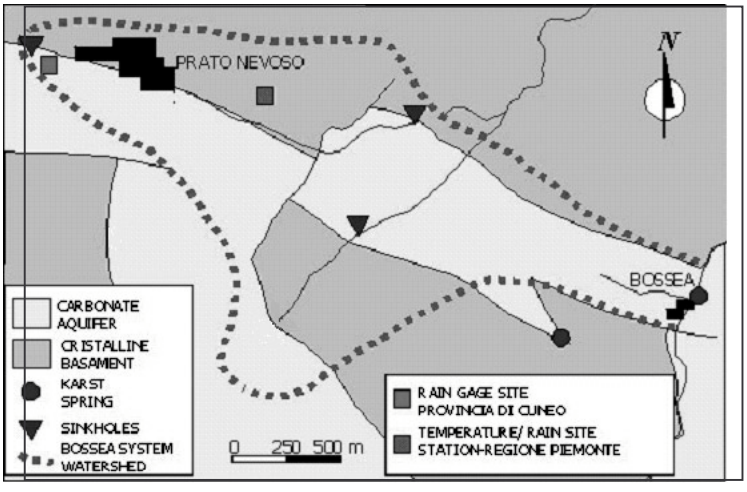

Fig. 2: The Bossea Cave system watershed.

The boundaries of the hydro-geological basin have been set according to the results of several artificial tracer tests and have been verified comparing the annual average balance with the average yield of the springs.

THE SCIENTIFIC STATION

The scientific station was set up in the Bossea cave in the early 1980s and has been continuously updated since then. In the initial phase a weir was built along the main stream and equipped with a water level measurement device to monitor the discharge. Automatic measurement devices for monitoring water conductivity and temperature were also implemented during this initial phase.
In the second phase new measurements were started. The new equipment was more reliable and gave the opportunity to increase the number of the monitored parameters (pH, dissolved oxygen, Radon).
Moreover, the secondary seepages and main percolation streams were also gauged to study the behaviour of the unsaturated section above the cave, from both a quantitative and qualitative viewpoint of the groundwater. In order to do so, several measurement systems were used and adapted to the conditions of the current experiments.
To measure the lower water-flow rates (seepages) rainfall gauges were used together with orifice buckets equipped with multi-parameter sensors for automatically measuring the water level, temperature and electric conductivity. Other small weirs were built up to measure the major water-flow rates, also equipped with multi-parameter sensors.

The study area contains a total of 16 monitoring locations to study the groundwater. Rainfall and air temperature are measured by several gauging stations located in Prato Nevoso, Borello and Monte Malanotte, as well as at the Bossea scientific station.

HYDRODYNAMICS OF THE SYSTEM

Discharge data from the main drain have been gathered since 1981. Data collection from the secondary input springs started in 1985 when devices were installed in the area of Polla delle Anatre and Stillicidio dell'Orso (Fig. 3).

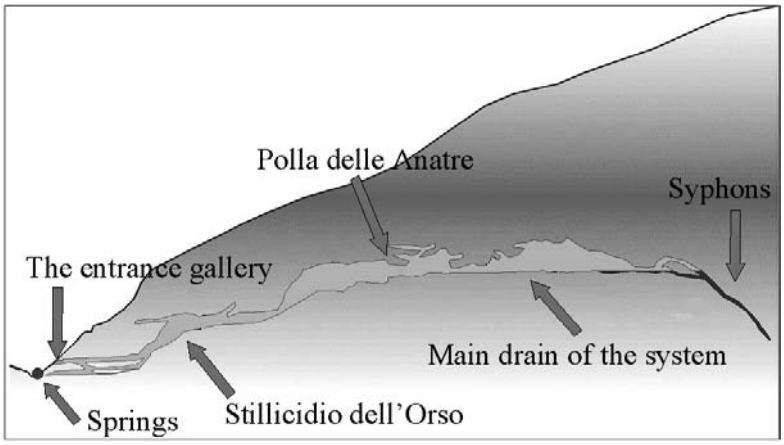

Fig. 3: The Bossea Cave hydrogeological section.

The annual trend of water-flow rates from the main drain can be easily identified, despite some slight differences (Fig. 4).
During winter, the water-flow rate is reduced and is tailing towards its minimum, about 0.04 -0.05 m^3/s, on at the end of February. This tailing is due to the low external air temperatures and the lack recharge due to snow accumulation.
A period of high flow rates occurs during spring, with highly variable discharge rates due to intense rainfalls and the melting of snow cover at high elevations. The maximum discharge exceeds 1 m^3/s, generally during May.

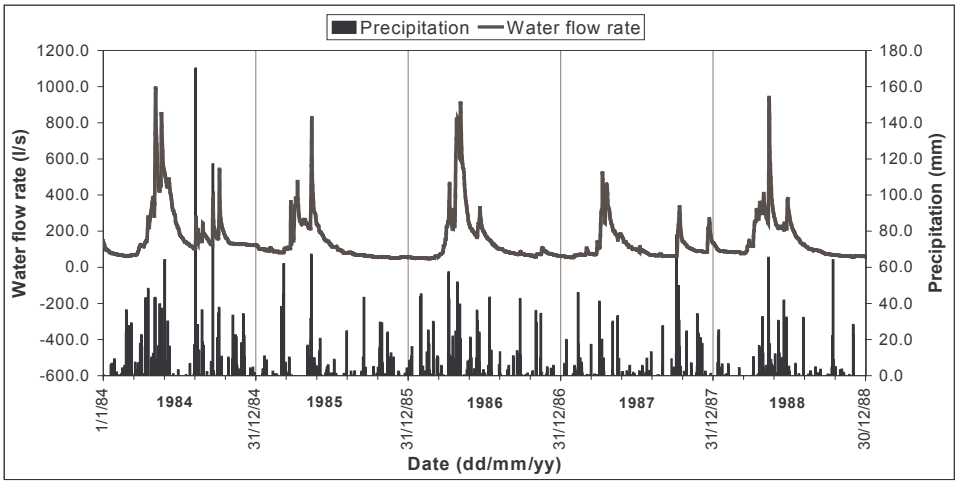

Fig. 4: The main drain annual trend of water flow rates.

There is then a progressive reduction in yield, sustained by storage in the system from which for long periods relatively high discharge levels may result without direct fresh infiltration. During summer and fall, heavy rain can cause a huge increase in the discharge rate, generating a number of hydrograph secondary peaks that deplete a few weeks after these storms. Throughout these months, even without rain, the water-flow rate is about 0.05-0.06 m^3/s.

The delay in the hydrodynamic response of the system to precipitation is influenced by the saturation level of the network.. When it rains in relatively dry conditions, it takes approximately 24 hours before any increase in water discharge is measured. However, when the discontinuities network is relatively saturated, the hydrodynamic response is immediate and characterized by a piston flow process due to the hydraulic head increase in the network.

Tracer tests show water displacement time of 3-15 days, depending on the various hydrodynamic conditions of the system. The hydrodynamic response times are highly variable and emphasize the importance of hydraulic pressure transmission inside the full-charge karstic network.

During the research period, it was possible to observe the reaction of the karstic system to two high flowage events, which took place in southern Piedmont in 1994 and in 1996. The system's behaviour in each case turned out to be very different, even if the rain events were similar.
In November 1994, the highest discharge peak reached 1.30 m^3/s - very close to the maximum value, which is normally measured in March. This emphasizes how the karstic system is unable to ingest the high recharge rates caused by heavy rains. Due to the steepness of the slopes and to the relatively overburdened karst superficial run-off occurs in the watershed, quickly feeding the surface water system but not the aquifer system.
During the October 1996 event, the response on heavy rainfall (205 mm) was quite different due to the exceptional nature of a phenomenon, which occurred inside the siphoning area of the cave (Fig. 5). The hydrograph showed a first peak of 1.23 m^3/s, two short periods with no flow at all, followed by an exceptional discharge exceeding 4-5 m^3/s and lasting for 10 hours. This event caused extensive damage to the station's gauge devices, to tourist equipment inside and outside the cave, to a 100m section of road and produced an anomalous flood wave in the Corsaglia stream. Moreover, during the peak discharge period a hyper-concentrated suspended transport flow occurred, containing sandy-silty dark yellow deposits. This high suspended load transport depleted in approximately 5 hours.

The processes that led to the extreme events in the Bossea cave were reconstructed by interpreting the data from the gauging stations, and by direct observations conducted by the scientific station researchers, guides

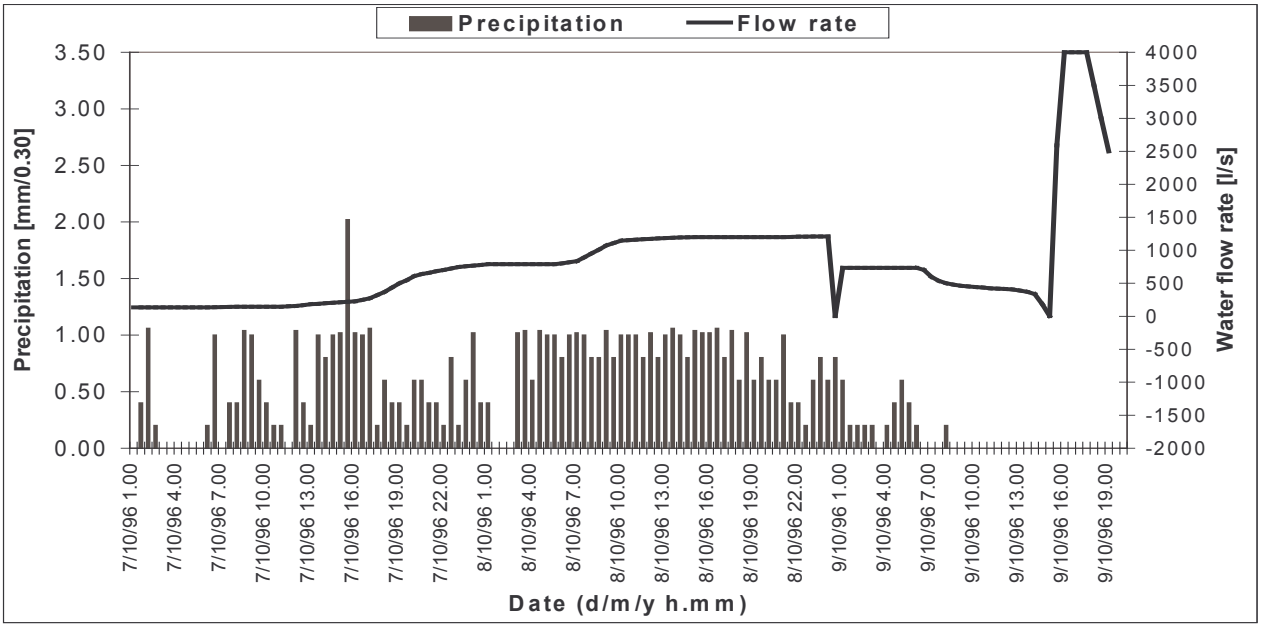

Fig. 5: Flow rate in the Bossea cave during the exceptional flowage in October 1996.

and diving speleologists within the siphoning area of the cave. This last section of the cave has a 45° gradient and is partially full of unstable sandy-silty deposits.
It was shown that these sedimentary deposits had progressively collapsed, blocking the conduit during the rain event, and thus stopping the flow of groundwater. This led to an upstream accumulation of a huge mass of water within the karstic network. Eventually the high water pressure destroyed the sediment plug, initiating an ejection of the fine-grained deposits and the flood wave.

Percolation stream water flows into the main drain and has generally low discharge rates, ranging from 1 l/h to a few l/s. These rates demonstrate the ground water flow dynamics in the discontinuities network of the unsaturated zone of the system. The annual hydrographs of the 16 examined percolation streams show very different trends. The general trend is relatively constant, but they can show significant increases due to rainfall events, and can also dry up due to a lack of infiltration. The recession curves of the different secondary flows feature significant differences associated with the extreme heterogeneity of each specific section of the drainage network. Despite this, the response to the infiltration inputs is similar for every spring and is characterized by significant piston flow phenomena. This is linked to the charge increase in the drainage networks.

Delay in the hydrodynamic response can vary depending on the saturation level of the network and can even last a few hours from when the recharge process starts. This response can be explained also by the hydrochemical changes. Dye tests carried out from the surface, approximately 120 meters above the cave, display the arrival of the tracers about 6 days after the input, showing a reduced (about 20 m/day) groundwater velocity within the discontinuities network.

PHYSICAL AND CHEMICAL CHARACTERISTICS OF GROUNDWATER

The main drain shows a reduced saline content within the groundwater, with a TDS value that ranges from 170-200 mg/l, a total hardness generally not exceeding 14°F and an electric conductivity range 190-250 µs/cm.
These values are normal for a mountain karstic system fed by both direct infiltration in the limestone complex and by groundwater coming from the well fractured metamorphic basement that borders the karstic structure (Civita et al., 1990).

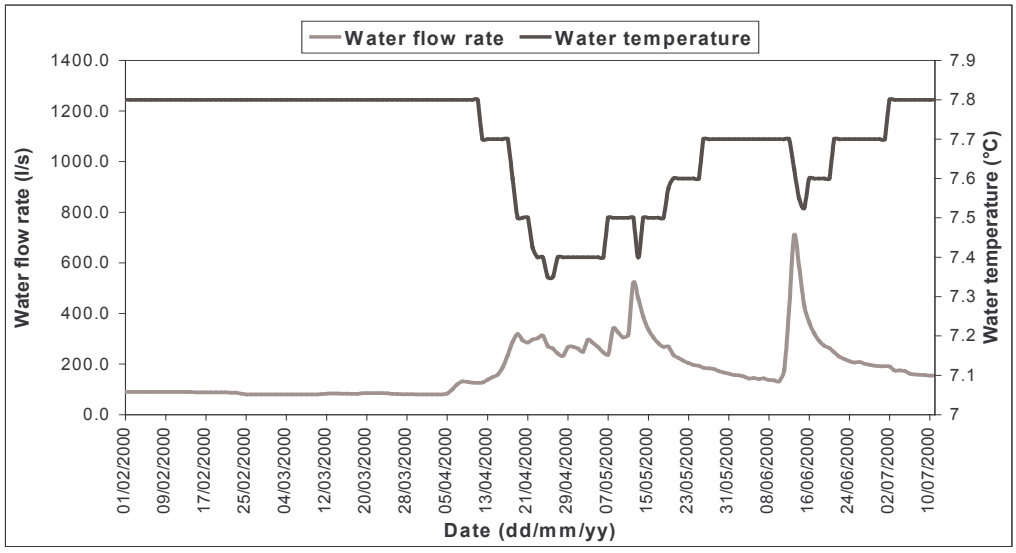

Fig. 6: Correlation between water temperature and water flow rate at Bossea system main drain.

The annual variations of the physical and chemical parameters are quite restrained, showing that water mineralization increases in connection to the high recharge events and to the piston effects generated by more mineralized waters located in less transmissive zones of the limestone system (Fig. 6). Only the groundwater temperature shows a gradual decrease (less than 1°C) during Spring time, due to the snowmelt waters mixed with the waters circulating within the saturated zone. The presence of reservoirs is confirmed by the artificial tracer restitution curves that showed rather long arrival times and a high dye dilution (Civita et al. 1990).

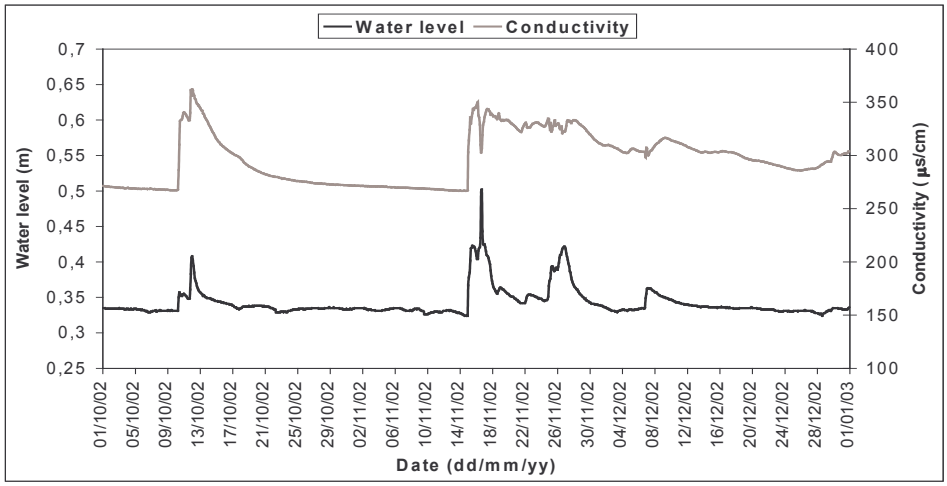

Fig. 7: Correlation between conductivity and water level at Polla delle Anatre percolation stream. The conductivity values are strongly influenced by the piston flow phenomenon.

Water mineralization of percolation streams is slightly higher than for the main drain, with TH values ranging from 13 to 26°F and conductivity ranging from 230 to 430 µs/cm (Peano et al. 1995; Civita et al. 1999), strongly influenced by piston-flow phenomena (Fig. 7). During the great flowage of November 1994 and October 1996, the greatest increases in the main hydrochemical parameters was detected, showing the importance of neo-infiltration water pressure in charging the underground network.

CONCLUSIONS

The research carried out on the Bossea karstic system yielded interesting information on this system's recharge-discharge process. There are in fact only a few studies that describe the role of the unsaturated zone in the infiltration processes both in underground hydrodynamics and geochemical interactions between rocks and water in a karstic system.
The definitions of precipitation, infiltration, and storage in a karstic system cannot be ignored in the assessment of water quantity and quality, together with the models on flood formation and the dynamics of complex land sliding events.

REFERENCES

Civita M., Peano G., Vigna B. (1984) - *La stazione sperimentale della Grotta di Bossea nel quadro delle ricerche idrogeologiche sui sistemi carsici del Monregalese*. Mem. Soc. Geol. It., 29, pp. 187-207.

Civita M., Olivero G., Vigna B. (1987) - *Analysis of recharge time dependent factors of Bossea Karstic System*. I.A.H. 21nd Congr. Proc., Guilin City (China), pp. 339-344.

Civita M., Gregoretti F., Morisi A., Olivero G., Peano G., Vigna B., Villavecchia E.,Vittone F. (1990) - *Atti della Stazione Scientifica della Grotta di Bossea.* Monography, L'Artistica Savigliano, Savigliano, pp. 136.

Civita M., Peano G., Vigna B. (1999) - *Primi risultati dello studio dell'insaturo carbonatico nel sistema di Bossea (Alpi Liguri - Piemonte Meridionale).* Atti "3° Conv. Naz. sulla Protezione e Gestione delle Acque Sotterranee per il III Millennio", Parma 13-15/10/1999, pp. 1128-1137.

Peano G., Vigna B. (1995) - *Le cavità naturali come via privilegiata per lo studio delle acque sotterranee: i rilevamenti effettuati nella stazione scientifica della grotta di Bossea*. Atti del Simposio Internazionale "Grotte turistiche e monitoraggio ambientale", Frabosa Sopra, (CN), 24-26 marzo 1995, pp. 333-348.

GROUNDWATER MODELING FOR THE ALLUVIAL BASIN OF THE JALOVECKY CREEK (SLOVAKIA) BY MEANS OF FIELD CAMPAIGN DATA

R. Dijksma[1], C.R. Stoof[1], L. Holko[2], H.A.J. van Lanen[1], G. Bier[1] and M. Kruitwagen[1]

[1]*Sub-department of Water Resources, Wageningen University, Nieuwe Kanaal 11, 6709PA Wageningen, the Netherlands*
[2]*Institute of Hydrology, Slovak Academy of Science (IH-SAS), Ondrasovecka 16, 031 05 Liptovski Mikulas, Slovakia*
e-mail Roel Dijksma: roel.dijksma@wur.nl

ABSTRACT

The alluvium of the Jalovecký Creek in the North of Slovakia is deposited by a braided river system whose source lies in the western Tatra Mountains. The rather thin Quaternary alluvium covers impermeable layers of Palaeogene claystone and flysch. Groundwater flow is concentrated in these Quaternary alluvial sediments. In autumn 2003, an intensive field campaign was carried out to improve the knowledge of such a hydro(geo)logical system as this. The type, thickness and permeability of the sediments, the creek elevation, discharge, infiltration/drainage and electrical conductivity were measured. The thickness of the alluvial aquifer showed a large variation on a small spatial scale, either due to height differences in the Palaeogene bedrock or due to differences in sedimentation. After the field campaign, the Jalovecký Creek catchment was simulated in MODFLOW 2000. In this model the Stream Package was used to simulate the infiltration and drainage of the Jalovecký Creek.

Key words: surface and groundwater flow, alluvium, modelling with MODFLOW2000, field campaign.

INTRODUCTION

The Liptov Basin is an intra-mountainous basin in Slovakia, between the Western Tatras in the north and the Low Tatras in the south. This depression is about 50 km long and up to 15 km wide. The elevation of the depression is 550 – 800 m a.s.l. In the axis, in an east-west direction flows the river Váh. Several small north-south and south-north oriented mountain creeks run parallel through the Liptov Depression towards the Váh.
The Jalovecký Creek is an example of such a north-south oriented creek. The catchment of this creek can be divided into an upper part (mountainous), and a lower part (the Liptov Depression). These catchments are called Upper Jalovecký Creek and Lower Jalovecký Creek respectively. Figure 1 shows the DEM of the total Jalovecký Creek.

At two locations the discharge of the Jalovecký Creek is measured (limnigraphs). The discharge of the Upper Jalovecký Creek, with its highest point at 2178 m a.s.l. at Banikov, is measured by the Priemstav limnigraph at a height of 830 m a.s.l. The discharge of the Lower Jalovecký Creek is measured by the Ondrašová limnigraph at an elevation of 570 m a.s.l. This implies an average surface gradient of 1348 m over approx. 5 km (26%) in the Upper Jalovecký Creek and an average surface gradient of 260 m over approx. 9 km (3%) in the Lower Jalovecký Creek. This implies that the surface gradient changes significantly at the Priemstav limnigraph.

The objective of this research was to gather as much field information as possible during a short field campaign and to test what the effect would be of different modelling concepts (averaging of variety at small scale versus detailed modelling; steady state versus transient modelling) on the output. An extra objective was to look into the effect of small scale water abstractions in the area.

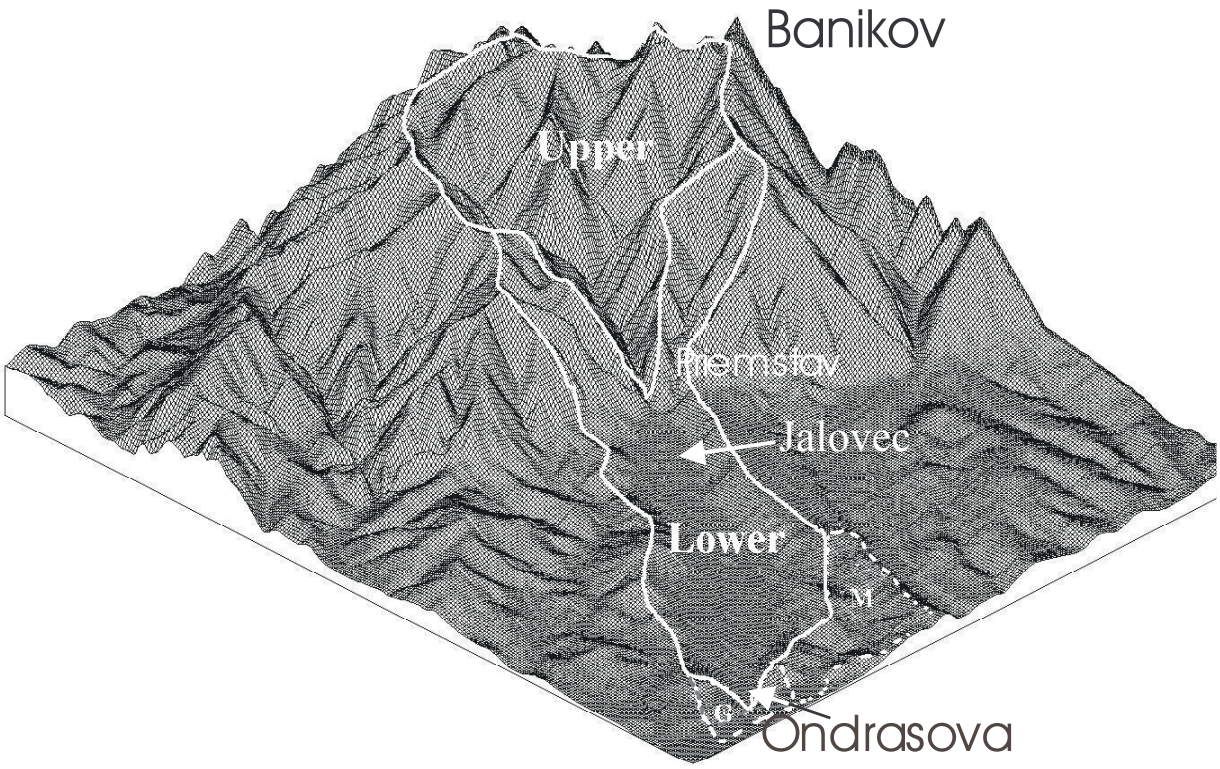

Fig. 1: DEM of the Jalovecký Creek catchment [after Kostka & Holko, 1997].

METHODS

The Inner Carpathians intra-mountainous depressions, like the Liptov Depression, are filled with Palaeogene marine –and in some places lacustrine- sediments, up to several hundreds of meters thick. These sediments are in general fine grained. The thickness and composition implies that these Palaeogene formations can be considered as impermeable. At the end of the Neogene, the sea receded and a river network was formed, with creeks which are several tens of meters lower than the surrounding Palaeogene ridges. During the Quaternary these rivers and creeks deposited several meters of sediments in the river valleys, such as fluvial sediments, travertine, slope-, proluvial- and organic sediments [Gross & Köhler, 1980]. Extended erosion terraces (Riss glacial) are observed. The surface of these terraces is generally flat and slopes towards the river Váh. During the Holocene, the Jalovecký Creek incised in its Riss sediments and new, lower-lying terraces were formed. Such permeable Quaternary and Holocene sediments underlain by impermeable Paleogene sediments result in an unconfined, coarse grained, but highly heterogeneous single aquifer system. In other words, the alluvium is actually a coarse grained channel lying under a relatively steep slope.

The saturated hydraulic conductivity of the alluvial sediments of the Lower Jalovecký Creek ranges between about 10 and 90 m d^{-1} [Gross & Köhler, 1980]. The mean annual precipitation is 817 mm at the Priemstav site and 646 mm at the Ondrašová site, where the mean annual actual evapotranspiration equals 500 mm. Figure 2 shows the mean monthly precipitation and the precipitation in 2003, when an intensive field campaign was performed (Stoof, 2004; Kruitwagen, 2004). The year 2003 was on the average a quite dry year.

Groundwater levels have been measured at different locations in the Lower Jalovecký Creek catchment. A set of piezometers was installed near Jalovec (Fig. 1) in the 1980s [Kostka & Holko, 2003]. From May 1988 until March 1990 these piezometers were frequently measured (Fig. 3). The groundwater fluctuation at this location can be more than 3 m. Moreover, the groundwater level can rise and decline very quickly (several

meters in a month). High groundwater levels are frequently observed in spring during the snowmelt period, and in the relatively wet August/September period.

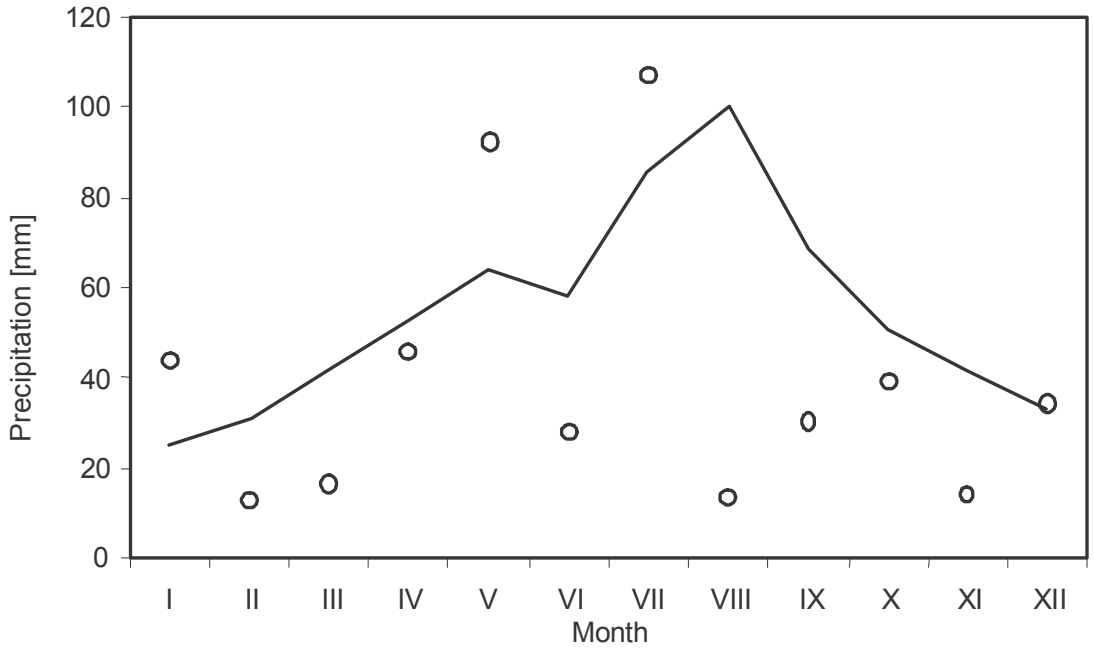

Fig.2: Mean monthly precipitation in Ondrašová in the period 1989-2002 (line) and monthly precipitation in the year 2003 (circles)[unpublished data IH-SAS].

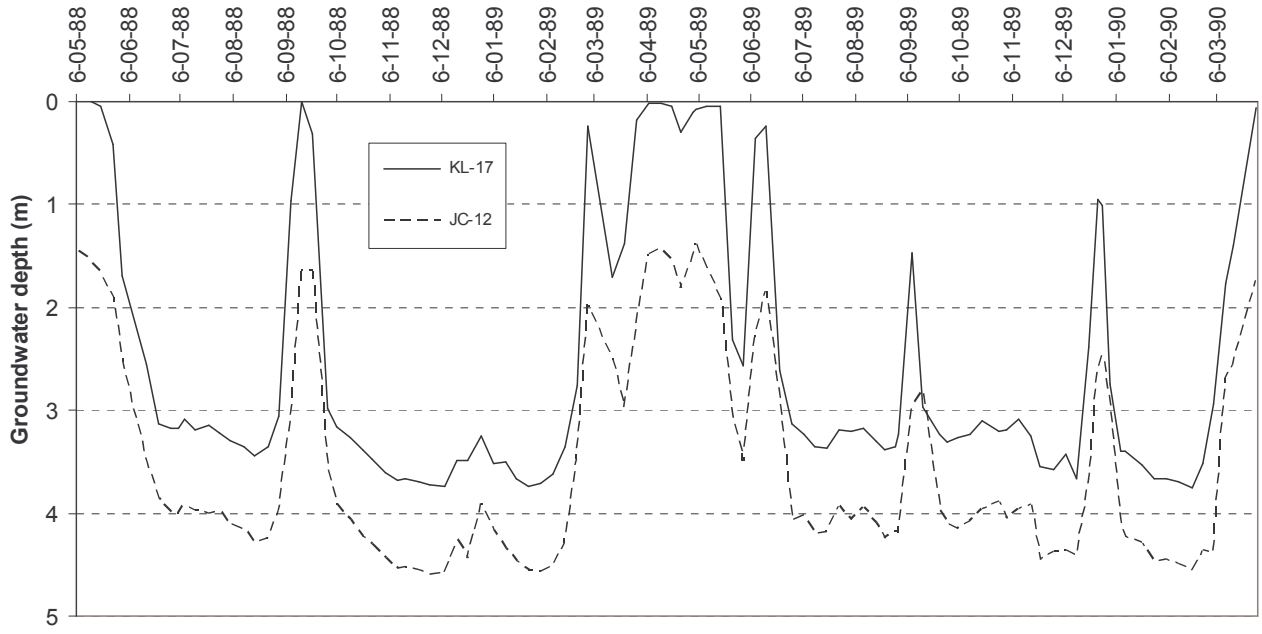

Fig. 3: Observed groundwater levels (below soil surface) near the village of Jalovec [IH-SAS].

From October to December 2003, an intensive field campaign was carried out in the Lower Jalovecký Creek catchment. Stream flow was measured along the stretch of the creek in combination with Electric conductivity routing in order to get information on the interaction between the stream and the aquifer, at about 50 locations geo-electric measurements were performed to get an insight into the spatial distribution of the sediments in the area, at four locations the hydraulic conductivity of the topsoil was measured, and the

groundwater level was measured frequently at the Jalovec site. Also a new observation well was constructed to derive the groundwater level in the downstream part of the Jalovecký Creek. Finally, the elevation and gradient of the Jalovecký Creek was measured.

These field data were used to build independently two groundwater flow models of the area. For both models the hydrological modelling software package MODFLOW2000 was used. Kruitwagen (2004) created a steady state model of the area, in order to look into the possibilities for small scale groundwater abstractions near Jalovec and Stoof (2004) created a transient model of the area to gain a better insight in the interaction in space and time between groundwater and surface water in catchment. The Stream Package of MODFLOW2000 was used to compute stream flow (discharge), stream stage (water level in the stream) and stream leakage of the Jalovecký Creek at a given inflow.

RESULTS AND DISCUSSION

Field campaign

Stoof [2004] and Kruitwagen [2004] found during their intensive field campaign in 2003 that the Lower Jalovecký Creek loses water to the alluvial aquifer (influent stream) in the upstream part and that it drains groundwater in the middle reach (effluent stream), whereas in the downstream part the brook seems to have lost hydraulic contact with the aquifer. It is likely that in this lower part the groundwater flows directly to the Váh and Liptovská Mara. They also found that the Quaternary sediments are highly variable at small spatial scales, which also implies that the hydraulic conductivity in these Quaternary formations is also highly variable at small scales. The hydraulic conductivity measurements of the topsoil (fine grained) showed an average hydraulic conductivity of 5 m d^{-1}.

Steady state modelling

According to the results of geophysical measurements (Kruitwagen, 2004; Stoof, 2004), 14 different geological formations were distinguished. After clustering of formations with similar physical properties only 9 formations remained, varying in hydraulic conductivity between 1.0 10^{-6} m d^{-1} and 218 m d^{-1}. Figure 4 shows the groundwater contour lines of the steady state modelling. The overall picture does resemble the results of the field measurements quite well. The groundwater contour lines indicate the Jalovecký Creek is losing some water in the upstream part, that it drains groundwater in the middle reach, and that it loses water in the downstream part. The water balance of the model suggests that about 7% of the groundwater leaves the area at the southern boundary, directly into the Váh and Liptovská Mara.

Three scenarios for groundwater abstraction for small scale drinking water supply were tested. The first scenario tested the effect of an abstraction of 30 m^3 d^{-1} and 150 m^3 d^{-1} respectively from the Jalovecký Creek banks, between Bobrovec and Priemstav. The model showed that the 60 days zone would already reach a holiday resort close to Priemstav. Such an abstraction would thus be vulnerable to pollution. The second scenario considered similar small abstractions as in scenario 1, but now from a well just upstream of Jalovec. The drawdown in the well is small, within 0.5 m. The intake area for this scenario is mainly northeast of the abstraction well, with only extensive agriculture and nature as land use. The third scenario was to test an abstraction well location between Bobrovec and Jalovec. The model showed that the intake area was interfering strongly with the main road between both villages. It was concluded that the second scenario offered the best possibilities for a small scale groundwater abstraction.

Transient modelling

The groundwater system of the Lower Jalovecký Creek is characterized by strongly varying fluxes and groundwater levels and can therefore best be reflected in a transient simulation, in which fluxes can vary over time. For this transient modelling, the Jalovecký Creek stream was divided into sixteen segments. Each

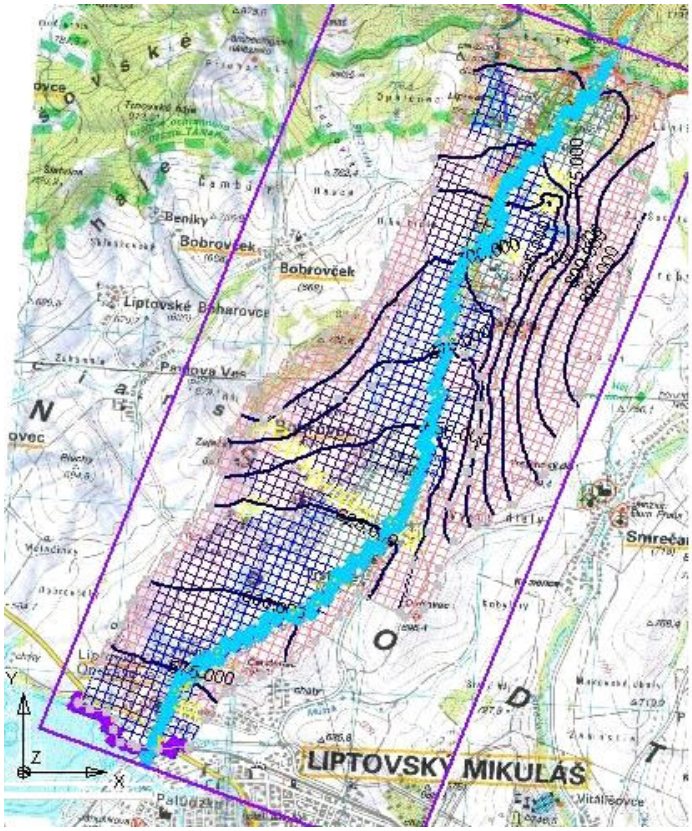

Fig. 4: Groundwater contour lines (25 m interval) of the steady state model (Kruitwagen, 2004).

segment represented the stream length between two locations where the creek elevation had been measured during the field campaign.

The conversion from field observations of the geological structure to a model grid can be done best with a conceptual approach in which the model defines the layers itself. At places where the geological structure is complex, a grid based approach is probably favourable. Therefore the model was developed using the conceptual and grid-based approach. To be able to test the difference between these approaches, two models were constructed. In the HETERO model the geometric mean of the coarse and fine sediments was used where a combination of both was expected, and for the profiles with only fine sediments the hydraulic conductivity of fine sediments was used. In the ZONES model the spatial distribution of the fine and coarse profiles was incorporated, roughly based on soil maps, geo-electrical soundings, the discharge of the creek and the pattern of groundwater levels and springs. Figure 5 shows the measured discharges at the inlet (Jalovecka Dolina or Priemstav) and outlet (Ondrašová) of the Lower Jalovecký Creek and the calculated discharges of a model with an averaged permeability (HETERO) and a model with permeability in zones (ZONES). The Quaternary sediments of the Jalovecký Creek consist of both (very) coarse and fine profiles, with large spatial variation. By averaging the permeability, the implication would be that equal amounts of water would flow through both fine and coarse sediments. The effect of the very coarse layers would then be minimized. Therefore preferably more detail should be incorporated in the model. However, even with the quite detailed geophysical study, the exact location and distribution of the coarse zones is not known. To incorporate the coarse layers in the model, hypothetical coarse zones had to be defined.

Figure 5 shows that the measured discharge at limnigraph Ondrašová (the outlet of the Lower Jalovecký Creek) is always higher than at limnigraph Priemstav/Jalovecka Dolina (the outlet of the Upper Jalovecký Creek, thus the inlet of the Lower Jalovecký Creek). The difference between the HETERO and ZONES concept is very small. Apparently the discharge at Ondrašová is not strongly affected by incorporating the high permeable zones. This conclusion is not very strong though, because the discharge at Ondrašová is

largely underestimated. This is maybe due to an underestimated recharge or due to a too high flux directly into the Váh and Liptovská Mara.

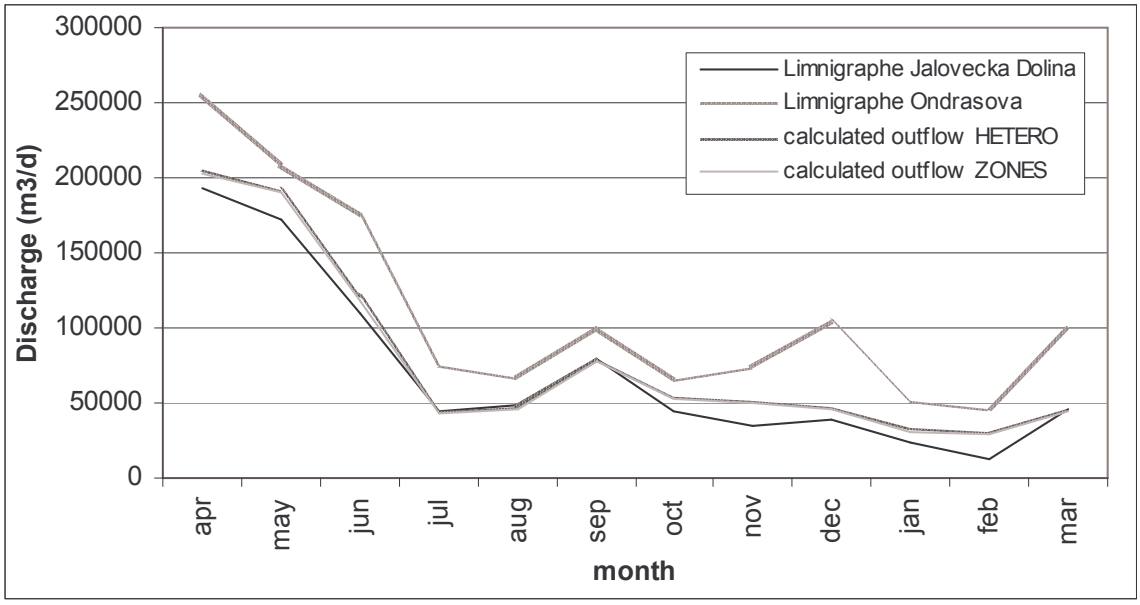

Fig.5: Mean monthly measured and calculated discharges (Ondrašová kindly provided by SMHI).

Discussion

The intensive field campaign of 2003 provided a good impression of the spatial variability of Quaternary sediments in intramountainous basins in general, like the Lower Jalovecký Creek. However, the exact location and distribution of the coarse and therefore highly permeable layers could not be found. Furthermore the differences between the independently developed models were not very large. The steady state models resembled the general water flow quite nicely, but the transient models need to be improved further to get a better match between measured and calculated discharges.

REFERENCES

Gross, P. and Köhler, E. (1980): *Geologia Liptovskej kotliny (Geology of the Liptov valley)*, Geologicky ustav Diobyza Stura, Bratislava, 242 pp.

Kostka, Z. and Holko, L. (1997): *Soil moisture and runoff generation in small mountainous basin*. Publication of the Slovak Committee for Hydrology 2, Institute of Hydrology SAS, Bratislava.

Kruitwagen, M. (2004): *Exploration of groundwater flow in the Lower Jalovecký catchment; Fieldwork and MODFLOW study for the abstraction of drinking water*. Doctoral thesis Wageningen University, Wageningen, the Netherlands, SHMI: Slovak Hydrometeorological Institute, Bratislava.

Stoof, C.R. (2004): *Interaction between a creek and its underlying aquifer in Tatra Mountains alluvium, Slovakia*. Doctoral thesis Wageningen University, Wageningen, the Netherlands.

INTEGRATED MONITORING OF SMALL RIVER BASINS IN LITHUANIA

Z. Gulbinas

Public Agency "Nature Heritage Fun" / Vilnius Paedagogical University, A. Juozapaviciaus 9, Vilnius, LT-09311 Lithuania
e-mail Zenonas Gulbinas: zenonas@gamta.lt

ABSTRACT

Three different procedures are used for **i**ntegrated small Lithuanian river basin monitoring. The first part of this article presents semi-natural ecosystem integrated monitoring in small 100 to 400 hectare catchments with natural pine/spruce vegetation in protected territories; the second agro-ecosystem integrated monitoring with watershed investigation providing an opportunity to analyse surface, drainage and ground water quality in various interacting pools in normal farming conditions; the third is natural 2000 site management and restoration through an Integrated River Basin Management Plan of the River Dovine Ditch PIN-Matra project, with the overall purpose of producing a River Dovine basin Management and Restoration Plan.

Key words: integrated monitoring, small river basins, hydrodynamic and hydro-chemical modelling, PIN-Matra project.

NATURAL ECOSYSTEM INTEGRATED MONITORING

Four different monitoring programmes were implemented for the UN/ECE Convention on Long-range Trans-boundary Air Pollution in the Eighties, all targeted at monitoring and assessing the environmental effects of air pollutants. In 1988, the UN/ECE recommended that participating countries contribute to a 3-year pilot programme involving so-called small catchment Integrated Monitoring or IMP. The Executive Body meeting of November 1992 decided that the IMP was to continue renamed as International Co-operative Programme in Integrated Monitoring of Air Pollution Effects on Ecosystems.

Lithuania started participating in this programme in 1993 and 17 sub-programme complying with IMP Regulations and Standards have been included in Lithuania's State Environmental Monitoring Programme and processed as global background monitoring.
Integrated ecosystem monitoring involves measuring different ecosystem departments at the same locations simultaneously over time, with physical, chemical and biological tools. Integrity is achieved by identifying the integrated monitoring territory IMT within the main landscape types extant in Lithuania. Such territories were identified in minimal anthropogenic impact areas and were combined with national park and reservation infrastructures as background territories.
Integrated ecosystem stationary investigation inclusive of rainfall, surface, ground and soil water, soil chemical composition and biota conditions surveys is performed in small 100 to 400 hectare catchments with natural pine/spruce vegetation in protected territories. The Author has previous experience in this field, having been responsible for stationary investigations of the soil and soil, ground and runoff water chemistry in integrated monitoring territories for ten years. Over 20 hydrological, physical and chemical parameters are measured, analysed and calculated as geo-indicators in each sub-programme.

The main purpose of the investigation is identifying pollutant accumulation and transformation in the sail, their leaching intensity, migration routes and input into open water basins. Field observation data are required to identify biogenic and pollutant flows, together with migration and accumulation links, budget calculations and modelling for anthropogenic process analysis and forecasting.

Agricultural pollution is absent in background monitoring territories, so atmosphere is the only source of dispersed pollution. Long-term regime investigation is firstly required to identify anthropogenic factor impact on environment quality, followed by water flow and chemical element balance calculation with atmosphere/vegetation/soil, ground, surface and atmosphere water chain modelling.

OBJECTIVES

Lithuania's first two IMTs were established in the National Park reservation zones of Aukstaitija in the east of the country and Dzukija its south in the year 1993 (Fig. 1). The third one was established in 1995 in the Zemaitija National Park in western Lithuania.

LT01 was established in the eastern Lithuania forest nature reserve of Aukstaitija at 55°26'N and 26°04'E that included the Gerveciai forest raised bog and adjoining tree plantation at 158-188 metres above sea level. The Verminis rivulet whose catchment area occupies 101.5 hectares and flows into a lake situated in the Gerveciu bog was selected for monitoring. Typical reliefs in the investigation area are glacial river plains and kames.

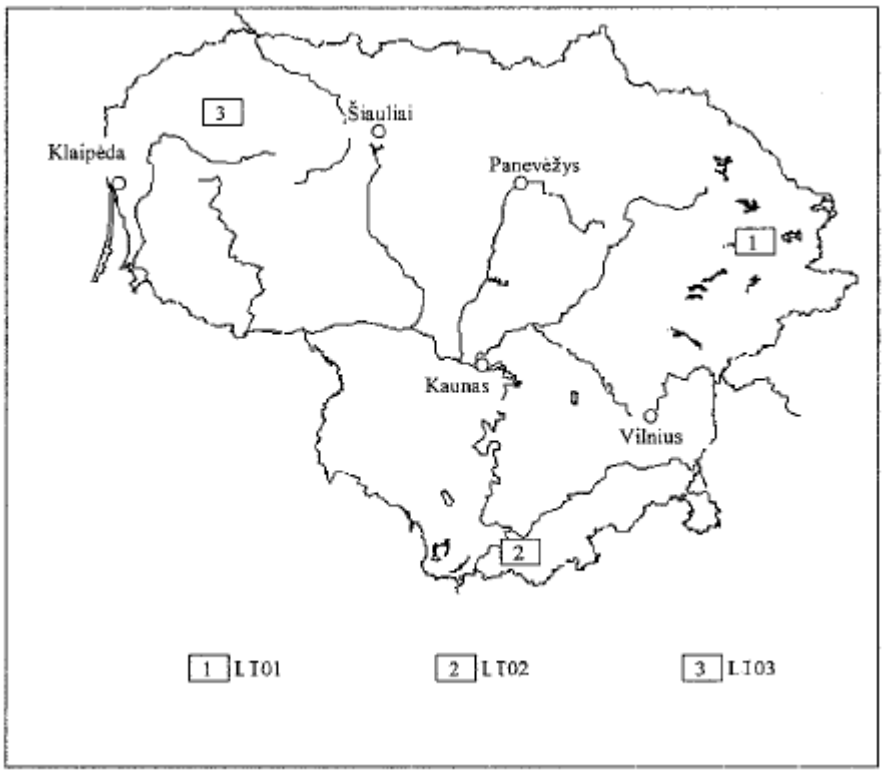

Fig. 1: Integrated monitoring territories in Lithuania.

LT02 was established in the Skroblus nature reserve at 54°05'N and 24°17'E, inclusive of the River Skroblus mid and lower course. The 380-hectare catchment area of the Slaitinis rivulet, a left tributary to the River Skroblus between the villages of Rudnia and Dubininkai, at 80-134 metres above sea level was selected for monitoring. Landscape reliefs are mostly the outcome of the last glacial melt waters that also deposited a wide glacial river plain whose sandy deposits were blown into complicated shape continental dunes.

LT03 was established in a western Lithuania nature reserve at 56°01'N and 21°52'E, 147-180 metres above sea level. The 147.3-hectare catchment area of the Juodupis rivulet, the right tributary to the River Uosna, was select for monitoring. The investigation area presents three genetic relief types, namely outer glacial sub-aerial accumulations in a hilly tract affected by water abrasion and accumulation of some 160-18 meters of the eastern part of the territory and chaotically scattered sand covered solitary flattop hills at basin edges; limnoglacial formations represented by wavy and sandy depressions between hills and bog accumulation forms stretching in the lowest depressions of the former limnoglacial basin, consisting of organogenic material, peat included (Table 1).

Table 1: Catchment features

IMT	Soils	Regional climate	Mean annual temperature [°C]	Mean annual rainfall [mm]
LT01	Podzolic, partly podzolised	Moderately cold and evenly humid	5.8	682
LT02	Weakly podzolised, nutrient- poor medium size grain sand size typically podzolised, developed on glacial origin sandy plains	Moderately cold and evenly humid	6.0	625
LT03	Pine forest podzolic on 51.3% of the area	Mild thin snow cover frequent thaw winters, comparatively warm springs and warm rainy autumns. High year-round air humidity, cloudiness and rainfall	5.9	788

Coniferous stands – mostly Scot pine trees with a mixture of Norway spruce – prevail in LT01. LT02 vegetation species diversity is much poorer, with pure Scot pine dominating and rarely found spruce and spruce pine forest stands. Coniferous stands dominate in LT03, mostly Norway spruce with 20 to 30% Scot pines mixtures (Gulbinas and Samuila, 1999).

A 40x40 m intensive soil measuring area subdivided into smaller 10x10 m lots was established near the intensive vegetation investigation area in view of dominant soils.

Soil water monitoring lysimeters were emplaced on three sides of the intensive soil-monitoring plot, featuring a 20x25 cm surface plate connected via a tube to a water collector. Three pairs of lysometers were installed, three individuals one at some 20 cm depth in the eluvial horizon and the other three at a depth of some 40 cm.

A cascade system of ground water sampling tubes, four in each IMT, was installed in the intensive vegetation area and soil was monitored for ground water level and samples were taken for chemical analysis.

A runoff monitoring station at the stream mouth recorded water level regularly. Water samples for chemical analysis were also taken regularly from the stream at this location.

METHODS

Chemical analysis soil samples were taken from representative sites. Soil profiles were dug out and descriptions written on site. The investigation site was divided into a 10x10 m grid, further subdivided into smaller 1x1m plots. Twelve to twenty four of previously unused 1x1 m plots were assigned to sampling, as they reflect the entire soil area. Wherever possible, soil samples for chemical analysis and bulk density were obtained from soil horizons 0-5, 5-10, 20-40 and 60-80. Decomposition and peat type were identified when describing peat soil. All samples were taken from the same horizons at 40 cm depth.

Soil chemical composition test samples were taken every 5 years in August/September.

Lysimeters were used for soil water chemical composition monitoring. These units can be produced from Teflon, porcelain or glass and are installed whenever possible into every observed horizon, but firstly in the upper 20 cm depth eluvial horizon and in the 40 cm depth B horizon below the root zone. Soil water samples for chemical analysis were taken every month in the frost-free period. Soil water flow from 1 km^2 at 20 and 40 cm depth was calculated at the same time. Thawing occurs frequently when the soil remains frost-free

during the winter, so water samples were taken and soil water flow calculated at the same frequency. No samples were taken in snow cover periods.

Soil water flow and moisture saturation were monitored at 20 m and 20 cm depth but were only calculated 4 to 6 times a year.

As soil water flow was only observed 6 times throughout a whole year, calculated values were set at a period of some 60 days, which means these findings are not very representative. Soil moisture saturation was monitored each month during the warmer season when the soil was not frozen and measurements could be performed.

Ground water level was measured every two weeks and during chemical analysis sampling operations. Ground water samples were taken bi-monthly 6 times a year after plummet measurements and stagnant water removal by pumping. Fifteen chemical parameters were checked in all.

Rivulet water sampling for chemical analysis was made monthly at 10 to 15 cm depth and daily river discharge calculated with automatic recorder data. Sixteen different parameters were checked in the runoff water sub-programme.

All water samples were analysed with standard *Methods for Integrated Monitoring* (1989, 1993) and *Manual for Integrated Monitoring (*1998), used by all IMP Member countries.

RESULTS

Main investigation results are reported in the scientific article by Z. Gulbinas and M. Samuila, which presents a review of the investigated inorganic soil horizon chemical features soil water properties, ground water chemical composition and long term fluctuation trends, calculation of water runoff and of some catchment chemicals as well as simulation of water balance elements with the SOIL model during the investigation period. Ten-year data analysis indicated the presence of a negligible amount of chemicals. Results confirmed that the catchments selected for integrated monitoring could be used as background monitoring material (Gulbinas and Samuila, 2002).

Stationary study results were presented at biannual conferences organised by the Nordic Hydrology Associated and published in the Reports of the Nordic Hydrology Programme (Gulbinas and Samuila, 1998; Gulbinas, 2000; Samuila, 2000b) and the paper Monitoring of Forest Ecosystems in Lithuania (Gulbinas and Samuila, 1999).

Minijus Samuila interpreted data collected with a mathematical modelling method based on the use of different computer model types.

An analysis of the mathematical modelling method showing how an actual computer model can be used to simulate soil water flow and moisture saturation in different forest soil profile sites was completed in 1999 (Samuila, 1999). Work with the SINSOIL computer model showed it could be applied quite successfully in Lithuanian conditions, as the correlation between model results and measurements of the same parameters is satisfactory. The model is convenient for checking certain assumptions necessarily made on the basis of inadequate field measurements

The purpose of the year 2000 study (Samuila, 2000a) was to simulate soil water balance and its elements with the WABTAL model with the same approach as for integrated Aukštaitija territory monitoring and assess its possible use. The model was calibrated on accurately measured *in situ* soil moisture saturation values and global radiation data measured at the nearest weather station. Work with he WABTAL computer model demonstrated its possible use in Lithuania, with certain reservations however. Modelling results are greatly generalised in time and should be interpreted as indications. The author of this study is rather sceptical as to winter and spring month results.

In the year 2001 study (Samuila, 2001), the Author attempted to model the Zemaitija IMT soil water balance with WINSOIL and WABTAL hydrodynamic models, compare data obtained and their reliability with the results of previous Aukštaitija IMT investigations. Models were then calibrated on accurately measured *in situ* soil moisture saturation values and global radiation data measured at the nearest weather station in Kaunas. The study confirmed previous WINSOIL and WABTAL model results and can be used as final proof that the models are applicable to the situation in Lithuania, provided proper account is taken of modelled territory local conditions. Table 2 shows the average measured and calculated water balance data for each integrated monitoring territory.

Table 2: Water balance of three integrated monitoring territories

IMT	Rainfall	Total evaporation	Transpiration	Total runoff
LT01	710.2	536.5	289.8	185.8
LTO2	721.2	522.5	294.5	190.8
LT03	951.2	545.9	210.2	396.0

The SMART regional model for acidification trends was selected in this study for analysing precipitation impact on surface water hydrology and chemical composition. SMART simulated some soil and water features of the IMT under review, based on the hypothetical scenario for future process development (Samuila, 2002).

AGROECONOMIC SYSTEM INTEGRATED MONITORING

Watershed level investigation enables analysing surface, drainage and ground water quality in different interacting pools in natural farming conditions. Water Management of the Lithuanian University pf Agriculture performed comprehensive monitoring, surface and ground water included, of the Graisupis watershed, which is covered by the national agroeconomic monitoring programme. The purpose is to analyse overall agricultural watershed water quality, including river quality and nutrient losses, drainage water and drinking water well quality.

The River Graisupis is the second rank tributary to the River Nevezis, and is located in the Middle Plains Kedainiai District of Central Lithuania. The area covers some 13.2 km^2 at the river monitoring station and the Graisupis watershed lies on a Silurian limestone bedrock. The quaternary sediment layer contains sandy loam soil; the landscape is flat and lies at 60 to 70 metres above sea level. The main spoil type is soddy gley, with loam and sandy loam soils dominating the watershed. Most soils are neutral, while those in the Graisupis watershed are saturated with phosphorus and rather low in potassium, content. Average mineral N content was found to be 0,65 mg per 100g of $soil^{-1}$ when 12 fields of various crops were investigated. All watershed agricultural land is subsurface drained, 54% of it being occupied by arable land with some 15% grassland. Forests cover 29% of the watershed (Gaigalis et al., 2003).

Lithuania's new State Environment Monitoring Plan is due to commence in 2005 and the national monitoring programme will also include the two additional watersheds of Vardas and Lyzena.

RIVER DOVINE BASIN INTEGRATED MANAGEMENT PLAN

The PIN-Matra programme "Management and Restoration of Natura 2000 sites through an Integrated River Basin Management Plan of the River Dovine" started in Lithuania in 2003, its overall purpose being the production of a Management and Restoration Plan for the River Dovine Basin covering a total area of 588.7 km^2, as an input for the Integrated Rivcr Basin Management Plan for the River Neumas Basin District.

The River Dovine Plan will include: a) a proposal to stop eutrophication and improve Lake Žuvintas hydrology and ecology as a contribution to reach a favourable conservation status of the Natura 2000 habitats and species by achieving a good ecological status of the River Dovine; b) a proposal for achieving a favourable conservation status for the Žuvintas mire and fen wetland areas adjacent the lake and other

wetlands and water bodies classed as Natura 2000 sites in the River Dovine catchment; c) preparation of a nature management and restoration plan for the drained Amalvas wetland and d) completion of a River Dovine Basin Geographical Information System.

Hydrodynamic and hydro-chemical process modelling in the basin will be completed with the Dutch integrated surface and ground water flow model SIMGRO (SIMulation of GROund water flow and surface water levels), which simulates regional ground water flow related to drainage, water supply, sprinkling subsurface irrigation and water level control (Querner, 1988).

The PCLake (Janse and Van Liere, 1995) model was proposed for modelling the Lake Žuvintas hydro-chemical situation. This model describes nitrogen and phosphorus nutrient cycles, mineral and organic nutrients included, three algae species, water plants, zooplancton, white and predatory fish and zoo benthos, as well as nutrient sorption to a water bottom sediment layer.

ACKNOWLEDGEMENTS

Support from the Dutch Government PIN-Matra project "Management and Restoration of Natura 2000 sites through an Integrated River Basin Management Plan of the River Dovine" (project Nr. 2003/040) is greatly appreciated.

REFERENCES

Gaigalis, K., Marculaniene, J. and Smitiene, A. (2003). Water quality in different Lithuanian geographic zones: comparison of two watersheds. *Water management engineering. LUA and LUA WMI Transactions,* 23 (45), pp. 69-78, Kedainiai, Lithuania.

Gulbinas, Z. (2000). Influence of precipitation on groundwater level and chemical composition in the integrated monitoring territories in Lithuania. *Nordic Hydrological Programme, NHP- Report no.* 46 *(ed Nilsonn, T). Vol.* 2; pp. 526-534, . Uppsala: SLU REPRO, Sweden.

Gulbinas, Z., Samuila, M. (1998). Water quality monitoring in the national parks of Lithuania. *Nordic Hydrological Programme, NHP Report no.* 44, *Volume I;* pp. 183-193, Helsinki, Finland.

Gulbinas, Z., Samuila, M. (1999). Soil, soil water, groundwater and runoff chemistry. *Monitoring of forest ecosystems in Lithuania;* pp. 182 - 186, Kaunas, Lithuania.

Gulbinas, Z., Samuila, M. (2002). Resu1ts of Integrated Monitoring in Small Wooded Catchments in Lithuania. *Geological Quarterly,* 46 (1), pp. 81-96, Warszaw, Poland.

Janse and Van Liere, (1995). PCLake: A modelling tool for the evaluation of lake restoration scenarios in *Wat. Sci. Techt. VoI* 31, *No.8,* pp. 371-374

Manual for Integrated Monitoring (1998). ICP 1M Programme Centre, Finnish Environment Institute, Helsinki.

Manual for Integrated Monitoring Programme Phase 1993-1996 (1993). Environment Data Centre, National Board of Waters and the Environment, Helsinki.

Methods for Integrated Monitoring in the Nordic Countries (1989). The Working Group far Environmental Monitoring, Nordic Council of Ministers, Copenhagen.

Querner, E.P. (1988). Description of a regional groundwater flow model SIMGRO and some applications. *Agric. Water Man* 14. 209-218.

Samuila, M. (1999). Simulation of some Hydrological indices in the Aukštaitija Integrated monitoring territory. *The Geographical Yearbook XXXII,* pp. 260-277, Vilnius, Lithuania.

Samuila, M. (2000a). Calculation of soil water balance elements by WATBAL model. *The Geographical Yearbook XXXIII,* pp. 430-444 (in Lithuanian).

Samuila, M. (2000b). Simulation of some Hydrological parameters in small wooded catchment. *Nordic Hydrological Programme, NHP- Report no* 46 *(ed. Nilsonn, T).* Vol. 1, pp. 291-298 Uppsala: SLU REPRO, Sweden.

Samuila, M. (2001). Utilization of soil water models in Žemaitija Integrated monitoring territory. *The Geographical Yearbook XXXIV* (2), pp. 103-120 (in Lithuanian).

Samuila, M. (2002). Modelling by SMART model in Lithuanian integrated monitoring territories *The Geographical Yearbook XXXV* (1-2), pp. 253-265 (in Lithuanian).

CHARACTERISTICS OF MINIMUM FLOW AND DROUGHT PHENOMENON IN THE SMALL BASINS IN ROMANIA. FORECASTING RELATIONS

P. Mita and S. Matreata

National Institute of Hydrology and Water Management Sos. Bucuresti-Ploiesti, 97 – Bucharest – Romania
e-mail Pompiliu Mita: pompiliu.mita@hidro.ro
e-mail Simona Matreata: simona.matrata@hidro.ro

ABSTRACT

For two areas in Romania– the western and north-eastern ones– this paper presents some of the major problems regarding minimum flow in small basins: the characteristics of minimum flow including drought and the forecast relations of these phenomena.
These problems are analyzed in four sections: 1. The characteristics regarding minimum flow in the Moneasa river basin (the water course has a permanent flow); 2. The relations of minimum flow forecasting for the Moneasa river basin; 3. The characteristics of the drought phenomenon within the Tinoasa-Ciurea and Tutova river basins (the water courses are subject to drought); 4. The forecasting relations of the drought phenomenon for the Tinoasa-Ciurea and Tutova river basins.
The influence of physiographic factors upon minimum flow is also presented in this paper.

Key words: minimum flow, drought phenomenon.

THE CHARACTERISTICS OF MINIMUM FLOW IN THE MONEASA RIVER BASIN (THE WATER COURSES HAVE A PERMANENT FLOW)

Brief presentation of the natural factors, rain-pattern regime and hydrometric observations

The Moneasa river basin is located in the mountain area of the western part of Romania. The mean altitude of the basin is 586m and the basin slopes are 40-45%. The prevailing soil types are forest brown and brown-reddish, and the vegetation covering most of the basin surface consists of deciduous forests (more than 80%). In order to carry out the study of the minimum flow, data from 7 gauging stations has been used. These stations cover areas ranging from between 0.146 km^2 and 76.2 km^2. The measurements were taken during the period 1975-2002. The mean annual amount of precipitation is 1020 mm (1975-2002).
Figure 1 shows the monthly flow depth resulting from rain, hr (mm), snow melting, hs (mm), and groundwater outflow, hg (mm), as determined for the hydrological year October 1988 – November 1989. The values for this year are very close to the long term mean, both in terms of precipitation quantity and distribution over time.

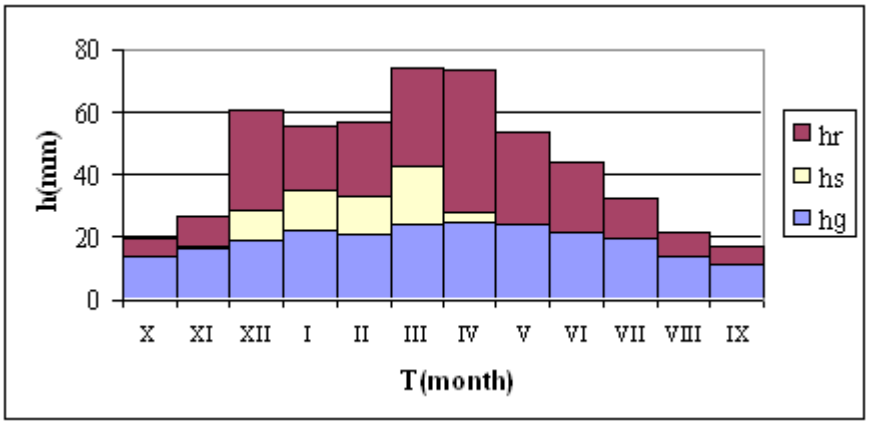

Fig. 1: Flow variation (the monthly mean depth, h). determined for hydrological year 1988- 1989 at Ranusa station.

As a result of the minimum amount of precipitation occurring between September and November, the smallest discharge volumes are measured in these months (Fig. 1).
From probability curves, 95% probability occurs at a minimum daily discharge value of 0.005 m^3/s at Ruja station (A=6.6 km^2) and 0.135 m^3/s at Ranusa station (A=76.2 km^2). Values of this kind were observed in October in the 1975 – 2002 period

In October but also in September and November values between 0.006 and 0.008 m^3/s at Ruja station and values between 0.135 and 0.180 m^3/s at Ranusa station are frequently measured and these values correspond to a probability of between 95% and 80%.

THE RELATIONS OF MINIMUM FLOW FORECASTING FOR MONEASA RIVER BASIN

The relations of the minimum flow forecast (annual minimum mean daily discharges) have been based on the following characteristics, as shown in Figure 2.

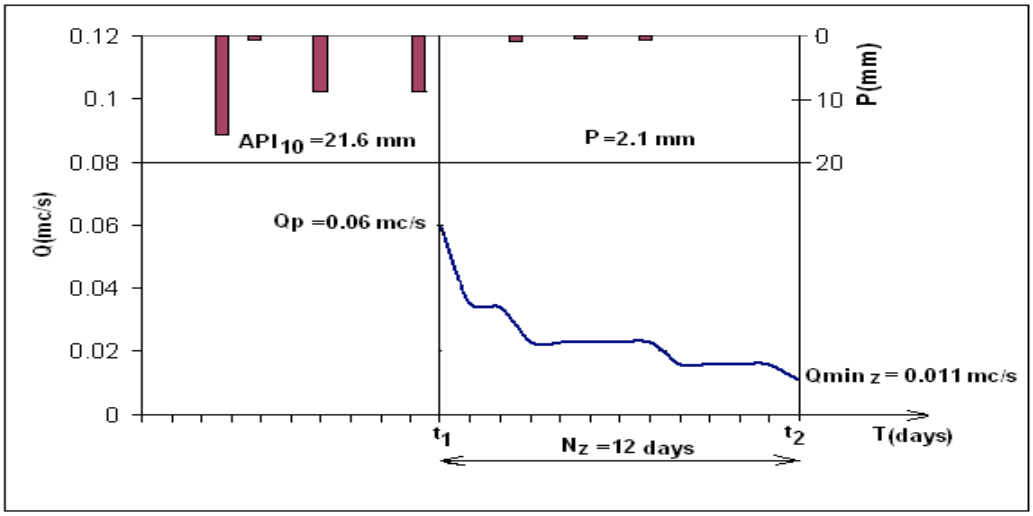

Fig. 2: Variation of the hydro meteorological characteristics at the Ruja station.

The characteristics used for the elaboration of the forecasting relations were the following:

- $Q_{min.Z}$ (m^3/s), is the minimum daily discharge. This discharge is the one to be forecasted.
- t_2 is time of $Q_{min.Z}$ (m^3/s) occurrence.
- Q_p (m^3/s) is the threshold discharge. The threshold discharge represents the initial point when elaborating the forecast. The fact that Q_p should exceed $Q_{min.Z}$ by at least 5-6 times has been taken into account, so that the interval between Q_p and $Q_{min.Z}$ should be efficient for surveying the flow evolution (10-20 days, for instance).
- t_1 is the time of Q_p occurrence.
- N_z (days) is the number of days between t_1 and t_2. This period is characterized by a continuous decrease in the flow.
- P(mm) - the amount of precipitation during the N_z interval.
- API_{10}(mm) - the amount of precipitation 10 days before the N_z interval. The value API_{10}(mm), was computed using the API (Antecedent Precipitation Index) model.

On the basis of these characteristics, the main parameter of this relation was obtained – *daily gradient of discharge decrease, G_s ($m^3/s/day$)*. This was determined for each of the N_z intervals (days) analyzed, taking into account the difference between Q_p, the point at which the forecast is elaborated, and $Q_{min.Z}$ which can be reached at the end of the N_z interval (Q_p - $Q_{min.Z}$). This difference is divided by the number of days of the N_z interval. Thus $G_s = (Q_p - Q_{min.Z})/ N_z$ ($m^3/s/day$).
Using this parameter for different conditions regarding the amount of precipitation P(mm) in the N_z interval and the precipitation that occurred 10 days before t_1 (API_{10}(mm)) the relation G_s= f(P, API_{10}) was determined (Fig. 3).

This relation makes the G_s (m^3/s/day) values available for the multitude of conditions regarding P and API_{10} values.

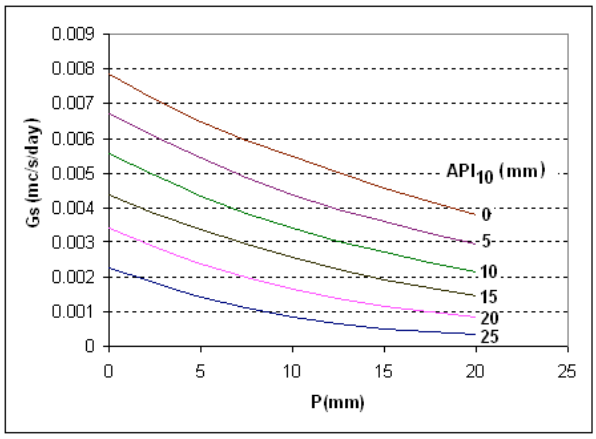

Fig. 3: Relation G_s= f(P, API_{10}).

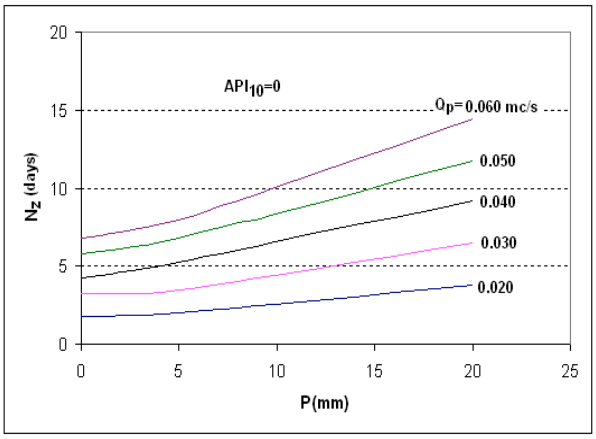

Fig. 4: Relation N_z = f(P, Q_p).

Ruja station (Moneasa representative basin)

Using the G_s values shown in Figure 3, the so-called forecast relation was determined, N_z=f(P, Q_p) for API_{10}=0 mm (Fig. 4). In this way the number of days can be determined, N_z, from the record of a certain threshold discharge Q_p, up to $Q_{min.Z}$ - the forecasted one - for different conditions regarding P and API_{10} values.

In the case of the Ruja station, for example, the Q_p values were of 0.060 m^3/s, 0.050 m^3/s, etc (Fig. 4). In order to have a valid relation for as long a forecast interval, N_z, as possible, it was established that $Q_{min.Z}$, the forecast one, should be $Q_{min.Z}$=0.005 m^3/s, the lowest flow ever recorded at Ruja station over the observed period. The $Q_{min.Z}$=0.005 m^3/s value was taken into account when calculating N_z in all the Q_p values.

The forecast of N_z is elaborated using both relations (Figg. 3 and 4). If the forecast is elaborated, beginning with the moment that Q_p=0.060 m^3/s for example, under conditions in which API_{10}=0 mm and P=0 mm, then G_s=0.0078 m^3/s/day (Fig. 3). After, for example, 5 days on such a gradient, the discharge will decrease to 0.021 m^3/s.

$$Q= Q_p-(N_z*G_s) = 0.060\ m^3/s - (5days*0.0078\ m^3/s/day) = 0.021\ m^3/s$$

The forecasting method of the minimum flow proposed by this paper (for rivers with areas up to 70 km^2 with permanent flow) could be used for larger rivers too. The reason is that the factors that lead to the decrease in flow of small rivers with permanent flow are the same as for rivers with areas larger than 70 - 80 km^2.

CHARACTERISTICS OF DROUGHT PHENOMENON WITHIN THE TINOASA-CIUREA AND TUTOVA RIVER BASINS

Brief presentation of the natural factors, rain-pattern regime and hydrometric observation

The Tinoasa and Tutova river basins are situated in the eastern part of Romania. The mean altitude of the sub-basins making up these basins varies between 250 and 320 m. The sub-basin slopes are 13-17%. The prevailing soils are forest brown-reddish and alluvial. The vegetation consists of leaf-bearing forests, pastures and hay fields, orchards and agricultural crops.

In order to elaborate the study of the minimum flow in small basins within this area, data from 4 gauging stations within the Tinoasa – Ciurea river basin with areas between 0.5 and 4.17 km^2 and from 2 gauging stations within the Tutova river basin with areas of 20.4 and 30 km^2 were used.
Hydrometric measurements at these gauging stations started in 1975.

The main factor determining a severe drought phenomenon (Q=0) is due to the excessive temperate-continental climate of the area. This climate is characterized by annual precipitation amounts which do not exceed 600–620 mm, frequently manifested as showers. After short intervals of only a few days or hours, precipitation can exceed 80 – 90 mm but this is followed by long periods of drought, sometimes longer than 30 – 40 days. Under such conditions, the drought phenomenon can persist for long periods.

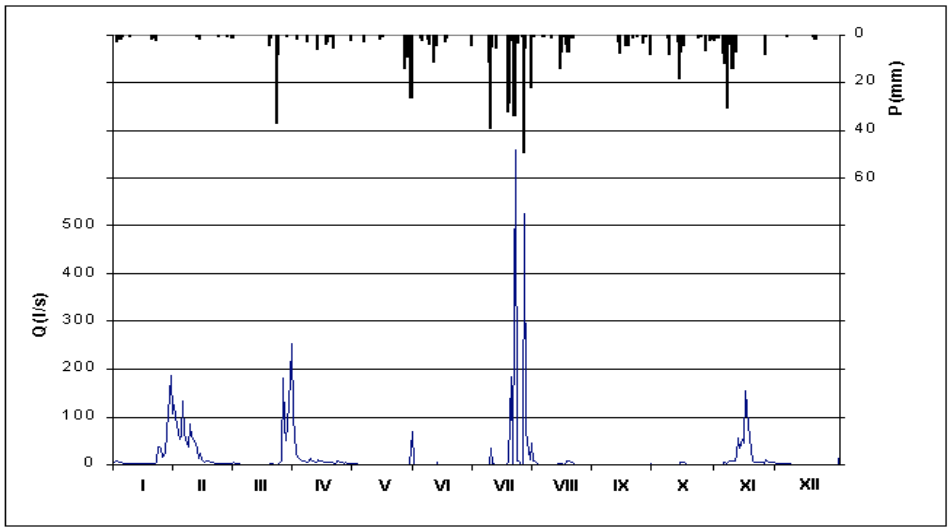

Fig. 5: The flow variation (the daily mean discharges) and the precipitation variation (quantities during 24 hours) observed in 2002 at Tinoasa station.

Figure 5 shows the precipitation and discharge variation in 2002 at the Tinoasa station (A=4.17 km^2) from the Tinoasa-Ciurea representative basin. 2002 was very close to the annual mean, both in terms of precipitation quantity and distribution over time and confirms the characteristics mentioned above concerning the pluvial regime in this area.

Another important factor amplifying the severe drought phenomenon is represented by the geological structure of the area. The thalweg of the low-flow channels of the water courses within the Tinoasa – Ciurea representative basin do not intersect the phreatic water. So, the stream flow is produced only by the precipitation on the surface of the basins.

In these conditions, the frequency of drought phenomenon (Q=0) occurrence, f(%), is between 40 - 50% for the basins in the 15 -20 km^2 area and over 90% for basins with an area smaller than 5 km^2. The frequency of drought phenomenon occurrence, f(%) was computed: f(%)=(n/N)*100 where: n is the number of years in which the drought phenomenon occurred and N is the number of years of the observation period.
For the Tinoasa-Ciurea representative basin (located in the Moldavian Central Plateau), flow continued throughout the entire year only in 1980.
Figure 6 shows the relation f(%)=f(A) for the studied area. For the area smaller than 2 - 3 km^2, the drought phenomenon occurs every year (f = 100%).

The annual mean duration of the drought phenomenon (Q=0), Ns(days), also shows very high values. At the Tinoasa station in the Tinoasa-Ciurea representative basin (A=4.17 km^2), the value Ns = 131days and at the Plopana station in Tutova representative basin (A=20.4 km^2) the value Ns = 39days.
The annual mean duration of the drought phenomenon Ns is over 100 days for the areas smaller than 5 - 6 km^2 and between 20-40 days for the areas between 20-25 km^2 (Mita and Haraga, 1996).

The maximum duration of the drought phenomenon (Q=0), observed in the small basins of this area was in 1987: 292 days for the Tinoasa station (A=4.17 km^2) and 326 days at the Humaria station (A=1.60 km^2) in the same basin (Tinoasa-Ciurea representative basin). Precipitation in 1987 amounted to 470 mm.

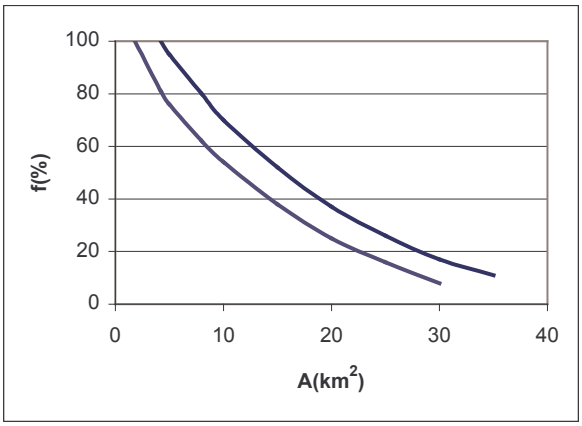

Fig. 6: Relation f(%)=f(A) for the Moldavian Central Plateau.

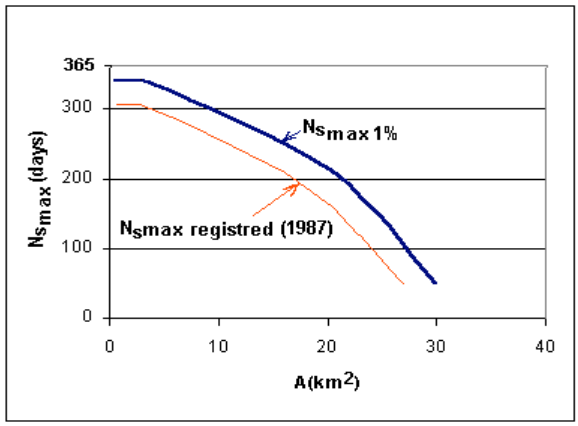

Fig. 7: Relation $Ns_{max1\%}$=f(A) for the Moldavian Central Plateau.

In this year, there were entire months (I, VII, IX, X) when flow did not occur at all, although there was some precipitation. This precipitation, however, occurred in the summer period, after some intervals of drought and was absorbed by the soil. This was especially the case for smaller quantities under 10-15 mm, but sometimes even for larger amounts.

The situation was different in 1986, when precipitation amounted to only 381 mm, 89 mm less than in 1987. Yet, the Ns value was smaller, only 255 days. This happened because the precipitation fell mainly during the spring period, when the humidity was higher and favored the flow.
Therefore, the length of duration of the drought phenomenon depends not only on the precipitation quantity, but also on when precipitation occurs.
Regarding the maximum duration of the drought, statistical analysis shows that for a probability of 1% and less the duration could be longer than 320 days for the basins with areas smaller than 5 km^2 and over 330days for the basins with a high degree of forestation (Fig. 7).

The drought phenomenon analysis in basins with different degrees of forestation showed that in years of low precipitation, drought duration is longer for forested basins than in basins that are not forested. The explanation is that in forested areas supplementary water can be retained in the trees as interception and especially in the soil of the forest floor, which has a large drainage capacity. For example, in the case of a 100-year-old forest, quantities of precipitation of over 20 - 25 mm can be retained after a long period of drought. This explains the longer duration of the drought phenomenon in forested areas.

FORECAST RELATIONS OF THE DROUGHT PHENOMENON FOR THE TINOASA-CIUREA AND TUTOVA RIVER BASINS

The forecast relations for the occurrence of the drought phenomenon in these basins have a similar structure to the relations for minimum flow forecasting in water courses with permanent flows. The same method was used here to obtain the relations, but some parameters may differ.

In Figure 8 the type of relation for the drought phenomenon forecast is shown for the Tinoasa station within the Tinoasa – Ciurea representative basin (A=4.17 km^2), $N_z = f(P, S_a)$ for Q_p=20 l/s, where:

- N_z (days) - is the number of days between the observation of a certain threshold discharge, Q_p, and a new occurrence of the drought phenomenon Q=0;
- Q_p(l/s) – is the threshold discharge. Q_p is the value established in elaborating the forecast;
- P (mm) – the amount of precipitation during the N_z interval;
- S_a – the number of days with drought phenomenon (Q=0) before reaching the threshold discharge, Q_p, due to precipitation.

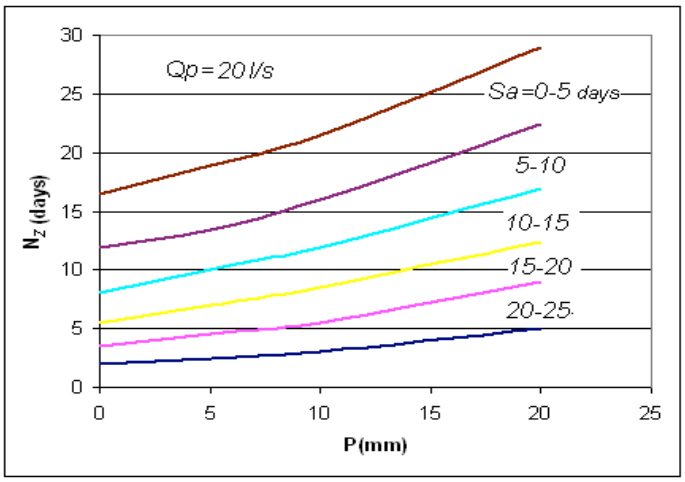

Fig. 8: Relation $N_z = f(P, S_a)$- Tinoasa station.

In the forecast relation, the S_a parameter was also introduced, reflecting the soil moisture conditions in the period preceding the threshold flow. In the case of a long period of drought (S_a>20 days), this parameter can indicate the depletion of the water storage in the soil. In this case, it is obvious that the flow should decrease much faster than in the case when such a period is absent (Mita, 1996).

As with watercourses with permanent flows, the threshold discharge Q_p exceeding 15-20 times the forecasting discharge, Q=0, has been taken into account in order to have an accurate forecast.

This forecasting method for the occurrence of the drought phenomenon could be used only for rivers with areas up to 20 - 30 km^2 from the low regions of the country, where this phenomenon occurs with over 10 - 15% frequency, as was the case for the observed period 1975-2002.

CONCLUSIONS

The presentation of some results concerning the minimum flow of small water courses in the two areas of the country highlights the main factors leading to the occurrence of low flows and even of drought (Q=0) in such rivers. The main parameters of the flow stages are specifically presented.

The parameters of the minimum flow, for example the minimum daily or monthly discharges of large probabilities (80 - 90%) in the case of rivers with permanent flow or the number of days (maximum, medium or 1 - 2% probability) with the drought phenomenon, are of great importance to water management because of the high number of small lakes in this area.

The relations carried out for the forecast of the minimum flow and of the drought phenomenon are based on the main factors determining the occurrence of these characteristics. Considered to be sufficiently accurate for operative hydrological purposes, they can be used on condition that the meteorological forecasting is accurate.

REFERENCES

Mita, P. (1996) Representative basins in Romania. *Printing House of the NIMH* Bucharest, Romania.

Mita, P., Haraga, St. (1996) Qualitative and quantitative estimates upon the draining phenomenon on the watercourses in the Central Moldovian Plateau. *Studies and Research, Hydrology*, 62, NIMH Bucharest, Romania.

SEAWATER INTRUSION AND GROUNDWATER QUALITY IN THE SOUTHERN ITALY REGION OF APULIA: A MULTI-METHOD APPROACH TO PROTECTION

M. Polemio

National Research Council (CNR) Institute for Geo-Hydrological Protection (IRPI), 122/i Via Amendola, 70126 Bari, Italy
e-mail Maurizio Polemio: m.polemio@ba.irpi.cnr.it

ABSTRACT

Remarkably fast socio-economic development over the past few decades stressed the Region of Apulia's hydrogeology by originating different hazard sources. Massive groundwater withdrawal increased and aquifers were also increasingly bound to be a sort of ultimate receptacle for domestic and industrial wastewaters. The entire region underwent twofold human-origin pollution caused by saline seawater and chemical-physical intrusion

The importance of impaired natural resources and situation severity called for an approach based on all scientific knowledge available, supplemented by up-to-date investigations on groundwater. The main objective was to identify quality trends, availability degradation and groundwater resource risks, by using different GIS integrated methodologies and developing management tools, the latter to be simple, quick, affordable and as low cost as possible. The proposed approach was based on groundwater vulnerability assessment and use of an automatic hydrogeology monitoring network, the analysis of rainfall, air temperature, river flow yield time series and, more importantly, piezometric level checks to quantify groundwater availability changes, salinity trend analysis to assess changing seawater intrusion effects, groundwater quality schematic mapping with available chemical-physical laboratory data and multi-parameter logging for fast groundwater quality classification. Each tool used is summarised with the main results of applications to Apulia's aquifers.

Key words: groundwater resources, degradation risk, seawater intrusion, pollution, monitoring methods.

INTRODUCTION

Apulia is the south eastern Region of Italy (Fig. 1); it features extremely scarce surface water, groundwater close to the surface giving in fact been the main water supply source in the past for towns, particularly in the Murgia area hinterland. Despite massive water import, Apulia's groundwater now satisfies over 20% of local drinking water demand. Groundwater is the also the only resource available for use in vast areas of the region, as an effect of stream flow incidence, due to the environment's widespread karstic nature. Groundwater thus is the region's main water source.

Apulia's aquifers are Mesozoic rocks outcropping in the Gargano Promontory, hereinafter refereed to as the *Gargano*, in the north, in the low Murge Plateau (*Murgia*) in the centre and Salento Peninsula (*Salento*) in the south (Cotecchia et al. 2004). Apart from the Tavoliere, the remaining hydrogeological structures show some common features (Cotecchia & Magri, 1966; Ippolito et al., 1958; Grassi, 1983; Maggiore & Pagliarulo, 2004). They are large and deep carbonate aquifers, mainly consisting of limestone and dolomite rocks. Carbonate rocks are affected by karstic and fracturing, which also occur well below sea level, whereas intruded seawater underlies fresh groundwater due to different density. Confined groundwater is more widespread in the Gargano and Murgia than the Salento hinterland; groundwater is phreatic along a narrow coastline strip surrounding the region. When the Salento and Gargano are schematized as quadrilaterals, the sea along three sides bound them. The Tavoliere hydrogeological structure features three aquifer types. Starting from the top, the first is a large shallow porous Pleistocene-Holocene aquifer within a less than sixty meters deep conglomerate sandy-silty sequence, with a clayey impermeable bottom. It is deep enough to allow seawater intrusion only close to the coast. Groundwater is phreatic inland and upward, but confined in the remaining aquifer part. The second is a group of NW-SE oblong aquifers within the sandy layers of the deep sequence of Plio-Pleistocene clays, marly clays, sandstones and sands underlying the shallow aquifer

and overlying the carbonate platform. The deepest is an aquifer within the sunken carbonate platform, hundreds of meters below ground surface in continuity with the Gargano and Murgia carbonate rocks.

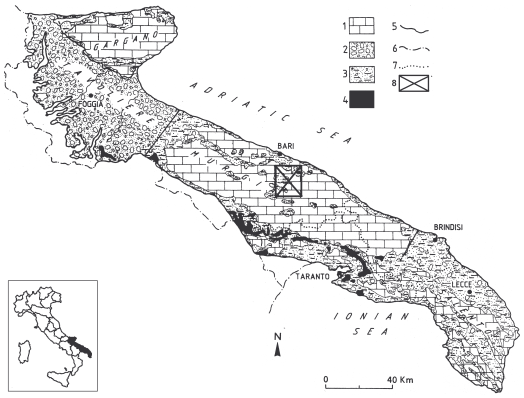

Fig. 1: Apulia's hydrogeology. 1) Carbonate rock outcrops in the Gargano, Murgia and Salento structures; 2) Tavoliere structure, shallow mainly conglomerate and sand aquifer; 3) shallow aquifers and permeable lithotypes, calcarenites, clayey sands, sands, gravel or conglomerates; 4) low permeable lithotypes, blue marly clays; 5) hydrogeology boundary, dashed where uncertain; 6) regional boundary; 7) provincial boundary; 8) Murgia experimental area.

Seawater intrusion-induced salt contamination of Apulia's groundwater is a well-known and thoroughly investigated phenomenon (Cotecchia, 1977; Grassi & Tadolini, 1996). A strong connection between salt contamination increase and t piezometric level lowering attributable to groundwater overdraft and/or natural groundwater recharge decrease, has been recognised today (Polemio & Limoni, 2001, Polemio et al., 2004). Aquifers have been considered a sort of ultimate receptacle for domestic and industrial wastewaters. The quantity of adequate quality groundwater is decreasing and chemical-physical and biological pollution is gaining importance, mainly due to widespread agricultural origin pollution or phenomena around urbanized areas (Tulipano & Fidelibus, 1993; Polemio 2000). Quality degradation of many pollution sources is noted as being due to outflow from coastline springs above and below sea level.
The importance of impaired natural resources and the severe situation require a strict approach based on all scientific knowledge available supplemented by up-to-date investigations of groundwater quality and availability changes. A multi-methodological approach is proposed to achieve sustainable exploitation of important natural resources such as groundwater. This approach should be based on procedures and as simple as possible technologies to be used not only by all public institutions, associations and professionals but also by as wide as possible number of users and citizens are proposed. The main objective is to identify quality and availability degradation trends and groundwater resource risks by using different GIS-integrated methodologies and developing management tools. These tools should to be simple, quick, affordable and as low cost as possible. The approach proposed is based on: groundwater vulnerability assessment; the use of automatic hydrogeological monitoring network; the analysis of rainfall, air temperature, river flow yield time series and, most importantly, piezometric level checks to quantify groundwater availability changes, salinity trend analysis to evaluate seawater intrusion effect variations, groundwater quality schematic mapping with available chemical-physical laboratory data and multi-parameter logging for fast groundwater quality classification. Each tool will be shortly summarised together with the main results of practical applications.

PROTECTION TOOLS

Groundwater Vulnerability Assessment

The location of any settlement that is a potential source of pollution must be planned based on detailed hydrogeological data and analyses, reported in a clear and straightforward form for use by decision-makers, where wide and vulnerable aquifers are located. The intrinsic aquifer vulnerability map is an effective

information tool for this planning activity. These maps quantitatively represent aquifer sensitivity to receiving and transporting pollutants that may degrade groundwater quality (Civita & De Maio, 1997).

Intrinsic aquifer vulnerability was evaluated with the SINTACS method (Civita & De Maio, 1997), an approach that divides the landscape into a grid with regularly spaced cells and assigns scores to selected variables for each cell. The variables used in this method were as follows: depth to water S, actual infiltration or net recharge I, unsaturated zone effect N, soil media effect T, aquifer media features A, hydraulic conductivity C, ground surface slope S. A weight factor was associated to each variable according to its contribution to vulnerability. These weights were defined as functions of the local hydrogeological setting based on many experimental assessments of Italian test sites. The intrinsic vulnerability index for each cell was computed by using the sum of the product of the scores and the weight of each variable.

Some experimental applications show procedure efficiency and clarify the criteria used (Polemio & Ricchetti, 2001). All data are converted into a digital format for implementation in a GIS Geographic Information System for vulnerability analysis, in the case of the Murgia experimental area (Fig. 1). Analysis was accomplished based on a 10 m spatial resolution raster grid (Polemio & Ricchetti, 2001). The data and analysis processes developed to produce the intrinsic vulnerability map are schematically described in the flow chart shown in Figure 2. A semi-variogram for each variable is obtained from point data to define the interpolation function. Then several 10 m resolution raster maps can be computed for the different variables by using kriging. The intrinsic vulnerability map shows the presence of four vulnerability index classes in the study area from 29 to 75% (100% is equivalent to maximum vulnerability); most of the area was classified as highly vulnerable (index over 50%).

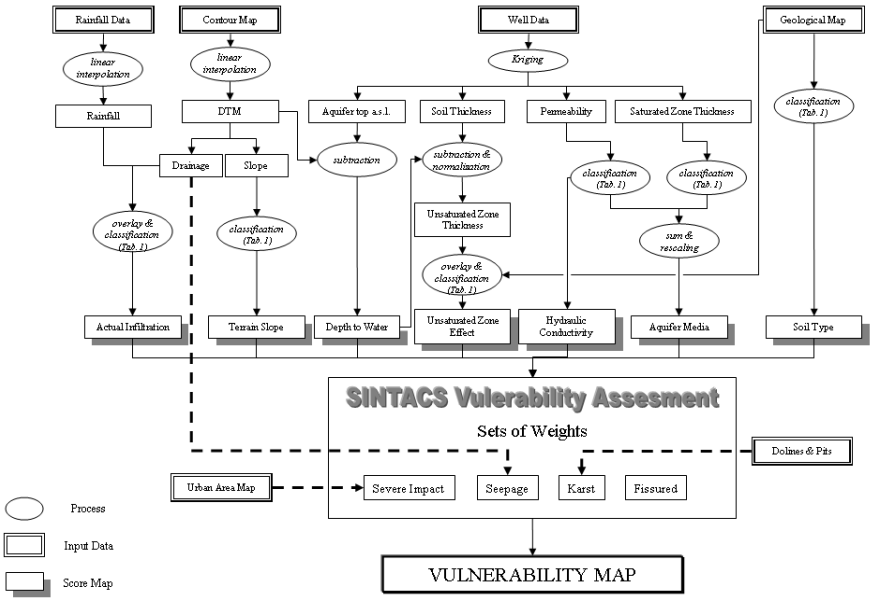

Fig. 2: Vulnerability analysis process diagram (Polemio & Ricchetti, 2001).

Automatic Hydrogeological Monitoring Network

All groundwater resource management and safeguarding activity was based on hydrogeological survey. A system was devised in the case of Apulia's groundwater, accessing the real-time electronic measurements required for proper groundwater supply planning, scheduling and management. Apulia's monitoring network includes: piezometric wells, salt-observation wells for measuring fresh-saline water equilibrium and quality control wells for assessing human-related pollution (Cotecchia & Polemio, 1999). Some 120 stations are currently used (Fig. 3) but plans are to increase the number of wells to 350, also including main coastal springs (Tedeschi, 2004).
Salt observation wells are located along a coastal strip and are deep enough to reach the transition zone between the surface fresh and underlying saline water and are equipped with multiple probes to measure piezometric level, temperature and specific electrical conductivity. Quality control wells are located where

withdrawal rate and groundwater contamination hazards are higher; the probes measure the piezometric level, pH, temperature, specific electrical conductivity and Eh. All data are used by a GIS for easy planning and management. It basically stores historical data gathered by other sources over the years as well as by the monitoring network. It manages information on soil cover type, hydrogeological features and groundwater quality. It then plots simulations against time and highlights hazards and emergencies.

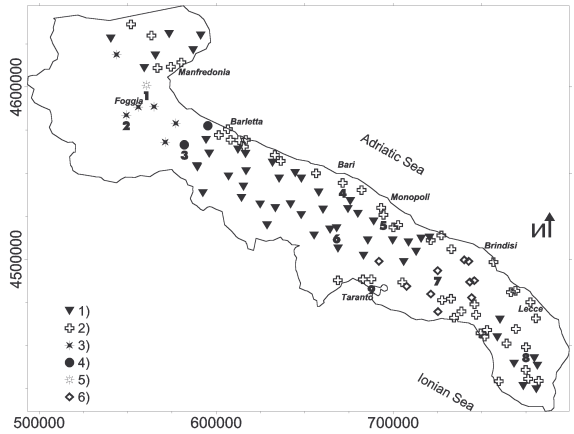

Fig. 3: Well map of monitoring network, logging wells and log types. Log type: 1) A, Inner or recharge area, 2) B, coastal strip or seawater intrusion area; 3) C, shallow Tavoliere aquifer; 4) D transition zone between the Murgia and the Tavoliere; 5) E, transition zone between the Tavoliere and the Gargano; 6) F, transition zone between the Murgia and the Salento.

Time Series Analysis and Groundwater Availability

The availability degradation risk could feature time series analysis of piezometric data, air temperature, well withdrawals, rainfall and river flow yield data, all currently widely available. This approach enable classifying water cycle, hydrology regimes and their variations in time as well. Trend, self-correlation and cross-correlation analyses and forecasting methods should be applied to all variables, as they are quite simple and can be extremely useful to identify available degradation hazards. Simple statistical GIS tools could thus be used to define spatial variation-based groundwater availability changes.
The analysis of Southern Italian monthly rainfall and temperature data time series from 1921 to 2001 highlights a vast decreasing annual rainfall trend at the end of the study period, equivalent: to a drop of 10% of Apulia's mean annual rainfall, with a mean value as low as 644 mm (Polemio & Casarano, 2004). The decrease is higher during the winter, Apulia's aquifer recharge season. The combined effect of annual rainfall and temperature trends and their regime variation is quite dramatic in terms of net rainfall, the trend decrease for which is evaluated as equivalent to 30% of mean annual net rainfall.

Data of 63 wells or piezometric gauges were considered (Polemio et al., 2004) (Table 1).

Table 1: Piezometric trends and data availability for each hydrogeological structure HS. MW) number of monitoring wells, AC) minimum trend (angular coefficient as m/year), MPST) more probable spatial trend at 2002

HS	MW	Data		AC	MPST (2002)
		from	to		
Tavoliere	12	1929	2002	-0,408	Decrease
Gargano	4	1975	1978	-0,036	Low decrease?
Murgia	30	1965	2003	-0,240	High decrease
Salento	17	1965	2003	-0,120	Decrease

Self-correlation piezometric coefficients show a progressively declining trend, starting from values slightly lower than 1. Apulia's groundwater is consequently subject to a consistent memory effect, that is to say the piezometric values recorded in any given month are strongly dependent on previous month values, the link being significant, decreasing the time lag increases, usually not less than a three month time span. This is a typical feature of groundwater of great importance during droughts. Apulia's aquifers show very strong and long-lasting memory effects, as further proof of its excellent hydrogeological potential. The links between piezometric and climatic variables are cross-correlated to a significant degree for a time lag of 1-4 months (Polemio et al., 2004). Rainfall effects are perceptible up to a maximum of 2/3 months, while the best correlation with temperature is felt with a time lag of 4 months, a situation typical of this semiarid area. The results of self- and cross-correlation analyses justify implementing simple and quite reliable piezometric forecasting models such as ARMA, ARIMA and multivariate modelling. The calculated piezometric trend is downward, as there is a widespread tendency, albeit in some cases very slow, towards a piezometric drop. The lowest piezometric decrements occur in the Salento area, with an Angular Coefficient AC of over -0.001 m/month. Minimum AC values occur in the Murgia and Tavoliere, where the lowest values are -0.240 and -0.408 m/year respectively. AC always approaches zero closer to the coastal areas as would be expected. Based on data available and irregular measurements made in 2002/2003, the most likely piezometric trend, ending in the second half of 2002 appears very serious indeed over the entire area (Table 1). Trend and cross-correlation analyses show that the steady and generalized piezometric drop is not entirely due to a rainfall: drop but that resource over-exploitation plays a very clear role in this process. The widespread and long-lasting piezometric decreasing trend implies water resource shortages; effects on seawater intrusion favoured by piezometric decreases and ensuing fresh groundwater salt pollution emphasize this dramatic degradation.

Salinity Trend Analysis and Seawater Intrusion

Two tools based on the use of data collected by private and public bodies are proposed assess seawater intrusion evolution and the ensuing saline contamination in a simple and reliable way.

The former is simple spatial analysis that can be applied if a threshold salinity value between pure fresh and seawater-contaminated groundwater is set for local hydrogeology.
The threshold is equivalent to about l to 0.5 g/l for Apulia's karstic and coastal aquifers. Using data measured by hundreds of wells, the threshold contour line can be measured with geo-statistic methods and its changes over the time can be underscored with GIS applications. Spatial evolution over the time was measured using 1981, 1989 and 1997 data (Fig. 4). Three area types were distinguishable. The first was where salinity is always below the threshold. It is an inland type; a vast part of inland Murgia and a restricted strip in the middle of the Salento peninsula were not been polluted so far. The second was linked to the areas where salinity is always greater than the threshold and groundwater saline pollution was found to be a long-standing phenomenon. This type can be identified in large areas along the Adriatic and Ionian shoreline. The third is an intermediate or transitory type; in each point of these areas, salinity is a sensible function of water cycle changes and, mostly, of human capacity to manage groundwater resources. The reference contour line receded gradually in the1981 to 1989 period, for instance, from the coast and groundwater in these areas too, was an effect of a great drought period and consequent greater groundwater over-exploitation. The phenomenon is either stopped or reversed, as in the case of some Murgia and Salento areas, as a consequence of rainy years.
The former tool assumes the existence of very high linear correlation between chlorine concentration and salinity for coastal aquifer groundwater. It should also be remembered that private individuals for several reasons caused chlorine concentration and law in many countries should regulate daily water use, when groundwater is supplied for drinking purpose.
The existence of this good correlation in Apulia's coastal aquifer is testified by 500 analysed groundwater samples, for which the linear correlation coefficient is equivalent to 0.98 (Polemio & Limoni, 2001). The increasing saline pollution of Murgia and Salento groundwater is confirmed by changes to chlorine ion concentration over 30 years in 18 wells. Data show that increased groundwater saline pollution is closely related to overexploitation. No significant concentration increase was reported in most wells before 1980. The phenomenon became apparent in the late 80s after some dry years leading to reduced recharge of aquifers and increased groundwater withdrawal. A clear increasing trend is observed in Salento, where the straight regression line angular coefficient is from 1.7 to 5.1-mg/L year.

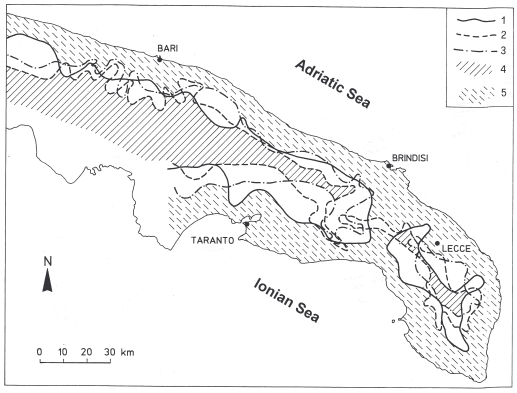

Fig. 4: Time modifications of 0.5 salt contour line g/l. Contour line of: 1) 1997, 2) 1989, and 3) 1981; 4) salinity always: less than 0.5 g/l, 5) greater than 0.5 g/l.

Laboratory Data and Schematic Quality Mapping

Schematic mapping groundwater quality with commonly available chemical-physical data enables defining groundwater quality and its variations starting from the natural features of groundwater as typical of each aquifer system. It is based on using ordinary determined parameter laboratory analysis data due, as required by health or drinking water laws, and from which to extrapolate historical groundwater resource features in time and space. The parameters should be chosen in function of availability in locally available historical data sources, simple laboratory assessment and their importance in connection to the different hydrogeological characteristics of the aquifer considered and potential water source pollution.
In the case of Apulia's groundwater, the proposal is to use concentration Ci of a group of chemical-physical parameters, total hardness, TDS, sulphates and chlorine, and a group of undesirable substances, nitrates, ammonium, iron and total coliforms. All these parameters play ab important role in identifying general water quality conditions (Civita et al., 1993; Polemio & Limoni, 1999). The former group of parameters should be strongly influenced firstly by natural hydrogeology conditions and secondly by anthropogenic phenomena. The latter group is typical of human pollution. The classification uses European Council Directive 80/778/EEC on the quality of water intended for human consumption, which defines Guide Level and Maximum Admissible Concentration MAC for each parameter, and it identifies 3 decreasing quality levels for each group, from A to C: A if Ci<GL for each parameter, B if Ci>GL at least for one parameter and Ci<MAC each parameter, C if Ci>MAC at least for one parameter. This means that 9 classes of groundwater, AA, AB, and the like can be obtained. Type AB is quality A and B respectively for the former and latter group of parameters. Quality degradation of Apulia's groundwater is summarised by applying the proposed tool, as shown in Figure 5. Quality is so low as to exclude use for drinking in 50% of the wells considered, while, the same treatment is often necessary in the remaining ones.

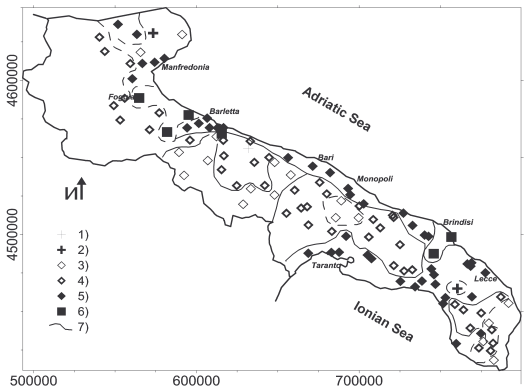

Fig. 5: Groundwater quality classification. Well with groundwater class 1) AA, 2) BA, 3) AB, 4) BB, 5) CB, 6) CC, 7) limit between groundwater classes.

Multi-parameter Logging for Fast Groundwater Quality Classification

Multi-parameter logs monitor some parameters, such as groundwater temperature T, specific electrical conductivity EC, TDS, dissolved oxygen DO and Eh, measured in well water columns. The method is based on identifying the trends of these parameters typical of an aquifer's natural hydrogeology. They are rather recurrent in space and time and enable extensive use of the method suggested, which can be easily applied to hydrogeology preliminary detection when natural or modified by anthropogenic activities, human-related pollution or seawater pollution amount and level. This may prove particularly useful for practical purposes, since these surveys are quite simple, fast and inexpensive.
The method was tested on some 120 wells of the Region of Apulia for one year, with quarterly surveys (Fig. 3) (Cotecchia et al., 1999). 6 typical multi-parameter log trends were identified. The chemical and physical properties of groundwater, as indicated by the tests, could somewhat correlate with the special hydrogeology of the inner: or recharge area type A, coastal strip type B, Tavoliere shallow aquifer type C, transition zone between the Murgia and the Tavoliere type D, transition zone between the Tavoliere and the Gargano type E)and between the Murgia and the Salento type F (Fig. 3). Field research highlighted that multi-parameter logs clearly show some special conditions where human acts cause groundwater degradation or modification, due to pollution or overexploitation. As regards the latter, this tool provides useful data on seawater intrusion evolution and on changes to the transition zone between fresh and saline water.

Conclusions

The complex issues appertaining to groundwater resource use, protection and management and the related socio-economic impact suggest applying an advanced multi-method approach as proposed. Each data collection and geographical processing step should be based on GIS platform. This system will give access to the real-time data required for proper groundwater resource planning and management.

REFERENCES

M. Civita, A. Dal Prà, V. Francani, G. Giuliano, G. Olivero, M. Pellegrini, A. Zavatti (1993) - Proposta di classificazione e mappatura della qualità delle acque sotterranee. Inquinamento, n° 12, Italia.

M. Civita, M. De Maio (1997) - S.I.N.T.A.C.S. - Un sistema parametrico per la valutazione e la cartografia della vulnerabilità degli acquiferi all'inquinamento. Pitagora Edizioni, Bologna, Italia.

V. Cotecchia, D. Grassi, M. Polemio (2004) - Carbonate aquifers in Apulia and seawater intrusion. 32nd IGC, "Some Engineering Geology case histories in Italy", 1-16, Florence, Italy.

V. Cotecchia, P.P. Limoni, M. Polemio (1999) - Identification of typical chemical and physical conditions in Apulia's groundwater (Southern Italy) through well multi-parameter logs. XXXIX IAH Congress "Hydrogeology and land use management", 353-358.

V. Cotecchia, M. Polemio (1999) - Apulia's groundwater (Southern Italy) salt pollution monitoring network. 15th Salt Water Intrusion Meeting, Ghent, Belgium, 1998, Flemish Journal of Natural Science, Ghent; Belgium, 197-204.

D. Grassi, T. Tadolini (1996) - The influence of water withdrawals in Apulia's Mesozoic platform upon inland propagation of seawater intrusion. 14th SWIM, Malmœ, Sweden.

D. Grassi (1983) - Difformità di ambiente idrogeologico promossa in seno alla piattaforma carbonatica appula da una evoluzione tettonico-carsica differenziata. Geologia Applicata e Idrogeologia, XVIII, parte I, 209-239, Bari, Italy.

F. Ippolito, V. Cotecchia, G. De Marchi, R. Dentice (1958) - Indagine sulle acque sotterranee del Tavoliere – Puglia. Cassa per il Mezzogiorno, Roma.

M. Maggiore, P. Pagliarulo (2004) - Circolazione idrica ed equilibri idrogeologici negli acquiferi della Puglia. Geologia e territorio, Supplemento. 1, Ordine dei Geologi, Bari, 13-36.

M. Polemio (2000) - Degradation risk owing to contamination and overdraft for Apulia's groundwater resources (Southern Italy). Water resources management in a vulnerable environment for sustainable development, published by K. Andah, UNESCO - International Hydrological Programme, Grifo Publishers, Perugia, 185-194.

M. Polemio, D. Casarano (2004) - Rainfall and drought in southern Italy (1821-2001). The Basis of Civilization - Water Science?, IAHS Publications. 286, 217-227.

M. Polemio, D. Casarano, V. Dragone (2004) - Trend termopluviometrici, siccità e disponibilità di acque sotterranee. Atti della giornata di studio: metodi statistici e matematici per l'analisi delle serie idrologiche, 123-132, Naples, Italy.

M. Polemio, P.P. Limoni (1999) - Mappatura speditiva della qualità delle acque sotterranee pugliesi. GNDCI Pubblicazione 2010, *Quaderni di Geologia* Applicata, Pitagora Editrice, Bologna, 1, 3-10.

M. Polemio, E. Ricchetti (2001) - Vulnerability Mapping of an Apulia's Deep Carbonate Aquifer Using GIS. II Simposio "Protezione delle acque sotterranee dall'intrusione marina e dall'inquinamento", Istituto Italo-Russo di formazione e ricerche ecologiche", 291-302.

G. Tedeschi (2004) - La rete di monitoraggio delle risorse idriche sotterranee pugliesi. Geologia e territorio, Supplemento 1, Ordine dei Geologi, Bari, 89-94.

L. Tulipano, V. Cotecchia, M.D. Fidelibus (1990) - An example of multi-tracing approach in the studies of karsting and coastal acquifers. Proceedngs of the International Symposium and Field Seminar on Hydrogeological Processes in Karst Terranes, Antalya, Turkey, IAHS publications 207, 381-389.

L. Tulipano, M.D. Fidelibus (1993) - Metodologie per la valutazione degli effetti del rilascio di rifiuti urbani sulla distribuzione dei nitrati nelle acque sotterranee delle unità idrogeologiche Murgia e Salento (Italia Meridionale). *Quaderni di Protezione Ambientale*, 49, Pitagora Edizioni, Bologna, Italia.

THE CASE OF THE "EFFIMERO" LAKE AT MONTE ROSA (ITALIAN WESTERN ALPS): STUDIES, FIELD SURVEYS, MONITORING

A. Tamburini[1] and G. Mortara[2]

[1] *CESI S.p.A.-ISMES, Via Pastrengo, 9 - 24068 Seriate, BG - Italy*
[2] *C.N.R. Istituto di Ricerca per la Protezione Idrogeologica, Strada delle Cacce, 73 - 10135 Torino Italy*
e-mail Andrea Tamburini: tamburini@cesi.it
e-mail Giovanni Mortara: giovanni.mortara@irpi.cnr.it

ABSTRACT

Glacial lakes represent a potential hazard due to the possibility of sudden outburst floods. This paper reports on the recent extraordinary evolution of the "Effimero" (short-lived) Lake at the Belvedere Glacier (Monte Rosa Group) and the actions carried out to prevent a glacial outburst or at least mitigate its consequences. During and after the emergency phase, studies and surveys were carried out in order to gain data relevant to the glacier's dynamics, the evolution of the lake and the englacial and subglacial drainage system pattern. GPS assisted bathymetric surveys were carried out in order to evaluate the lake volume (about 3 million m^3) and the lake bottom morphology. GPS assisted GPR (Ground Penetrating Radar) surveys, both from helicopter and from the glacier surface, were performed in order to measure the depth of the glacial bed. According to the results of tracer experiments, hypotheses about englacial and subglacial lake water flow and its seasonal variations were proposed. Due to both the need to collect the requested data in the shortest time possible and the need to minimize the number of operators and their stay in such a dangerous situation, a Mobile GIS station integrated with DGPS was used in order to assist navigation and data collection.

Key words: outburst flood, glacial hazards, differential GPS, echo sounder, GPR, tracers, Mobile GIS, Italian Alps.

INTRODUCTION

Glacial lakes offer fresh examples of glacial dynamics and assume a special importance in relation to climate and environment. However, the appearance of a glacial lake constitutes a reason for concern about potential Glacial Lake Outburst Floods (GLOF or jökulhlaup, an Icelandic term). The effects of a GLOF can often be disastrous, as documented by a lengthy case series for all glaciated areas, including the Alps (Ives, 1986; Dutto & Mortara, 1992; Walder & Costa, 1996; Raymond et al., 2003).

Once a glacial lake is formed, the thermokarst process causes a gradual deepening of the lake bottom that can lead to critical situations in the lake-glacier system (Kääb & Haeberli, 2001; Mercalli et al., 2002). Under such conditions, the stability of the glacial ice dam depends on the relationship between lake depth and ice thickness. The water pressure may destabilize the ice dam, which tends to be buoyed up (iceberg model). Within a few hours, a hydraulic breach may open, leading to the development of an uncontrollable sub/endoglacial GLOF. This is why knowledge of the glacial basin and the ice thickness is so important (Clague & Matthews, 1973; Kääb et al., in press).

THE CASE HISTORY

The Belvedere Glacier originates at the base of the huge eastern face of Monte Rosa and pushes its forked tongue almost as far as the village of Macugnaga, a well known holiday resort. The glacier and its tributaries have experienced at least seven sudden, huge discharges of water which seriously threatened Macugnaga. Memories of the 1970, 1978 and 1979 GLOF issuing from the proglacial Locce Lake are still very vivid (Haeberli & Epifani, 1983).

Fig. 1: The Belvedere Glacier supraglacial lake as it appeared in the second half of June 2002, when the maximum water level was reached.

Since the spring of 2001, the Belvedere Glacier has undergone an extraordinary surge-type movement, unequalled in the present scenario of Alpine glaciers, with astonishing changes in ice velocity, volume growth and morphological features, including a large depression that formed at the foot of the east wall of Monte Rosa (Haeberli et al., 2002).

The width of the depression and the lake basin gradually reached its maximum extent during an anomalous heat wave in the second half of June 2002. Fed by abundant supplies of meltwater from ice and snow, the lake extended over 15 hectares in area, with an estimated volume of about 3 million m3 (Fig. 1). The presence of the lake (named Lago Effimero, "short-lived lake") presented two scenarios, both equally alarming for the possible consequences downstream:

- the possibility of an overflow due to a rapid rise in the level of the lake (up to 1m/day)
- the increasing probability of a glacial outburst flood, a much less predictable phenomenon that offers no warning signs for the civil defence authorities to take the necessary, timely emergency measures.

A pumping system was installed at the lake. In the meantime, a system to monitor lake stage and glacial outlet stream discharge and turbidity was set up and a number of field investigations, such as topographic/bathymetric/geo-radar surveys and tests with tracers were carried out (Tamburini et al., 2003a).

By early July 2002, a combination of cold weather,, pumping and naturally occurring subglacial drainage began to lower the lake level, restoring it by the end of October to its previous size as of autumn 2001.

In the second half of May 2003, another period of exceptionally high temperatures again caused the lake to grow as rapidly as it had done the year before. Very soon, however, a natural flow path opened inside the glacier and partially on its surface. Between June 18th and 20th an active outburst took place, with a

maximum discharge of 15-20 m3 s-1. The total volume released was 2.3 million m3. No significant morphological effect or relevant damage occurred (Kääb et al., in press).

BATHYMETRIC SURVEYS ON THE "EFFIMERO" LAKE

Bathymetric surveys were carried out using a boat equipped with a DGPS positioning system connected with an echo sounder for the measurement of the lake bottom.

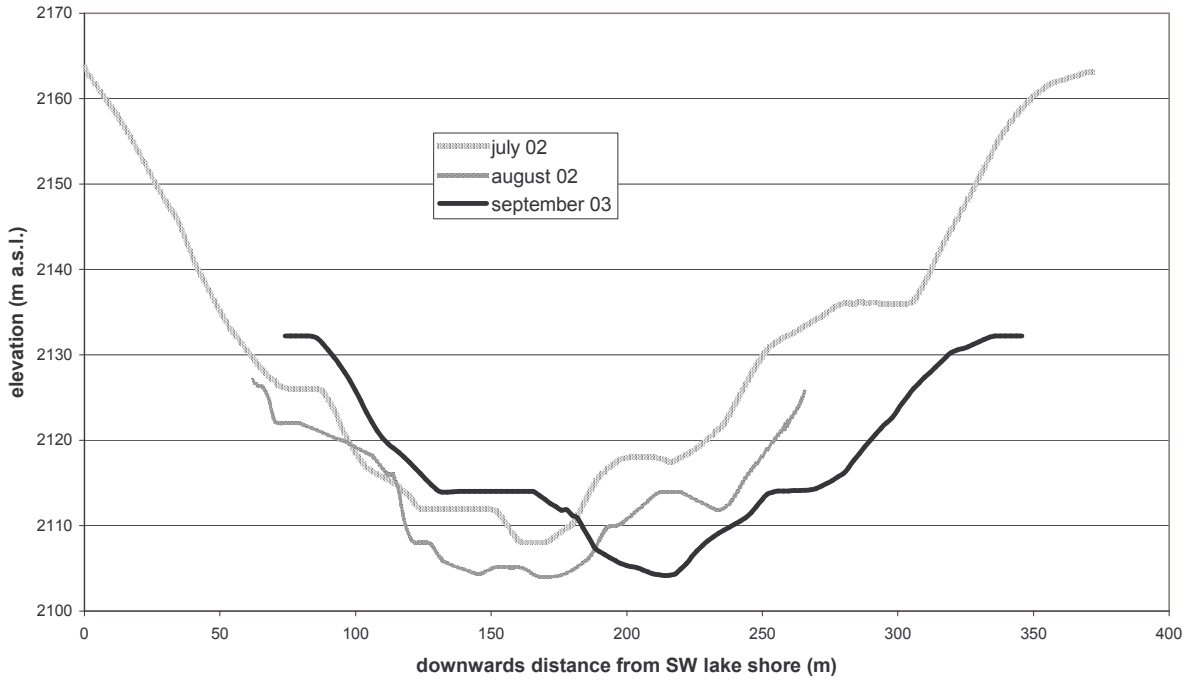

Fig. 2: Belvedere Glacier supraglacial lake longitudinal profile: lake bottom topography evolution from July 2002 to September 2003, obtained after repeated bathymetric surveys (courtesy Enel.Hydro and G. Viazzo).

The first survey was completed in one day (3rd July 2002); the lake's total volume, a map of the lake bottom contour lines and the level-volume ratio were available the same evening. The overall volume was calculated at 3 million cubic metres with a measured maximum depth of 57 metres.

Repeated bathymetric surveys confirmed the efficiency of the thermocarst process, giving measurements of the lake bottom as it deepened and lake migration and growth downwards over subsequent years, as shown in Fig. 2.

GPR SURVEYS ON THE BELVEDERE GLACIER

GPS assisted GPR surveys, both from helicopter and directly from the glacier surface, were carried out in order to determine the ice thickness and thus the depth of the glacial bed in the area around and downstream from the lake.

The interpretation of the data was extremely difficult, mainly because of the glacial till cover and of water and debris inside the ice. However, it was possible to clearly identify the course of the lateral moraine up to maximum depths ranging from 120 to 140 m and then to extrapolate the glacier's approximate thickness. The estimated thickness of the ice in the surveyed area varied between a minimum of 120 m beneath the lake bottom to a maximum of about 220 m in the area located downstream from the supraglacial lake.

DYE TRACER TESTS ON THE BELVEDERE GLACIER

Hydrological tracer tests were carried out in order to obtain qualitative and quantitative information about the englacial and subglacial water dynamics of the Lago Effimero and the Belvedere glacier.

Three tracing campaigns using fluorescein dye were performed in October 2002, June 2003 and October 2003 . In the first two experiments passive captors (activated charcoal) were located at five points downstream, collected at different times and analysed. In the last test, in addition to the passive captors, a field fluorometer was employed to record at regular and frequent time intervals the Anza Stream waters, 50 m from the left snout.

Tracer concentration breakthrough curves were analysed to characterize the englacial and subglacial hydrological system and identify the main drainage lines. Tracer transit velocities obtained after each tracer test were compared in order to evaluate the efficiency of the drainage system. In the last experiment the percentage of tracer recovery was estimated: a low loss or storage within the glacier's drainage system resulted (Tamburini et al., submitted).

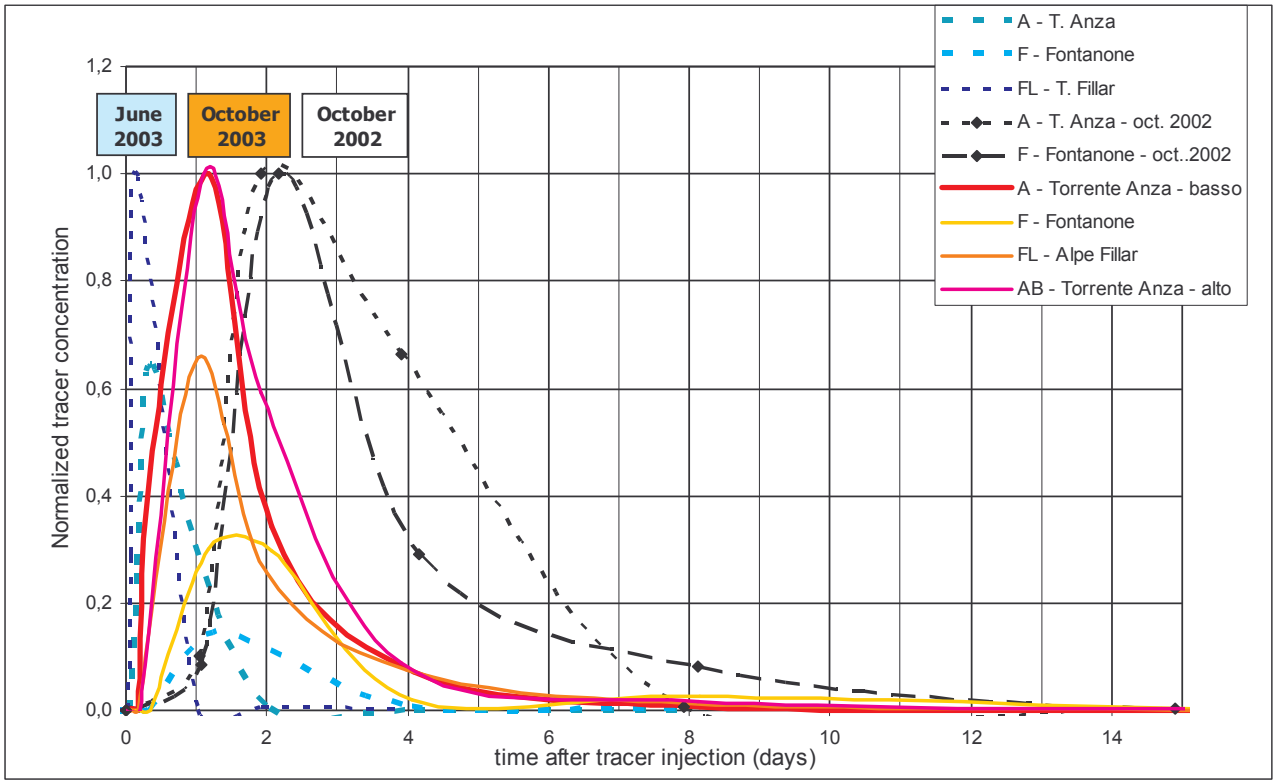

Fig. 3: Results of the traced tests performed at the "Effimero" Lake in summer 2002, fall 2002 and fall 2003: normalized tracer concentration vs time curves obtained after the tests are compared.

A comparison between the normalized tracer concentration curves obtained after the tests is shown in Fig. 3.

The following comments can be made:

- a comparison between tests performed in June and October 2002 respectively shows a higher efficiency of the englacial-subglacial drainage system at the beginning of the ablation period
- after the lake outburst (June 2003) the englacial-subglacial drainage system underwent important modifications resulting in improved efficiency, if compared with the results obtained one year before in the same season

THE JUNE 2003 OUTBURST

A glacial outburst occurred on June 18th-20th 2003. Fortunately it was not a sudden event but a progressive enlargement of the drainage channels.

Continuous lake level monitoring provided lake volume variation during the outburst, obtained by applying the volume vs water level curve obtained from the bathymetric surveys. By processing the water volume variation it was possible to obtain the average outflow-inflow balance during the event. The computed outflow-inflow vs time values are shown in Fig. 4.

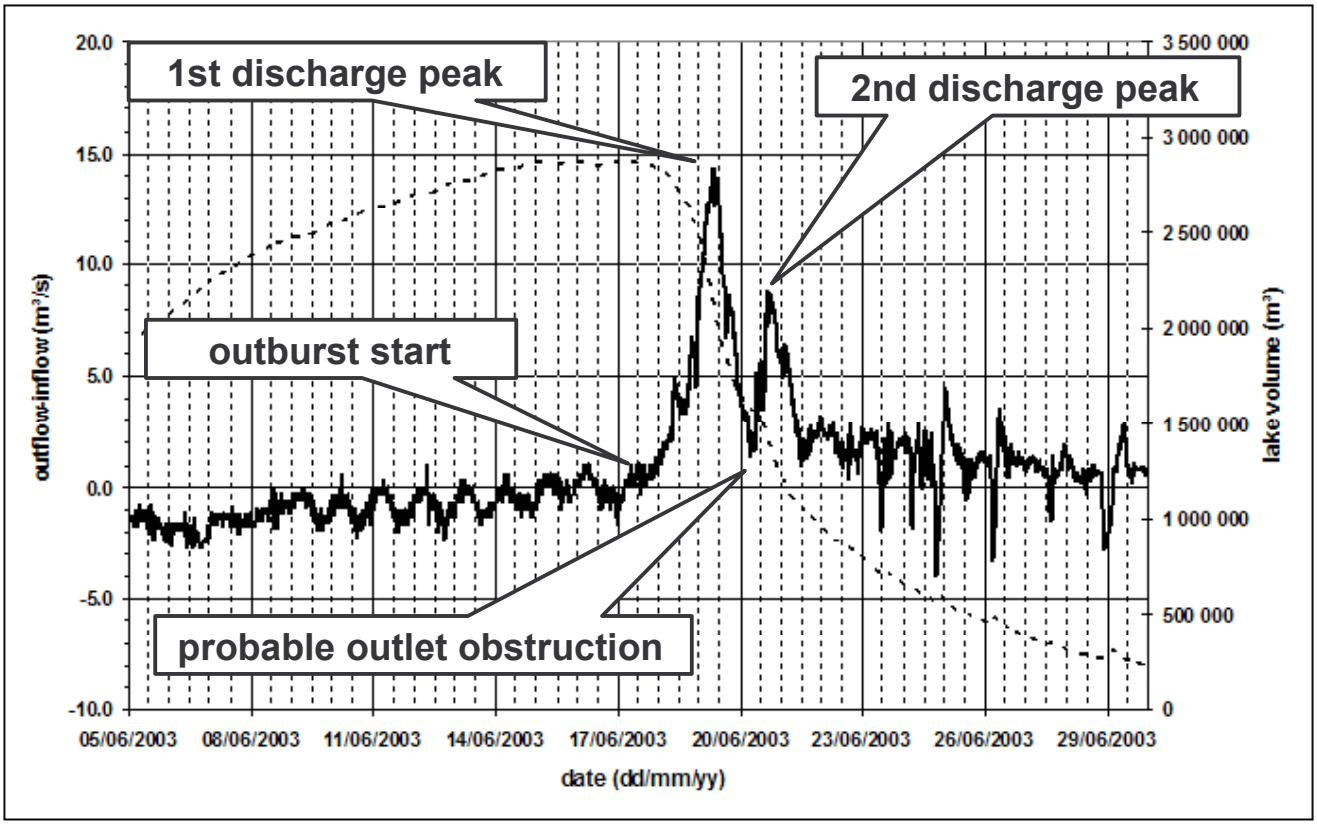

Fig 4: Discharge balance (continuous line) and water volume (dotted line) vs time curves for the Effimero lake obtained from continuous lake level monitoring.

The following comments can be made:

- a first discharge peak (outflow-inflow about 14 m^3/s) occurs on June 19th around 9 a.m.
- after the first peak, a rapid discharge decrease can be observed: this decrease has been interpreted as a probable obstruction of the main outlet;
- a second peak (outflow-inflow about 9 m^3/s) can be observed on June 20th around 4 p.m.
- after the event improved efficiency of the englacial and subglacial drainage system can be observed (discharge balance >0), confirming the results of the tracer tests

CONCLUSIONS

The emergency created by the *Lago Effimero* on the Belvedere Glacier provided an opportunity to test the efficiency of the most up-to-date survey techniques and to gather reliable data quickly while appropriately managing monitoring the event. A significant role was played by the Mobile GIS station, which provided the real time position of equipment and operators, reducing their presence in dangerous areas to a minimum (Tamburini et al, 2003b).

The experience described in this article provides a valuable contribution to the effort to reduce the adverse effects of large accumulations of water on or inside a glacier. This kind of scenario is likely to become more and more frequent in the glacial environment as a consequence of global warming.

ACKNOWLEDGEMENTS

The authors wish to express their gratitude to Paolo Federici for tracer data processing and Alessandro Cadore for discharge data calculation and analysis.

REFERENCES

Clague, J.J. & Mathews, W.H. (1973). The magnitude of jökulhlaups. Journal of Glaciology 33: 501-504.

Dutto, F. & Mortara, G. (1992). Rischi connessi con la dinamica glaciale nelle Alpi Italiane. Geografia Fisica e Dinamica Quaternaria 15: 85-99.

Haeberli, W. & Epifani, F. (1983). Mapping the distribution of buried glacier ice – an example from Lago delle Locce, Monte Rosa, Italian Alps. Annals of Glaciology 8: 78-81.

Haeberli, W., Kääb, A., Paul, F., Chiarle, M., Mortara, G., Mazza, A., Deline, P. & Richardson, S. (2002). A surge-type movement at Ghiacciaio del Belvedere and a developing slope instability in the east face of Monte Rosa, Macugnaga, Italian Alps. Norwegian Journal of Geography 56: 104-111.

Kääb, A. & Haeberli, W. (2001). Evolution of a High-Mountain Thermokarst Lake in the Swiss Alps. Arctic, Antarctic and Alpine Research 33: 385-390.

Kääb, A., Huggel, C., Barbero, S., Chiarle, M., Cordola, M., Epifani, F., Haeberli, W., Mortara, G., Semino, P., Tamburini, A. & Viazzo, G. (in press). Glacier hazards at Belvedere Glacier and the Monte Rosa East face, Italian Alps: processes and mitigation. Int. Conf. Interpraevent 2004.

Ives, J.D. (1986). Glacial lake outburst floods and risk engineering in the Himalaya. Int. Centre Integrated Mount. Development (Icimod), Occasional Paper n.5, Kathmandu.

Mercalli, L., Cat Berro, D., Mortara, G. & Tamburini, A. (2002). Un lago sul ghiacciaio del Rocciamelone, Alpi occidentali: caratteristiche e rischio potenziale. Nimbus 7: 3-9.

Raymond, M., Wegmann, M. & Funk, M. (2003). Inventar gefährlicher Gletscher in der Schweiz. Mitteilungen Versuchsanstalt Wasserbau 182: 5-368.

Tamburini, A., Mortara, G., Belotti, M. & Federici, P. (2003a). L'emergenza del Lago "Effimero" sul Ghiacciaio del Belvedere nell'estate 2002. Terra Glacialis 6: 37-54.

Tamburini, A., Mortara, G. & Belotti, M. (2003b). Uso di Mobile GIS nell'emergenza del Ghiacciaio Belvedere (Macugnaga, 2002). Atti della 6° Conferenza Italiana Utenti ESRI, Roma, 9-10 aprile 2003.

Tamburini, A., Federici, P., Predonzani, S., De Vittor, C., Mortara, G. & Semino, P. (submitted). Hypotheses about the englacial and subglacial drainage system of the Belvedere Glacier, Italy, from dye tracer tests. Incontro scientifico congiunto CoNISMa – AIOL, 18-22 ottobre 2004, Città del mare – Terrasini (PA).

Walder, J. & Costa, J.E. (1996). Outburst floods from glacier-dammed lakes: the effect of mode of lake drainage on flood magnitude. Earth Surface Processes and Landforms 21: 701-723.

MORPHODYNAMIC CHANNEL NETWORK IDENTIFICATION: FIELD MEASUREMENTS AND *GIS* INTEGRATION

A. Vianello

Dept. of Land and Agroforest Environments, University of Padova, Agripolis, Viale dell'Università 16, 35020 Legnaro (PD), Italy
e-mail Alessandro Vianello: alessandro.vianello@unipd.it

ABSTRACT

The study is oriented both to channel network identification and to the distinction between hillslope, colluvial and alluvial reaches. Field research was carried out in an alpine basin in the Dolomites, characterized in the upper part by a developed ephemeral colluvial network and by a main channel dominated by rapid and step pools. Measurements were made along the upper Cordevole stream. Cross section geometry (channel width and depth at the bankfull stage), local bed slope, and water discharge were measured in the main channel and in five colluvial reaches at the head of the basin.
The investigation is focused on the transition from colluvial to alluvial reaches and on the analysis of those variables which can play a primary role in the identification of the morphodynamic attitudes of the channel network. Stream power, which expresses the rate of potential stream energy loss per channel unit length , has proved to be consistent for representing the threshold conditions from the colluvial to the alluvial morphologies. Even considering simple water discharge at the bankfull stage as a threshold parameter, separation between hillslope, colluvial reaches and alluvial net gives satisfactory results.
The validation of the inferred thresholds criteria was then conducted at basin scale through geographic information system (*GIS*) techniques.

Key words: alluvial reaches, bankfull discharge, colluvial reaches, GIS techniques, stream power.

INTRODUCTION

The hydrographic network of some alpine basins can be divided into two distinct channel typologies: colluvial and alluvial reaches. The first developed at the upper part of the hydrographic basin. The colluvial incisions can be considered as small headwater channels, which exhibit a weak or ephemeral transport capacity (Montgomery & Buffington, 1997). They represent, then, the transitional form from non-incised rills to a headwater channel network (Montgomery & Dietrich, 1989).
The main objective of this work is in the analysis of those factors which can play a role in differentiating between colluvial and alluvial channels. This suggests an analysis of relations between morphometric and hydraulic variables, such as local slope (S), drainage area (A) and hydraulic stream power (Ω) and formative (or bankfull) discharge (Q_{bk}). Stream power defines the rate of energy expenditure per unit length of the channel (Bagnold, 1966; Brummer & Montgomery, 2003). It varies locally (W/m) and may be expressed as a function of bankfull discharge (Q_{bk}), according to the law (Ferguson, 1981-1987; Richards, 1982; Keller & Brookes, 1983; Nanson & Croke, 1992; Van den Berg, 1995):

$$\Omega_{bk} = \gamma Q_{bk} S \quad \text{(W/m)} \quad (1)$$

where: $\gamma = 9810$ N/m^3; Q_{bk} = bankfull discharge.

The work concentrates on an analysis of the formative conditions for the hydrographic network. A new type of approach is based on the determination of the parameter to be used, if extended at basin scale, as an element of identification between colluvial and alluvial reaches on the basis of both measured and calculated values and the use of *GIS* techniques. The analysis was carried out using field measurements in a mountain basin in the Dolomites (Italian Alps), considering the main channel (D'Agostino and Vianello, 2004) and five colluvial reaches at the head; the analysis was supported by direct measurements of discharge along the network.

STUDY SITE

The study was conducted at the head of the Cordevole basin (7.08 km^2), closed to Vizza. The basin is located in the Eastern Dolomites (Belluno, Veneto, Italy) (Fig. 1); it has a mean elevation of 2274 m and a mean slope of 55.7 %.

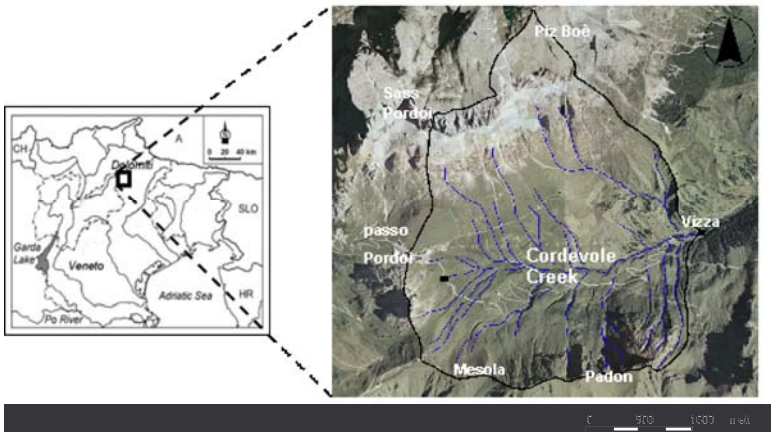

Upper Cordevole basin	
Area	7.08 km^2
Max. elevation	3152 m a.s.l.
Min. elevation	1820 m a.s.l.
Mean elevation	2274 m a.s.l.
Mean slope	55.7 %
Hydrographic network length	29.42 km
Main channel length	2.74 km

Fig. 1: Cordevole basin near Vizza; geography, location map and morphometric parameters.

With the exception of the sites adjacent to the watershed where the dolomitic series (left side of the valley) and the volcanic ones (right) are located, the geological formation of San Cassiano is the most representative. Over these soils the largest extent of the hydrographic network develops, comprising the main 2.36 km-long alluvial channel (Cordevole Creek: Fig. 2B) and a dense network made up of small tributaries. Many of them are incisions associated with a colluvial network (Fig. 2A).

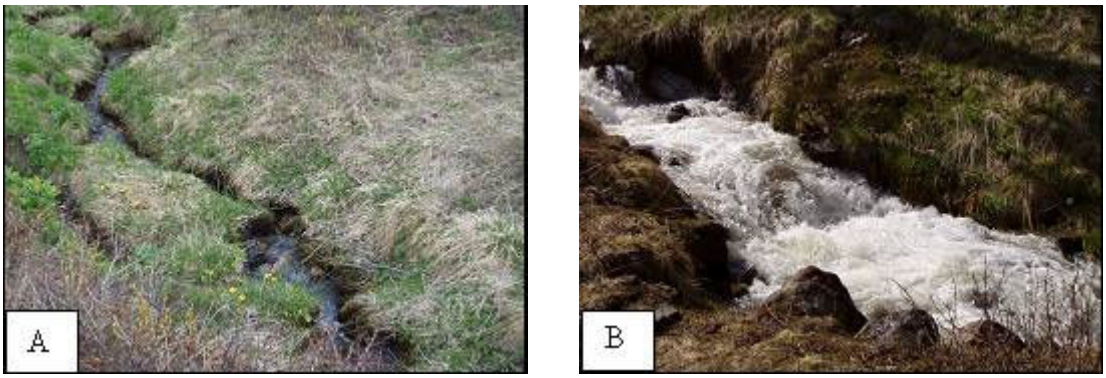

Fig. 2: Colluvial reaches, developed on the San Cassiano formation (A); Cordevole Creek (alluvial reach, B).

ANALYSIS OF DATA AND RESULTS

A field analysis was conducted on five colluvial reaches at the upper part of the basin, and on the entire main channel, measuring channel lengths (L), local slopes (S) and calculating, the values of formative (or bankfull) discharge (Q_{bk}) along the hydrographic network by starting with direct measurements of channel flow. Among the hydraulic variables, stream power (eq. 1) was chosen. The Ω values were calculated both in correspondence with alluvial channel sections (n = 104) and with some colluvial reaches (n = 77). Ω_{bk} , typically for small basins, grows rapidly and continuously with an increasing drainage area (Fig. 3) and defines that portion of the basin (< 10 km^2) dominated by high transport capacity (Brummer and Montgomery, 2003; Fonstad, 2003).

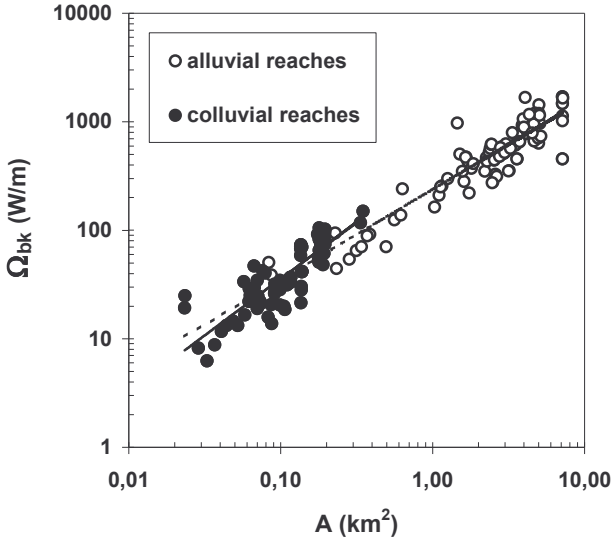

Fig. 3: Colluvial and alluvial reaches - logarithmic plot of drainage area (A, in km^2) versus calculated stream power values (Ω_{bk}, in W/m).

The alluvial reaches have the highest values. That is, a downstream increase in Q and a slight decrease in S. For the colluvial reaches and the alluvial channel, the equations assume the form of power laws; Colluvials: $\Omega = 528.9A^{0.92}$ (eq. 2) with $R^2 = 0.67$; Alluvials: $\Omega = 303.5A^{0.73}$ (eq. 3) with $R^2 = 0.81$. With the intention of analyzing the conditions for the formation of the hydrographic network and the differentiation between colluvial and alluvial reaches, the Ω values were put as a function of the local slope (S); the relation between S and Ω is shown in figure 4.

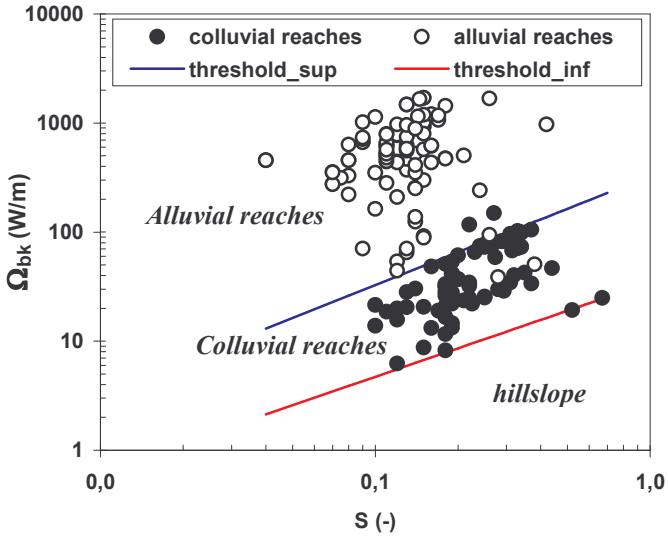

Fig. 4: Logarithmic plots of local slopes S (-) versus Ω_{bk} (W/m), for colluvial and alluvial reaches. The threshold which separates the two channel morphologies is defined by eq. 4 (blue line).

The colluvial reaches are scattered in the lower part of figure 4; on the same slope, they can be formed in correspondence with stream power values lower than those which refer to the alluvial channel. The colluvials are more easily incised, although the drainage area values were small. An evident separation between

colluvial reaches and alluvial morphologies may be found; it takes the form of a linear law, defining the threshold conditions from the colluvial incisions to the alluvial channel (eq. 4):

$$\Omega = 326.9S \qquad (4)$$

while the linear equation 5 (threshold_inf) defines the formative conditions at which the colluvial incisions (and the whole hydrographic network) begin (separation between hillslope and channel network):

$$\Omega = 37.3S \qquad (5)$$

On the basis of eq. 4 and 5, applying to eq. 1, the two threshold conditions depend only on the bankfull discharge (Q_{bk}); the threshold condition for the origin of the hydrographic network corresponds to the Q_{bk} value of 4 l/s, while the threshold between colluvial and alluvial morphologies is equivalent to the formative discharge of 33 l/s. This result can be verified in the graph in figure 5, where we can observe that the Q_{bk} threshold conditions are slope independent, on the basis of the disposition of colluvial and alluvial data.

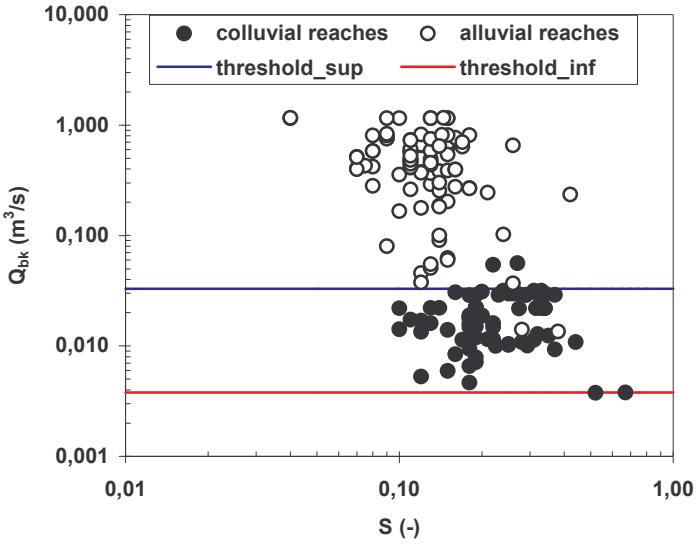

Fig. 5: Fields of existence of the colluvial and alluvial reaches, as a function of bankfull discharge (Q_{bk}) and of local slope (S).

The relationship between Q_{bk} and the drainage area of the basin (A), in the case of the upper Cordevole river, follows a linear form (eq. 6):

$$Q_{bk} = 0.162A \qquad (6)$$

On the basis of eq. 6, the two threshold values of Q_{bk} can be associated, in terms of drainage area, to the values of 2.4 ha (threshold between hillslope and hydrographic network) and 20.4 ha (colluvial – alluvial threshold).

These criteria were subsequently applied to and distributed at basin scale, in order to verify whether the automatic identification of hillslopes and of the hydrographic network assures satisfactory results, in particular for that great portion of the network not included in the field measurements. For this purpose, the analysis concentrated on the application of *GIS* techniques. The raster map of a threshold area of 20.4 ha was calculated and subtracted from the raster map of the drainage area; the values lower than zero identify the colluvial network, while the alluvial channel corresponds to values higher than zero (Fig. 6A). These results were verified through field observations in that part of the network which had not been previously analyzed; such observations confirmed a good overlap between the morphodynamic identification, made using *GIS* techniques, and the real situation.Starting from the limited study of colluvial reaches (n = 5), it was possible

to identify the whole colluvial network of the basin. The alluvial morphologies are limited to the single main channel and to another lateral tributary. In figure 6B the different segments of the hydrographic network are shown, characterized by ranges of stream power values. The highest values ($\geq$ 1000 W/m) can be observed at the final part of the channel network.

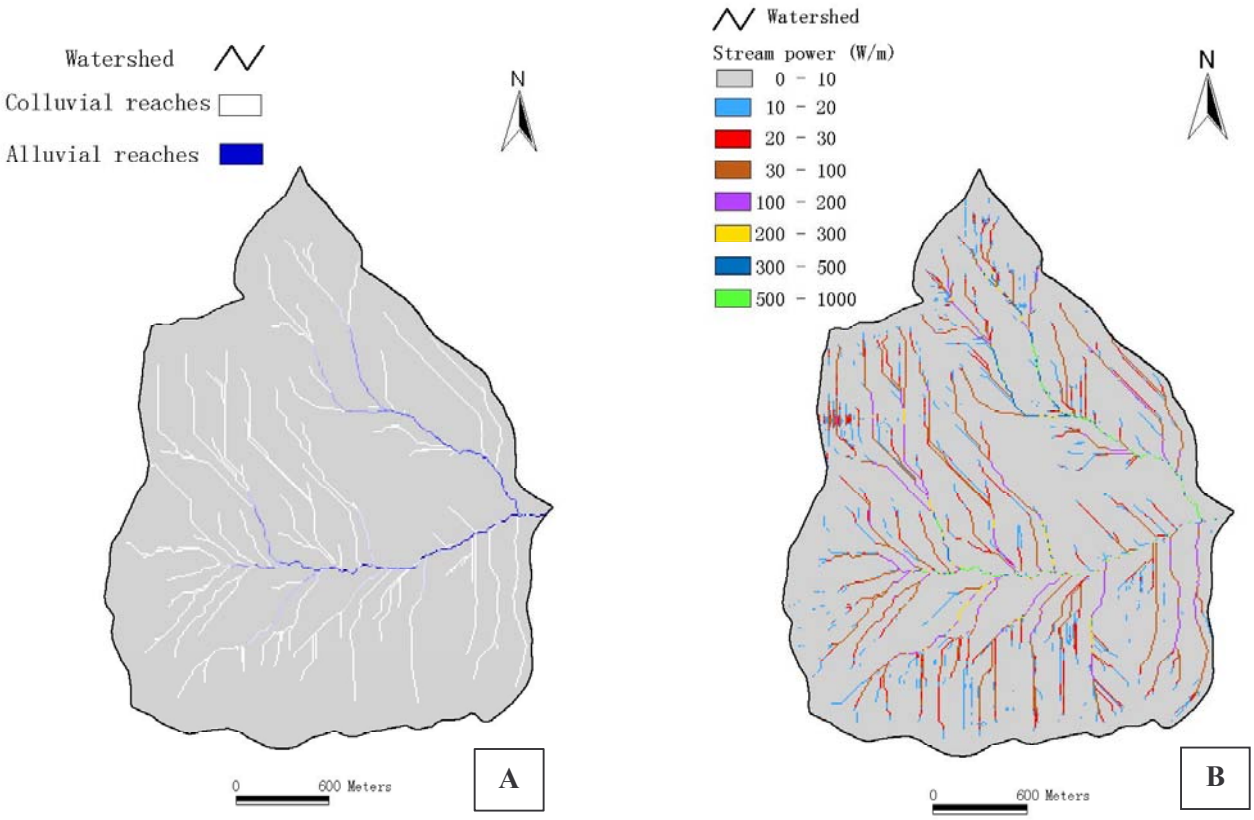

Fig. 6: Raster map (A) of the basin - colluvial reaches (white lines) and alluvial channel (black lines). Ω_{bk} (W/m) intervals assigned to the different portions of the network (B). The uniform grey zones correspond to the basin hillslopes.

CONCLUSIONS

Among the factors which play a role in differentiating between colluvial and alluvial channels, the morphometric (local slope) and hydrologic variables (discharge and stream power) have to be analyzed in detail. The formulation of analytical equations allows the threshold conditions between hillslope and colluvial reaches to be distinguished, and those which correspond to the evolution from colluvial to alluvial morphologies. The bankfull stream power (Ω_{bk}), in particular, can be used as a threshold parameter which identifies colluvial and alluvial reaches. From this assumption, two threshold values of Q_{bk} and of drainage area (A) can be used for the definition of the formative conditions of the hydrographic network. Applying *GIS* techniques, the validation of field analysis can be obtained on basin scale. The result is the identification of the whole colluvial hydrographic network and its separation from the alluvial morphologies.
These criteria, developed from field measurements, and then applied using *GIS*, to the whole hydrographic basin can be considered as good instruments for the prediction of the channel morphodynamic attitude.

REFERENCES

Bagnold R. A. (1966). *An approach to the sediment transport problem from general physics*. USGS Professional Paper, 422-J, Washington D.C.

Brummer C. J., Montgomery D. R. (2003). *Downstream coarsening in headwater channels*. Water Resources Research, 39, (10), 1294 pp..

D'Agostino V., Vianello A. (2004). *Analisi di campo sulla larghezza a piene rive in un torrente delle Dolomiti*. Rivista di Ingegneria Agraria, 4 (in press).

Ferguson R. I. (1981). *Channel form and channel changes*. In: J. Lewin (Editor), British Rivers, Allen and Unwin, London, pp. 90 – 125.

Ferguson R. I. (1987). *Hydraulic and sedimentary controls of channel pattern*. In: K. S. Richards (Editor), River Channels, Environment and Process, Blackwell, London, pp. 129 – 158.

Fonstad M. (2003). *Spatial variation in the power of mountain streams in the Sangre de Cristo Mountains, New Mexico*. Geomorphology, 55, pp. 75 – 96.

Keller E. A., Brookes A. (1983). *Consideration of meandering in channelization projects: selected observations and judgements*. River Meandering, Proc. Conf. Rivers, pp. 384 – 397.

Montgomery D. R., Buffington J. M. (1997). *Channel-reach morphology in mountain drainage basins*. Geological Society of American Bulletin, 109 (5), pp. 596 – 611.

Montgomery D. R., Dietrich W. E. (1989). *Source areas, drainage density, and channel initiation*. Water Resources Research, 25, (8), pp. 1907 – 1918.

Nanson G. C., Croke J. C. (1992). *A genetic classification of floodplains*. Geomorphology, 4, pp. 459 – 486.

Richards K. S. (1982). *Rivers, form and processes in alluvial channels*. Methuen, London, 358 pp..

Van Den Berg J. H. (1995). *Prediction of alluvial channel pattern of perennial rivers*. Geomorphology, pp. 259 – 279.

Annex

List of posters presented at the conference

Session 1: Surface and subsurface water flow

Brocca L., Melone F., Moramarco T., Stelluti M.
Soil water content monitoring in an experimental basin in Central Italy.
Key words: Soil moisture, rainfall-runoff, experimental basins.

Chormanski J., Ignar S., Cabanski P.
Application of the Green-Ampt infiltration model to watershead modelling.
Key words: Watershead rainfall-runoff modelling, GIS, parameter evaluation, Green – Ampt, SCS curve number.

Ferrero A., Usowicz B., Liepic J.
Soil thermal properties in relation to management of a sloping vineyard.
Key words: Hillside catchment, soil water-content, statistical-physical model, 3D map.

Sútor J., Gombo M., Ivan J.
Threshold phenomena of soil draught starting.
Key words: Soil drought, cracking process, hydrolimits in soil.

Van der Velde R., Warmerdam P., Stricker J.
Comparison of methods to compute reference evapotranspiration with lysimeter measurements.
Key words: Lysimeter, evapotranspiration.

Villagarcía L., Were A., Cantón Y., Fernández F., Moro M.J., Domene M.A., Solé-Benet A., Domingo F.
Daily soil water content fluctuations in rangelands from semi-arid SE Spain.
Key words: Water vapour absortion, semi-arid, range management, dew, monitoring.

Session 2: Precipitation-runoff processes

Anselmo V., Guiot E., Tesar M.
SCS-Curve Number derivation from rainfall-runoff data collected in forested experimental catchments of ERB network (Rio della Gallina, Italy; Liz, Czech Republic).
Key words: Curve Number, rainfall-runoff, experimental basin.

Brilly M., Toman M., Vidmar A.
Monitoring of revitalisation measures of urban rivers.
Key words: Urban river, revitalisation, fish habitat.

Demeterovà B., Kullman E., Poorovà J., Zuzana P., Velcicka L.
Hydrological Monitoring in vegetation Period 2003 on Wetlands in the Ltorica River Basin.
Key words: Wetlands along the Latorica River, monitoring of hydrological regime, The Tisza River Project.

Pérez F., López M. S., Echeverría M. T., Ibarra P.
Fire and hydrological behaviour in two prepyrenean forest basins (Aragon, Spain).
Key words: Runoff, precipitation, infiltration, fire.

Gutry-Korycka M.
Catchment model as a tool for research of surface and subsurface water interaction.
Key words: Mathematical modelling of hydrological processes, surface and groundwater river alimentation, hydrological systems and subsystems, lowland catchment.

Hlavcová K., Poórová J., Kalas M., Danihlík R.
Hydrological balance modelling in the Hornad River.
Key words: Hydrological balance modelling, Tisza River project, potential evapotranspiration.

Holko, L., Kostka, Z., Pecusova, Z.
Hydrological regime of the upper Hron river basin in 1962-2001.
Key words: Mountainous basin, long-term data series, snow cover, changes in hydrological regime.

Li X.Y., Contreras S., Villagarcía L., Sánchez J., Cantón Y., Solé-Benet A., Domingo F., Lázaro R., Van Wesemael B., Puigdefábregas J.
Influence of soil surface types on runoff in a karstic area (Sierra de Gador, SE Spain). Implications for aquifer recharge.
Key words: Runoff, vegetation, rock fragments, rock outcrop, rainfall simulation.

Martinez-Fernandez J., Ceballos A., Moran C., Hernandez V., Casado S.
Hydrological processes along a mediterranean rainfall gradient.
Key words: Rainfall gradient, Mediterranean conditions, land use, soil moisture, runoff.

Ninov P., Ribarova I., Nikolaidis N., Tsoraki R., Kalinkov P., Kukurin K., Topalova J.
Application of the HSPF model for the River Iskar inflow into the Reservoir Iskar.
Key words: Hydrology, HSPF model, calibration, GIS-data.

Salvia M., Barnich F., Hofmann H., Iffly J.-F., Kies T., Matgen P., Pfister L., Tailliez C., Tosheva Z.
Chemically based hydrograph separations in two experimental micro-basins of the Attert catchment.
Key words: Hydrograph separation, EMMA, water chemistry.

Swiatek D., Chormanski J., Okruszko T.
Hydraulic numerical model verification techniques for wetland river valley.
Key words: Flood routing, surface water flow, numerical modelling, remote sensing, wetland.

Walczak R. T., Slawinski C.
Procedure of rainfall intensity estimation for runoff prediction on structured soils.
Key words: Rainfall intensity, runoff, structured soils.

Session 3: Water quality and quantity relationships

Alvera B.
Pluriannual variations of the three kinds of erosion in a small Pyrenean watershed.
Key words: Sediment transport, suspended sediments, solutes, bed-load, runoff.

Casazza M., Piano A.
Industrial areas precipitation intensity and aerosol emissions.
Key words: Precipitation processes, aerosol, humidity.

Diliberto L., Canè G., Botti P.
Water quality dynamics of a Sardinian temporary river during flood events.
Key words: Temporary river, first flush, water quality dynamics.

Gambillara R., Terrana S., Bernasconi S., Figaroli M., Centurini A., Martin S.
Chemical features of the springs in north-western area of the Como Lake basin: preliminary results (Northern Italy).
Key words: Como Lake, Springs, Groundwater, Hydrochemistry, Geochemistry.

Rzonca B., Buczynski S., Druzynski A.
Chemical variety of spring waters surrounding Radochowska cave (Sudety Mts., SW Poland).
Key words: Spring water chemistry, crystalline waters, karst waters, cave.

Session 4: Water and sediment relationships in channel and slope erosion, sediment transport, mass movement and debris flow

Centurini A., Gambillara R., Figaroli M., Martin S.
Debris flows in the S. Vincenzo basin (West Como Lake): a first report.
Key words: S. Vincenzo basin, Structural setting, Debris flow events.

Conversini P., Salciarini D., Felicioni G.
Debris flow hazard in the Appennine area: the case study of S. Giorgio creek in eastern Umbria.
Key words: Channeled debris flow, small basin, triggering precipitation.

Ramon J., Hereter A.
Influence of flat areas and terraces on intense water erosion episodes.
Key words: Precipitation-runoff processes.

Konícek A., Miklánek P., Pekárová P.
Sediment transport from the agricultural soils in the upper Torysa basin.
Key words: Sediment transport, erosion simulation, AGNPS model, Torysa basin.

Maraga F., Anselmo V., Caroni E., Di Nunzio F., Godone F., Massobrio R., Pelissero C.
Runoff and bed load 1982 - 2003 in a small Alpine basin (Valle della Gallina, Italy).
Key words: Bed load, sedimentary trap, sediment supply, topographic survey, Italian Alps.

Marchi L., Arattano M., Dini M.
Benefits of long-term debris flow monitoring in instrumented basins
Key words: Debris flow, monitoring, instrumented basins, time-series, magnitude assessment.

Nadal-Romero E., Martí-Bono C., Lana-Renault N., Regüés D.
Regolith development and dynamics in a Pyrenean badland area: methodology and preliminary results.
Key words: Central Spanish Pyrenees, badland, weathering, bulk density, precipitation, moisture, temperature.

Tropeano D., Turconi L.
The Marderello catchment (Western Alps, Italy): a ten years's survey on geo-morphodynamical processes with special regard to debris flows.
Key words: Landscape evolution, geomorphological processes, debris flow analysis.

Session 5: Approaches and experiences on earth process studies involving development on innovative devices

Allasia P., Lollino G.
First applications of advanced tecnologies for the measurement of deep bed load.
Key words: Innovative field monitoring, sediment transport, water flow.

Buachidze G.
Diminish of Geoecology Risk in the Water Systems on the Borjomi Catchment of Baku-Tbilisi-Geyhan Pipeline.
Key words: Geoecology Risk, Surface and undergraund waters, Borjomi, Georgia.

Civita M., Gandolfo M., Peano G., Vigna B.
Study of the unsaturated zone of Bossea cave system.
Key words: Groundwater basin, Karst system, gauging station, floods.

Corniello A., Ducci D.
Groundwater Quantitative Status Assessment: an example in the Northwestern Basin of Campania (Southern Italy).
Key words: Water Framework Directive, groundwater levels, GIS, Campania Region, Italy.

Latron J., Rubio C., Llorens P.
Investigating local scale soil moisture dynamics and its relation to catchment scale hydrological response.
Key words: Moisture dynamics, hydrology.

Van den Bos R., Iffly J-F., Matgen P., Salvia M., Hofmann H., Tosheva Z., Kies A., Pfister L.
Constraining conceptual rainfall-runoff responses by incorporating imprecise tracer data information into the calibration process.
Key words: Conceptual model, uncertainty, tracer, GLUE, fuzzy, parameter constraining.